# AN EVALUATION OF THE ELECTRONIC TONGUE FOR THE TASTE ASSESSMENT OF DRUGS AND PHARMACEUTICAL FORMULATIONS

**XOLANI DERECK GONDONGWE**

School of Pharmacy

Department of Pharmaceutics

University College London

**Thesis submitted for degree of Doctor of Philosophy**

**May 2015**

I **Xolani Dereck Gondongwe** confirm that the work presented in this thesis is my own. Where information has been derived from other sources, I confirm that this has been indicated in the thesis.

## ABSTRACT

The publication of the European Paediatric Regulation (EC No. 1901/2006) in January 2007 brought the issue of taste assessment of medicines to the forefront. This regulation requires the early submission of a paediatric investigation plan (PIP).In most cases the applicant is required to provide an overview of planned measures / performed studies of which taste masking and assessment are of particular relevance. Therefore, there has been an increased interest in the development of objective taste assessment methods.

The first area in this thesis focused on investigating and understanding the mechanism of detection of the Insent® electronic tongue TS 5000Z. Within this area, sensor responses to molecules possessing similar structures were analysed. In addition, metformin hydrochloride, paracetamol and ibuprofen were also analysed.

In the development of objective taste assessment methods, such methods have to correlate with human taste perception. To this end, the second area investigated the correlation of taste assessment between an untrained human taste panel (n=24) and the electronic tongue. The human taste panel were presented with extemporaneously prepared amlodipine suspension which they graded in a visual analogue scale (VAS). These scores were compared to those obtained from the electronic tongue.

It is widely accepted that hot melt extrusion is useful for generating solid dispersions that have taste masking capability. However there are limited reports in the literature that assess taste masking efficacy using electronic tongues. The third area of this thesis focuses on generating solid dispersion of Eudragit®EPO and quinine hydrochloride dihydrate.

Overall, three key messages are concluded from the work detailed in this thesis. Firstly, the detection mechanism is dependent on the ionic / ionisation of the molecule under investigation. Secondly, strong correlation is shown between taste scores from the human panel and those obtained from the electronic tongue. Lastly, melt extrudates with 30% and 50% of quinine hydrochloride released less than 10% of drug in the first three minutes of dissolution therefore showing taste masking via both UV spectrophotochemical and electronic tongue analysis.

## ACKNOWLEDGEMENTS

I would like to thank my supervisors Professor Duncan Craig and Dr Susan Barker to whom I am eternally indebted for their guidance, technical assistance, vast knowledge and never ending patience which they exercised all throughout my PhD. I would also like to thank Dr Catherine Tuleu and Dr Mine Orlu Gul for their invaluable time and expertise.

My thanks also go to the members of thermal underground drug delivery group at UCL School of Pharmacy for their support and assistance during my period of study. In particular I would like to single out Dr Bahijja Raimi-Abraham and Dr Ziyi Yang (and our mutual friends green man special and sauvignon blanc) for their kind words of encouragement and support. Without them I would have not laughed, danced, eaten, travelled or drank so much throughout my PhD.

I would also like to thank my friends Miss Glynnis Masuku-Zinhumwe, Mr Lee Wyatt, Mr Matthew Gavan, Miss Michelle Gedge, Mrs Tonye Oboroh, Mr Robert Gonouya and Mr David Mitchell, who provided words of encouragement and understanding over the past few years. To the “Berlin crew” I thank you, you have no idea how much our trips contributed to this thesis.

Above all, I would like to say a heartfelt thank you to my mother (Catherine), sister (Cynthia) and brother (Dylan). Without their purses, patience, understanding, support, guidance and unconditional love, I would have not been able to complete my PhD!

*For umama and*

*loving memory of ubaba and madawu*

# TABLE OF CONTENTS

**TABLE OF CONTENTS**

**TABLE OF CONTENTS**

**TABLE OF CONTENTS**

## TABLE OF CONTENTS

# LIST OF FIGURES

## CHAPTER 1



## CHAPTER 2

## LIST OF FIGURES



## CHAPTER 3

## LIST OF FIGURES

## LIST OF FIGURES

## LIST OF FIGURES



## CHAPTER 5

## LIST OF FIGURES

## LIST OF FIGURES

## LIST OF FIGURES

# LIST OF TABLES

## CHAPTER 1



## CHAPTER 2



## CHAPTER 3



## CHAPTER 4

## LIST OF FIGURES

## LIST OF FIGURES

### CHAPTER 5

## LIST OF ABBREVIATIONS

| | |
|---|---|
| 5-HT | 5-hydroxytryptophan |
| AADC | amino acid decarboxylase |
| AAPS | American Association of Pharmaceutical Scientists |
| ANOVA | Analysis of Variance |
| ATP | Adenosine triphosphate |
| API | active pharmaceutical ingredient |
| BATA | brief access taste aversion |
| BP | British pharmacopoeia |
| CNS | central nervous system |
| ChemFET | Chemically modified field effect transistor technology |
| DSC | Differential scanning calorimetry |
| E | Electrode potential |
| $E^o$ | standard electrode potential |
| ENaC | epithelial sodium channel |
| EMEA | European Medicines Agency |
| ESC | European Society of Cardiology |
| ESH | European Society of Hypertension |
| F | Faraday constant |
| FDA | Food and Drug Administration |
| FIP | International Pharmaceutical Federation |
| GAD67 | glutamate decarboxylase |

| | |
|---|---|
| GLAST | glutamate aspartate transporter |
| GRAS | generally recognised as safe |
| GPCR | G-protein coupled receptor |
| HME | hot melt extrusion |
| HPLC | high performance liquid chromatography |
| $IP_3$ | Inositol phosphate 3 |
| ISO | The International Organisation of Standardisation |
| LAPV | Large amplitude pulse voltammetry |
| MSG | monosodium glutamate |
| MX | methylxanthine |
| NCE ` | New chemical entity |
| NCAM | neural cell adhesion molecule |
| NET | norepinephrine transporter |
| NICE | National Institute of Health and Care Excellence |
| NSAID | non-steroidal anti-inflammatory drug |
| ODT | orodispersible tablets |
| OXTR | oxytocin receptor |
| Panx1 | pannexin 1 |
| PCA | Principle component analysis |
| PIP | paediatric investigation plan |
| PLCβ2 | phospholipase c beta 2 |
| PROP | 6-n-propylthiouracil |

**LIST OF FIGURES**

| | |
|---|---|
| PTC | phenylthiocarbamide |
| PXRD | powder x-ray diffraction |
| Qn | quinine |
| QHD | quinine hydrochloride dihydrate |
| QhS | quinine hemisulphate dihydrate |
| R | Universal gas constant |
| RESS | Rapid expansion supercritical solution |
| ROMK | renal outer medullary potassium channel |
| SAPV | Small amplitude pulse voltammetry |
| SEM | scanning electron microscope |
| SCF | Supercritical fluid |
| TGA | Thermogravimmetric analysis |
| TCR | Taste receptor cell |
| THF | Tetrahydrofuran |
| VAS | Visual analogue scale |
| WHO | World Health Organisation |

# CHAPTER ONE
# INTRODUCTION

# CHAPTER 1 – INTRODUCTION

The taste of medicine is an important determinant of patient compliance with treatment regimens. The issue of unpleasant taste is particularly important in paediatric and geriatric populations. Generally, bitter taste is masked using solid dosage forms such as tablets or capsules. However, these are becoming increasingly inappropriate for both patient groups. In paediatrics, tablets and capsules are only recommended by the World Health Organisation (WHO) for children (6-12 years) and adolescents (12-18 years). Oral liquid dosage forms such as suspensions, syrups and oral drops are universally recommended for neonates (0-30 days), infants (1 month – 1 year) and young children (2-6 years). Among the elderly, there is an increase in the incidence of dysphagia (a swallowing disorder resulting from neurological / physical impairment of oral pharyngeal or oesophageal mechanism). 1.1 million people in England in 2013 are living with effects of stroke; the Royal College of physicians estimates that 40% of those surviving stroke have a swallowing difficulty (Royal *et al.* 2012). 50-75% of nursing home residents have some degree of dysphagia (O'Loughlin *et al.* 1998). These numbers are set to increase with the increasing ageing population. Therefore, in these patient groups it is necessary to use liquid dosage forms where they are commercially available. Taste masking is more difficult (or impossible) in liquid dosage forms especially if the drug is highly soluble. In addition, liquids have a high propensity to interact with taste buds because they spread all over the tongue and oral cavity, which means taste becomes more apparent to the patient.

During formulation development, the poor taste of a medicine does not become known until late into clinical studies. At this point, if the taste is noticeable and resulting in aversion then it may be necessary to find a different salt of the active pharmaceutical ingredient (API) which has a better taste profile or in the worst case scenario, an alternative candidate is selected. It would be valuable to be able to screen molecules and /or salt forms early in the development phase (preferably at the pre-candidate

stage), to enable formulators to work with the optimum API in terms of taste amongst other parameters. To perform this screening in humans has numerous limitations, of which the most important is ethics. Participants in such studies would be exposed to several new chemical entities (NCE) for which the toxicology data are limited or unknown. Hence, there is a need for other techniques for selecting candidate APIs at the pre-clinical stage. Such method(s) would also benefit formulators when designing a taste masking strategy for the NCE at a very early stage of development, which would ultimately be timely and cost effective. In order to develop such in vitro methods, it is important to understand the basic physiology of taste and taste transduction in mammals.

## 1.1 HUMAN PERIPHERAL GUSTATORY SYSTEM

Taste perception serves as a primary gatekeeper, controlling voluntary ingestions of substances in mammals. The peripheral gustatory system has two distinct functions, which are believed to be evolutionary in origin i.e. to detect nutritionally beneficial compounds and distinguish them from those that are potentially toxic of harmful. Taste is often confused with flavour (McBurney *et al.* 1979). The latter is a combination of different sensory signals, namely taste and aftertaste (gustatory system) and somatosensory modalities such as appearance (vision), texture (touch), smell (olfactory) and temperature (Chaudhari *et al.* 2010). The brain integrates these signals, the outcome of which is explained as flavour (Boltong *et al.* 2013). In this thesis, taste refers to the output obtained from the gustatory system alone. Signals from the olfactory system (nose) are only detected if the ingested substance is also volatile; this is not normally the case for most pharmaceuticals products therefore for the purposes of this research focus will be diverted from the taste-smell interaction under the assumption stated above.

### 1.1.1 FUNCTIONAL ANATOMY AND PHYSIOLOGY OF THE GUSTATORY SYSTEM

Spatial testing has dismissed the historical myth of the tongue map illustrated in Figure 1.1. This stated that the four basic tastes are spatially distributed such that sweet tastes are only detected on the anterior section of the tongue, while sour and salty are detected on the lateral section and bitter on the posterior. In fact, taste detection not only occurs on the tongue but throughout the oral cavity.

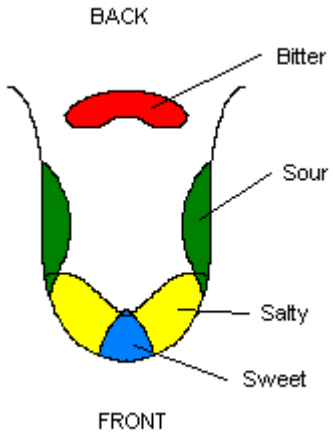


FIGURE 1. 1 THE TONGUE MAP (HTTP://FACULTY.ETSU.EDU/MILLERH/TONGUE/TONGUE4.GIF)

This is because taste recognition in mammals is mediated by specialised epithelial cells called taste receptor cells (TCR) that are arranged in taste buds on the tongue and throughout the oral cavity. Humans have taste receptors in several fields within the oral cavity including: all edges of the tongue, soft palate and in the pharyngeal and laryngeal regions of the throat. These cells are made up of gustatory cells, transitional cells and supportive basal cells and exhibit a rapid turnover; their average lifespan is about 10 days (Beidler *et al.* 1965). Taste receptor cells are not neuronal cells. Rather, they are specialised epithelial cells that share the same properties as neuronal cells but they lack an axon. The cells bodies of these taste fibres occur within the sensory ganglia of cranial nerves VII, IX and X. TRC predominately reside within multicellular rosette clusters labelled as “taste buds”.

Each taste bud contains approximately fifty to one hundred taste receptor cells collected together in a spherical structure that is 20-40µm in diameter and 40-60µm in

length. Taste buds are distributed throughout the oral cavity in the lingual and extra-lingual locations. Two thirds of these taste buds are localised on the tongue in three specialised structures known as fungiform, foliate and circumvallate papillae. Circumvallate papillae, found in the posterior region of the tongue can contain thousands of taste buds. Foliate papillae, are distributed most densely at the tip and on the edges of the tongue. Fungiform papillae which are located in the anterior third of the tongue only contain a few taste buds (Roper 1992, Breslin *et al.* 2006, Chandrashekar *et al.* 2006)

Taste buds display some similarity regardless of their location within the oral cavity. The individual taste receptor cells within the taste buds are diverse and as such they are classified into four cell types of which three are shown in Figure 1.2. Type I cells are also known as dark cells. They are the predominant cell type in taste bud consisting about 55-75% of all the cells (Finger 2005). Type II cells are considered the light cells and are distinguished by the presence of electron-lucent cytoplasm and large oval nuclei. Furthermore, they have smooth endoplasmic reticulum and constitute 20% of all cells in a taste bud. Type III are intermediate cells largely similar to type II cells but differ in that they have numerous dense-core vesicles particularly in their basal portions. Their unique feature is their unequivocal synaptic connections to afferent nerve synapses. Type IV cells, which are located at the basal parts of the taste bud, are a pool of undifferentiated precursor cells devoted to replacing the other cell types throughout life (Chaudhari *et al.* 2010).

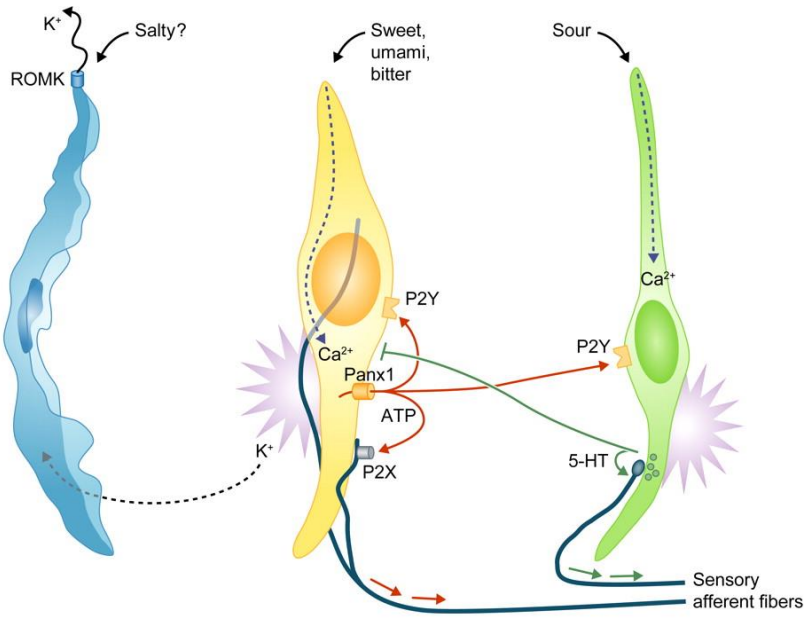


| Type I glial-like cell | |
|---|---|
| ***Neurotransmitter clearance*** | |
| GLAST | Glutamate reuptake |
| NTPDase2 | Ecto-ATPase |
| NET | Norepinephrine uptake |
| ***Ion redistribution and transport*** | |
| ROMK | $K^+$ homeostasis |
| ***Other*** | |
| OXTR | Oxytocin signaling? |

| Type II receptor cell | |
|---|---|
| ***Taste transduction*** | |
| T1Rs, T2Rs | Taste GPCRs |
| mGluRs | Taste GPCRs |
| Gα-gus, Gγ13 | G protein subunits |
| PLCβ2 | Synthesis of IP3 |
| TRPM5 | Depolarizing cation current |
| ***Excitation and transmitter release*** | |
| $Na_v1.7$, $Na_v1.3$ | Action potential generation |
| Panx1 | ATP release channel |

| Type III presynaptic cell | |
|---|---|
| ***Surface glycoproteins, ion channels*** | |
| NCAM | Neuronal adhesion |
| PKD channels | Sour taste? |
| ***Neurotransmitter synthesis*** | |
| AADC | Biogenic amine synthesis |
| GAD67 | GABA synthesis |
| 5-HT | Neurotransmitter |
| Chromogranin | Vesicle packaging |
| ***Excitation, transmitter release*** | |
| $Na_v1.2$ | Action potential generation |
| $Ca_v2.1$, $Ca_v1.2$ | Voltage-gated $Ca^{2+}$ current |
| SNAP25 | SNARE protein, exocytosis |

FIGURE 1. 2 THE THREE MAJOR CLASSES OF TASTE RECEPTOR CELLS. THE CLASSIFICATION INCORPORATES ULTRA-STRUCTURAL FEATURES, PATTERNS OF GENE EXPRESSION AND FUNCTIONS OF EACH. (CHAUDHARI ET AL. 2010)

### 1.1.2 CELLULAR MECHANISMS OF TASTE TRANSDUCTION

The qualitative range of human taste is not yet fully established. Traditionally, the majority of taste research has presumed the existence of five basic taste attributes namely: sweet, sour, bitter, salty and umami. These are illustrated in Figure 1.3.

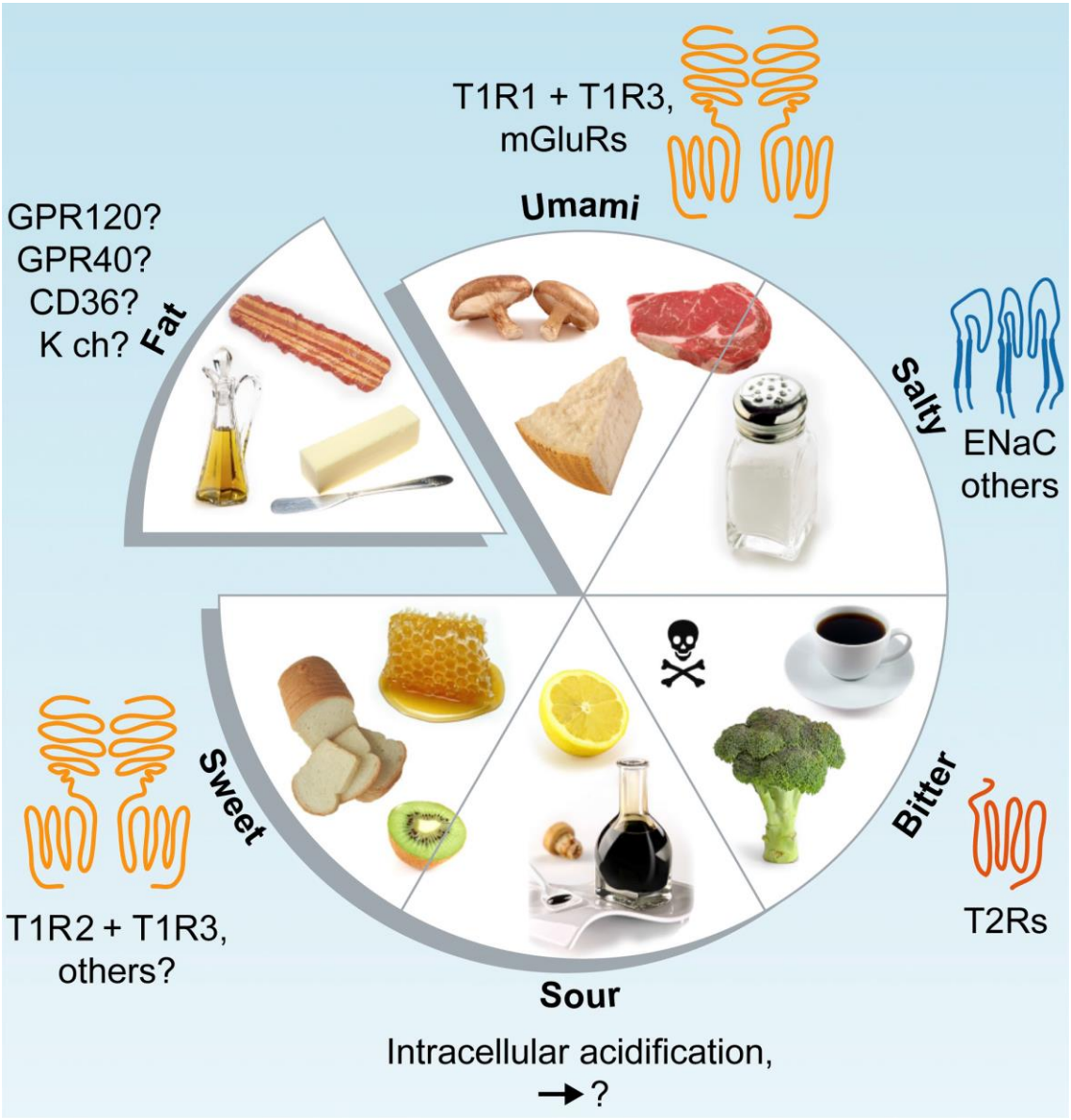


FIGURE 1. 3 FIVE RECOGNISED TASTE ATTRIBUTE I.E. SWEET, SOUR, BITTER, SALTY AND UMAMI, TASTE RECEPTOR THAT DETECT THEN AND EXAMPLES OF STIMULI (CHAUDHARI ET AL. 2010)

Data are accumulating that suggest that other sensory qualities such as fatty (Gilbertson 1998, Mattes 2011), astringency (Schiffman *et al.* 1992) and metallic (Lawless *et al.* 2004) are also carried by taste nerves. Thus, while the terms sweet, sour, salt, umami and bitter maybe familiar and have linguistic relevance, they do not describe the entire range of tastes perceived by humans.

As illustrated in Figure 1.3, each taste attribute has a specific coding mechanism which is mediated by specialised taste receptor. T2R family of G-protein coupled receptors

(GPCR) for bitter; T1R GPCRs for sweet and umami taste; ion channels candidate receptors for salt and sour. Figure 1.4 shows a schematic of the taste signal transduction pathways of the five basic taste attributes. Essentially, bitter sweet and umami are triggered by the activation of TCR on the tongue and palate. Tastant molecules bind to and activate a phosphoinositide pathway that elevates cytoplasmic $Ca^{2+}$ and depolarises the membrane via a cationic channel, Trpm5. The combined action of the elevated $Ca^{2+}$ and membrane depolarisation opens the large pores of the gap junction hemi-channels, likely composed of panx1, resulting in adenosine tri-phosphate (ATP) release. This thesis will focus on bitter taste transduction which is described in further detail in **section 1.1.3**.

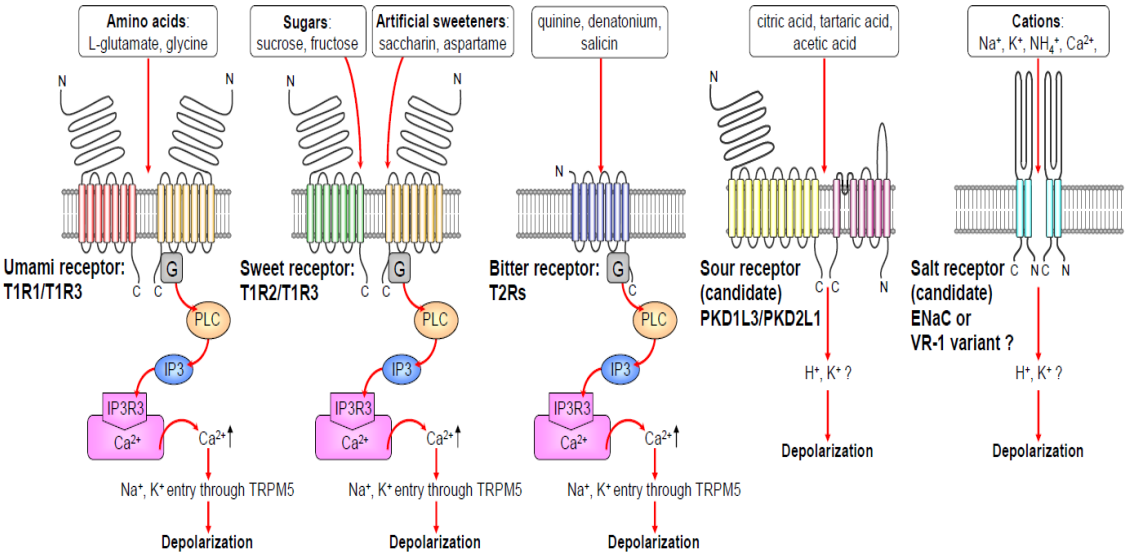


FIGURE 1. 4 SCHEMATIC OF TASTE SIGNAL TRANSDUCTION PATHWAYS OF EACH OF THE FIVE BASIC TASTE QUALITIES.(KOBAYASHI ET AL. 2010)

### 1.1.3 BITTER TASTE

The bitter taste is generally known as an aversive taste. It warns mammals to avoid the ingestion of potentially harmful compounds. Since some APIs are developed from plant alkaloids or animal toxins they have a bitter taste; therefore the understanding of the taste transduction of bitterness is crucial. Bitter taste does not originate from one single type of chemical agent but a diverse range of substances. These are transduced by GPCR and at present 25 bitter taste receptor genes and 11 pseudo-genes have

been identified in humans. These bitter receptors were named T2Rs (also termed Tas2Rs). At present, a focused search for ligands that activate the 25 human T2Rs is underway, with at least nine bitter-taste receptors and their ligands already been identified. These have been highlighted in Table1.1.

TABLE 1. 1 BITTER RECEPTORS CURRENTLY IDENTIFIED TOGETHER WITH THEIR CORRESPONDING LIGANDS (ADAPTED FROM (REED ET AL. 2006)

| Receptor | Ligand | Reference |
|---|---|---|
| **$hTaSR_{16}$** | Salicin | (Bufe *et al.* 2002) |
| **$hTaS2R_{38}$** | Phenythiocarbamide, polythiouracil | (Bufe *et al.* 2005) |
| **$hTaS2R_{43}$** | High concentration saccharin and acesulpham K | (Kuhn *et al.* 2004) |
| **$hTaS2R_{44}$** | High concentration saccharin and acesulpham K | (Kuhn *et al.* 2004) |
| **$hTaS2R_{46}$** | Absinthin, strychnine, denatonium | (Sakurai *et al.* 2010) |
| **$hTaS2R_{4}$** | Denatonium, PROP | (Chandrashekar *et al.* 2000) |
| **$hTaS2R_{10}$** | Strychnine | (Bufe *et al.* 2002) |
| **$hTaS2R_{14}$** | Broadly tuned | (Behrens *et al.* 2004) |
| **$hTaS2R_{61}$** | 6-nitro-saccharin | (Kuhn *et al.* 2004) |

The precise signal transduction pathway that results in bitter taste sensation is not yet fully understood. However, studies on the subject so far allude to the following second messenger signal transduction process. Tastant molecules bind to the GPCR activating the hetero-trimeric GTP-binding proteins. Upon ligand binding, the Gβγ subunits are freed from the taste GPCR and interact functionally with a phospholipase $PLC\beta_2$, which in turn stimulates the synthesis of $IP_3$. This is followed by the $IP_3R_3$ ion channels on the endoplasmic reticulum open resulting in the release of $Ca^{2+}$ into the cytosol of the receptor cells. The elevated intracellular $Ca^{2+}$ appear to have two targets in the plasma

membrane: a taste-selective cation channel TRPM5 and a gap junction hemi channel, both found in taste receptor cells. The $Ca^{2+}$ dependent opening of TRPM5 produces a depolarisation potential in receptor cells. In summary, two signals are elicited by tastant molecules: strong depolarisation and increased $Ca^{2+}$. These are both integrated by gap junction hemi channels resulting in ATP and possible other molecules are secreted through hemi channel pores into the extracellular space surrounding the activated receptor cell.

### 1.1.4 FACTORS AFFECTING TASTE

*NATURE OR NURTURE*

Parents provide genes and, especially during the early years of a child's life, they create the child's eating environment, making it difficult to separate genetic and environment factors (Plomin *et al.* 1993). To ask the question "nature or nurture" has become obsolete. The question has become how genes expressed in differing environmental contexts produce particular phenotypes. Taste preferences are phenotypic behaviours that result from genes, genetic polymorphism and environment interactions (Birch 1999).

The genetic basis of taste is exemplified by studies into the ability of certain individuals to taste phenylthiocarbamide (PTC) and its chemical relation 6-*n*-propythiouracil (PROP). These investigations date back to a serendipitous accident in Fox's laboratory in 1931. Synthesised PTC blew into the air and a nearby colleague complained of a bitter taste that Fox himself could not perceive. To date, literature has concluded that PTC tasting is produced by dominant allele (T). Individuals that are homozygous recessive (tt) are non-tasters, while heterozygotes (Tt) are medium tasters and homozygous dominant (TT) are super tasters. Polymorphisms in a single gene $hTaS2R_{38}$ have been shown to account for most (60-85%) of the variation in PTC/PROP sensitivity among individuals. Unfortunately the question of genetic variation in bitterness has primarily focused on the PTC/PROP phenomenon. It is

understood that supertasters find quinine and caffeine bitterer when compared to non-tasters (Tepper *et al.* 1997), however the taste preferences (phenotypic behaviours) of raft of pharmaceutical agents has not been fully elucidated.

*AGE*

In humans, specialised taste cells first appear around the seventh or eighth week of gestation and structurally mature taste buds are recognisable at thirteen to fifteen weeks (Cowart 1981). The foetus engages in episodic swallowing of amniotic fluid which changes composition throughout gestation. However, there is no direct evidence relating to the gustatory sensitivity in utero to behaviours in neonates or subsequent years of development. What is clear is that children are not merely miniature adults. Their responses to certain tastes differ markedly from adults. They exhibit heightened preferences for sweet-tasting and greater rejection of bitter-tasting substances (Mennella *et al.* 2003).

It is well established that taste acuity diminishes with increasing age. Changes in taste threshold increase after the age of 70 (Cowart 1981, Stevens *et al.* 1993, Schiffman 1997, Ng *et al.* 2004). Such changes include ageusia (absence of taste), hypogeusia (diminished sensitivity to taste) and dsygeusia (distortion of normal taste). Research and clinical studies indicate that hypogeusia and dsygeusia commonly occur in the elderly population, whereas ageusia is relatively rare. At present there is anecdotal evidence to suggest that it is not uncommon for the elderly to exhibit both hypogeusia and dsygeusia. This evidence suggests that it may be challenging to predict taste perception in the elderly population given that the loss or alteration of taste can differ in intensity and magnitude even between the basic taste senses.

Studies comparing an elderly population (n=24, mean age = 75± 6.0), and young adults (n=24, mean age = 28±3.4) showed that the elderly population judged caffeine (bitterness stimuli) and citric acid (sour stimuli) as tasting less intense than did the young adults. The same study illustrated that the aging effects on suprathreshold taste

perception were greatest for bitter, marginal for sour and least for sweet and salty stimuli (Hyde *et al.* 1981). In another study, detection thresholds in the elderly were on average 4.7 times higher than those of the younger population (Schiffman 2009).

Age related decrease in taste sensitivity was once thought to be a result in decrease in the number of taste buds whereas more recent studies have found no significant decrease in numbers with age. Since taste receptor cells have a life span of approximately 10 days, it has been suggested that an increase in the taste receptor cell's life span results in the deterioration of taste cell responses (Fukunaga *et al.* 2005).

### *MEDICINES AND DISEASE*

A range of medical conditions have been reported to affect the sense of taste. However, in most of these reports, the patients who were evaluated for taste perception were also being treated with medications for their medical conditions, so, it is impossible to determine the relative contribution of the disease state or the medicines to the taste alteration. Cancer is a classic example. It is a chronic condition in which patients are vulnerable to taste disorders. Taste receptor cells are rapidly dividing cells so therefore in theory they can be targeted by chemotherapy agents. This implies that it is not clear that taste distortion can only be attributed to the chemotherapy agents alone because disease progression is some cancers also affects taste perception. It is important to note that of those medicines where taste alteration has been identified, in most cases the nature of the taste alteration is not clearly identified and whether the taste alteration is transient or permanent is also not generally established. Therefore further investigation is required.

## 1.2 TASTE ASSESSMENT METHODS

A comparative summary of the most commonly used taste assessment methods is given Table 1.2 and Table 1.3; however, each of the methods has been described in brief below.

### 1.2.1. HUMAN TASTE PANEL STUDIES

At present, human taste trials also known as gustatory sensation studies or taste trials remain the "gold standard" for taste assessment (Anand *et al.* 2007) The International Organisation of Standardisation (ISO) provides a series of standards that safeguard the running of efficient and safe human taste panels. In such studies, trained healthy adult volunteers are used typically to evaluate the taste of formulations in statistically designed analysis. Evaluation of the formulation is usually performed on an objective scale, such as a visual analogue scale (VAS), which panellists use to evaluate a particular property of the formulation. Although taste trials are the gold standard, they are not without their limitations. The recruitment, training and retention of panellists are difficult and running these trials is costly. Furthermore, ethical and /or safety considerations often limit taste trials e.g. for cytotoxic agents, it would be deemed unethical to expose panellists to medicines that may cause potentially harmful side effects. Whilst such studies are designed to reduce bias, panellists remain subjective. Taste trials conducted in adults are not representative of paediatric taste preferences. These trials are also time-consuming and laborious, which leads to inaccurate taste evaluation from fatigued assessors. In view of highlighted limitations of the taste trials, researchers have focused on other methods to evaluate taste. A number of technologies have been proposed for screening APIs and their formulations. Most of them require the API to be in solution for testing, so they cannot address the issue of mouth feel. However, they give valuable insight into other aspects of the APIs taste profile.

### 1.2.2 ELECTROPHYSIOLOGICAL STUDIES

In these studies, the use of isolated tongue models from animals is employed (Oakley 1985). Electrodes are implanted in the chorda tympani nerve bundle or glossopharyngeal nerve; tastant solutions are passed over the tongue for a controlled period. Electrophysiological recordings from the nerve fibres provide a means of directly measuring dose response curves of taste stimuli. However, use of these

studies is limited due to involvement of surgery, capital investment on equipment. The low throughput is low due to the limited life isolated tongue. These studies are rife with difficulties in data analysis and interpretation. Animal ethical considerations also remain an issue.

### 1.2.3 IN-VITRO DRUG RELEASE STUDIES

These studies are commonly used to measure the effectiveness of taste masking. They are an indirect method of assessing taste because they offer no contribution to the evaluation of the taste of the API. Pharmacopeia release tests have been modified in recent years by altering the chemical component of dissolution media or reducing the volume of the dissolution media (Preis *et al.* 2013). Taste masking is achieved when, in the early times points for 0-5mintues; the API is either not detected or detected in amounts below the API's detection threshold. Drug content is analysed spectrophotochemically or using high performance liquid chromatography (HPLC).

### 1.2.4 IN-VITRO ASSAY METHODS

In these studies, e.g. cell based assays, taste receptor cell lines are cultured to maturity (which in itself is difficult), then they are exposed to tastant molecules while gustducin / transducing release is measured. Cell lines used include human enteroendocrine NCI-H716 cells and STC-1 cells (Hui *et al.* 2012). These methods are generally specific to bitterness but are only useful if bitterness response is gastducin / transducing dependant (Ruiz-Avila *et al.* 2000).

### 1.2.5 ANIMAL TASTE PREFERENCE STUDIES

Two commonly used models include the two bottle taste preference and the brief-access taste aversion (BATA) model. Typically, rats, mice, cats or dogs are used in these studies. In the two bottle preference study animals are given free access to two bottles, one which contains water and another containing an equal volume of tastant solution. The volume missing from each bottle after the test period (typically between

twenty four and forty eight hours) is measured and a preference ratio of tastant solution to water consumed is calculated (Danilova *et al.* 2006). In the BATA model, animals are mildly water deprived and therefore are motivated to sample from one of the multiple spouts that are presented one at a time through a port, usually in random order, in an apparatus called the Davis Rig, or "lickometer" (Boughter *et al.* 2002). Each bottle contains only a few millilitres or either water or tastant solution. The animals only have a short period to sample (lick) a solution. The time period should be short enough to allow animals enough time to lick but not too long so as to alleviate the animal's thirst such that they lose motivation to continue licking. Therefore, this is generally limited to fifteen seconds. Typically, a thirsty mouse will emit thirsty to fifty licks of water per five second period. Lick rates are diminished by a highly aversive tastant e.g. 1mM quinine hydrochloride (Glendinning *et al.* 2002). These studies tend to be qualitative, have low throughput and involve animal ethical issues and as such their use is limited (Devantier *et al.* 2008).

### 1.2.6 BIOMIMETIC TASTE SENSING SYSTEMS

These are also known as electronic tongues, e-tongues, taste sensors, taste chip and electronic sensor array systems. They are analytical sensor array systems which are able to detect specific substances by means of different artificial membranes and /or electrochemical techniques. The principle of detection of the electrodes can generally be divided into: potentiometric, voltammetric, impedimetric, optical and mass sensors. Potentiometric sensors are among the most popular sensors adapted for electronic tongues. This is illustrated in Table 1.2 which shows electronic tongues in development. Furthermore, the two commercially available electronic tongues are based on this principle. In potentiometry, a potential across a working electrode is measured when an equilibrium state is reached, corresponding to a state where the net current is equal to zero. The most significant advantage of potentiometry is the availability of a large number so different, both specific and less specific membrane material available such as glass, solid crystals, ionophores and lipid membranes. In voltammetry, a potential is

applied to a working electrode, and the resulting current obtained when redox active species are reduced or oxidised on the electrode surface. Voltammetric analytical systems include cyclic, stripping and pulse voltammetry. The latter is used most often. It can either be large amplitude pulse voltammetry (LAPV) and small amplitude pulse voltammetry (SAPV). An extensive review on the different voltammetric systems and the basic principles is described by (Winquist 2008). It is therefore not discussed any further because this research focuses on the potentiometric electrodes. Impedimetric sensors take the voltage-current ratio at a particular frequency as the detection signal and simultaneously another important interfacial property, capacitance, can also be detected. Impedence sensors have been widely used for taste assessment and have proven to be a feasible and effective methods due to their cross-selectivity, high sensitivity and reproducibility (Pioggia *et al.* 2007a, Pioggia *et al.* 2007b). Optical and mass electrodes have not been discussed in this context as there are currently no mentions in the literature of the development of electronic tongue which use these two principles.

As previously mentioned, there are currently two commercially available models of the electronic tongues available on the market i.e. AlphaMoss Astree2 and Insent TS5000Z. The latter, which is investigated in this thesis, is discussed in detail in **section 1.3** whilst the former is discussed below in brief. The Astree2 is equipped with a seven-sensor probe, an Ag/AgCl reference electrode and an auto sampler with sixteen to forty eight possible sample positions. There are three types of sensor sets available i.e. food analysis, pharmaceutical analysis and bitterness intensity measurement for new chemical entities. The underlying sensor technology is based on chemically modified field effect transistor technology (ChemFET) which is similar to the ion selective FET technology. The ChemFET sensors are composed of two highly conducting semiconductor regions: a source and a drain. These regions are surrounded with an insulator. A sensitive layer (coated membrane) is deposited above the insulator between the source and the drain. The composition and nature of the coat remains

undisclosed by the manufactures however it is suggested that it is able to form Van der Waals or hydrogen bonds with tastant molecules. There are also other electronic tongues in various development phases, a summary of which is given in Table 1.2. Thus far several reviews have been published in the literature, a selection that focus on commercially available electronic tongues have been highlighted (Kobayashi *et al.* 2009, Savage 2012, Tahara *et al.* 2013). This thesis will focus on the commercially available Insent TS 5000Z, which was developed and manufactured by Intelligent Sensor Technology Co. Ltd.(Insent®) in Japan.

## 1.3 ELECTRONIC TONGUE INSENT® TS5000Z

### 1.3.1 DEVELOPMENT OF INSENT® ELECTRONIC TONGUE

Research into so called “electronic tongue” was first recorded in the literature in the 1980s; Toko et al applied for a patent for their taste sensor in 1989 (Hayashi *et al.* 1990). They then developed a taste sensor equipped with multichannel electrodes using a lipid/polymer membrane for a transducer thus commercialising the first version of the electronic tongue TSS SA 401 (Toko *et al.* 1994). This taste sensor was considered to be an electronic tongue with “global selectivity”. Toko defined global selectivity as the decomposition of the characteristics of a chemical substance into those of each type of taste and their quantification, rather than the discrimination of individual chemical substances (Toko 1996). Essentially, Toko suggested that these taste sensors were able to describe a chemical substance in terms of its taste composition (based on five basic tastes) and furthermore quantify each of these taste attribute. This was based on the fact that in human taste transduction which is described in **sections 1.12** and **1.1.3**, humans recognise taste attributes rather than individual chemical substances. This was a departure from previous work in the literature which sort to discriminate individual chemical substances. Other models of the electronic tongue include the TSS 402 and the TSS 402B which were commercialised in 1996 and 2000 respectively.

It was found that the sensors used in the SA401 model had low taste selectivity, thus causing difficulties in the evaluation of sample with unknown taste qualities. In order to improve selectivity and sensitivity of taste sensors, the developers modulated the electrical charge density and the hydrophobicity of the membrane surface. This was achieved by incorporating varying amounts of lipid in the membrane. For example, in the development of the bitter sensor AN0, developers focused on the adsorption of the bitter molecule on the surface of the membrane. In this case the researchers focused on Log D, which is known to be correlated to hydrophobicity. With this in mind, taste sensors with eight plasticisers of different hydrophobicity were examined for sensitivity. The study showed that sensors with bis(1-butylpentyl) adipate (BBPA), bis(2-ethylhexyl) sebacate (BEHS), phosphoric acid tris(2-ethylhexyl) ester (PTEH) and tributyl o-acetylcitrate (TBAC) were selective to quinine hydrochloride and the selection of the eventual composition of the sensor was based on the polymer – lipid composition that gave the highest voltage reading (Kobayashi *et al.* 2009). Similar methods were applied in the development of the other sensors. Sensor composition and fabrication is discussed in further detail in **section 1.3.2**.

The SA402 and SA402B models needed improvement in the automation of the robotic arm and software for operating the electronic tongue and proceeding data analysis. The automation of the electronic tongue is not discussed any further in this thesis because this was outside the scope of the objectives presented for this research. However, data analysis is an integral part of the results obtained from the electronic tongue therefore attention is given to this issue in **chapter 2** (which explains the basic principles of principle component analysis). In **chapters 3, 4** and **5** a practical application and interpretation of the data analysis is described.

An image of the TS 5000Z which was used in this research is given in Figure 1.5

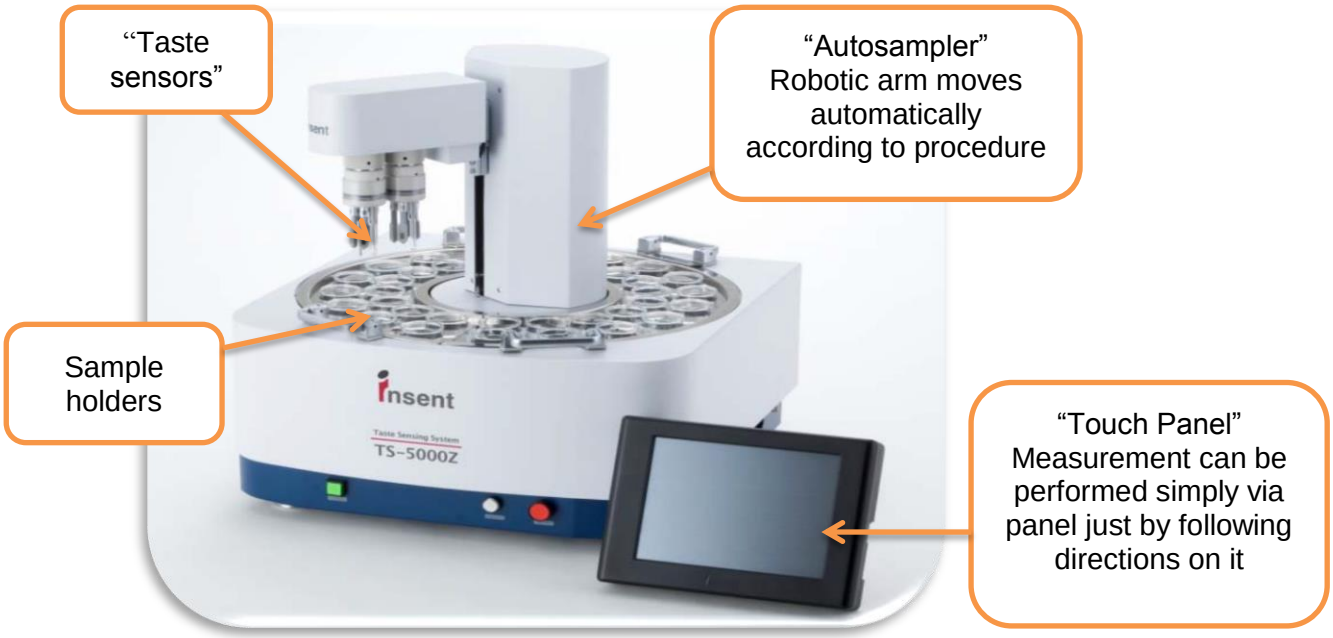


FIGURE 1. 5 IMAGE OF ELECTRONIC TONGUE INSENT® TS 5000Z, SHOWING THE POSITIONING OF SENSOR ELECTRODES, SAMPLE HOLDERS, ROBOTIC ARM AND TOUCH PANEL FOR RUNNING INSTRUMENT

TABLE 1. 2 A COMPARATIVE SUMMARY OF THE CURRENT IN VITRO AND IN VIVO TASTE ASSESSMENT METHODS – PART 1.

| Methods | Description | Applications | limitations |
|---|---|---|---|
| **Taste panel studies** | Sensory Analysis of tastants in trained healthy human volunteers | Well established and standard method for the taste assessment of drugs and drug products | Extensive training, subjectivity, toxicity, low throughput, time consuming, human ethical issues. |
| **Electrophysiological studies** | Response of tastants from glossopharneal or chordi tympani nerve | Screening of new molecules by assessment of taste difference | Involvement of surgery, capital investment on equipment, low throughput, difficulties in data analysis and interpretation, animal ethical issues |
| **Animal taste preferences tests** | Animal taste behaviour methodology to obtain data that parallels physiological investigations | Screening of new molecules by assessment of animal preference | Qualitative test, low throughput, animal ethical issues |

TABLE 1. 3 A COMPARATIVE SUMMARY OF THE CURRENT IN VITRO AND IN VIVO TASTE ASSESSMENT METHODS – PART 2

| Methods | Description | Applications | limitations |
|---|---|---|---|
| **In vitro drug release studies** | Study of release of tastant from pharmaceutical formulations | Formulation development tool, quality control | not applicable in case of liquid medicines namely solutions |
| **In vitro assay method** | Biochemical assay involving measurement of activation of gustducin and /or transducin | Rapid-throughput of bitterness and bitterness inhibitors, determination of molecular mode of action | Not applicable in gustducin/transducin independent taste modifiers |
| **Biomimetic taste sensing systems** | Electrochemical sensors coupled with chemometric methodologies for qualitative and quantitative analysis | Rapid-throughput screening of tastants and taste – masking agents, formulation development and optimisation, benchmark analysis, buccal dissolution simulation and quality control. | Require completely dissolving or suspending of the oral medicine in water. |

TABLE 1. 4 SUMMARY OF EXPERIMENTAL TONGUES IN DIFFERENT STAGES OF DEVELOPMENT -ADAPTED FROM (WOERTZ *ET AL.* 2011D)

| Sensor type | No. of sensors | Measurement principle | Where developed | Reference |
|---|---|---|---|---|
| **2 x chalcogenide glass membrane with pronounced redox sensitivity or plasticised PVC cation / anion sensitivty** | 27 | potentiometric | Chemistry department, University of St Petersburg, Russia | (Legin *et al.* 2004, Rudnitskaya *et al.* 2013) |
| **Ion selective electrodes** | 8 | potentiometric | Warsaw University of Technology, Department of Chemistry, Warsaw, Poland | (Ciosek *et al.* 2007) |
| **Nanostructured films adsorbed on Pt integrated electrodes** | 6 | impedence spectroscopy | Faculdade de Ciencias e Technologia, UNESP, Sao Paulo, Brazil | (Aoki *et al.* 2008) |
| **Lipid membrane sensors** | 8 | potentiometric | School of Pharmaceutical Sciences, Universiti Sains, Penang, Malaysia | (Ahmad *et al.* 2006) |
| **Ion selective electrode coated PVC membranes** | 1/drug | potentiometric | Department of Physical Chemistry, Kyoto University, Kyoto, Japan. | (Funasaki *et al.* 2006) |
| **Electrodes composed of gold, iridium, palladium, platinum and rhodium** | 5 | voltammetric | Swedish Sensor Centre, Linköping University, Linköping, Sweden | (Winquist 2008) |

### 1.3.2 SENSOR COMPOSITION AND FABRICATION

Various amounts of lipids and plasticisers were mixed for one hour in 10ml of tetrahydrofuran (THF). The mixture was dried in a petri dish at room temperature for three days to form a transparent layer (artificial membrane) which is about 200µm thick. The membrane is attached to the sensor platform using a solution of 800mg polyvinyl chloride (PVC) in 10ml of THF(Kobayashi *et al.* 2010). The sensor platform is illustrated in Figure 1.6. The sensor membrane is mounted on the part of the plastic tube, which has a hole, such that the inner part of the cylinder is isolated from the outside. The end of the cylinder is sealed with a stopper that holds the Ag/AgCl electrode. The lipids and plasticisers used are detailed in Table 1.4. The purpose of the plasticiser is to increase hydrophobicity of the lipid membrane which is the case of basic bitterness increases the adsorption of quinine hydrochloride dihydrate. In contrast the saltiness sensor has a higher lipid concentration and subsequently a lower plasticiser concentration therefore increasing the hydrophilicity of the sensor therefore allowing formation of electrostatic interactions with ions. The structures of the lipids and sensors used in the fabrication of the sensors are given in Figure 1.7.

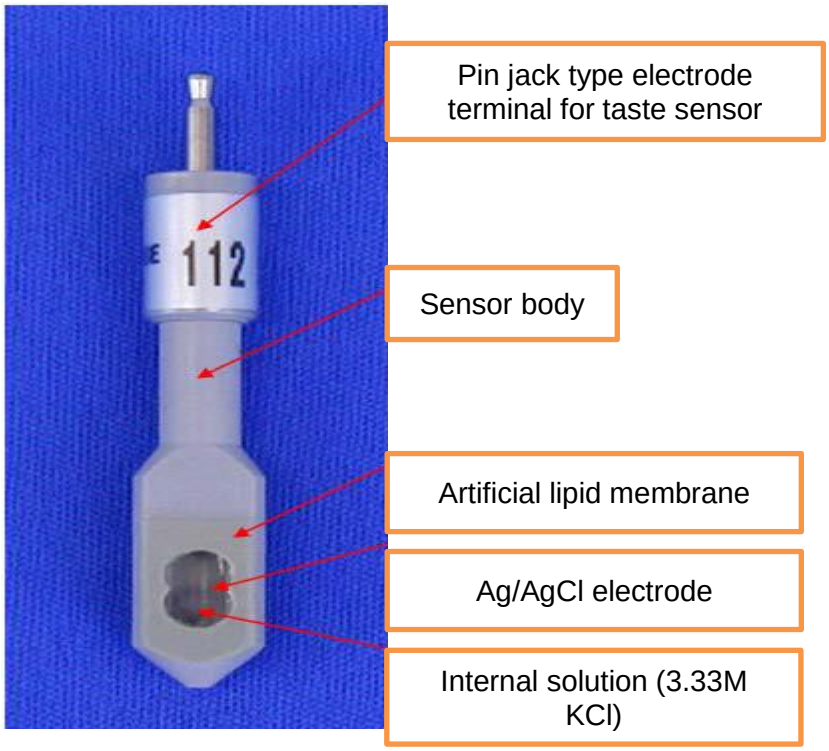


FIGURE 1. 6 IMAGE SHOWING A TYPICAL SHOWING. THE PIN JACK ELECTRODE TERMINAL PLUGS INTO THE SENSOR HOLDER. THE LIPID MEMBRANE DIFFERS DEPENDING ON THE SENSOR. ALL THE HANDLING OF THE SENSOR IS DONE VIA THE SENSOR BODY.(INSENT® TASTE SENSING SYSTEM MANUAL 2010).

TABLE 1. 5 COMPOSITION OF SENSORS – ADAPTED FROM INSENT® TASTE SENSING SYSTEM MANUAL (2010)

| | Name of Taste Sensor | Characteristic | Composition (Artificial lipid + plastisicer |
|---|---|---|---|
| **Positively charged membrane** | C00 | acidic bitterness | Tetradodecylammonium bromide and 2-Nitrophenyl octyl ether |
| | AE1 | astringency | Tetradodecylammonium bromide and dioctyl phenylphosphonate |
| **Negatively charged membrane** | AC0 | basic bitterness | 1-hexadecanol + dioctyl phenylphosphonate |
| | AN0 | basic bitterness | phosphoric acid di-*n*-decyl ester and dioctyl phenylphosphonate |
| **Blend membranes** | CT0 | saltiness | Tetradodecylammonium bromide *n*-Tetradecyl alcohol and phosphoric acid di-*n*-decyl ester |
| | CA0 | sourness | phosphoric acid di-*2*-ethylhexyl) ester, oleic acid, Triomethylammonium chloride and dioctyl phenylphosphonate |
| | AAE | umami | phosphoric acid di-*2*-ethylhexyl) ester, Triomethylammonium chloride and dioctyl phenylphosphonate |
| | BT0 | sweetness | Tetradodecylammonium bromide, Trimeritic acid + dioctyl phenylphosphonate |

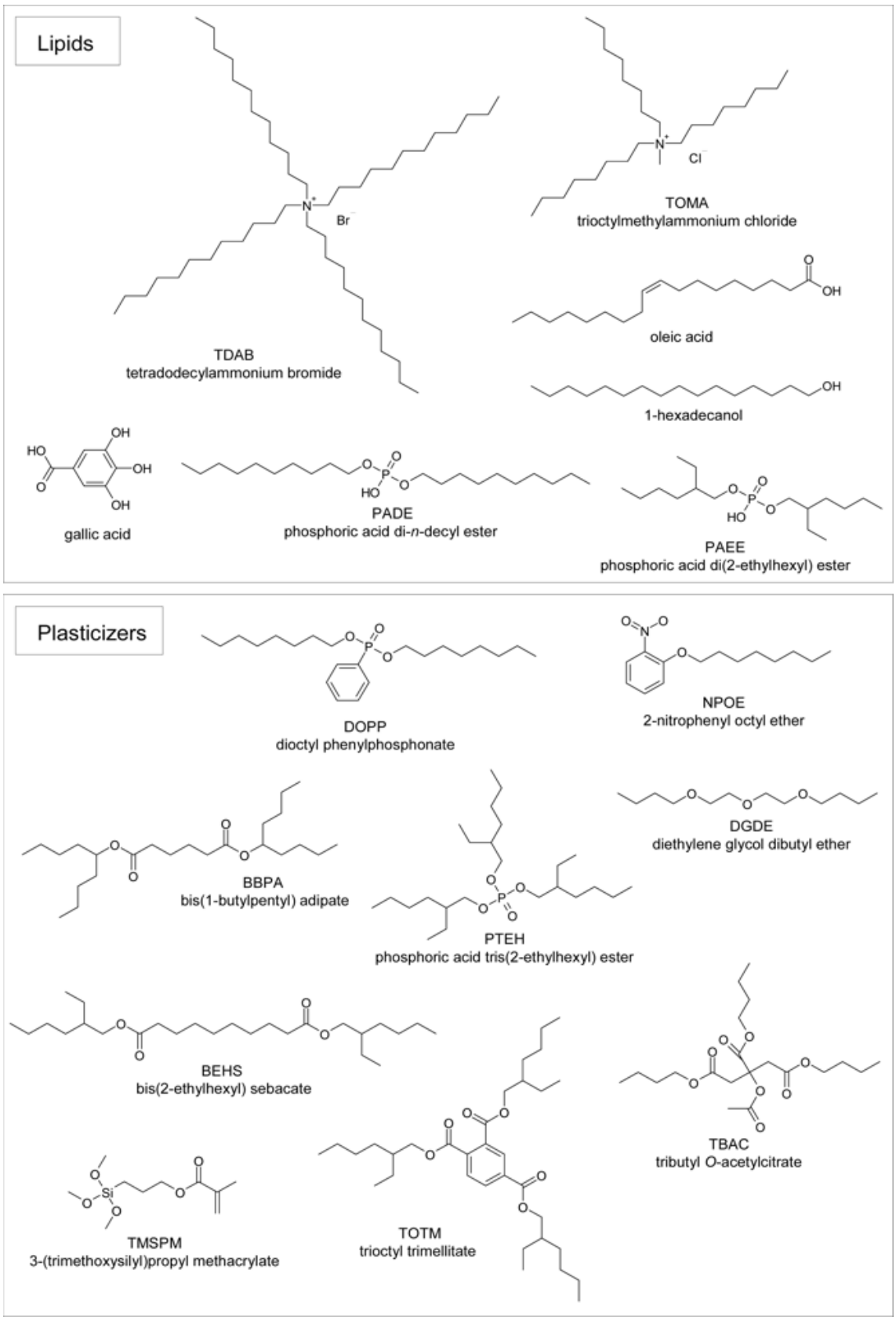


FIGURE 1. 7 FIGURE OF STRUCTURES OF LIPIDS AND PLASTICISERS USED IN THE FABRICATION OF TASTE SENSOR ELECTRODES FOR THE INSENT® TASTE SENSING SYSTEM (KOBAYASHI ET AL. 2010)

### 1.3.3 MECHANISM OF DETECTION

The mechanism of detection as described by the developers of the electronic tongue is illustrated in Figure1.8. Essentially, it is based on the Gouy Chapman theory, which states that when a lipid-based membrane is immersed in an aqueous solution, an electrical double layer (stern and diffuse layers) is formed at the membrane surface as shown in Figure 1.8A. The double layer is a result of dissociation of acid group of lipid molecules hence causing a membrane potential. The Stern layer either positive or negative comprises of ions adsorbed directly onto the membrane due to chemical interactions. The diffuse layer is composed of ions attracted to the surface charge via Coulombic force, electrically screening the Stern layer. The membrane potential can be calculated using the Poisson – Boltzmann equation which is a differential equation that describes electrostatic interactions between molecules in ionic solutions. The addition of a drug i.e. HCl (sour - Figure 1.8B), NaCl (salt - Figure 1.8C) and quinine (bitter – Figure 1.8D) to the aqueous solution can affects the membrane potential. In the case of an acid, the protons ($H^+$) prevent dissociation of the acid groups. In the case of a salt e.g. NaCl, the $Na^+$ cation provides a screening effect leading to a change in membrane potential. Quinine however, is believed to adsorb onto the surface of the lipid membrane therefore changing the membrane potential (Kobayashi *et al.* 2010). It is important to note that when the considering the Gouy-Chapman stern theory, the charge density of the solute, the concentration and charge of the ion are important determinants of the electrostatic interactions. While determining the responsiveness of the artificial membranes used on the electronic tongue the manufacturers make no reference to investigating molecules /ions which have the same charge at the same concentration with a view of explore the effect of these variables on responsiveness of sensors.

As previously mentioned, during the development of the electronic sensor, Toko suggests that these sensors possessed global selectivity, a term already defined in **section 1.3.1**. Essentially, an assumption is made that it is not necessary to detect the precise molecule in the formulation but however it is the overall taste quality of the formulation that is important, which in some respects describes taste synergy. Caution should be taken when accepting this assumption. The cellular mechanisms described in literature and summarised in **section 1.1.2** suggests that in human each molecule is detected but the overall taste quality depends on the processing in the brain centres. How this processing occurs in the brain remains unclear. Although taste synergy is important, it is equally important to understand the basic taste detection and quality of each molecule in the formulation before addressing the issue of taste synergy. This is because in order to establish synergistic or suppressive taste effects, it is important to establish the detection of each molecule before investigating their effect in combination.

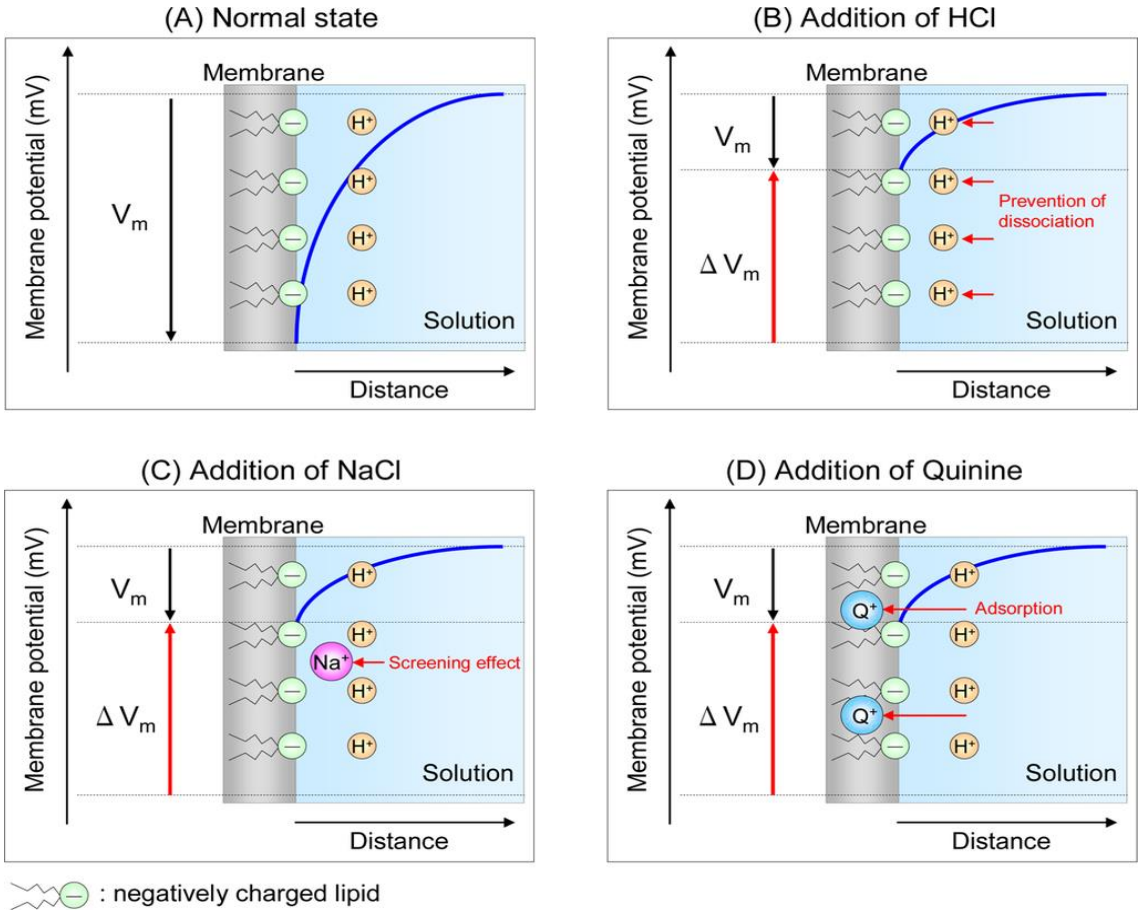


FIGURE 1. 8 PICTORIAL REPRESENTATION OF MECHANISM OF DETECTION OF HCL, NACL AND QUININE WITH THE CORRESPONDING CHANGES IN MEMBRANE POTENTIAL (KOBAYASHI ET AL. 2010).

The issue of molecule detection by the taste sensor has also been investigated in two studies (Woertz *et al.* 2011c, Guhmann *et al.* 2012). The former suggested that cationic and anionic molecules were easier to detect compared to neutral molecules, while the latter described successfully distinguishing diclofenac acid from its sodium and potassium salts, suggesting that differentiation observed was largely due to the presence of different cations. Woertz et al suggested that the underlying measurement principle is potentiometric and is best explained using Nernst Equation (Equation 1.1).

$$E = E^0 + \left(\frac{RT}{zF}\right) \ln a_i$$

EQUATION. 1.1

where, E = electrode potential, $E^o$ = standard electrode potential, R = universal gas constant, T = temperature ($^o$K), *z* = ionic valence of substance, F = Faraday constant, $a_i$ = activity of substance.

The potentiometric response (mV) of the chemical sensors depends logarithmically on the activity of the substance $a_i$ (Equation 1.2)

$$a_i = f c_i$$

EQUATION. 1.2

where, $f$ = activity coefficient of substance, $c_i$ = concentration of substance.

Application of these formulae suggests that, in the case of detection of diclofenac, the differences observed were largely due to the different cations. This observation raises the question that, are the sensors on the taste sensor detecting the leaving group cations i.e. $H^+$, $Na^+$, $K^+$ and not the parent diclofenac molecule. This therefore suggests that the resultant taste quality observed relates to the cation and not the parent diclofenac molecule which is the active ingredient.

Furthermore, questions still remain as to whether the detection process is a function of concentration or a function of intrinsic bitterness of the molecule in question. It is necessary to understand whether the bitterness described by the electronic tongue is attributed to the underlying bitterness of the API or its concentration in the formulation.

Also of interest to be investigated is the issue of how the physical characteristics of the molecule i.e. solubility in water, extent of ionisation in solution (pKa) and salt dissociation profile affect the detection of the molecule by the electronic tongue.

### 1.3.3 PHARMACEUTICAL APPLICATION

Reports in literature have established the utility of the electronic tongues in validating various taste masking strategies. A study evaluated the bitterness of clarithromycin which was coated with an aminoalkyl methacrylate polymer using the spray congealing technique (Uchida *et al.* 2003). An electronic tongue was used to confirm that the polymer was successful in almost completely masking the bitter taste of clarithromycin. Taste masking efficiency of quinine pellets produced via extrusion-spheronisation and coated with Eudragit® EPO was evaluated using the *Astree 2* electronic tongue (Kayumba *et al.* 2007). They demonstrated taste masking ability of this formulation. The evaluation of ibuprofen suspensions using the *Insent TS500Z* in a top down fashion with the aim of developing a taste masked generic formulation has been successfully demonstrated in a recent study (Woertz *et al.* 2010b). The *Astree 2* was used to illustrate the taste masking efficiency of hot melt extruded paracetamol granules containing Eudragit® EPO or Kollidon® VA64. The best taste masking effect was observed with VA64 at 30% paracetamol loading (Maniruzzaman *et al.* 2012). In another study, the *Astree 2* was used to evaluate taste masking efficiency of paracetamol powder formulations. The powders were produced via spray drying of aqueous paracetamol dispersions containing sodium caseinate and lecithin. The "coating" containing sodium caseinate and lecithin had a significant role in decreasing the release of drug in the first 2 minutes and therefore was able to mask the bitterness of paracetamol (Thia *et al.* 2012). Orodispersible films containing dimenhydrinate and cyclodextrin / maltodextrin prepared using the solvent casting method where investigated for taste masking efficacy using both the α-Astree and the TS-5000Z. In both cases, taste masking effect of the excipients was demonstrated (Preis *et al.* 2012). In another study, the α-Astree2 was used to evaluate the bitterness of eight antihistamines namely: cetirizine dihydrochloride, diphenhydramine hydrochloride,

chlorphenamine maleate, epinastine hydrochloride, ketotifen fumarate, olopatidine hydrochloride, fexofenadine hydrochloride and azelastine hydrochloride. The antihistamines were compared to quinine hydrochloride and water. The Euclidean distances between API and quinine / water were calculated. However, it was not possible to establish a bitterness scale as the main sensor response was acidity (Ito *et al.* 2013). With the exception of Uchida et al (2003) and Ito et al (2013), all the other studies highlighted here did not attempt to illustrate correlation between the taste masking efficiency shown on the electronic tongue with a human taste panel study. In addition, again with the exception of Ito et al (2013), all the studies did not use known comparators like quinine hydrochloride or water in proving taste masking efficacy of their new formulations. With this in mind this thesis will aim to describe the correlation of taste prediction / perception between a human taste panel and the Insent® electronic tongue.

## 1.4 TASTE MASKING

There are three general taste masking strategies, namely; the use of physical barriers, chemical or solubility modification and solid dispersions. Table 1.6 gives a list of the different techniques currently used for taste masking. Physical barrier methods are described in brief because they are the most common method. Solid dispersion strategies are discussed in further detail as one of these strategies is going to be used in this thesis.

TABLE 1. 6 SUMMARY OF CLASSIFICATION AND EXAMPLES OF TASTE MASKING STRATEGIES

| Taste Masking Strategies | | |
|---|---|---|
| **Physical Barriers** | **Chemical modification** | **Solid dispersion** |
| Fluidised bed coating | Chemical derivitisation | Melt granulation |
| Micro-encapsulation | Complexation | Spray congealing |
| Supercritical fluids | | Melt extrusion |

### 1.4.1 PHYSICAL BARRIERS

The simplest and most common method to taste mask a bitter API, especially chewable and liquid formulation is via physical barriers. A barrier coated onto the API could successfully provide a palatable oral dosage form, as sometimes such barriers prevent early dissolution of API in the oral cavity.

#### *FLUIDISED BED COATING*

This technology is commonly used to apply a continuous coat around the core particle. Generally coating can be achieved using polymeric solutions or molten material. The atomisation of polymeric systems dispersed as solutions/suspensions in volatile organic solvent(s) and/ or aqueous vehicles are used to apply the film coat. While the use of organic solvents is generally fast with simplified film formation processes due to the dissolved nature of the polymer, the use of aqueous systems remains the preferred option. Aqueous systems are advantageous because of the absence of solvent toxicity, increase process safety and lower production costs. Despite these benefits, cases still remain where aqueous systems are inappropriate namely: API sensitivity to water resulting in degradation and migration of water leading to compromised quality of product (Bose *et al.* 2007). Alternatively, a solvent free process i.e. the atomisation of molten materials commonly known as melt coating has been adopted. This process requires application of low melting point materials maintained at temperature of about 40 – 60$^{o}$C above the melting point of the wax or polymeric component. When fatty acids or glycerol ester or low melting polymers such as polyethylene glycols are applied; the melt coating is performed in fluid bed coater with the aid of heating systems for atomised air to provide a molten spray plume (Cerea *et al.* 2008). A study has reported the preparation of diclofenac sodium granules with Eudragit L30 D-55® by fluidised bed system. The subsequent dissolution studies confirmed the effectiveness of fluidised bed for applying enteric coated on diclofenac granules (Silva *et al.* 2006).

*MICROENCAPSULATION*

Microencapsulation is defined as a process by which small discrete solid materials, liquid droplets or gases are completely enveloped within an intact membrane. Taste masking is often achieved by applying an encapsulating barrier around an API. The barrier remains intact while the dosage form in administered. Following administration, the barrier allows API release either immediately or in a modified fashion. Ethyl cellulose microcapsules containing theophylline exhibited modified release performance. It was reported that the microcapsules demonstrated excellent taste masking properties (Golzi *et al.* 2004). This is because the API was released slowly. Therefore an insufficient amount was release into the mouth to trigger a taste response prior to swallowing. There are several methods to achieve microencapsulation. The most common include: temperature-induced phase separation, emulsion solvent evaporation, solvent evaporation, film coating, non-solvent addition and spray drying. A very comprehensive review is described by Rogers et al (2011). The authors describe microencapsulation in terms of background and materials used (Rogers *et al.* 2011a), techniques used to make microcapsules (Rogers *et al.* 2011b) and applications (Rogers *et al.* 2011c).

*SUPERCRITICAL FLUIDS*

This is a rather limited approach which involves the use of supercritical fluids (SCFs). It is a one step process. The supercritical state is defined as a state where both the pressure and temperature of a substance are greater than its critical pressure ($P_c$) and critical temperature ($T_c$). The thermal and physical properties of SCFs fall in between pure liquids and pure gases. In a critical isotherm (between $T_c$ and $1.2T_c$), the density, viscosity, diffusivity and other physical properties, such as solvent strength and dielectric constant, can be varied in a range from gas like to liquid like with small changes around the critical pressure ($0.9 – 2.0P_c$) (Subramaniam *et al.* 1997). Carbon dioxide is one of the most commonly used supercritical solvents because of its relatively low critical temperature and pressure ($T_c$ = 31.1$^o$C, $P_c$= 78.3bar)

(Bose *et al.* 2007). In this technique, essentially, the drug and polymer are dissolved in an organic solvent and then sprayed into a high pressure chamber filled with supercritical carbon dioxide ($scCO_2$). Rapid expansion supercritical solution (RESS) is the most common supercritical fluid process in pharmaceutical applications. The coating agent is solubilised in $scCO_2$ in a high pressure vessel. The API is dispersed in the SCF. The suspension is rapidly expanded by passing through a heated nozzle at supersonic speed. By so doing, the solvent power of carbon dioxide is reduced. This results in the coating material precipitating onto the particle of drug dispersed in the medium (Thies *et al.* 2003, Moribe *et al.* 2008). SCFs offer considerable promise for taste masking through the formation of micro-particles. However, this technique is not widely used because of its expensive running costs, limited polymer /drug solubility in carbon dioxide and insufficient drug loading in some cases.

### 1.4.2 SOLID DISPERSION

#### *MELT GRANULATION*

This process involves the dispersion of the API into a molten mixture of highly water soluble sugars e.g. mannitol and xylitol. The mixture is heated above the eutectic temperature and then rapidly cooled to form a glassy solid. In some cases, solvents such as methanol, ethanol and polyethylene glycol are used to facilitate lower melting temperatures. The solvents are removed via cooling and solidification. In cases where the API is heat sensitive, a low melting point polymer can be used.

#### *SPRAY CONGEALING*

This method is used to change the structure of a material with the aim of obtaining free flowing powders. Generally, the API is allowed to melt, disperse or dissolve in a hot melt of an inert polymer and other additives. This molten mixture is sprayed into an air chamber where the temperature is below the melting point of the formulation components, the product of which are spherical congealed pellets which usually range from 0.25 to 2.0mm in size (Yajima *et al.* 2003). Spray congealing presents noticeable

advantages including the absence of solvent evaporation which makes the pellets non-porous, strong and remain intact on agitation. It is also a single step continuous process. However, the high temperature exposure of the API presents a problem for APIs that are thermally labile. If amorphous / anhydrous forms of the API are generated this alters the dissolution behaviour and by extension the release profile. Furthermore, coated particles maybe perceived as gritty in the mouth due to the fact that water-insoluble polymers remain intact in the mouth after all the other excipients have disintegrated or dissolved.

*PRECIPITATION AND DRYING*

This is a method of preparing stable dispersions of poorly soluble APIs in the presence of one or more stabilisers free of any toxic solvents. Initially, the poorly water soluble API is dissolved in a suitable solvent. This solution is added to another solution containing at least one surface stabiliser to form a second solution. The formulation is precipitated by adding an appropriate non solvent usually a polymer. The API is entrapped within the polymer matrix by in-situ complexation which eliminates the bitter taste and provides a good mouth feel. Any salt formed is removed by dialysis or filtration and concentrations of the dispersion by conventional means. Although precipitation can be applied to several APIs, in some cases, it is necessary to use harmful solvents. In addition, increased polymer-drug ratios are necessary to mask the bitter taste, resulting in a slow release profile.

*MELT EXTRUSION*

Melt extrusion is a well-known, solvent free approach which is generally accepted as a method to enhance the dissolution characteristics of poorly water soluble drugs. In taste masking, melt extrusion is performed by mixing API with an extrudable material e.g. Eudragit®. The process and pharmaceutical application of melt extrusion are described in detail in section 1.5

## 1.5 HOT MELT EXTRUSION (HME)

Hot melt extrusion technique was first invented for the manufacturing of lead pipes at the end of the 18th century. Since then, it has been widely used in plastic, rubber and food manufacturing industries. The technology has proven to be a robust method of producing drug delivery systems, via the production of solid dispersions. Put simply, extrusion can be described as conveying raw materials with a rotating screw under controlled temperature and pressure through barrel. The output (extrudates) are of uniform shape and density (Breitenbach 2002).

An extruder is composed of a control panel, inlet feeding hopper, steel barrel with different heating zones, screws for extrusion, a die attached to the end to specifically shape the product, a cooling system and downstream processing machinery. Two types of pharmaceutical grade extruders are available, ram and screw. The latter is available as single and twin screw types. The single screw has a long history but may not provide sufficient mixing of different materials if the screw is not long enough (Crowley *et al.* 2007). Single screw extrudates showed streaks and shaded areas indicating incomplete mixing whereas materials processed using twin-screw extrusion was homogenous.

The vast majority of extruders manufactured for pharmaceuticals needs are twin-screw types. The screws can be oriented in a number of configurations depending on the desired level of shear and speed operation. Depending on required intensity of mixing, the two screws can be designed to rotate in the same direction (co-rotating) or in opposite (counter rotating). Co-rotating screws are primarily used in pharmaceutical formulation.

### 1.5.1 PROCESSING

Theoretically, HME can be divided into five steps, namely: feeding, melting and plasticising, conveying and mixing, flow through the die, stripping and downstream processing. These are illustrated in Figure 1.9.

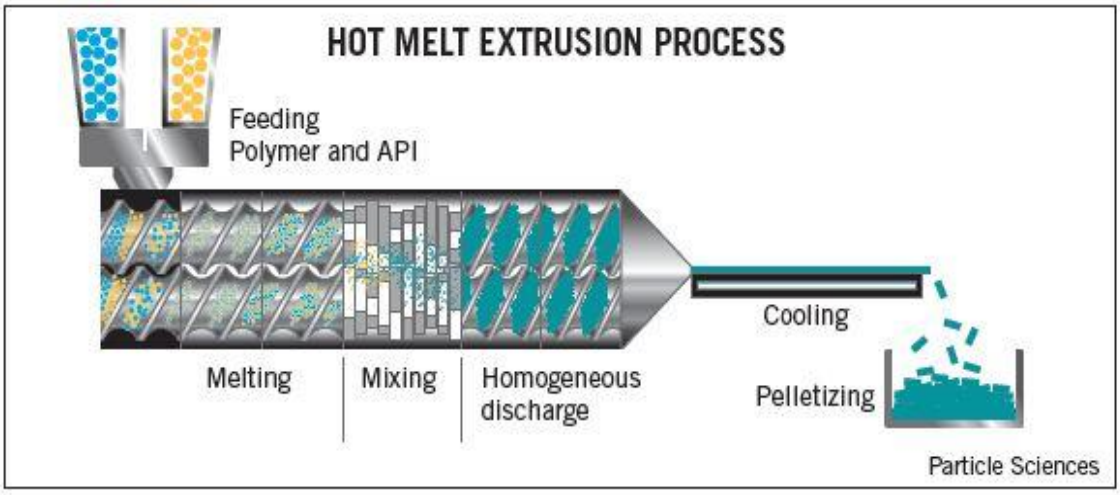


FIGURE 1. 9 HOT MELT EXTRUSION ILLUSTRATED. HTTP://WWW.PARTICLESCIENCES.COM/IMAGES/TB/HOT-MELT-EXTRUSION-PROCESS.JPG

Each of these steps affects the properties of the final extrudate. In brief, the material to be extruded is introduced into the feed section via a hopper. It is essential that the angle of the feed hopper always exceeds the angle of repose of the feed material in order to ensure good flow properties of the feedstock and avoid formation of solid bridges at the throat of the hopper which often results in erratic flow. The feed section has flights of greater pitch as illustrated in Figure 1.10. As the material is conveyed along the screw to the mixing zone, the flight depth decreases gradually. This increases the pressure on the material (through a squeezing effect) that, when combined with the external heating to the barrel and increased shear causes the material to melt. The final metering point zone has the smallest depth but is held constant to provide and even flow of material to the die (Wilson *et al.* 2012).

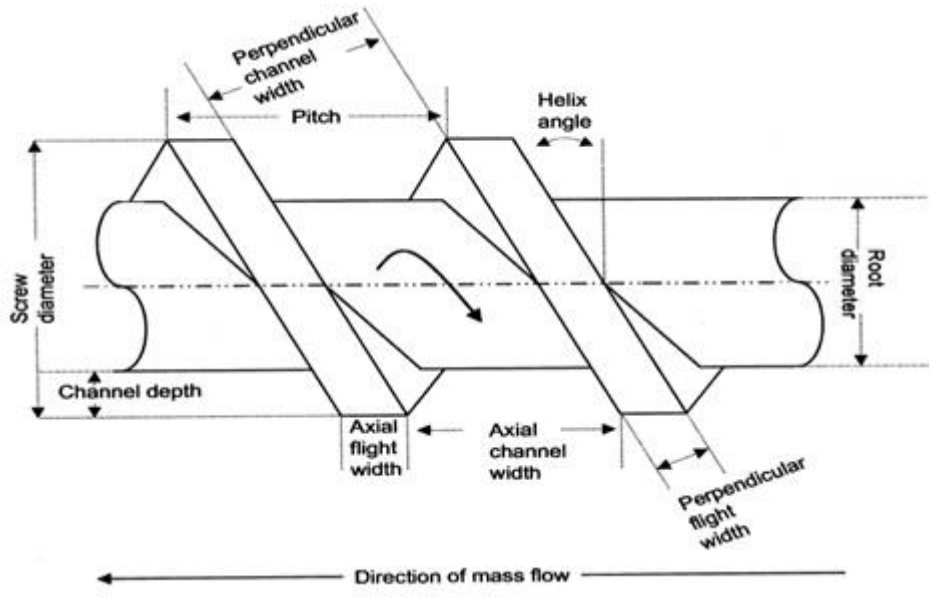


FIGURE 1. 10 SCREW DIMENSIONS SHOWING FLIGHT/ CHANNEL DEPTH, AXIAL CHANNEL WIDTH, PITCH, AXIAL FLIGHT WIDTH AND HELIX ANGLE (BREITENBACH 2002).

The processing parameters play a key role in determining the properties of the final extrudate. Some of the most commonly adjusted parameters include screw speed, processing temperature and feeding rate (Henrist *et al.* 1999). As HME is a non-ambient process, often high temperatures are required to facilitate extrusion and as such plasticising agents play a pivotal role in providing acceptable drug delivery systems. They can be used to lower the processing temperature required therefore preventing the thermal degradation of the API. In some cases, interactions between the drug and the polymer may be used to this effect. However, certain minimum temperatures are required in order to reduce the torque needed to rotate the screws. Typically, the temperature of the melting zone is set to 15 – 60$^{o}$C above the melting point of the semi-crystalline polymer or the glass transition of an amorphous polymer (Repka *et al.* 2008).

Torque is directly proportional to the viscosity of the molten feedstock (Repka *et al.* 2007). This relationship can be expressed using the Arrhenius equation (Equation 1.3)

$$\eta = K' \times e^{\frac{Ea}{RT}}$$

EQUATION 1.3

where, η = viscosity of polymer melt, $K'$ is a constant dependant on the structure and molecular mass of polymer. $Ea$ is the activation energy of the polymer for the flow process and is constant for the same type of polymer while $R$ is the gas constant and $T$ is the temperature ($^oK$).

The screw speed and feeding rate are also related to shear stress, shear rate and mean residence time, which will affect the dissolution rate and stability of the final products. Although heat conduction from the electrical bands on the barrel contributes to the melting process, heat is also generated by shearing of the polymer melt. "Viscous heat generation" is the process of transforming energy from shearing into thermal energy (Li *et al.* 2013). The rate of heat generation per unit volume due to viscous heat dissipation follows Equation 1.4

$$E = m \times \gamma^{n+1}$$

EQUATION 1.4

where, $m$ is a constant, $\gamma$ is the shear rate and $n$ is the power law constant.

The materials used in the production of hot melt extruded dosage forms are similar to those used in traditional dosage forms. However, as already eluded above, thermal stability of the individual components is a pre-requisite for the process. It is noteworthy that the short processing time afforded by using HME does not entirely limit thermo-labile compounds.in addition to the API. Other materials include carrier molecules, plasticisers, release modifying agents and/or other functional excipients. Carriers used in hot melt extrusion are broadly classified as either polymeric or non-polymeric. Needless to say, that the selection of the carrier compound is important in the formulation and design of hot melt extruded dosage forms. This is because the

properties of the carrier material often dictate the processing conditions necessary for the production of the dosage unit. These properties also often modulate the release of the active from the final dosage form. Some examples of carries used in the pharmaceutical industry include Eudragit®, Kollidon® and Soluplus®, these will be discussed further when considering the pharmaceutical application of HME in **section 1.5.3**.

Plasticisers are sometimes necessary in order to improve the processing conditions or to improve the physical and mechanical properties of the final product. They are typically low molecular weight compounds capable of softening polymers thus making them more flexible. Plasticisation of a polymer is generally attributed to the intermolecular secondary valence forces between the plasticiser and the polymer. Therefore plasticisers are able to decrease the glass transition temperature and the melt viscosity of a polymer by increasing the free volume between polymer chains (Aharoni 1998). Release modifying and other functional excipients have not been discussed in this thesis due to the fact that there were not used in the formulation design and therefore deemed not relevant to this discussion.

### 1.5.2 PHARMACEUTICAL APPLICATIONS

HME stands out in the pharmaceutical industry because it is associated with increased throughput, efficient mixing and material modification during processing. Furthermore, HME presents a highly versatile technology capable of producing a wide range of different drug-delivery products, including pellets, controlled release tablets, fast dissolving systems, transdermal/ trans- mucosal delivery systems and implants. Several comprehensive reviews covering this issue are available in the literature (Breitenbach 2002, Repka *et al.* 2008, Jones *et al.* 2010).

Although it is widely accepted that HME is useful in taste making, there are limited reports where this has been evaluated using the taste assessment techniques

described in **Section1.2**. Instead, reports in the literature have detailed the mechanisms and dissolution profiles of solid dispersions created via HME (Qi *et al.* 2008a, Qi *et al.* 2010b, Jijun *et al.* 2011). Other reports in the literature have focussed on the analytical techniques to characterise such solid dispersions (Qi *et al.* 2008b, Yang *et al.* 2013). In other reports, the mechanical properties of hot melt extrudates were investigated (Campbell *et al.* 2009). Reports in the literature detailing the taste masking efficacy of hot melt extrusion following taste assessment using the electronic tongue are both reported by Douromis' working group. In the first report, they produced hot melt extruded paracetamol formulations using Eudragit® EPO and Kollidon VA64 as carriers. The taste masking efficacy was evaluated using a panel of six untrained volunteers and the α-Astree electronic tongue. The best taste masking effect was observed for Kollidon VA64 at 30% paracetamol loading. The authors reported good correlation between in-vivo and in-vitro taste assessment methods (Maniruzzaman *et al.* 2012). In another study, the same group produced hot melt extrudates of cetirizine hydrochloride and verapamil hydrochloride with various grades of Eudragit L100 and Eudragit L100-55. Taste assessment was carried out in similar fashion to their previously reported work. This study concluded that HME was able to mask the bitter taste of drug by enhancing the drug polymer interactions (Maniruzzaman *et al.* 2014). The work detailed in this thesis seeks to add to this limited pool of evidence by describing the taste masking effects of hot-melt extrudates using the Insent® electronic tongue for which there are currently no reports in the literature.

## 1.6 DISSOLUTION TESTING OF TASTE MASKED SOLID DOSAGE FORMULATIONS

Historically dissolution testing has been used to assess taste masking efficiency because it allows the researcher to make a prediction of the taste masking capability of the formulation by estimating the likely release in the oral cavity. The British Pharmacopoeia (BP) has recommended dissolution tests for delayed release dosage forms, however, these are not appropriate for taste masked particles as they are

designed to mimic the stomach and the small intestine with the use of an acid stage followed by a buffer stage. This does not give consideration of the oral cavity because the oral cavity solvent composition (saliva), volume and residence time is considerably different.

Natural saliva is a complex aqueous solution containing 99% water and a diverse spectrum of inorganic ions, small organic molecules and proteins. The inorganic ions include bicarbonate and phosphate which contribute to the buffer capacity of the saliva. Electrolytes such as sodium, potassium, magnesium, zinc, calcium, chloride, fluoride, iodide, thiocyanate and nitrates are present. In addition, small molecules such as steroid hormones, amino acids, glucose, creatinine and urea have been identified. The proteins present include immunoglobulins, mucins (which contribute to the viscosity of saliva), enzymes including lingual lipase and amylase, growth factor, and antimicrobial factors such as lactoferrin and lysozyme (Gibson *et al.* 1994). It is clear that the complexity of natural saliva renders it challenging to prepare artificially in the exact composition of natural saliva. Saliva is generated in the oral cavity by three salivary glands namely: parotid, submandibular and sublingual, which together produces 90% of total saliva. Studies have shown that unstimulated saliva flow rate range between 0.05 – 2.87ml$min^{-1}$, with mean values between 0.37 and 0.56ml$min^{-1}$ (Rudney *et al.* 1995, Aframian *et al.* 2006). Other studies have reported that the volume of saliva present in the oral cavity ranged from 0.09 – 1.86ml, with a mean or median values in the range of 0.37 – 0.70ml and only approximately 30% of saliva is swallowed in each unforced swallow (Lagerlöf *et al.* 1984, Müller *et al.* 2010). In addition, the pH of saliva has been shown to range from 5.45 – 7.8 (Kalantzi *et al.* 2006, Shpitzer *et al.* 2007).

Ideally, dissolution testing of taste masked solid dosage form should mirror the oral cavity environment. Few studies have been reported in the literature relating to the modelling of the oral cavity. Lee at al evaluated coated nanohybrid particles of sildenafil at neutral pH in de-ionised water for 2 minutes as a model of the oral cavity

(Lee *et al.* 2012). However, this test was carried out using 900ml of media and a paddle dissolution apparatus. Such a large volume is not representative of the volumes found in the oral cavity. Smaller volumes were used in a study evaluating polymer coated diclofenac particles in 50ml of simulated salivary fluid which was comprised of potassium dihydrogen phosphate (12mM), sodium chloride (40mM), calcium chloride (1.5mM), sodium hydroxide (to pH 7.4) (Guhmann *et al.* 2012). Several examples of modelling the oral cavity are discussed in a review by Gittings et al (2014). What is clear from this review is that more research is needed into the development of an in-vitro dissolution model that mimics the oral cavity in terms of media composition, volume, agitation and residence time (Gittings *et al.* 2014).

This inappropriateness of traditional dissolution testing was initially highlighted by the International Pharmaceutical Federation (FIP) and American Association of Pharmaceutical Scientists (AAPS) who jointly issued guidance on dissolution testing of novel dosage forms (Siewert *et al.* 2003b). Although these guidelines cover formulations such as suspensions, orally disintegrating tablets, chewable tablets, transdermal patches and suppositories, it also highlights the need for more research for powders and granules and micro particulate formulations. To this end, the research presented in this thesis also demonstrates a proof of concept study for dissolution testing of taste masked powders produced via hot melt extrusion.

## 1.7 RESEARCH OBJECTIVES

The overall aim of the research detailed in this thesis was to further the understanding of the electronic tongue (Insent® TS-5000Z) and how it can be used for taste assessment during or after the formulation process. The work detailed in this thesis is composed of three main areas.

The first area concerns the analysis of sensor responses to different molecules in solution with the view to gain further understanding of the mechanism of detection.

Within this area, the first objective was to address the issue of detection of molecules with similar structure. To this end methylxanthines, namely caffeine, theobromine and theophylline were investigated. This work detailed in **Chapter 3, Section 3.2** highlighted the need for using sensor response curves in order to establish whether molecules were being detected. The second objective (based on results from Chapter 3, Section 3.2) was to investigate a series of molecules for which detection had been previously reported. The work described in **Chapter 3**, **Sections 3.3** and **3.4**, led to identification of factors that influenced the detection of the molecules, i.e. the interaction between detecting sensor and ions, extent of dissociation / ionisation of electrolyte, concentration and the effect of solvent. The relevance of these factors is discussed in detail in **Chapter 3, Section 3.5**.

The second area of this thesis has three objectives. The first objective which is described in **Chapter 4, Section 4.3.1** was to investigate the utility of the electronic tongue in predicting which salt of amlodipine had the best taste profile. For the second objective, three extemporaneous formulations of amlodipine were investigated in order to compare their taste masking efficiency if any, with a view to provide objective data that could potentially influence decision making for clinicians when it comes to which extemporaneous formulation to use. The final objective in this area was to investigate the correlation in taste prediction of the electronic tongue to the perception of a human taste panel. This would further validate the use of electronic tongues for development of pharmaceutical formulations.

The third area addressed in this thesis was to evaluate the taste masking efficacy of formulation prepared using hot melt extrusion. Within this area (detailed in **Chapter 5**, **Section 5.3**), the first objective was to produce a hot melt extruded formulation using Eudragit® EPO as a polymeric carrier and quinine hydrochloride dihydrate as the model drug. The second objective was to characterise this formulation by performing a series of thermal, spectroscopic and X-ray diffraction techniques. The third objective in

this area was to evaluate the taste masking efficacy of this formulation. Two methods were employed in this objective: i) electronic tongue ii) modified dissolution apparatus with spectrophotochemical analysis, with a view to demonstrating a proof of concept for a dissolution apparatus to mimic the oral cavity.

# CHAPTER TWO
# MATERIALS AND METHODS

# CHAPTER 2 – MATERIALS AND METHODS

## 2.1 MATERIALS

All materials used were of analytical grade. Caffeine, theobromine, theophylline, quinine, quinine (Qn) hydrochloride dihydrate (QHD), quinine hemisulphate monohydrate (QhS), maleic acid and benzenesulfonic acid were obtained from Sigma-Aldrich UK and used as received. L-(+)-tartaric acid, absolute ethanol (≥99.8%) and tannic acid were also obtained from Sigma-Aldrich UK. Potassium chloride (KCl) was obtained from Lancaster UK. Monosodium glutamate (MSG) and iso-α-acid was supplied by Insent® Japan. Eudragit® EPO was kindly donated by Evonik Industries AG, Darmstadt Germany. Amlodipine maleate, amlodipine mesilate and amlodipine besylate tablets were purchased from AAH Pharmaceuticals UK. The electronic tongue sensors were purchased from Insent ® Japan as used as received.

### 2.1.1 EUDRAGIT® EPO

Eugradit ® EPO is a cationic polymer with the chemical name poly (butyl methacrylate-co- (2-dimethylaminoethyl) methacrylate-co-methacrylate (1:2:1). The monomer structure is given in Figure 2.1. It has an approximate molecular weight of 47,000g/mole and a glass transition temperature ($T_g$) of 45$^oC$ ±5$^oC$. It is naturally amorphous. It is presented as a white powder with a characteristic amine like odour. Eudragit® EPO is soluble in gastric fluid up to pH 5 and swellable and permeable at pH values above 5. It is routinely used in film coating, due to the dimethyl aminoethyl group forming a swellable and permeable coat at pH 5 or higher but also rapidly dissolving by forming salts at acidic pH values lower than pH 5. Even very thin film coats of approximately 10µm are effective. It is ideal for taste masking because it is insoluble in saliva which has a pH values ranging between 6 and 7. However, due to its swellable and permeable nature, it is possible for drug release to occur in the oromucusal cavity.

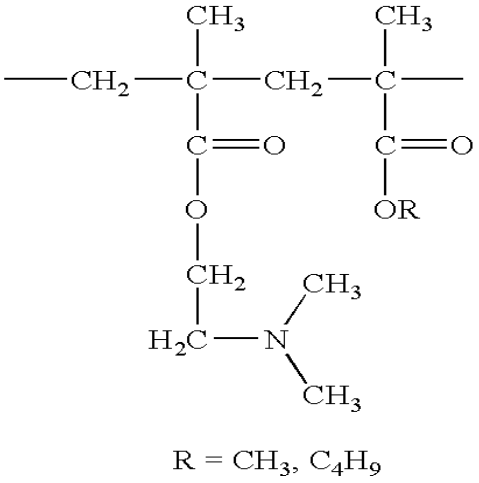


FIGURE 2. 1 CHEMICAL STRUCTURE OF EUDRAGIT®EPO

Besides coating, granulation and melt processes have been applied to taste masking using Eudragit® EPO. In these techniques, complexes are reversibly formed when an anionic API interacts with large cationic Eudragit ® EPO at a molecular level. This API-polymer composite prevents the API directly interacting with taste receptor cells in the oral cavity, thus achieving taste masking (Douroumis 2007). Recently, Eudragit® EPO was used in amorphous solid dispersions to increase the dissolution of poorly water soluble drugs (Feng *et al.* 2012, Sathigari *et al.* 2012). Additionally, the phase behaviour of Eudragit® EPO in amorphous solid dispersion has been studied (Qi *et al.* 2008b, Qi *et al.* 2010a). In these studies, it is reported that the drug-polymer solid solubility is drug dependent and as such different drugs formulated with the same polymer can present significantly different physical stability. The efficacy of Eudragit® EPO in taste masking has been studied using ondansetron (Khan *et al.* 2007), donepezil (Yan *et al.* 2010) and paracetamol (Maniruzzaman *et al.* 2012). All three studies reported successfully taste masking of API using Eudragit® EPO. This polymer was chosen for this project due to the fact that there is some interest on physical stability of the API in a solid dispersion of this polymer, and more importantly interest in its taste masking ability.

## 2.1.2 MODEL DRUGS

### 2.1.2.1 CAFFEINE

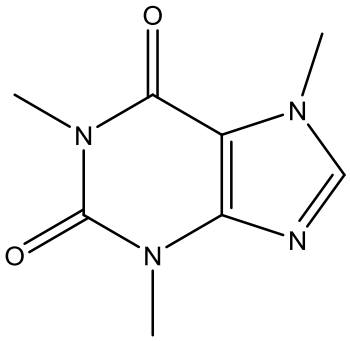


FIGURE 2. 2 STRUCTURE OF CAFFEINE

Caffeine is a naturally occurring xanthine derivative that is similar in structure to theobromine and the bronchodilator theophylline. It is found in coffee, black tea and milk chocolate at concentrations of 350µg/ml, 217µg/ml and 5µg/ml respectively. Its chemical name and formula are 1, 3, 7-trimethyl-2, 3, 6, 7-tetrahydro-1H-purine-2, 6-dione and $C_8H_{10}N_4O$ respectively. It is used a central nervous system (CNS) stimulant, mild diuretic and respiratory stimulant (in neonates with premature apnea). It antagonises the A1 and A2 subtypes of the adenosine receptor which results in stimulation of the respiratory centre, this increases minute ventilation, and decreases response to hypercapnia. It also increases muscle tone, metabolic rate and oxygen consumption while decreasing diaphragmatic fatigue and threshold to hypercapnia. Often, it is combined with analgesics in various all-in-one formulations for treating colds and flu symptoms particularly headaches. A study with ergotamine alkaloids indicate that the enhancement effect by the addition of caffeine may also be due to improved gastrointestinal absorption of ergotamine when administered with caffeine (Schmidt *et al.* 1974). Depending on the formulation, caffeine or caffeine citrate can be used. Citrated caffeine is generally used for orodispersible tablets or solutions due to it being more soluble than caffeine. Their respective solubilities at 20$^{o}$C are 18.7g/L and 95g/L. Caffeine citrate solution is currently available unlicensed in UK and US for the treatment of neonatal apnoea.

It is well understood that caffeine is bitter and as such it has been used as a model drug in research to elucidate the physiology of bitter taste transduction (Koyama *et al.* 1972b, Kurihara 1972). Caffeine has also been the subject of a significant amount of research on taste masking strategies (Warmke *et al.* 1993, Schiffman *et al.* 1994, Schiffman *et al.* 1995, Zheng *et al.* 2006, Woertz *et al.* 2011a).

### 2.1.2.2 THEOBROMINE

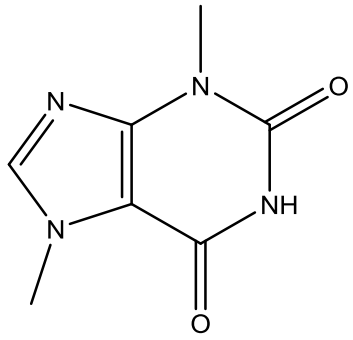


FIGURE 2. 3 STRUCTURE OF THEOBROMINE

Contrary to its name, theobromine contains no bromine; its name is derived from the theobora, the name of the genus of the cocoa tree. Its chemical name and formula are 3, 7 – dimethyl-1H-purine-2, 6-dione and $C_7N_8N_4O_2$ respectively. Theobromine is generally recognised as safe (GRAS) by the Food and Drug Administration (FDA). Human metabolism of caffeine produces theobromine as a metabolite. It is present in coffee, black tea and milk chocolate at concentrations of 17µg/ml, 12µg/ml and 21µg/ml respectively. Historically, the bitter taste of cocoa beans was attributed to the presence of theobromine (1.5%) and caffeine (0.15%) (Pickenhagen *et al.* 1975, Stark *et al.* 2005). However, Stark et al (2005) revealed that besides theobromine and caffeine, the flavan -3-ols epicatchin, catechin, polycynadin B-2, procyanidin B-5, procyanidine C-1, epicatechin – $(4\beta\rightarrow8)_3$ and epicatechin – $(4\beta\rightarrow8)_4$ were among the key compounds contributing to the bitter taste as well as the astringent mouthfeel upon consumption of roasted cocoa.

Theobromine was shown to be effective as a diuretic as well as in the treatment of angina pectoris. However, patients experienced severe nausea and heartburn when large doses were given in an attempt to achieve sufficient diuresis (Riseman *et al.* 1941). Therefore, there are currently no licensed medicinal products in the UK, US or European markets. Theobromine is found in a wide range of food products including beverages, yoghurt drinks, powdered fruit flavoured tea, coffee and chocolate.

Theobromine stimulates medullary, vagal, vasomotor and respiratory centres, promoting bradycardia, vasoconstriction and increased respiratory rate. This action was previously believed to be due to increase intracellular cyclic 3'5'-adenosine monophosphate (cAMP) following the inhibition of phosphodiesterase. It is now thought that xanthines such as theobromine and caffeine act as an antagonist at the adenosine receptors within the plasma membranes of cells. Since adenosine acts as an autocoid, inhibiting the release of neurotransmitters from the presynaptic sites but augmenting the actions of norepinephrine or angiotensin, antagonism of adenosine receptors promotes neurotransmitter release (Knox *et al.* 2011).

### 2.1.2.3 THEOPHYLLINE

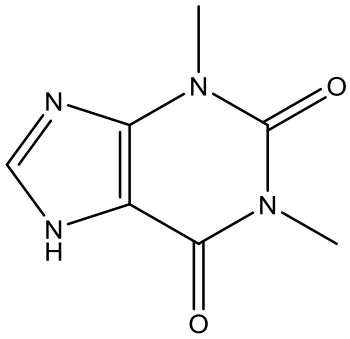


FIGURE 2. 4 STRUCTURE OF THEOPHYLLINE

Theophylline has the chemical name 1, 3-dimethyl-2, 3, 6, 7-tetrahydro, 1H-purine-2, 6-dione and molecular formula $C_7H_8N_4O_2$; it is found in trace amounts ($<10^{-7}$ µg/ml) in tea, coffee or milk chocolate (Bispo *et al.* 2002). Like the other two methylxanthines

already discussed, theophylline is also known to be bitter. It has been used in the literature as a model drug for comparing taste masked formulations (Burleson *et al.* 1978), and novel taste masking strategies (Pearnchob *et al.* 2003).

The mechanism of action of theophylline remains unclear. Traditionally, it was classified as a bronchodilator; however the ability of theophylline to control chronic asthma is disproportionately greater than its relatively small degree of bronchodilator activity. In fact, it is believed that theophylline has immune-modulatory, anti-inflammatory and bronco-protective effects that potentially contribute to its efficacy as a prophylactic anti-asthmatic drug. Several mechanisms of action have been suggested including:

- Inhibition of phosphodiestarase enzyme leading to raised cAMP levels
- Antagonism of adenosine receptors
- Inhibition of intracellular release of calcium
- Stimulation of catecholamine
- Anti-inflammatory action possibly involving the inhibition of submucosal action.

Although these mechanisms have been proposed to explain action of theophylline, inhibition of phosphodiesterase isoenzymes and non selective antagonism of specific cell-surface receptors for adenosine are the only ones known to occur at clinically relevant drug concentrations. Theophylline increases intracellular concentration of cyclic nucleotides in airways smooth muscle and inflammatory cells by inhibiting phosphodiesterase mediated hydrolysis of these nucleotides. Non-specific antagonism of adenosine receptors appears to be the mechanism of action by which theophylline increases ventilation during hypoxia, decrease fatigue in diaphragmatic muscles and decreases adenosine stimulated mediator release from mast cells (Weinberger *et al.* 1996).

2.1.2.4 QUININE

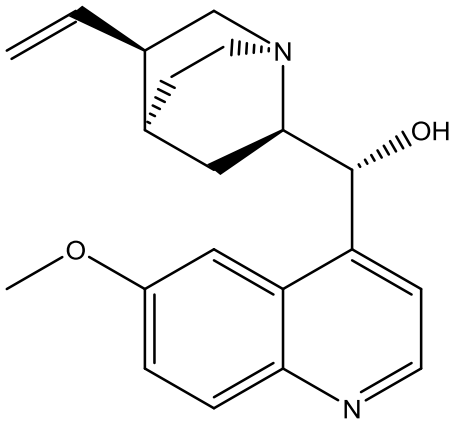


FIGURE 2. 5 STRUCTURE OF QUININE

Quinine (Qn) has the chemical name (R) -6- methoxyquinolin -4-yl) ((2S, 4S, 8R) -8-vinylquinuclidine –2-yl) methanol and molecular formula ($C_{20}H_{24}N_2O_4$). It is an alkaloid derived from the cinchona bark. It is used mainly as an anti-malarial agent. The precise mechanism of action of quinine remains unclear but current literature suggests that it may interfere with lysosome function or nucleic acid synthesis in the malaria parasites (Golenser *et al.* 2006). It is a rapidly acting blood schizontocide with activity against *Plasmodium faciparam*, *P vivax*, *P ovale* and *P malariae*. It has activity against gametocytes of *P malariae* and *P vivax*, but not mature gametocytes of *P falciparam*. Quinine is also used to treat nocturnal cramps as it has effects on the motor end-plate of skeletal muscle and therefore prolong the refractory period (El-Tawil *et al.* 2010). Quinine is also used as sodium channel blocker and as such as local anaesthetic and both anti and pro-arrhythmic activity. In this study, quinine (base), and its hydrochloride and sulphate salts are investigated. Table 2.1 gives a summary of the physical characteristics of the quinine and its salts. Quinine hydrochloride dihydrate is used in intravenous injections for the treatment of malaria, while its less soluble counterpart quinine sulphate is used in the treatment of nocturnal muscle cramps in film coated tablets. Quinine has two pKa values i.e. 4.1 and 8.5; it is neutral at pH 10, monoprotonated at pH 6 and diprotonated at pH 2.

The bitter taste of quinine is well recognised in the literature and evidenced by the fact that the elucidation of bitter taste transduction pathways used quinine as the standard of bitterness (Koyama *et al.* 1972a, Price 1973). Subsequently, there is significant interest in the literature on taste masking of quinine. Reid at al (1956) used cocoa syrups to mask the bitter taste of quinine. A series of studies formulated taste masked quinine sulphate in pellets and tablets for the treatment of malaria in Rwanda (Kayumba *et al.* 2007, Kayumba *et al.* 2008, Kayitare *et al.* 2010). Another study used sucrose, aspartame and sodium chloride as taste masking agents for quinine hydrochloride (Nakamura *et al.* 2002). Finally, quinine has been used as a bitterness standard when comparing taste assessment strategies (Woertz *et al.* 2011a).

TABLE 2. 1 BASIC PHYSICAL CHARACTERISTICS OF QUININE AND QUININE SALTS

| Drug | Structure | Appearance | Molecular weight (g/mol) | Melting point ($^oC$) | Solubility in water @ 25$^oC$ | Taste masking |
|---|---|---|---|---|---|---|
| **Quinine (Qn)** | 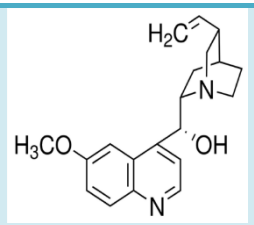 | White to off white crystalline powder | 324.42 | 173-175 | Slightly soluble | No data available |
| **Quinine hydrochloride dihydrate (QHD)** | 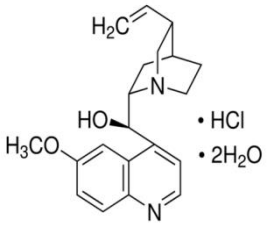 | White to off white crystalline powder | 396.91 | 115-116 | Soluble | (Reid *et al.* 1956, Schiffman *et al.* 1994) |
| **Quinine hemisulphate dihydrate (QhS)** | 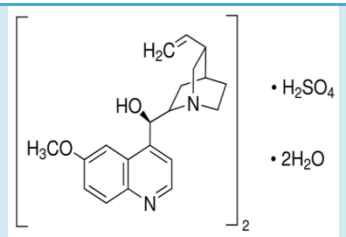 | White to off white crystalline powder | 391.47 | 225 | Slightly soluble | (Kayumba *et al.* 2007, Kayumba *et al.* 2008) |

### 2.1.2.5 PARACETAMOL

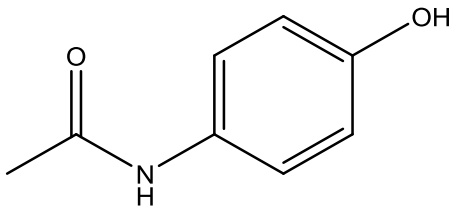


FIGURE 2. 6 STRUCTURE OF PARACETAMOL

Paracetamol (acetaminophen) has the chemical name N-(4-hydroxyphenyl) acetamide and molecular formula $C_8H_9NO_2$, is one of the most popular and widely used drugs in the treatment of pain and fever. In the UK there are over 200 licensed paracetamol containing preparations. Although paracetamol has been used clinically for more than a century, its mode of action has remained unclear until recently. Data have been published in the literature demonstrating that the analgesic effect of paracetamol is due to the indirect activation of cannabinoid $CB_1$ receptors. In the brain and spinal column, paracetamol, following deacetylation to its primary amine (p-aminophenol) is conjugated with arachidonic acid to form N-arachidonoylphenolamine, a compound already known (AM404) as an endogenous cannabinoid. This suggests that paracetamol acts as a pro-drug with active metabolite AM404 formed in the brain by action of the fatty acid amide hydrolase (Bertolini *et al.* 2006).

The bitter taste of paracetamol is well recognised in the literature. Most of the paracetamol oral suspension products currently licensed in the UK market contain varying concentrations of sweetening agents such as maltitol liquid, sorbitol liquid and sodium saccharin. Strawberry, orange or cherry flavour is also used in these formulations. Furthermore, the orodispersible preparations also contain some of the sweetening agents listed above. Paracetamol has also been the subject of investigation for taste masking strategies (Miyazaki *et al.* 2005, Zheng *et al.* 2006, Maniruzzaman *et al.* 2012, Thia *et al.* 2012).

### 2.1.2.6 IBUPROFEN

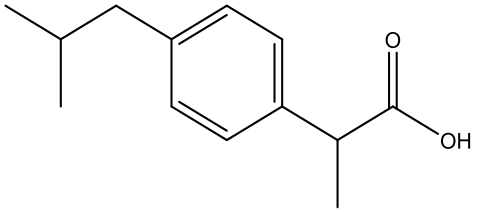


FIGURE 2. 7 STRUCTURE OF IBUPROFEN

Ibuprofen has the chemical name 2-[4-(2-methylpropyl)phenyl] propanoic acid and molecular formula $C_{13}H_{18}O_2$ is a commonly used non-steroidal anti-inflammatory drug (NSAID) with analgesic and antipyretic effects. The exact mechanism of action is not fully understood, however, it is believed to be a non-selective inhibitor of the cyclo-oxygenase (COX) enzyme, which is involved in prostaglandin synthesis via the arachidonic acid pathway. The pharmacological effects are believed to be due to the inhibition of COX-2 which decreases the synthesis of prostaglandins involved in the mediation of inflammation, pain, fever and swelling. Antipyretic effects are thought to be due to the action on the hypothalamus, resulting in an increased peripheral blood flow, vasodilation and subsequent heat dissipation.

The taste of ibuprofen is described in the literature as “peppery” and as such all the liquid formulations available commercially are taste masked. For example, a popular brand of ibuprofen suspension, Nurofen® is taste masked with maltitol syrup, glycerol and orange flavour.

### 2.1.2.7 METFORMIN HYDROCHLORIDE

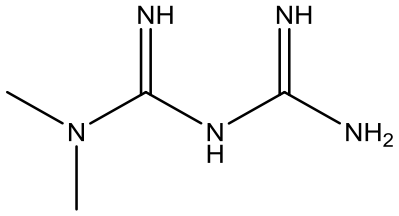


FIGURE 2. 8 STRUCTURE OF METFORMIN HYDROCHLORIDE

Metformin has the chemical name 1-carbamimidamido-N,N-dimethanimidamide and molecular formula $C_4H_{11}N_5$ is a biguanide anti-hyperglycaemic agent used for treating type 2 diabetes formally called non-insulin dependent diabetes mellitus. It is recommended as first line therapy by the National Institute for Health and Care Excellence (NICE) in patients who are overweight and for whom dietary management and exercise alone has not achieved adequate glycaemic control (NICE 2009). Metformin lowers both basal and postpradial plasma glucose. It does not stimulate insulin secretion and as such does not induce hypoglycaemia. The following mechanisms have been proposed for the mode of action of metformin:

- Reduction of hepatic glucose production by inhibiting gluconeogenesis and glycogenolysis
- In muscle tissue, increasing insulin sensitivity, improving peripheral glucose uptake and utilisation
- Delaying intestinal glucose absorption
- Stimulating intracellular glycogen synthesis by acting on glycogen synthase
- Increasing the transport capacity of all types of membrane glucose (GLUTs) known to date.

The bitterness of metformin is not clear in the literature. The manufactures of metformin hydrochloride report a taste disturbance as a common side effect i.e. $1/100 \geq n \leq 1/10$ (where n = proportion of patients taking drug). This takes the form of a metallic taste which is believed to decrease over time, taking anything from one to twelve weeks of taking metformin. The current thinking suggests that the metallic taste is caused by the accumulation of metformin in saliva. The mechanism by which this happens is still unclear. Metformin tablets on the market in the UK are film coated with hypromellose and macrogol. The film coat was applied to aid taste masking and making the tablet easier to swallow (Hetal 2014). Both metformin suspensions currently available commercially are taste masked using liquid maltitol, caramel, peppermint and peach flavours.

### 2.1.2.8 AMLODIPINE

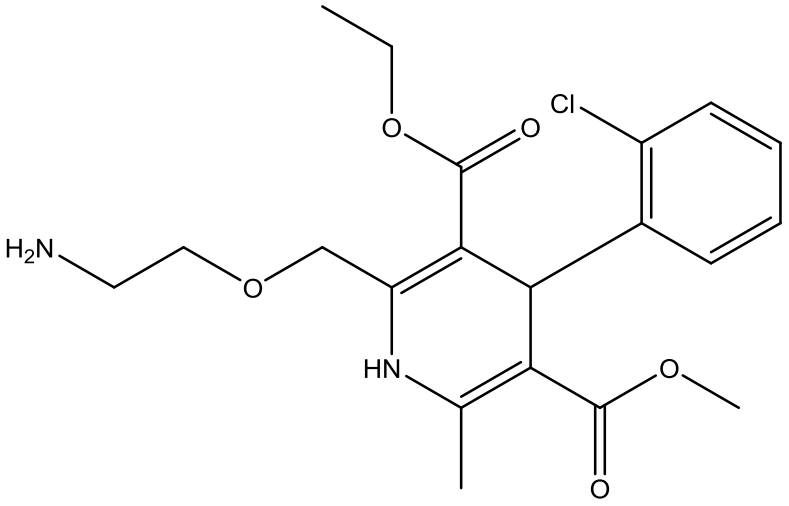


FIGURE 2. 9 STRUCTURE OF AMLODIPINE

Amlodipine has the chemical name, (R, S)-3-ethyl 5-methyl 2-[(2- amoniethoxy) methyl] -4-(2-chlorophenyl)-6-methyl-1, 4-dihydropyridine, 3-5-dicarboxylate. It is commonly used for the treatment of hypertension, chronic stable angina pectoris and vasospastic angina. It is a long acting dihydropyridine calcium channel blocker that exerts effect by blocking the trans-membrane influx of calcium ($Ca^{2+}$) into cardiac and vascular smooth muscle tissues. It also reduces vascular resistance and lowers BP by causing a direct vasodilation in peripheral arteries of vascular smooth muscle. Amlodpine is used to treat high blood pressure in both paediatric and adult populations. Its therapeutic action on angina is thought to be through the decrease in peripheral resistance and inhibition of coronary spasms (vasospastic angina).

The taste of amlodipine is assessed in a study which compared children's taste perception of pulverised amlodipine to lercanidipine. Both tablets were crushed and presented to the participants with no attempt to taste mask the powders. This study demonstrated that children aged 4-7 years and 8-11 years both preferred crushed lercanidipine tablets over amlodipine (Milani *et al.* 2010). The generic manufacturers of amlodipine tablets including Aurobindo®, UK, Discovery Pharmaceuticals®, UK and Actavis®, UK did not have any information regarding the taste of amlodipine.

## 2.2 METHODS

### 2.2.1 INSENT TS5000Z ELECTRONIC TONGUE MEASUREMENT PROCEDURE

A schematic of the measurement procedure is illustrated in Figure 2.10. To start, the sensors are washed in the reference solution twice, each wash lasting 120s. The reference solution is composed of 30mM KCl + 0.3mM tartaric acid has no taste and is designed to mimic human saliva. Between four and ten pairs of reference solution are available and a different pair is used for each rinse. The two rinsing steps are followed by the stabilising step in which the sensor is dipped into a separate reference solution and voltage reading is recorded. Essentially the voltage difference is expected to remain constant when the sensor is placed in the reference solution (*Vr*). If sensor recordings are not constant the stabilising process is repeated up to twenty times, until a constant is reached. A sensor is deemed to be stable if the value of the membrane potential becomes less or equal to the previous value recorded. If after twenty readings (*Vr*), and the recordings are not constant, then the sensors is deemed unstable and therefore cannot be used. Once stabilisation is complete, the sensors move on to the first sample (position designated A), were the sensors are immersed in the sample for 30 seconds and the voltage difference is recorded (*Vs*). Therefore *Vs – Vr* gives the voltage reading for the initial taste. The sensors are then briefly washed twice in two different reference solutions. Each wash lasts only three seconds. The sensors are then immersed in another reference solution where another voltage reading is recorded (*Vr'*). *Vr' – Vr* then denotes the after taste or change in membrane potential after adsorption (CPA). Finally the sensors are rinsed in positive or negatively charged washing solution for 90 seconds.

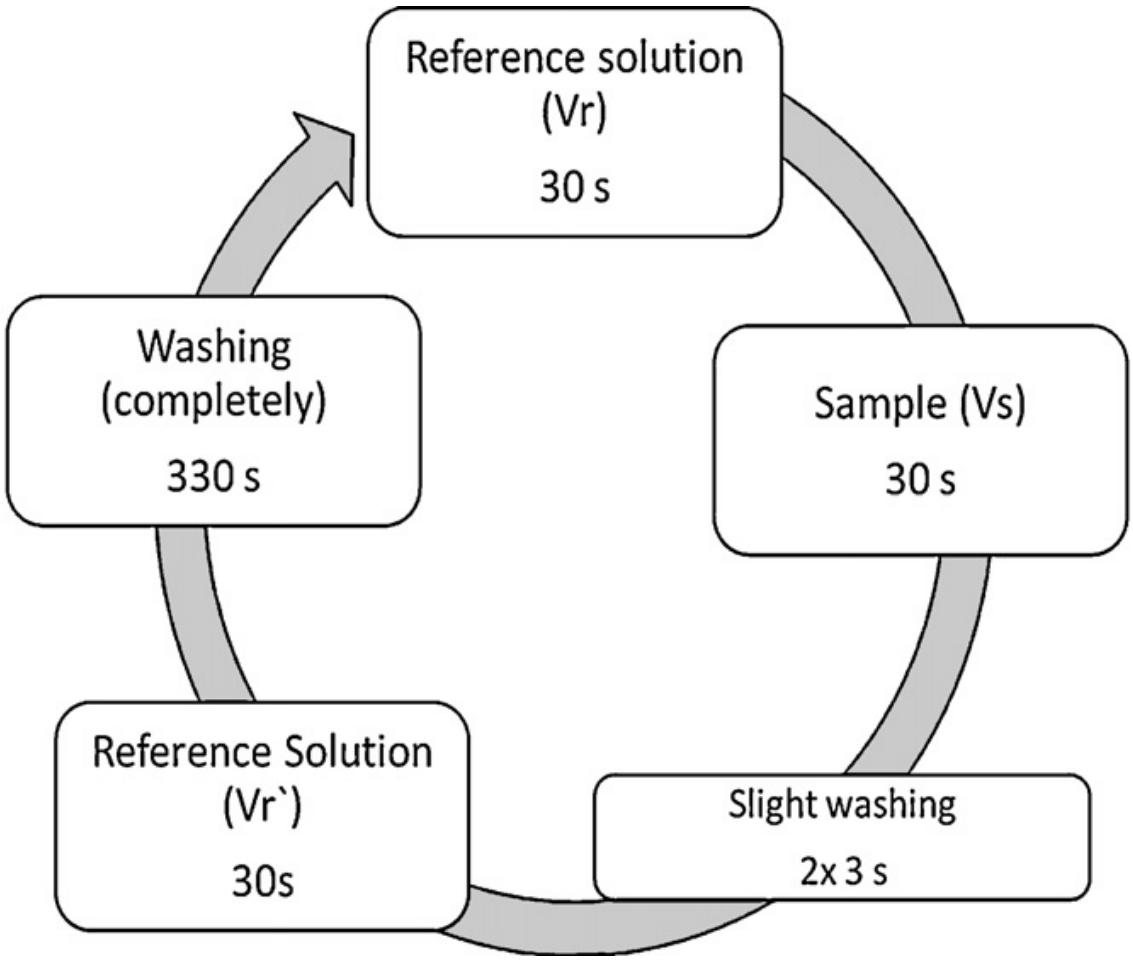


FIGURE 2. 10 SCHEMATIC OF ONE CYCLE OF THE MEASUREMENT PROCEDURE ON THE ELECTRONIC TONGUE TS5000Z (WOERTZ *ET AL.* 2011A)

#### 2.2.1.1 SENSOR CHECK

Prior to commencement of each measurement cycle a sensor check was carried out. This is not strictly recommended by the manufacturer but however it was performed nonetheless before every measurement. During the sensor check, the sensors are washed thoroughly in the positive and negative washing solutions for 2 x 120s. This was followed by a 90s wash in the reference solution. There are four to eight pairs of reference solutions which can be used. Following the 90s wash, the sensors are immersed in a different reference solution. The voltage readings for each sensor are displayed as shown is Table 2.2. This is repeated up to twenty times until the sensor reads the required voltage reading on three consecutive occasions. If after twenty attempts, the desired voltage reading is not recorded the sensor is deemed to be defective. It is possible for sensors to pass the sensor check and fail the maintenance measurement (discussed in section 2.4.3) therefore routine maintenance measurement

is required. At this junction it is worth noting that the sensor types and the reasoning behind choice of sensor types will be discussed in each chapter. The sensors currently available from the manufactures have already been described in detail in **chapter 1, section 1.3.2.**

TABLE 2. 2 VOLTAGE READINGS FROM EACH SENSOR DURING SENSOR CHECK

| Sensor | Voltage reading (mV) |
|---|---|
| **AN0** | -63 ± 2.0 |
| **AC0** | -65 ±2.0 |
| **C00** | 47± 2.0 |
| **AE1** | 119± 2.0 |

#### 2.2.1.2 MAINTENANCE MEASUREMENT

The maintenance measurement was carried out once a month as recommended by the manufacturers and at all times when sensors were changed. In this measurement the sensors are exposed to standard solutions whose composition is given in Table 2.3. Put simply, each sensor is expected to only respond to the taste attribute for which it is designed. For example, the astringency sensor (AE1) is expected to respond only to the astringency sample during maintenance. If any of the sensors respond to a standard solution for which they are not designed to, they are deemed as defective and need replacing.

#### 2.2.1.3 PREPARATION OF STANDARD SOLUTIONS

All standard solutions were adapted from Insent TS5000Z (2008) manual and the composition of each is given in Table 2.3. The method of preparation of each of the solution is described in **Appendix A1**

TABLE 2. 3 COMPOSITION OF STANDARD SOLUTIONS USED IN MAINTENANCE MEASUREMENT.

| Sample | Composition |
|---|---|
| **Reference** | 30mM KCl + 0.3mM tartaric acid |
| **Salty** | 300mM KCl + 0.3mM tartaric acid |
| **Sour** | 30mM KCl + 3.0 mM tartaric acid |
| **Bitter (+)** | 30mM KCl + 0.3mM tartaric acid + 0.1mM quinine hydrochloride |
| **Bitter (-)** | 30mM KCl + 0.3mM tartaric acid + 0.01% vol iso-α-acid |
| **Astringency** | 30mM KCl + 0.3mM tartaric acid + 0.05mM tannic acid |

#### 2.2.1.4 PREPARATION OF SAMPLE SOLUTIONS

Details of sample preparation are given in the chapters where the samples are investigated.

#### 2.2.1.5 DATA ANALYSIS – PRINCIPLE COMPONENT ANALYSIS (PCA)

Principle components analysis finds the principle components in a given data set. In other words, this statistical method aims to find linear combinations of original variable which account for maximal amounts of variation in the data set. The principle components are the underlying structure of the data set. They encompass both the direction of the greatest variance and extent to which the data is spread out. This underlying structure is defined by eigenvectors and eigenvalues. Eigenvectors which exist in pairs describe the direction of variation while the eigenvalues describe how the data is spread out. Therefore, the eigenvector with the highest eigenvalue is the first principle component (PC1). It follows that the second principle component (PC2) is the eigenvector with the second highest eigenvalue which is calculated disregarding data that has already been included in calculating PC1. By convention, data is plotted as a two dimensional (2D) scatter plot. PC1 is plotted on the x-axis while PC2 is plotted on the y-axis. PCAs main strength lies in its ability to reduce dimensions i.e. it reduces data down into its basic components, while stripping away any unnecessary

information. Figure 2.11 illustrates the use of PCA in evaluating the taste of a cola soft drink.

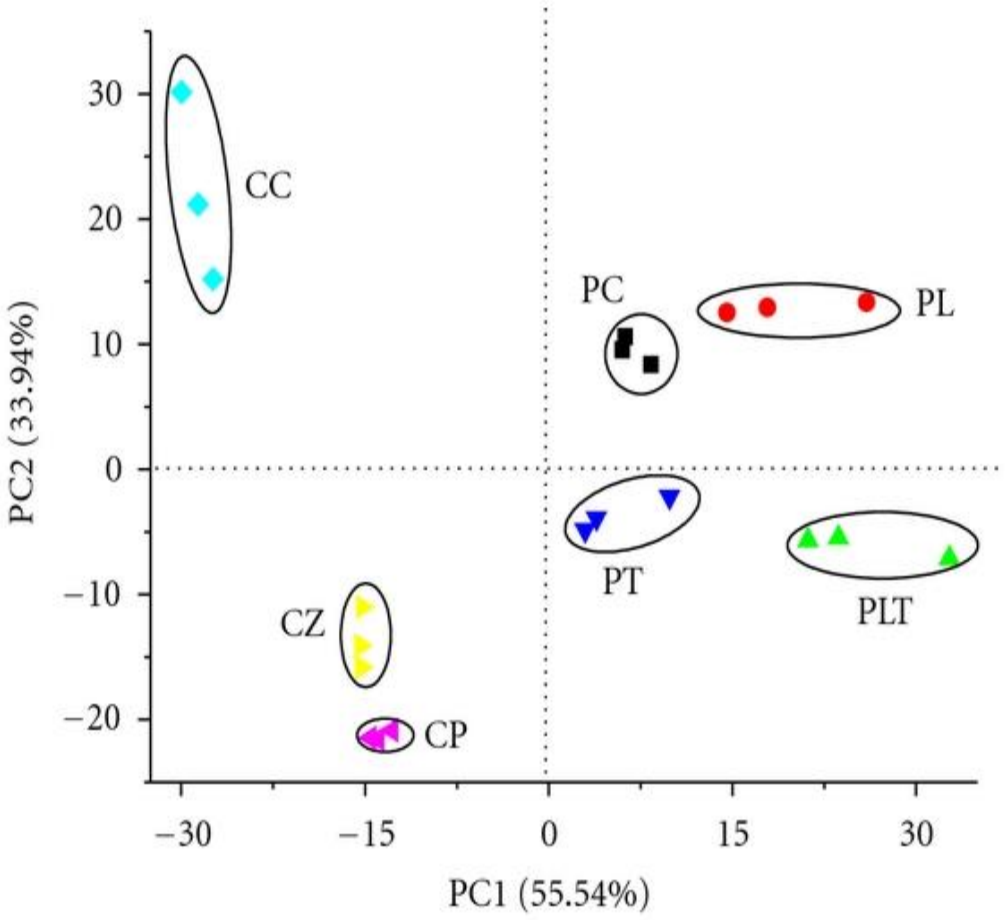


FIGURE 2. 11 PCA PLOT SHOWING TASTE ASSESSMENT OF COMMERCIALLY AVAILABLE COLA DRINKS. ABBREVIATIONS: PEPSI CLASSIC (PC), PEPSI LIGHT (PL), PEPSI LIGHT TWIST (PLT), PEPSI TWIST (PT), COCA-COLA CLASSIC (CC), COCA-COLA ZERO (CZ) AND COCA-COLA PLUS (CP) (BUENO L. 2012)

In this study, principle component analysis was used to identify which sensors were responsible for the data recorded on each sample. By so doing, biplots are plotted (illustrated in Figure 2.11); this was used to draw conclusions regarding the taste on the samples under investigation. In essence, the first principle component dictates which sensor gives the most response and equally so the second principle component will provide the second sensor. Therefore, the samples are described by their association with the principle components. In addition, the samples are grouped by similarity using hierarchical agglomerative cluster analysis which for ease of explanation has been described in **chapter 4, section 4.3.2**. Combining both sets of

analyses allows interpretation of not only taste attribute as described by sensors but also allowing comparison and contrasting of sample under investigation.

#### 2.2.1.6 DATA ANALYSIS – ANALYSIS OF VARIANCE (ANOVA)

Analysis of variance (ANOVA) is a parametric method for means comparison of several groups and it is also an extension of the independent sample t-test. However it differs from an independent sample t-test in that ANOVA allows for analysis across more than two data sets whereas independent sample t-test is limited to only two. The essence of ANOVA lies in testing the hypothesis that for a given data set, the means are equal. This hypothesis is tested under the assumption that a) the observation are random and independent, b) the distribution of the data set from which the samples are selected is normal, c) the variances of the distribution in the data are equal. If after hypothesis testing $p \leq 0.05$, then the hypothesis is true and the means are equal, if $p \geq 0.05$ then the hypothesis is false and the means are not equal. A ONE-WAY ANOVA is so named because only one variable ($x$) across the data sets is analysed. Multiple factors can also be analysed for example, two way ANOVA analyses two factors ($x,y$) and three way ANOVA analyses three factor ($x,y,z$). One way ANOVA is used in chapters 3 and 4 to demonstrate the statistical difference if any between the data under investigation. The data set is question is integral data i.e. measurement in mV, and independent. It is normally distributed (testing for normality will be illustrated when one way ANOVA is reported). In this instance the assumption that variances are equal was made.

### 2.2.2 HOT MELT EXTRUSION (HME)

Invented in the 18$^{th}$ century for the manufacturing of lead pipes, HME is now widely viewed in the pharmaceutical industry as an efficient technique of producing drug delivery systems (Jones *et al.* 2010). Extrusion is defined as a process of converting a raw material into a product of uniform shape and density by forcing it through a die under controlled conditions. The principle and pharmaceutical applications of HME

have been described in detail in **Chapter 1 section 1.5**. In this study all Eudragit® EPOQHD melt extrudates were prepared using a Thermo Scientific Process 11 twin screw extruder (Thermo Scientific UK) with co-rotating screws. The advantages of using a twin screw over a single screw barrel have been discussed in Chapter 1, section 1.5. However, to recap, twin screw barrels allow for betting mixing of the raw material therefore extrudates are characterised by a more even distribution of API in the polymeric carrier. The barrel temperature was set as follows: heating zones 2 and 3 were set at 120$^{o}$C while the rest of the zones were set at 140$^{o}$C. This temperature setting was selected because as previously mentioned in **section 2.3.4** the melting point of quinine hydrochloride is given as 115-116$^{o}$C, therefore as suggested by Repka et al (2008) the processing temperature was set to 15-60$^{o}$C above the melting point of the crystalline material or the glass transition of amorphous polymer (Repka *et al.* 2008). The glass transition of Eudragit®EPO has already been given in **section 2.2**. Therefore the processing temperature used in this was above the melting point of quinine hydrochloride and the glass transition of Eudragit®EPO.

Aside from the processing temperature, other process parameters play a key role in determining the properties of the final extrudate (Henrist *et al.* 1999). The screw speed and feeding rate are related to shear stress, shear rate and mean residence time which in turn affects dissolution rate and stability of the final products (Li *et al.* 2013). In the study, the feeding rate was set at 10rpm; this was selected because at this rate no solid bridges were formed therefore suggesting uniform mixing. It is important to note that Eudragit®EPO has poor flow properties. Rotation speed was set at 100rpm unless otherwise stated. The processing parameters adapted from a study by (Xin *et al.* 2007). However, modifications were made i.e. feed rate was decreased to 10rpm because at 60rpm the powder that contained 10 and 30% quinine hydrochloride formed bridges therefore reducing the feed rate solved this issue. The screw speed was adjusted to torque. Excluding the 70% drug loading, all other concentrations were processed at 100rpm screw speed. However, at 70% drug loading, using screw speed of 100rpm

resulted in torque running up to 100% which meant that the screws could not rotate; as such screw speed was reduced to 50rpm. It is also worth pointing out that, increasing the screw speed meant reduction in residence time. The significance of the residence time has already been pointed out in chapter 1.

### 2.2.3 MILLING

In the pharmaceutical industry milling is primarily used to reduce particle size. In this study, it was used to obtain powders from Eudragit®EPO QHD melt extrudates. There are several types of commercial mills available and these can be classified according to their mechanical processes. These include: cutting, compression, impaction, attrition and combined methods (Aulton 2007). For cutting mills, a series of knives attached to a horizontal motor which act against a series of stationery knives to generate high shear rates. Size reduction by compression can be carried out on a small scale in the laboratory using a pestle and mortar. Samples are pulverised through the friction from the weight of the pestle compressing the sample against the mortar. Impact methods such as hammer mills consist of a series of four or more hammers hinged on a central shaft. These swing out rapidly creating an angular velocity which produces strain rates of up to $80s^{-1}$. The rates are so high that most of the particles undergo a brittle fracture. As size reduction continues, the inertia of particles hitting the hammers decreases remarkably and subsequent fracture is less probable. Attrition mills such as roller mills use horizontally mounted rollers which rotate at different speeds such that the material is sheared as it passes through the gap and is transferred from slower to faster rollers.

Ball mills such as the one used in this study combine both impaction and attrition of particles. They consist of a hollow cylinder mounted such that it can be rotated on its horizontal longitudinal axis. The cylinder contains balls that occupy 30-50% of the total volume. These balls move with the cylinder until the forces of gravity exceed frictional forces and balls slide back to the base of the cylinder. At high angular velocities, the balls are thrown against the walls of the cylinder. To ensure that the material is

subjected to attritional and impaction forces often two or more cylinders are mounted onto a turntable which enable two modes of rotation.

In this study milled samples of Eudragit®EPO – QHD melt extrudates were prepared in a pulverisette 5 planetary ball mill (Fritsch) at a rotational speed of 350rpm for 30 minutes. The agate grinding chamber had a capacity of 500ml, with four 20mm agate grinding balls. The pulverisette 5 contains four sample chambers to enable simultaneous milling. Approximately 15g of melt extrudate was placed in two of the four chambers during processing. The samples were allowed to cool for 30 minutes when the milling process was completed, before being removed from the chamber, sieved and stored in three different temperature and humidity conditions which will be discussed in **chapter 5**.

### 2.2.4 DIFFERENTIAL SCANNING CALORIMETRY (DSC)

Differential scanning calorimtery (DSC) is a technique that measures difference in the heat flow between a sample and an inert reference as a function of time and temperature when subjected to a specified control program (temperature, time, atmosphere and pressure). This gives both qualitative and quantitative information such as crystallisation kinetics and identification of structural relaxations. There are two forms of DSC namely: heat flux (the most common) and power compensation. The former is described in detail as it is used in this study.

Heat flux DSC (illustrated in the schematic shown in Figure 2.12 consists of sample (S) and reference (R) pans placed symmetrically in a furnace. Both pans share a common heat source (the thermo electric disc) and are heated at the same rate. The temperature difference between the two pans is measured and resultant signal is converted to heat flow. The differential heat flow measured during a DSC experiment can be expressed using the thermal equivalent of Ohm's law:

$$\frac{dQ}{dt} = \frac{\Delta T}{\mathrm{R}}$$

EQUATION. 2.5

Where $\frac{dQ}{dt}$ is the heat flow (Q is heat energy and t in time), ΔT is the temperature difference between the sample and the reference and R is the thermal resistance in the heat flow path between the furnace and the sample.

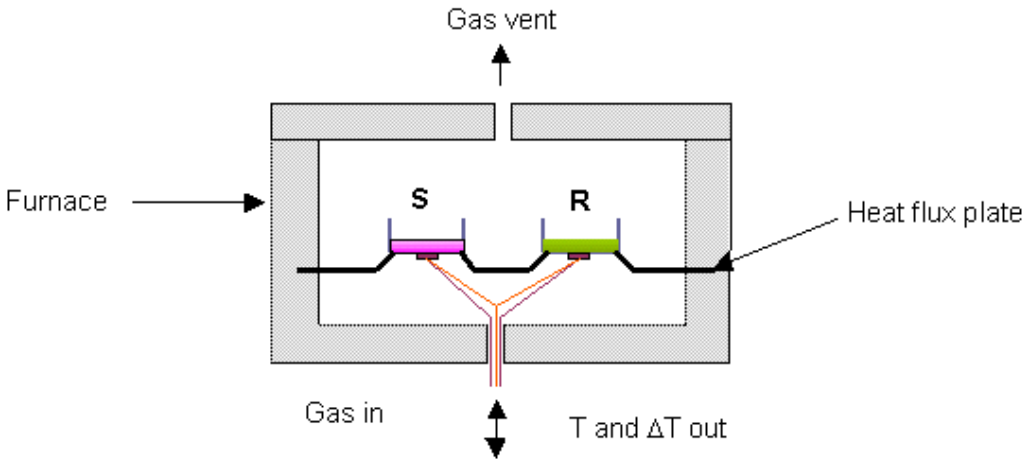


FIGURE 2. 12 SCHEMATIC OF HEAT FLUX DSC CELL SET UP. (TAKEN FROM HTTP://WWW.ANASYS.CO.UK/LIBRARY/DSC1_3.GIF)

During heating of a material, the heat flow signal is determined by the heat capacity (Cp) of the material. Heat capacity is defined as the amount of heat required to raise the temperature of one gram of the material by one degree Celsius. Hence, heat capacity can be expressed as:

$$Cp = \frac{dQ}{dt} \times \frac{dt}{dT}$$

EQUATION. 2.6

Where Q is the heat energy and $\frac{dt}{dT}$ is the reciprocal heating rate. This can be re-written as:

$$Cp = \frac{dQ}{dT}$$

EQUATION. 2.7

A schematic of a typical DSC plot is shown in Figure 2.13. The data is usually presented as a plot of heat flow against temperature. Identical heat capacities for the

sample and the reference result in the heat flow signal appearing as a horizontal line on the abscissa. Changes in the heat capacities between sample and reference result in the displacement of the horizontal baseline. Endothermic and exothermic processes are displayed and troughs and peak respectively. These are characterised according to position, size and shape. The size of peak represents the amount of material and energy of the reaction, while the shape points to the kinetics of the process.

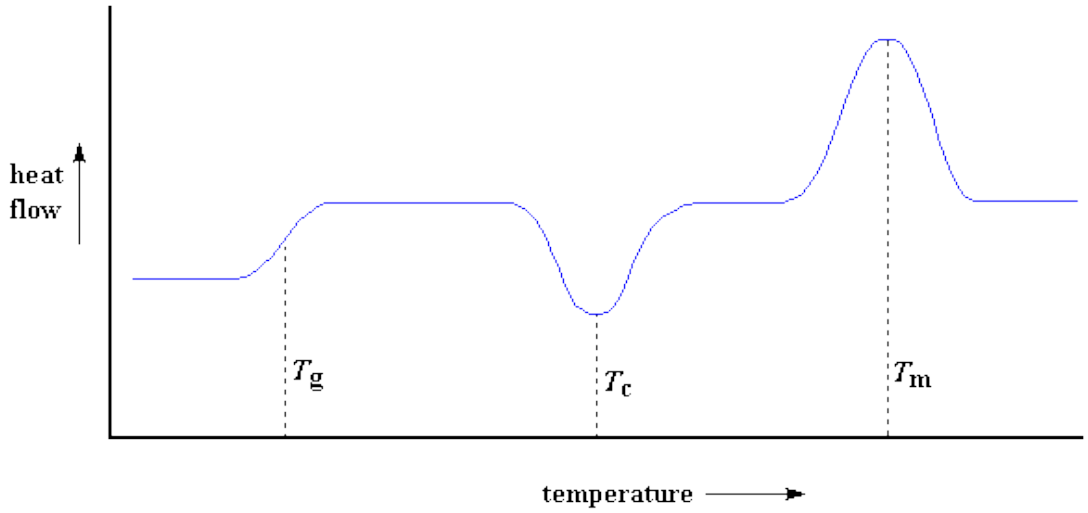


FIGURE 2. 13 SCHEMATIC OF TYPICAL DSC PLOT. TG REPRESENTS GLASS TRANSITION, TC IS RECRYSTALLIZATION AND TM IS MELTING TEMPERATURE. (TAKEN FROM HTTP://WWW.PSLC.WS/MACTEST/IMAGES/DSC08.GIF)

DSC measurements were performed on TA instruments DSC Q2000 with a refrigerated cooling system (RCS) attached. The purge gas, oxygen free nitrogen, was used at a flow rate of 50ml/min. All DSC experiments and calibration were performed using PerkinElmer 40µl, 0.15mm aluminium pans. Samples were accurately weighed directly into the pans using a Mettler Toledo XS205 dual range balance. The sample mass used was between 3-5mg. The samples were equilibrated to 25$^{o}$C before heating to 250$^{o}$C at a heating rate of 10$^{o}$C/min. Each set of DSC experiments was repeated three times to ensure reproducibility. Further details on pan types and variation heating rates are outlined within the relevant experimental section.The instrument was calibrated monthly or every time experimental parameters were changed to ensure optimal performance. The routine calibrations performed included the instruments baseline,

temperature and cell constant. High purity indium ($T_m$, 156.60°C), benzoic acid ($T_m$, 122.37°C) and *n*-octadecane ($T_m$, 28.24°C) were used as temperature calibrants.

### 2.2.5 POWDER X-RAY DIFFRACTION (PXRD)

X-rays were discovered by Wilheim Röntgen in 1895. The powder diffraction methods which use conventional X-ray sources were devised independently in 1916 by Debye and Scherrer in Germany and in 1917 by Hull in the United States. In PXRD experiments, X-rays are generated by a cathode ray tube which is directed towards the sample. Diffraction is governed by Braggs law given in Equation 2.4, which occur when the crystalline material interacts with the focused X-ray beam.

$$n\lambda = 2d\sin\theta$$

EQUATION. 2.8

where *n* is the order of the diffracted beam, $\lambda$ is the wavelength of the incident X-ray beam, *d* is the distance between adjacent planes of atoms (the *d*-spacing) and $\theta$ is the angle of incidence of the X-ray beam. By altering θ during scanning, different *d*-spacing can be obtained. A plot of the beam intensity against the angle of emergence produces a diffractogram with peaks seen corresponding to lattice spacing this providing an insight into the orientation and molecular arrangement within a sample. Materials exhibiting long-range order (i.e. crystalline) produce XRPD diffractograms containing clearly defined sharp peaks of varying intensities which corresponds to the uniform lattice spacing, arrangements and orientation of molecules within the crystal.

Applications in the pharmaceutical industry include: determining the crystal structure (Evans *et al.* 2004) and degree of crystallinity of a material (Grisedale *et al.* 2011), and the recognition and quantification of amorphous content in partially crystalline mixtures / solid dispersions (Wulff *et al.* 1996). X-ray powder diffraction analysis of quinine hydrochloride dihydrate and Eudragit EPO® extrudates and physical mixtures were performed at ambient temperature using the Rigaku miniflex 600 equipped with a copper X-ray tube (1.54Å). Samples were exposed to an X-ray beam with a voltage of

40kV and a current of 15mA. The PXRD patterns were recorded using diffraction angles (2θ) from $2^o$ to $70^o$ at scan rate of $3^o$/min. Resultant data was exported into Microsoft excel 2010® for analysis.

### 2.2.6 SCANNING ELECTRON MICROSCOPY (SEM)

Scanning electron microscopy (SEM) differs from standard light microscopy in that it uses electrons instead of light waves to magnify the surface of a sample. This enables samples to be examined at higher magnification and resolutions than light microscopy. SEM has three major benefits namely: upper magnification of about 250 000X, a large depth of field and lateral spatial resolution better than 3nm. A schematic diagram of a SEM set up is shown in Figure 2.14. Briefly, a beam of electrons is emitted from a cathode which is maintained under a very high vacuum to keep it stable and minimise beam scatter caused by electrons colliding with gas molecules. Electrons are accelerated using high voltage. As the electron beam collides with the sample, electrons and x-rays are emitted and detected by an array of detectors that are positioned a few millimetres away. The sample can be moved in X, Y and Z directions, rotated or tilted to allow creation of 3-dimensional images. The transfer of energy to the sample as the electron beam decelerates can cause localised heating which may degrade or melt material under observation. Hence, coating the sample with a conduction metal can help dissipate heat and reduce beam damage.

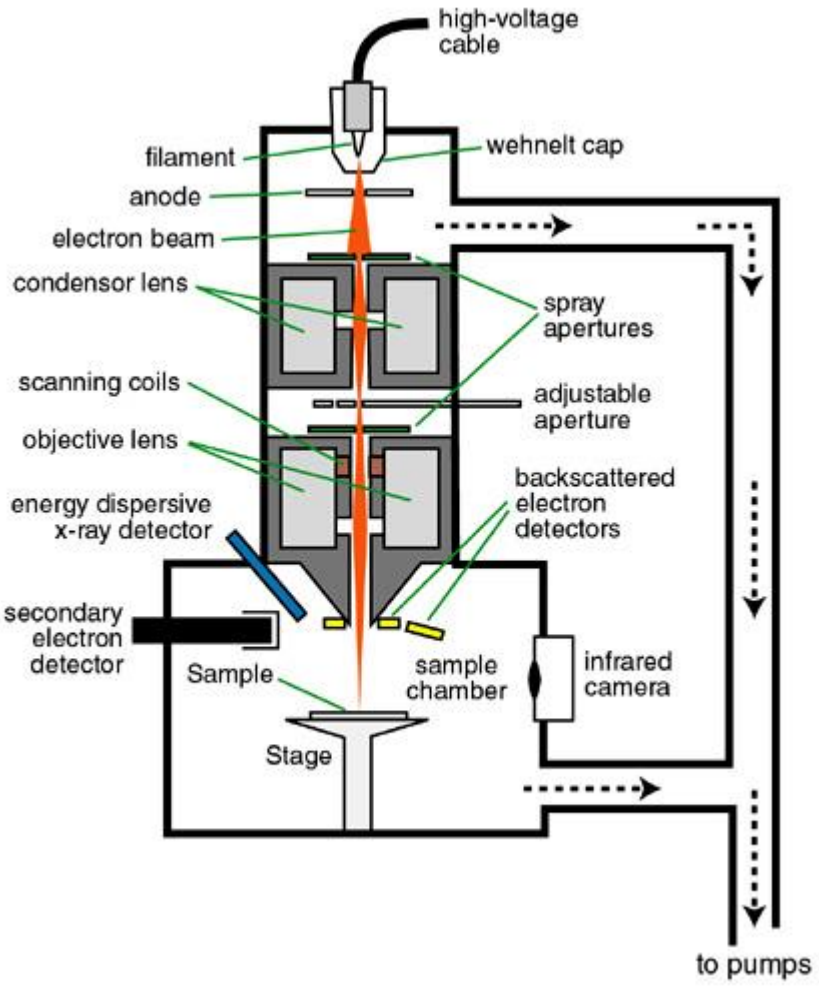


FIGURE 2. 14 SCHEMATIC DIAGRAM OF A SEM SET UP. (TAKEN FROM HTTP://WWW4.NAU.EDU/MICROANALYSIS/MICROPROBE-SEM/IMAGES/SEM_SCHEMATIC.JPG)

In this study, SEM images were taken using a FEI Quanta 200F (Eindhoven, The Netherlands). The samples were mounted on aluminium stubs with double sided carbon sticky pads and then coated with gold in order to protect the samples from heat generated by the electron beam.

### 2.2.7 HOT STAGE MICROSCOPY (HSM)

HSM is also known as thermo-microscopy. It is the combination of microscopy and thermal analysis to enable the study and physical characterisation of materials as a function of temperature and time. Sample changes upon controlled heating can be visually observed through a microscope which is attached to a computer where footage can be recorded as well as images captured. It is very useful tool for rapidly

distinguishing between crystalline and amorphous forms of pharmaceutical materials. When used in conjunction with other thermal techniques, hot stage microscopy can provide useful insight into thermal events seen.

In this study, a LeicaDM2700M microscope with a 10X magnification lens was connected to a FP82HT Mettler Toledo instruments heating stage unit and a FF90 Mettler Toledo instruments central processor unit. Samples were heated from 30$^{o}$C to 250$^{o}$C at a heating rate of 10$^{o}$C/min. Studio4 design capture software was used to record and capture thermal events in real time.

### 2.2.8 THERMOGRAVIMETRIC ANALYSIS (TGA)

Thermogravimetric analysis (TGA) is a technique in which weight change(s) of a material are measures as a function of increasing temperature or isothermally as a function of time under a controlled atmosphere. A typical TGA instrument consists of a sample holder, a sensitive electro balance, furnace and a recorder. The balance operates on a null balance principle. At the point zero or “null” position equal amounts of light shine on the two photodiodes, at which point a current is applied to the meter for movement to return the balance to the null position. The amount of current applied is proportional to the weight loss or gain. The furnace is purged with a gas such as air or nitrogen in order to maintain a controlled atmosphere surrounding the sample and to rapidly remove any evolved volatiles. The temperature within the furnace is monitored by a thermocouple located close to the sample and is used to control the furnace temperature.

Weight changes can occur in any material and may be caused by decomposition, oxidation or dehydration. The moisture content within a sample is an important quality control parameter as it can affect long-term stability and effectiveness as well as short term processability. Free surface water and bound water are present in most formulations. Free water refers to water that is absorbed from the environment and is

not chemically attached to materials while bound water(s) of hydration that are chemically bound to the surface. TGA was used in this study to detect water content of samples immediately after HME processing as well as after storage of melt extrudates in differing humidity conditions. It is important to measure the water content in solid dispersions since water can act as a plasticiser that can increase molecular mobility of amorphous drugs and compete against drugs in forming hydrogen bonds with polymers. This increases the physical instability of solid dispersions. This technique was also used to generate anhydrous forms of QHD and QhS.

TGA was carried out using a TA instruments Hi Res 2950 thermogravimetric analyser. The thermobalance was calibrated monthly using the melting transition of an indium standard. The magnitude and linearity of the balance were calibrated using milligram masses as per the manufactures instruction manual. Samples weighing 3- 5mg were placed in tarred aluminium pans on the sample holder. Oxygen free nitrogen was used as the purge gas. The flow rate through the furnace and TGA head were 60mlmin$^{-1}$ and 40mlmin$^{-1}$ respectively. Weight changes were recorded over a temperature range from 30$^{o}$C to 250$^{o}$C with a heating rate of 10$^{o}$Cmin$^{-1}$. Data obtained was analysed using Universal Analysis 2000 software for Windows 2000/XP/Vista version 4.5A (TA instruments).

### 2.4.9 DISSOLUTION TESTING

The basic premise of taste masking is to deter the interaction between the API and the taste receptor cells in the oral cavity. The different types of taste masking strategies have been discussed in chapter 1 (**section 1.4**). The release of the API in the oral cavity is critical in taste masking. An analysis of the release profile of the API, i.e. dissolution testing, is therefore essential to confirm taste masking. However, there are no set pharmacopeial standards for dissolution testing of taste masked particles. Guidance published jointly by the Federation International Pharmaceutique (FIP) and the American Association of Pharmaceutical Sciences (AAPS) for orally disintegrating

tablets (ODT) recommends the use of neutral medium where the drug should have typically less than or equal to 10% drug dissolved in 5 minutes to achieve taste masking (Siewert *et al.* 2003a). However, this criterion is heavily dependent of the bitterness and human detection threshold of the API. Highly bitter APIs have lower acceptable limits of release and vice versa, thus there is no set limit of acceptable drug release for all drug candidates. More importantly, this criterion is limited to APIs for which bitterness intensity and detection threshold have been identified.

The British Pharmacopoeia (BP) has recommended dissolution tests for immediate and delayed release dosage forms; however these are not appropriate for taste masked particles. This is because the tests aim to mimic the stomach and the small intestine and no consideration is given for the oral cavity. The lack of appropriate pharmacopoeial standard dissolution test for taste masked particles has led to a wide variety in dissolution methods being adopted. The challenge revolves around selection of dissolution media, the volume of dissolution media and agitation of sample if necessary.

In this study, dissolution studies have been designed to give a near representation of the oral cavity in terms of type of dissolution media, its volume and agitation time of tastant sample. 90ml of deionised water was used as dissolution media. The samples were agitated using an incubated shaker (Incu Shaker mini XHWY series, Shropshire, UK), temperature was set at 37$^{o}$C and shake speed of 50rpm was used. Samples were withdrawn at time intervals (3min, 30 minutes and 3 hours), filtered using a Millex GP filter unit (0.22µm) then analysed spectrophotochemically on the Jenway 6305 (Bibby Scientific, UK). UV absorbance values were recorded at 316nm.

# CHAPTER THREE
# MECHANISM OF DETECTION

# CHAPTER 3- MECHANISM OF DETECTION

## 3.1 BACKGROUND

At the time of the study presented here, studies into the responsiveness of the electronic tongue Insent®TS500Z had not investigated the responsiveness of the taste sensor to caffeine and its salts or quinine and its salts in comparison to water. Comparison of caffeine and caffeine citrate was briefly addressed in a study where the authors reported logarithmic dose response to caffeine citrate and no such response for caffeine (Woertz *et al.* 2011a). The same group also compared two salts of quinine namely, hydrochloride and sulphate. They reported that both salts recorded high responses to bitterness in comparison to quinine benzoate and sodium benzoate. However, in both cases, it is not clear from the literature reports as to whether negative controls i.e. de-ionised water was used. The objective of the work detailed in this section was to understand the responsiveness of taste sensor to different salts of the same molecule with the aim of explaining the precise mechanism by which objective taste measurement is achieved using the taste sensor. Another objective was to establish the extent to which the dissociation profile and other physical properties i.e. solubility and electrolyte behaviours of the drug affects its detection by the TS5000Z electronic tongue.

## 3.2 PRELIMINARY WORK

### 3.2.1 STUDY OBJECTIVES

In this study, the responsiveness of four sensors, namely AC0, AN0, C00 and AE1, (which collectively make up the bitter drug sensor set), were explored. For ease of explanation, sensor AC0 will be referred to as basic bitterness1, sensor AN0 is referred to as basic bitterness2, sensor C00 is referred to as acidic bitterness and sensor AE1 is referred to as astringency. The composition of these sensors has been discussed in **Chapter 1**, **Section 1.3.2, and Table 1.5.** Sensor response was evaluated using increasing concentrations of aqueous solutions of methylxanthines i.e. caffeine and

caffeine citrate, theobromine and theophylline with the aim of describing sensor response and sensitivity to molecules with similar structure. The increasing concentrations of the methylxanthines were each compared to de-ionised water (negative control).

### 3.2.2 GENERAL METHODOLOGY

Solutions of the methylxanthines (MX) were prepared by the addition of the required quantity of MX powder gently into the vortex created by the action of a magnetic stirrer in the deionised water. The stirring was continued until all the powder had dissolved. With the exception of theobromine, all solutions were stirred for 15 minutes. All solutions were prepared at room temperature on the day of testing. In the case of theobromine which did not dissolve after 15 minutes, dissolution was aided by using sonicator. A volumetric flask containing undissolved powder of theobromine and de-ionised water where placed in a sonicator for 30 minutes at 25$^{o}$C. The concentrations used in this study were all within the maximum solubility of each methylxanthine i.e. only solutions were used.

### 3.2.3 RESULTS

Concentrations ranging from 0.5 – 25mM of caffeine were investigated using the bitter drug sensor set and sensor response curves were plotted in Figure 3.1. These concentrations were adapted from a study by Woertz et al (2010). De-ionised water was used as a placebo for comparison. The plot in Figure 3.1 shows that there was no difference in the sensor response values between placebo and increasing concentrations of caffeine. A one-way ANOVA ($p$ = 9.9 x $10^{-12}$) showed that there was no statistical difference between the sensor responses of caffeine and those observed for de-ionised water (shown on the zero point concentration data point).

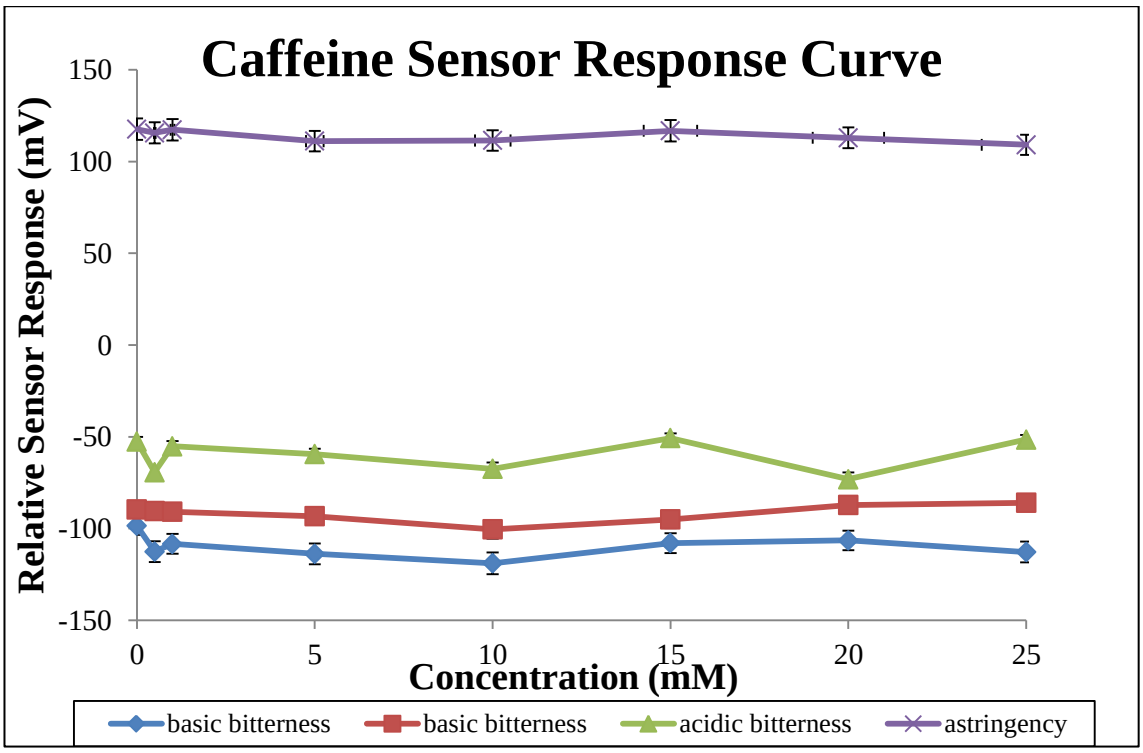


FIGURE 3 1 RELATIVE SENSOR RESPONSE FOR CAFFEINE SHOWING THE RESPONSES OF FOUR SENSORS WHICH CORRESPOND TO DIFFERENT TASTE SPECIFICATIONS, AS A FUNCTION OF CONCENTRATION (N=9, $\bar{x}\pm$ SD)

In order to understand why there was no difference between de-ionised water and caffeine it was necessary to investigate concentrations of caffeine ranging from 0.05 to 1.0mM (lower concentrations). The rationale for this was that the concentrations already investigated could have been too high therefore saturation effect on sensors would have led to no difference being observed. The response curve for the investigation of the lower concentrations is illustrated in Figure 3.2. It is noteworthy that mV recorded at the lower concentration were similar to recordings presented in Figure 3.1, which were also similar to those observed for deionised water. A *one-way ANOVA (p=0.001)* revealed that there is no statistical difference between the readings for de-ionised water and those observed for the lower concentrations of caffeine.

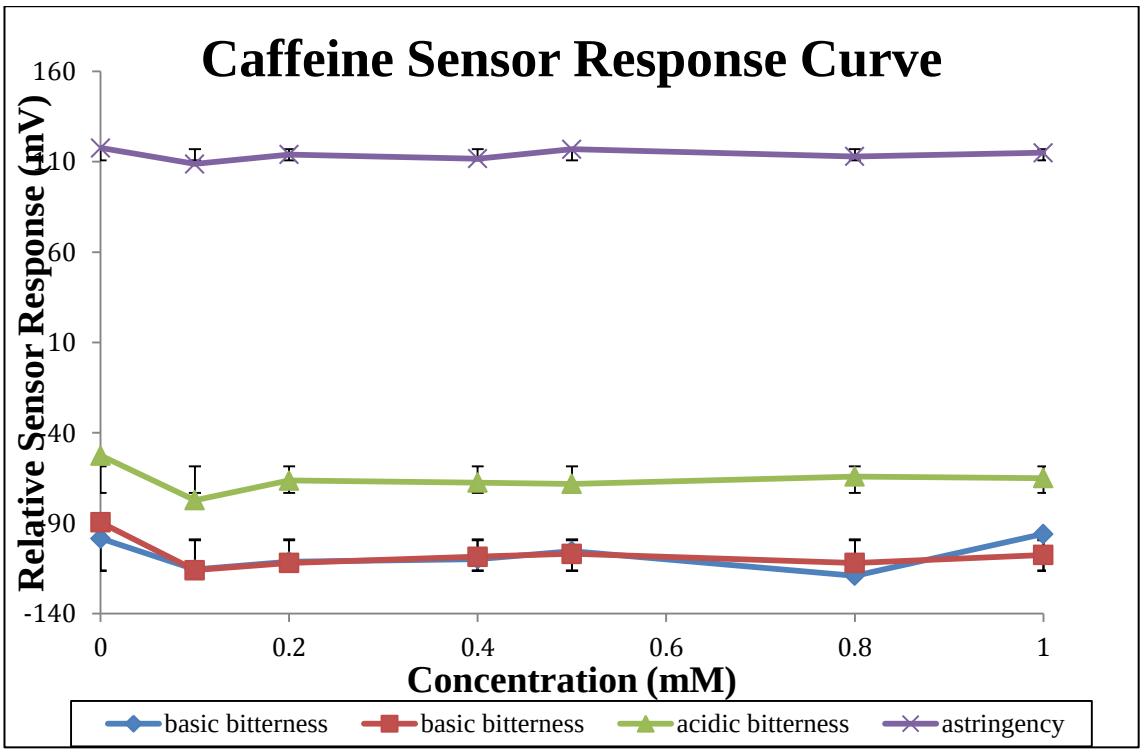


FIGURE 3. 2 RELATIVE SENSOR RESPONSE CURVE FOR CAFFEINE (LOW CONCENTRATIONS), SHOWING THE RESPONSES OF FOUR SENSORS WHICH CORRESPOND TO DIFFERENT TASTE SPECIFICATIONS, AS A FUNCTION OF CONCENTRATION (N=9, $\bar{x}\pm$ SD)

Investigations thus far have focused on concentrations ranging from 0.1 to 25mM. However, it was necessary to investigate sensor response to higher concentrations, right up to maximum solubility of caffeine in water, with a view to establish whether the smaller concentrations were below the minimum detection threshold of the taste sensor. Figure 3.3 shows sensor response curves of high concentrations of caffeine. Similar to Figures 3.1 and 3.2, a *one-way ANOVA (p= 0.001)* showed that there is no statistical difference in response in higher concentrations (60 to 110mM) of caffeine to de-ionised water.

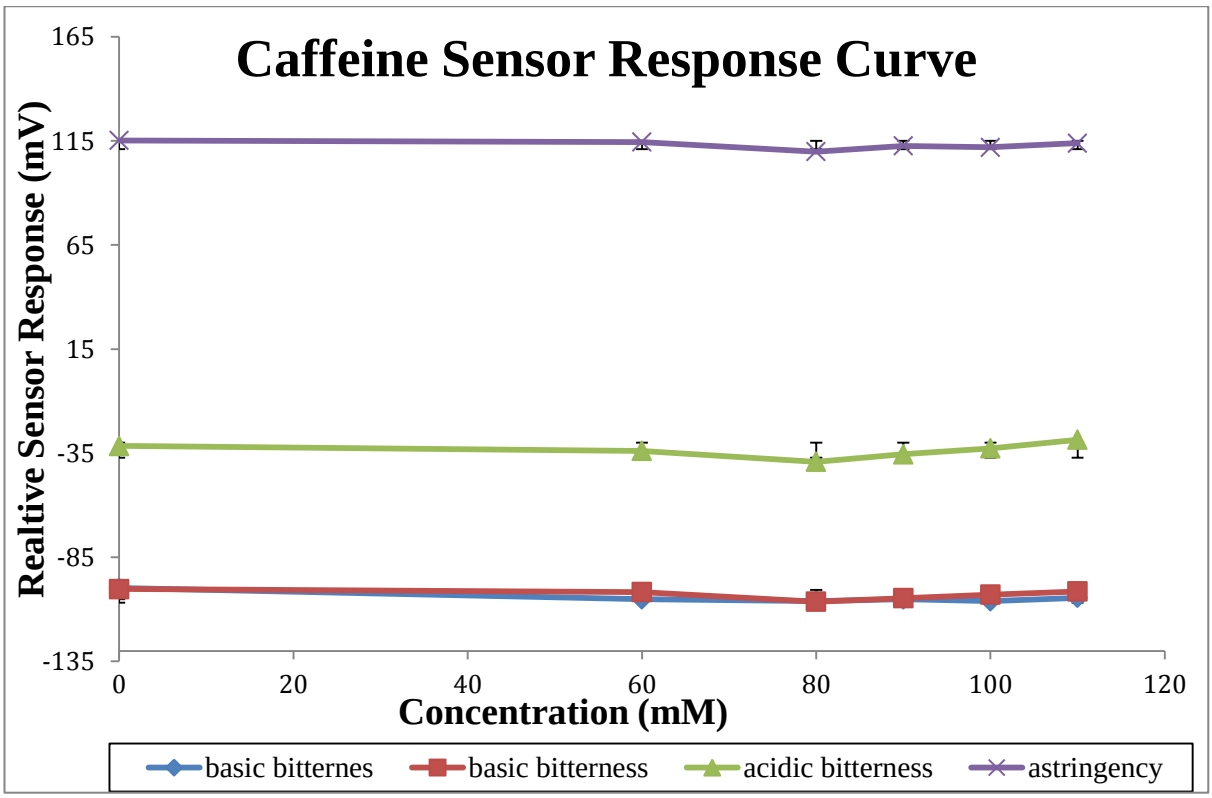


FIGURE 3. 3 RELATIVE SENSOR RESPONSE CURVE FOR CAFFEINE (HIGH CONCENTRATIONS), SHOWING THE RESPONSES OF SENSORS AS A FUNCTION OF CONCENTRATION (N=9, $\bar{x}\pm$ SD)

In summary, investigation of sensor response (mV) of caffeine concentrations ranging from 0.01 to 110mM has revealed no difference with deionised water. The results observed suggest that caffeine was not being detected by the taste sensor. Furthermore, increasing concentration of caffeine did not affect the detection of caffeine. Also noteworthy is that the relative sensor response for acidic bitterness increases between each measurement cycle i.e. in the case of water, in Figure 3.1 and 3.2 the relative sensor response was approximately -52mV however this increased to approximately -31mV in Figure 3.3. A comment will be made on this phenomenon in **section 3.5**.Theobromine is slightly soluble in water i.e. < 0.1g /100ml therefore concentrations ranging 0.05 – 2.5mM were used. Interestingly, results obtained for theobromine illustrated in Figure 3.4 are similar to those already observed for caffeine. A one-way ANOVA ($p$= 2.09x10$^{-14}$) showed that no statistical difference was observed between the sensor response readings for theobromine to water, as already observed with caffeine.

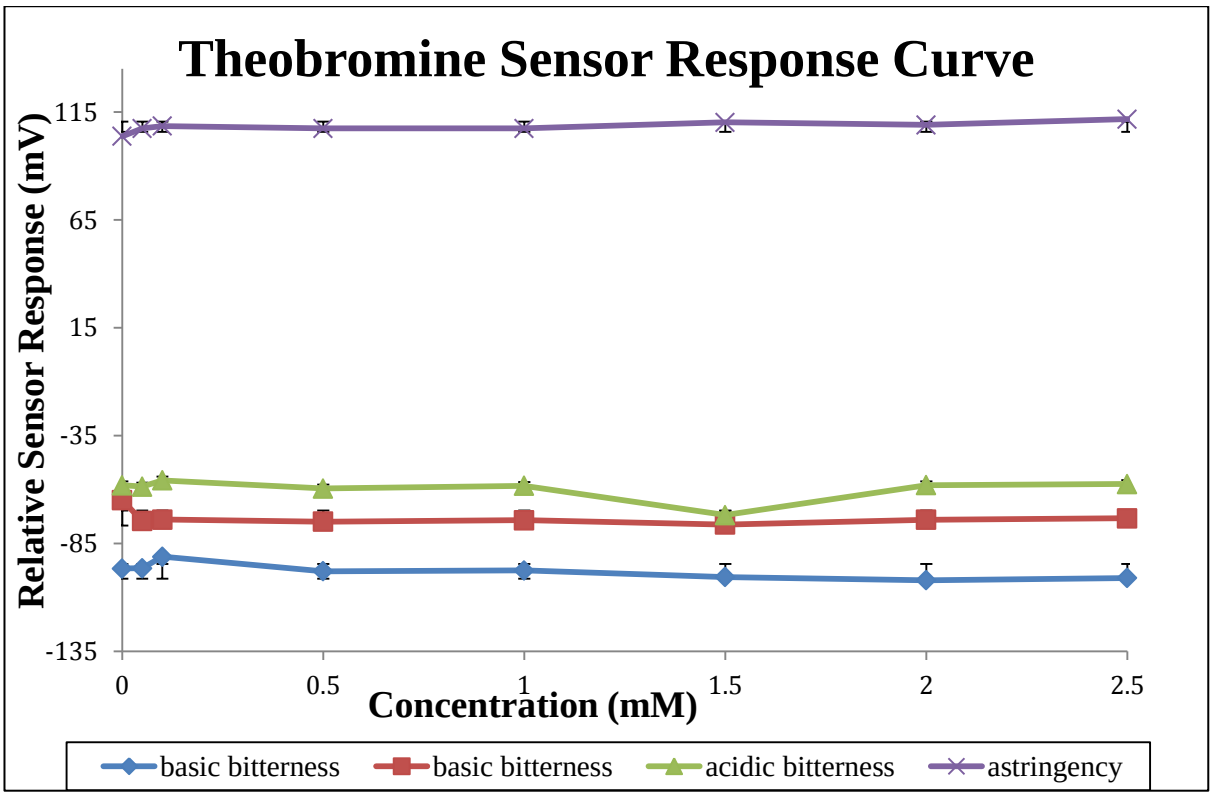


FIGURE 3. 4 RELATIVE SENSOR RESPONSE CURVE FOR THEOBROMINE, SHOWING RESPONSES OF SENSORS AS A FUNCTION OF CONCENTRATION (N=9, $\bar{x}\pm$ SD)

The investigation of theophylline at concentrations ranging from 0.5 – 25mM revealed results similar to caffeine and theobromine. The sensor response curves are shown in Figure 3.5. There was no statistically significant difference between relative sensor responses for theophylline and de-ionised water as evidenced by a *one-way* ANOVA ($p$= 2.24x10$^{-14}$).

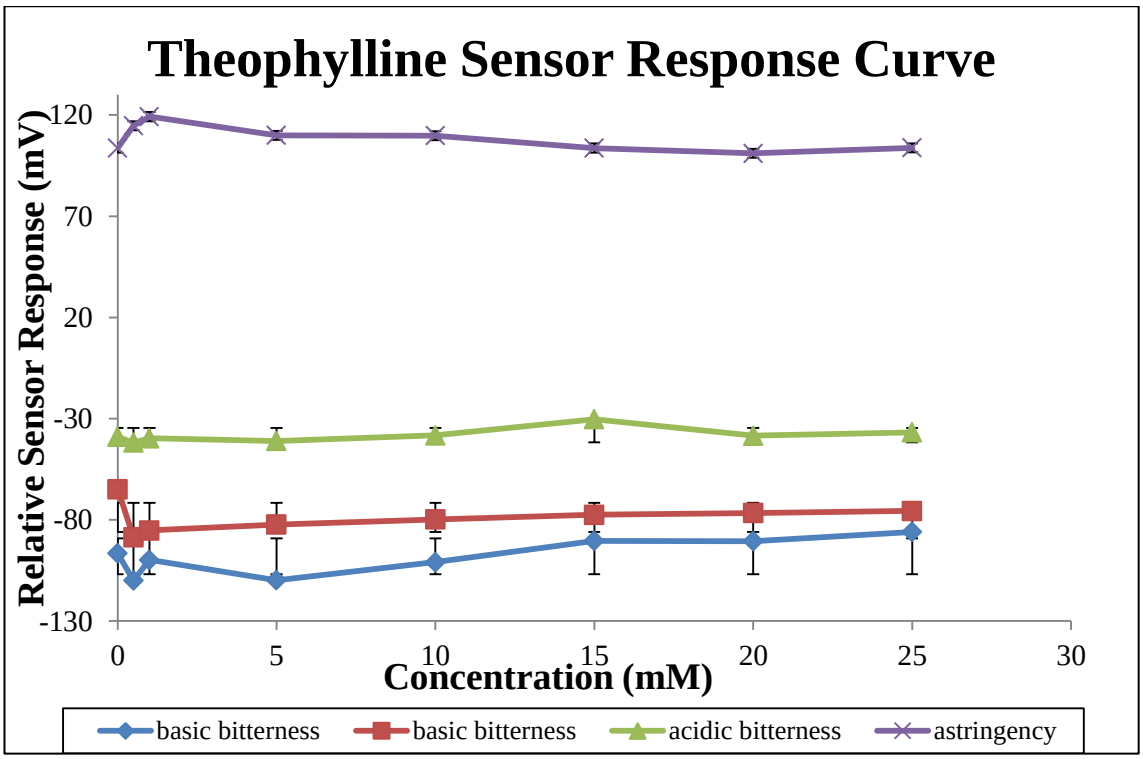


FIGURE 3. 5 RELATIVE SENSOR RESPONSE CURVE FOR THEOPLHYLLINE, SHOWING RESPONSES OF FOUR SENSORS AS A FUNCTION OF CONCENTRATION (N=9, $\bar{x}$± SD)

Following investigations of caffeine (Figures 3.1, Figure 3.2 and Figure 3.3), theobromine (Figure 3.4) and theophylline (Figure 3.5) at varying concentrations it became apparent that these three methylxanthines were not being detected by the electronic tongue. Furthermore, variations in concentrations across the methylxanthines did not change detectability by the taste sensor. There are no reports in the literature suggesting that theophylline or theobromine is detectable on the electronic tongue.

The detection of a caffeine salt i.e. caffeine citrate, which had already been described in literature as being detectable, was then investigated. Concentrations of caffeine citrate investigated were derived from literature reports but also matched the range that was used for caffeine in order to facilitate a direct comparison at equimolar concentrations (Woertz *et al.* 2010a). Reports in the literature suggest a concentration dependent relationship for caffeine citrate; a similar relationship was illustrated in Figure 3.6. The two basic bitterness sensors both showed an increase in relative

sensor response values with increasing concentration. However, there is no further increase in relative sensor response after 60mM. The acidic bitterness sensor shows a sharp increase in relative sensor response values between 0.5mM and 1.0mM, following this there is a gradual decrease in values which also level off after 50mM. The astringency sensor response values decrease gradually and then levelling off at 60mM. Overall, a *one-way ANOVA (p=0.57)* reveals that there is a statistical difference between response values of caffeine citrate and de-ionised water. Furthermore, sensor response values change with increases in concentration.

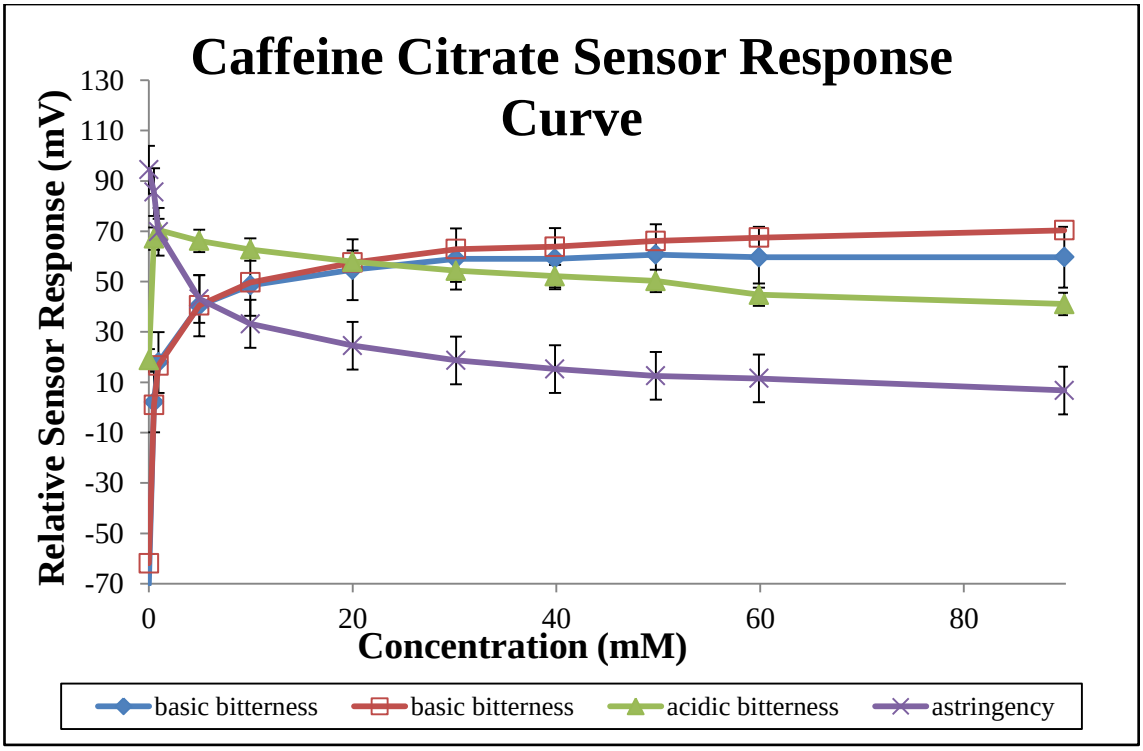


FIGURE 3. 6 RELATIVE SENSOR RESPONSE CURVE FOR CAFFEINE CITRATE, ILLUSTRATING SENSOR RESPONSES TO FOUR SENSORS AS A FUNCTION OF CONCENTRATION (N=9, $\bar{x}$± SD)

Various concentrations of caffeine revealed no difference in response patterns between deionised water and caffeine; however, caffeine citrate illustrates concentration dependence. At this juncture it was necessary to investigate citric acid (Figure 3.7), in order to give an indication as to which species is responsible for response identified with caffeine citrate. Interestingly, sensor response patterns for citric acid were similar to those observed for caffeine citrate. This suggests that the citrate in caffeine citrate could be responsible for the response patterns observed.

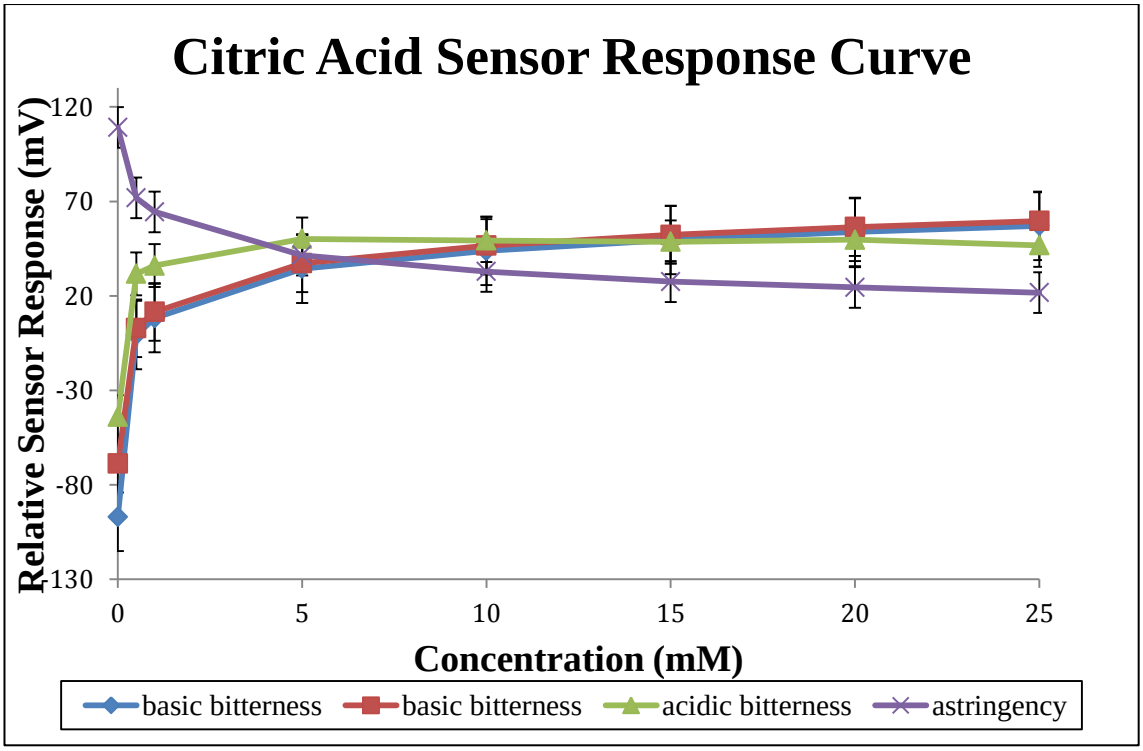


FIGURE 3. 7 RELATIVE SENSOR RESPONSE CURVE FOR CITRIC ACID, SHOWING SENSOR RESPONSE PATTERNS AS A FUNCTION OF CONCENTRATION (N=3, $\bar{x}$± SD).

Woertz et al (2010) reported that caffeine was detectable on the taste sensor although the report also stated that the results were inconclusive as only a few sensors showed ranges of linearity. The authors go on to add that the responses were quite small and not incongruent with the whole shape of the concentration curve. The work reported here contradicts this finding in that caffeine was not detectable using this sensor set. Therefore, in order to elucidate how detection may have been observed in previous reports, it was necessary to investigate the effect of the solvent used. As such, caffeine was dissolved in the reference solution instead of water. Figure 3.8 illustrates caffeine

solutions from reference solution while Figure 3.9 illustrates caffeine dissolved in water but reference solution used as a blank. Figure 3.8 shows a difference in voltage is observed between the reference solution and increasing concentrations of caffeine for all sensors except astringency. This difference was only observed for concentrations up to 10mM for both basic bitterness sensors. After this concentration, there is no statistical difference in the voltage reading observed for the other sensors as shown by a *one-way ANOVA ($p= 4.05x10^{-5}$).* Only the acidic bitterness sensor demonstrates response with different concentrations, however this does not appear to be concentration dependent.

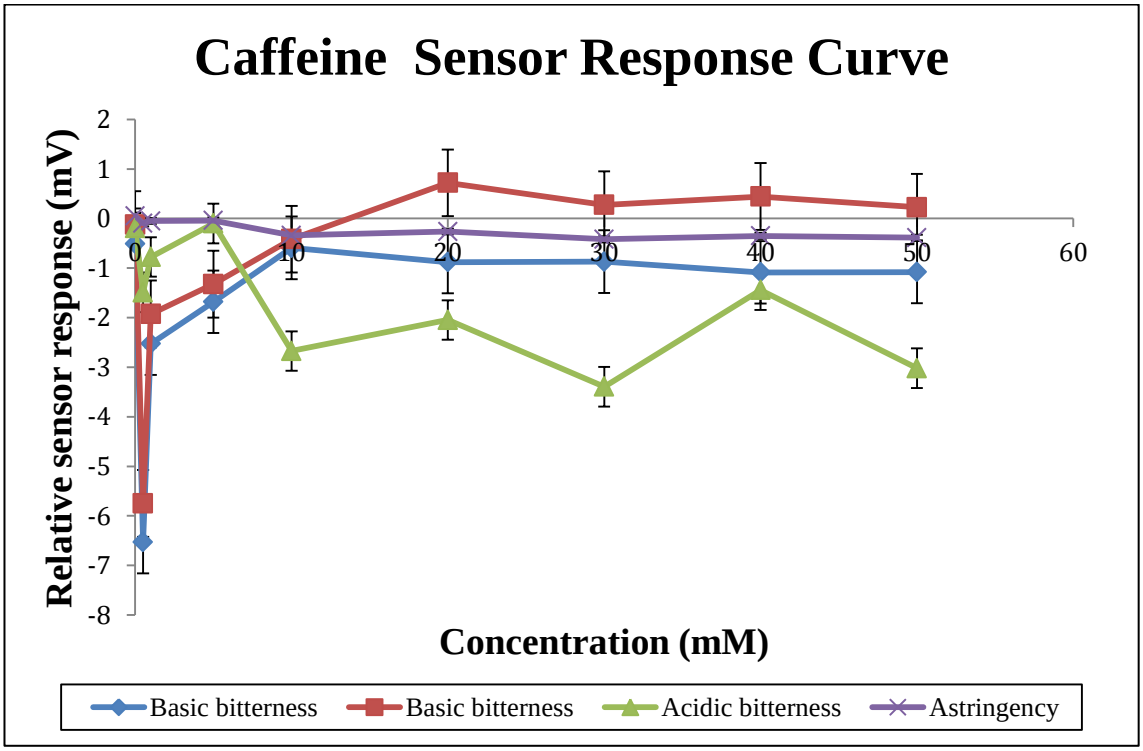


FIGURE 3. 8 RELATIVE SENSOR RESPONSE CURVE FOR CAFFEINE DISSOLVED IN REFERENCE SOLUTION, SHOWING SENSOR RESPONSE PATTERNS AS A FUNCTION OF CONCENTRATION (N=6, $\bar{x}$± SD)

Figure 3.9 shows the comparison of reference solution (0.03mM tartaric acid + 0.3mM KCl, shown on the zero concentration data point) to increasing concentrations of caffeine dissolved in de-ionised water. At 0mM the voltage reading recorded i.e. 0mV is the reference solution. The concentrations ranging from 0.5mM to 25mM are caffeine dissolved in de-ionised water. Comparison of increasing concentrations of caffeine dissolved in de-ionised water with the reference solution, showed a difference between

reference solution and 0.5mM. However, as already observed in Figure 3.1, no concentration dependence is seen with increasing concentrations of caffeine. A one-way ANOVA showed that there was no statistical difference between the increasing concentrations of caffeine ($p$= 2.89x10$^{-14}$)

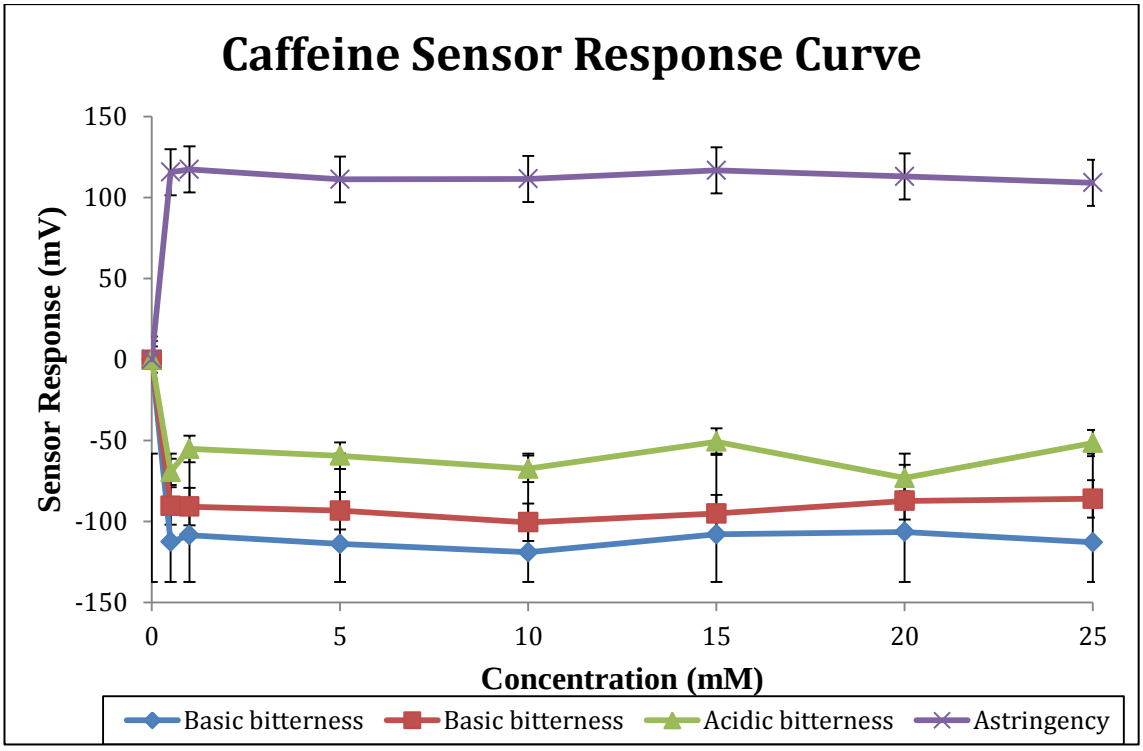


FIGURE 3. 9 RELATIVE SENSOR RESPONSE CURVE FOR CAFFEINE DISSOLVED IN WATER AND REFERENCE SOLUTION (0.03MM TARTARIC ACID AND 0.3MM KCL) USED A STANDARD COMPARATOR. THIS SHOWS SENSOR RESPONSE PATTERN AS A FUNCTION OF CONCENTRATION (N=6, $\bar{x}$± SD).

### 3.2.4 PRELIMINARY DISCUSSION AND CONCLUSION

In general, there is no difference in relative sensor response between de-ionised water (control) and the different methylxanthines across all four sensors used to detect bitterness of pharmaceutical products. Furthermore, the relative sensor responses show no dependence to concentration. A study by Woertz et al (2011) showed that caffeine did not have a clear log linear relationship. The authors also report that the results were inconclusive as basic bitterness1 and 2 showed no response with increasing concentrations of caffeine. The other sensors used in the study showed response albeit the responses were quite small and incongruent with the whole shape of a concentration curve. The authors attribute the non-detectability of caffeine by the bitterness sensors to the fact that the molecule is neutral (Woertz *et al.* 2011a). The

work reported here shows that caffeine has not been found to be detectable. A possible reason for this difference in findings is that, the work reported here uses de-ionised a negative control therefore eliminating the possibility of false positives. This is the first time that theobromine and theophylline have been investigated in such a study and also compared to a control (de-ionised water).

The results thus far point to the fact that caffeine is not being detected and furthermore neither are theobromine and theophylline when they are dissolved in deionised water. In the case of dissolving caffeine in reference solution, sensor responses were observed for all but the astringency sensor. It is important to note that this behaviour is observed at the lower end of concentrations of caffeine i.e. 0.5mM – 10mM. A possible explanation for this is that; caffeine is an amine; therefore, it has basic nitrogen which will react with a proton source. As previously mentioned in **chapter 2, Table 2.3**, the reference solution is composed of 0.3mM tartaric acid and 30mM potassium chloride. Hence, tartaric acid acts as a proton source. The reaction with the acid produces the conjugate acid (an ammonium ion) as illustrated in Equation 3.3. It is this conjugate form of caffeine that gives a change in membrane potential on the sensors thus it can be detected. However, the formation of the conjugate acid is limited by the concentration of tartaric acid (0.3mM). This is to say that there is a finite amount of caffeine conjugate that can be formed, therefore at concentrations higher than 10mM the concentration of caffeine exceeds that of the conjugate form, which means detection by the taste sensor is diminished in comparison to concentrations lower than 10mM. The significance of these finding will become apparent in section 3.5, however it is worth mentioning that the solvent used has an effect on the detectability of caffeine.

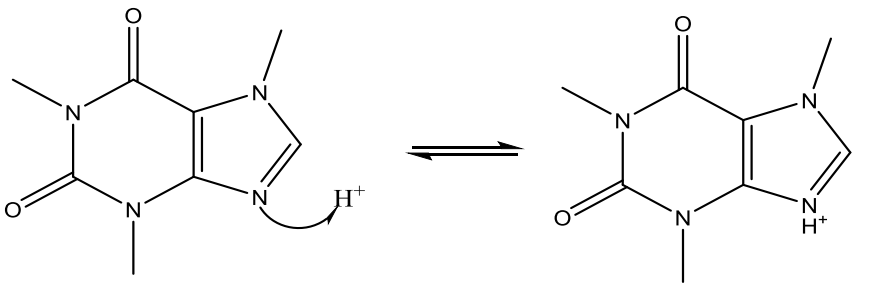


caffeine | caffeine conjugate acid

EQUATION 3.9

The pKa values of the methylxanthines are given in Table 3.1, together with pH values of solutions measured. In general, the solutions used had a pH below the pKa which suggests that the molecules were unionised in solution therefore did not affect the stern layer or diffuse layers of the double electrical layer. Woertz et al (2011) suggested that the increased conductivity of ionic substances leads to better detection by the electronic tongue; hence caffeine being a neutral molecule is difficult to detect. However, it is not possible to explain the mechanism of detection when investigating a system that is not being detected. This is to say that since methylxanthines are not being detected, that lack of detection does not validate the theories already suggested. It is therefore imperative to investigate a system that has some data regarding detectability.

TABLE 3. 1 SUMMARY OF CAFFEINE, THEOBROMINE, THEOPHYLLINE

| Molecule | Structure | Weight ($gmol^{-1}$) | Solubility (g/L) | pKa | Sensor Response compared to water | [Conc] dependence of sensor response |
|---|---|---|---|---|---|---|
| **Caffeine** | 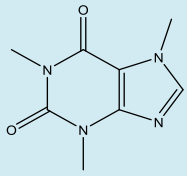 | 194.19 | 22 | 10.4 (Wishart *et al.* 2008) | No | None |
| **Theobromine** | 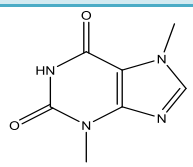 | 180.16 | 1.5 | 9.9 (Wishart *et al.* 2008) | No | None |
| **Theophylline** | 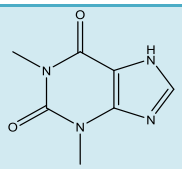 | 180.16 | 0.33 | 8.81 (Wishart *et al.* 2008) | No | None |
| **Caffeine citrate** | 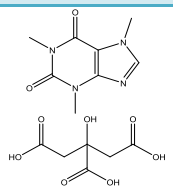 | 386.31 | Freely soluble | ----- | Yes | Response varies with [conc] |
| **Citric acid** | 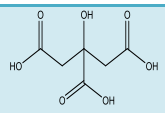 | 192.19 | 106 | 3.08, 4.74, 5.40 | Yes | Response varies with [conc] |

## 3.3 QUININE AND QUININE SALTS

### 3.3.1 STUDY OBJECTIVES

In line with preliminary work outlined in **section 3.2**, sensor response was evaluated using increasing concentrations of aqueous solutions of quinine, quinine hydrochloride and quinine sulphate with the aim of describing sensor response and sensitivity to molecules that are known to be bitter and detectable by the taste sensor. Exploring these molecules would give an indication as to whether the bitterness detection was attributed to the parent compound or the corresponding salt.

### 3.3.2 GENERAL METHODOLOGY

Solutions of quinine and the salts were prepared by the gentle addition of the required quantity of quinine or its salts into a vortex created by the action of a magnetic stirrer. The stirring was continued until all the powder had dissolved for 15 minutes.

*DATA MANIPULATION AND STATISTICAL ANALYSIS*

Six sensor response reading (mV) was obtained for each sample at each concentration; the average ($\bar{x}$) was obtained and plotted against the concentration. Principle component analysis (PCA) was carried out using the following formulae described in **chapter 2**. In addition, in order to establish statistical significance of findings, a one-way analysis of variance (ANOVA) was used. This statistical test was selected because the data being analysed was interval data and more than two means are compared.

### 3.3.3 RESULTS

The relative sensor response patterns of all four sensors are shown in Figure 3.10. Both basic bitterness sensor responses are similar showing clear concentration dependence. In both cases, sensor response does not increase after concentrations of 30mM. Furthermore there is no difference in magnitude of response between the two bitterness sensors at concentrations higher than 30mM. The astringency sensor response gradually decreases from approximately 120mV to 0mV with increasing

concentration. The relative response for acidic bitterness has a sharp increase between 0.1mM and 1.0mM, which was followed by a gradual decrease in sensor response as concentration increases. A one-way ANOVA ($p$= 0.06) showed that there was a statistical difference between the samples under investigation.

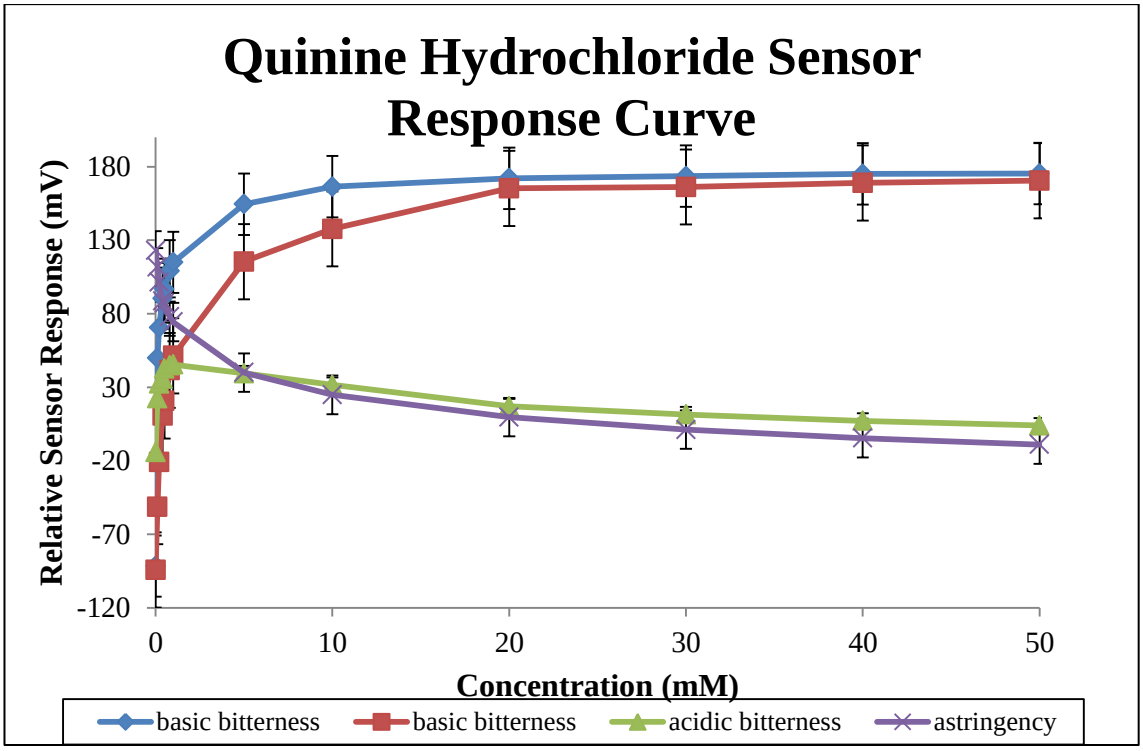


FIGURE 3. 10 RELATIVE SENSOR RESPONSE CURVE FOR QUININE HYDROCHLORIDE DIHYDRATE (QHD), SHOWING RESPONSES OF SENSORS AS A FUNCTION OF CONCENTRATION (N=6, $\bar{x}$± SD)

Figure 3.10 illustrates sensor response across concentration ranging from 0.1mM to 50mM; however the highest rate of change was observed between 0.1mM and 1.0mM, therefore it was necessary to observe sensor response across these concentrations. The sensor response pattern in the region where highest rate of change was observed is illustrated in Figure. 3.11. Both basic bitterness sensors show an increase in sensor response with increasing concentration. This observation is also mirrored by the acidic bitterness sensor. The astringency sensor shows a decrease in sensor response magnitude with increase in concentration. Statistical analysis using a one-way ANOVA ($p$= $4.44x10^{-4}$), showed that there was no statistically significant sensor response with increasing concentrations of quinine hydrochloride. It is worth pointing out that this

analysis only refers to the low concentrations of quinine hydrochloride described in Figure 3.11.

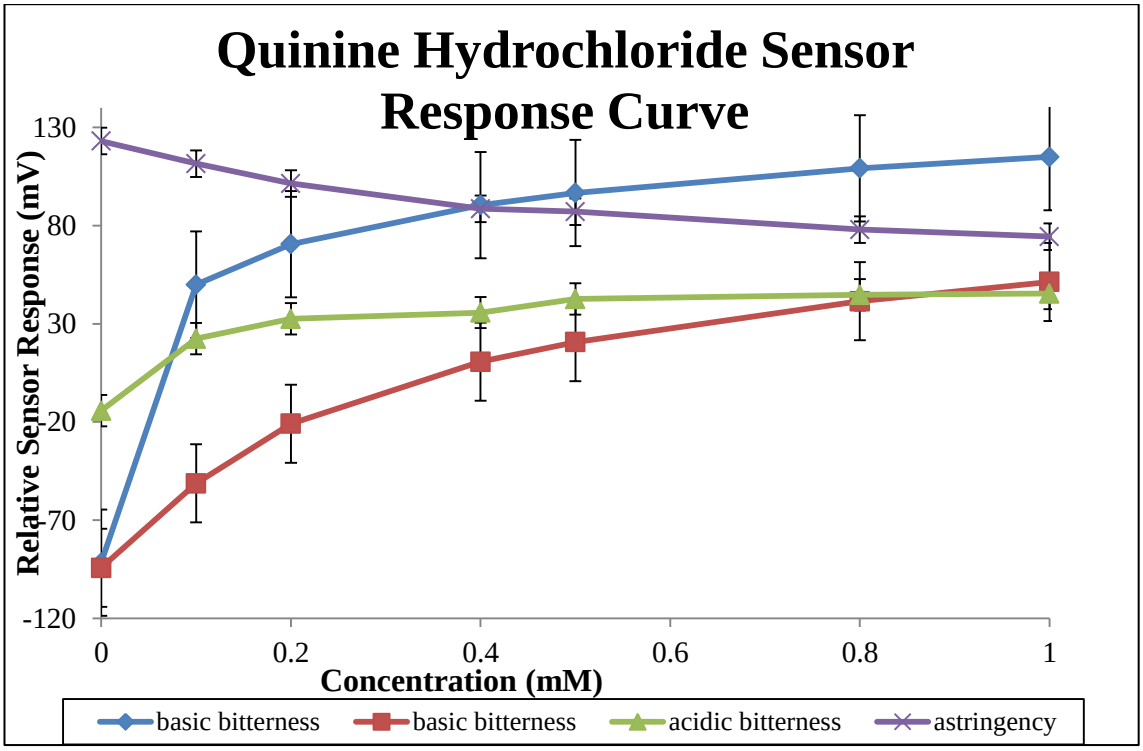


FIGURE 3. 11 RELATIVE SENSOR RESPONSE CURVE FOR QUININE HYDROCHLORIDE DIHYDRATE (LOW CONCENTRATIONS), SHOWING THE RESPONSES AS A FUNCTION OF CONCENTRATION (N=6, $\bar{x}\pm$ SD)

Quinine sulphate, another quinine salt was also investigated. The sensor response patterns are illustrated in Figure 3.12. Both basic bitterness and acidic bitterness sensors exhibit a concentration dependant response to quinine sulphate. Furthermore, the pattern of response is similar to those observed for quinine hydrochloride at similar concentrations. Interestingly, the astringency sensor does not demonstrate concentration dependence. There is no difference in the relative sensor response value between de-ionised water and the quinine sulphate which is confirmed by a one-way ANOVA test ($p= 5.57x10^{-7}$). This suggests that the astringency sensor is not detecting quinine sulphate. This behaviour was not observed with quinine hydrochloride.

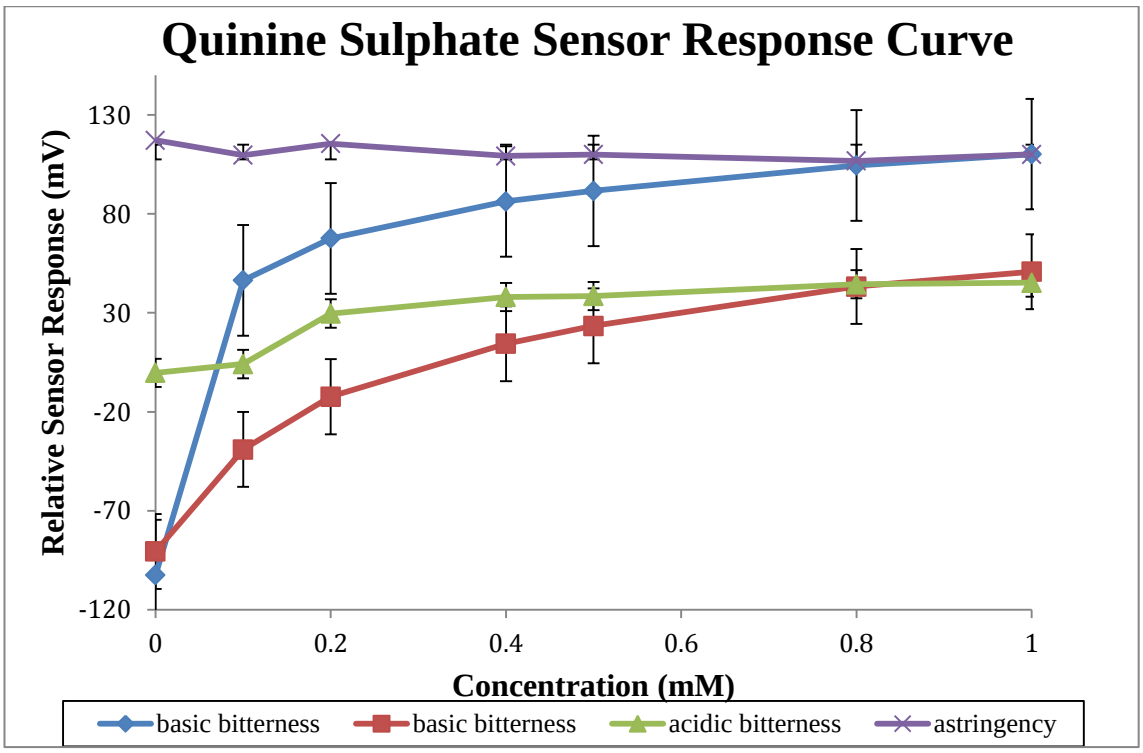


FIGURE 3. 12 RELATIVE SENSOR RESPONSE CURVE FOR QUININE SULPHATE, SHOWING THE RESPONSES OF SENSORS AS A FUNCTION OF CONCENTRATION (N=6, $\bar{x}$± SD)

The preliminary work demonstrated that ionic molecules were easier to detect as compared to neutral molecules, hence it was necessary to investigate quinine base in order to assess the taste sensor's responsiveness. Figure 3.13 illustrates the sensor response patterns to quinine base. Similar to quinine sulphate, both basic bitterness and acidic bitterness sensors show a concentration dependant response. The astringency sensor does not show definitive concentration dependence. The patterns of response for quinine bear resemblance to those observed for quinine sulphate. A one-way ANOVA ($p = 0.003$) showed that there was statistically significant difference between the increasing concentrations of quinine base. Therefore even though quinine is not an ionic molecule it is still detectable. This is because quinine is ionised in water therefore it is detectable. Further explanation is given in section 3.5.2.

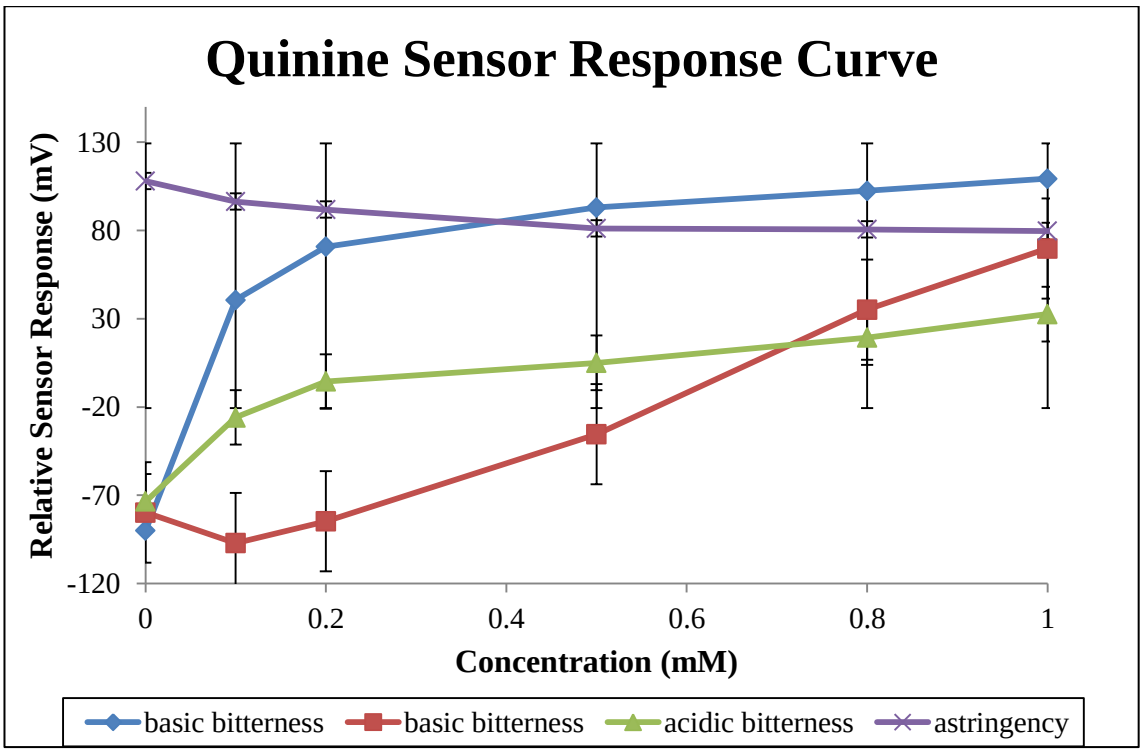


FIGURE 3. 13 RELATIVE SENSOR RESPONSE CURVE FOR QUININE (QN), SHOWING RELATIVE SENSOR RESPONSE AS A FUNCTION OF CONCENTRATION (N=6, $\bar{x}$± SD)

Quinine hydrochloride and quinine differ on a molecular level by the presence of the hydrochloride ion in quinine hydrochloride. Since sensor response patterns were also different, it was necessary to ascertain as to whether the difference was a result of the presence of the hydrochloride ion. Figure 3.14 demonstrates the sensor response patterns of hydrochloric acid which would give the same effect as hydrochloride ion in quinine hydrochloride. The basic bitterness sensors both exhibit concentration dependence. Statistical analysis using a one-way ANOVA ($p$=0.63), showed that there was a statistical difference between the sensor responses with increasing concentrations of hydrochloric acid. Furthermore, there is no difference in response between the two basic bitterness sensors, as shown by an independent sample t-test ($p$= 0.15). The acidic bitterness sensor has a marked increase between 0.1mM and 1.0mM, which is followed by a gradual decrease in sensor response. The astringency sensor also illustrates a gradual decrease in relative sensor response with increasing concentration. In general, all four sensors show concentration dependence and furthermore the rate of change tails off after 50mM. Interestingly, the results observed

for hydrochloric acid are similar to those observed for quinine hydrochloride. However, it is noteworthy that the magnitude of sensor response is markedly different between quinine hydrochloride and hydrochloric acid.

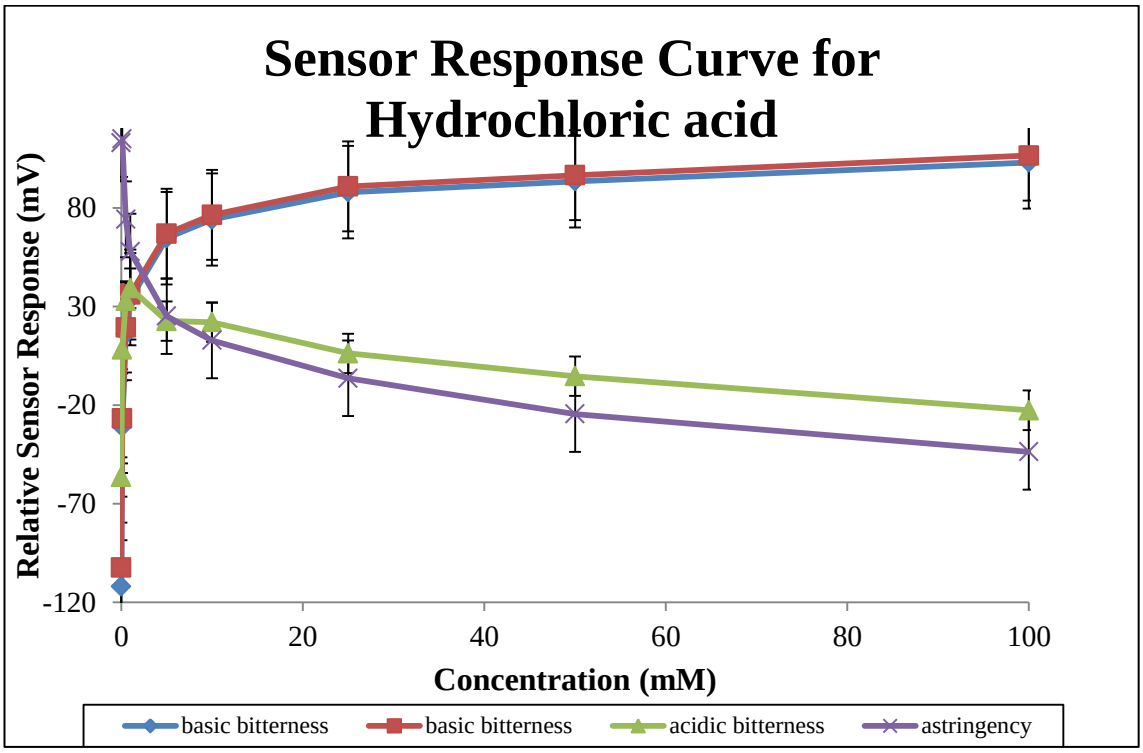


FIGURE 3. 14 RELATIVE SENSOR RESPONSE CURVE FOR HYDROCHLORIC ACID (HCL), SHOWING RELATIVE SENSOR RESPONSE AS A FUNCTION OF CONCENTRATION, (N-6, $\bar{x}$± SD)

In similar fashion to quinine hydrochloride and hydrochloric acid, quinine sulphate was compared to sulphuric acid. The relative sensor response patterns for sulphuric acid are illustrated in Figure 3.15. Both basic bitterness sensors show clear concentration dependence. There is no difference in response between the two sensors. The acidic bitterness sensor show marked increase in response between 0.1mM and 1.0mM, which is then followed by a gradual decrease in relative response. The astringency sensor demonstrates a gradual decrease with increasing concentration of sulphuric acid. Interestingly, the results observed for sulphuric acid are not similar to those observed for quinine sulphate, however they show resemblance to those observed for hydrochloric acid in Figure 3.14. A one-way ANOVA ($p$=0.29), revealed that there was a statistical difference in the sensor responses as the concentration of sulphuric acid increased.

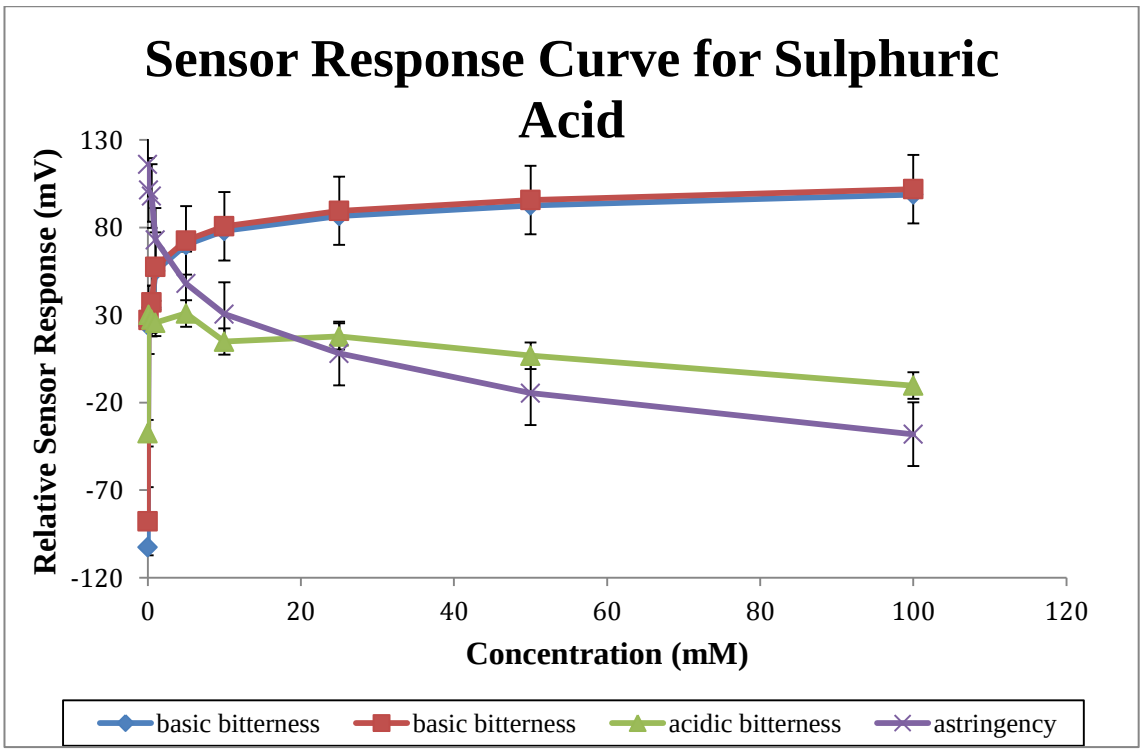


FIGURE 3. 15 RELATIVE SENSOR RESPONSE CURVE FOR SULPHURIC ACID, SHOWING RELATIVE SENSOR RESPONSE AS A FUNCTION OF CONCENTRATION (N=6, $\bar{x}$± SD)

The magnitude of response varies between the drugs as described in Table 3.2, which compares the magnitude of relative sensor response at a single concentration of 1.0mM. When considering basic bitterness sensor 1, there is no statistically significant difference in relative sensor response values between quinine and both its salts investigated. This is verified using a one-way ANOVA ($p$=0.02).However, a marked difference is observed between HCl, sulphuric acid and their quinine salts respectively ($p$=0.47). Possible explanations will be given in **section 3.5**.

For basic bitterness sensor 2, a one-way ANOVA ($p$=0.009), revealed that there is no significant difference between quinine hydrochloride, quinine sulphate and sulphuric acid in terms of magnitude of response. The quinine bases' response is significantly different from that of its salts ($p$=0.10), and similarly HCl response is different of all the other response at this concentration.

The acidic bitterness sensor's values are similar between quinine hydrochloride and quinine sulphate, however the quinine bases' response is significantly different from its respective salts. The relative sensor response magnitude for HCl and sulphuric acid are different from those recorded for quinine and its salts as well as from each other. In relation to astringency, quinine hydrochloride and quinine display statistically similar relative response values. The highest magnitude of response is recorded with quinine sulphate, however it should be noted that this response value has no difference to that recorded for de-ionised water.

TABLE 3. 2 RELATIVE SENSOR RESPONSE VALUES FOR QUININE, QUININE SALTS, HYDROCHLORIC AND SULPHURIC ACIDS.

| Drug | Concentration (mM) | Mean Sensor Response (mV) | | | |
|---|---|---|---|---|---|
| | | Basic bitterness (AN0) | Basic bitterness (AC0) | Acidic bitterness (C00) | Astringency (AE1) |
| **Quinine hydrochloride** | 1.0 | 115 | 51 | 45 | 74 |
| **Quinine Sulphate** | 1.0 | 110 | 50 | 45 | 110 |
| **Quinine base** | 1.0 | 109 | 69 | 32 | 80 |
| **Hydrochloric acid** | 1.0 | 33 | 36 | 39 | 58 |
| **Sulphuric acid** | 1.0 | 55 | 57 | 26 | 73 |

Similar to preliminary work, the responsiveness of the sensors to QHD was investigated when QHD was dissolved in reference solution (QHD-R). Contrary to response patterns observed when QHD in water (QHD-W), only basic bitterness 2 and acidic bitterness sensors responded. As illustrated in Figure 3.16, both these sensors

show an increase in sensor response with increasing concentration. However, for basic bitterness sensor 1 and astringency no concentration dependent behaviour is observed. Moreover, these two sensors appear not to detect QHD-R. The relative sensor response values are not statistically different from that observed for the reference as illustrated by a one-way ANOVA (*p= 0.002*).

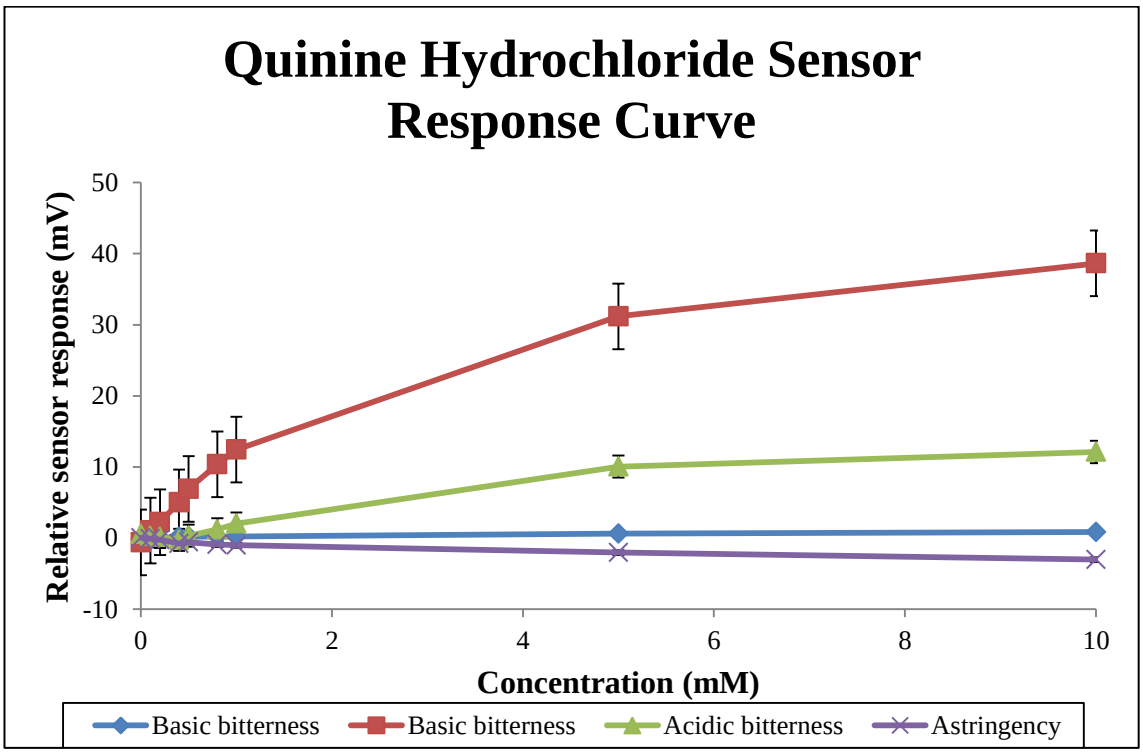


FIGURE 3. 16 RELATIVE SENSOR RESPONSE CURVE FOR QHD DISSOLVED IN REFERENCE SOLUTION (QHD-R), SHOWING RELATIVE SENSOR RESPONSE AS A FUNCTION OF CONCENTRATION (N=6, $\bar{x}$±SD).

*SUMMARY OF RESULTS*

This section has reviewed the detection capability of the Insent® TS5000Z electronic tongue on quinine, quinine hydrochloride and quinine sulphate. All three molecules were detectable on the electronic tongue with statistical significance being shown by a one-way ANOVA. Hydrochloric and sulphuric acids which are comparatively corresponding acids to quinine hydrochloride and quinine sulphate respectively were also detectable, though their magnitude of detection differed from the quinine salts. The significance of these findings will be highlighted in **section 3.5**.

## 3.4 PARACETAMOL, IBUPROFEN AND METFORMIN HYDROCHLORIDE

### 3.4.1 STUDY OBJECTIVE

In the previous section, the detection of quinine and its hydrochloride and sulphate salts was described. However, in order to fully elucidate the mechanism of detection it was necessary to investigate the detection of other active pharmaceutical ingredients (API) which have been reported to be bitter in the literature. The main objective of this study was to investigate the nature of sensor response to paracetamol; ibuprofen and its salt and metformin hydrochloride with a view of describing the mechanism of detection.

### 3.4.2 METHODOLOGY

Solutions of the paracetamol, ibuprofen, and ibuprofen sodium and metformin hydrochloride were prepared by the gentle addition of the required quantity of the API into a vortex created by the action of a magnetic stirrer. The stirring was continued until all the powder had dissolved for 15 minutes. In the case of ibuprofen, each of the ibuprofen solutions was stirred for 4 hours. Due to the long stirring time, solutions for ibuprofen were prepared 24 hours before they were used, whereas all other solutions were prepared on the day of testing. The concentrations used in this section matched those already used in previous work with quinine hydrochloride detailed in **section 3.2.2**. The solutions were tested according to procedure discussed in **chapter 2**.

### 3.4.3 RESULTS

In general, there is no clear concentration dependence observed for paracetamol as illustrated in Figure 3.17. Both basic bitterness sensors do not demonstrate a clear distinction between de-ionised water and the paracetamol samples. The acidic bitterness sensor illustrates a difference in response between de-ionised water and paracetamol however no clear concentration dependence is established. The astringency sensor does not show a clear difference between the de-ionised water and concentration. Overall, these results suggest that paracetamol is not being detected. Woertz et al (2010) published results suggesting a linear log relationship between

sensor response and concentration of paracetamol; however similar results have not been observed despite using similar methodology.

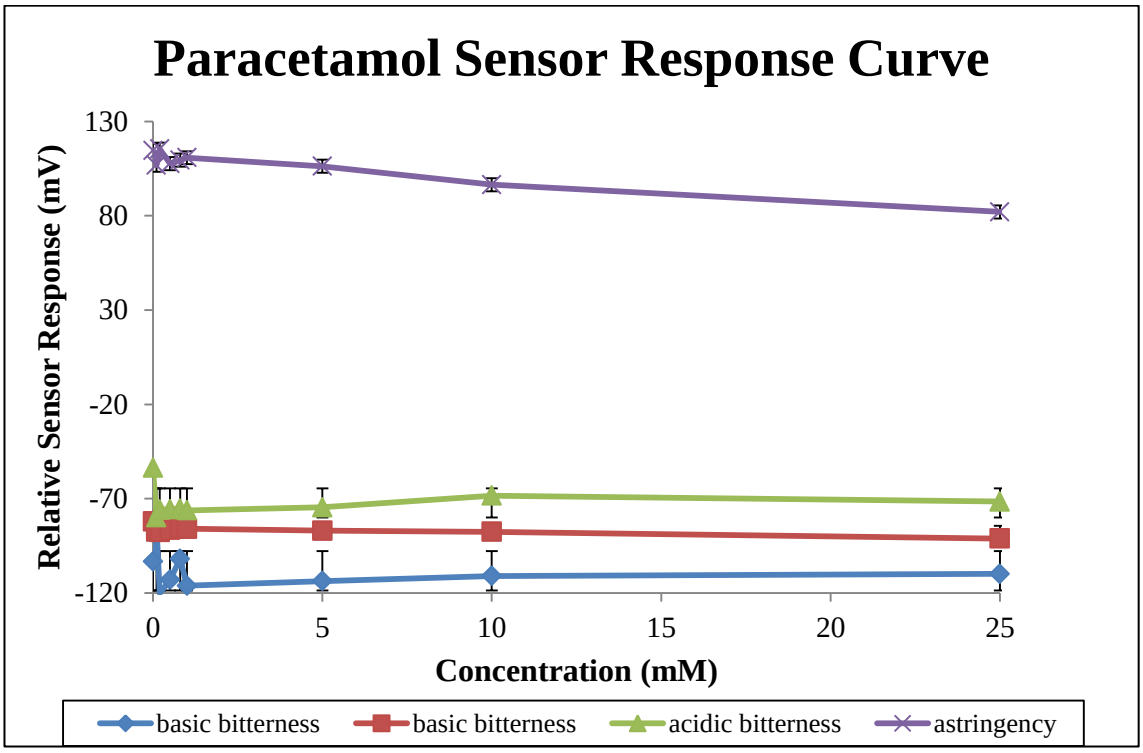


FIGURE 3. 17 RELATIVE SENSOR RESPONSE CURVE OF PARACETAMOL DISSOLVED IN DE-IONISED WATER, SHOWING SENSOR RESPONSES AS A FUNCTION OF CONCENTRATION (N=6, $\bar{x}$±SD)

In-keeping with work already reported for caffeine (**section 3.2.3**) and quinine hydrochloride (**section 3.3.3**), it was prudent to investigate the effect of the solvent on the detection of paracetamol. Dissolving paracetamol in water (Figure 3.17), has shown that there is no statistical difference in the sensor response values of all four sensors with increasing concentrations of paracetamol (one-way ANOVA, $p$= 0.0001). The sensor response patterns of paracetamol after it was dissolved in reference solution (0.3mM tartaric acid + 30mM potassium chloride) are shown in Figure 3.18. The astringency sensor shows a concentration dependent sensor response while the other three sensors show no significant change in sensor response with concentration (one-way ANOVA, $p$=0.007). An explanation for this observation will be given in **section 3.5**.

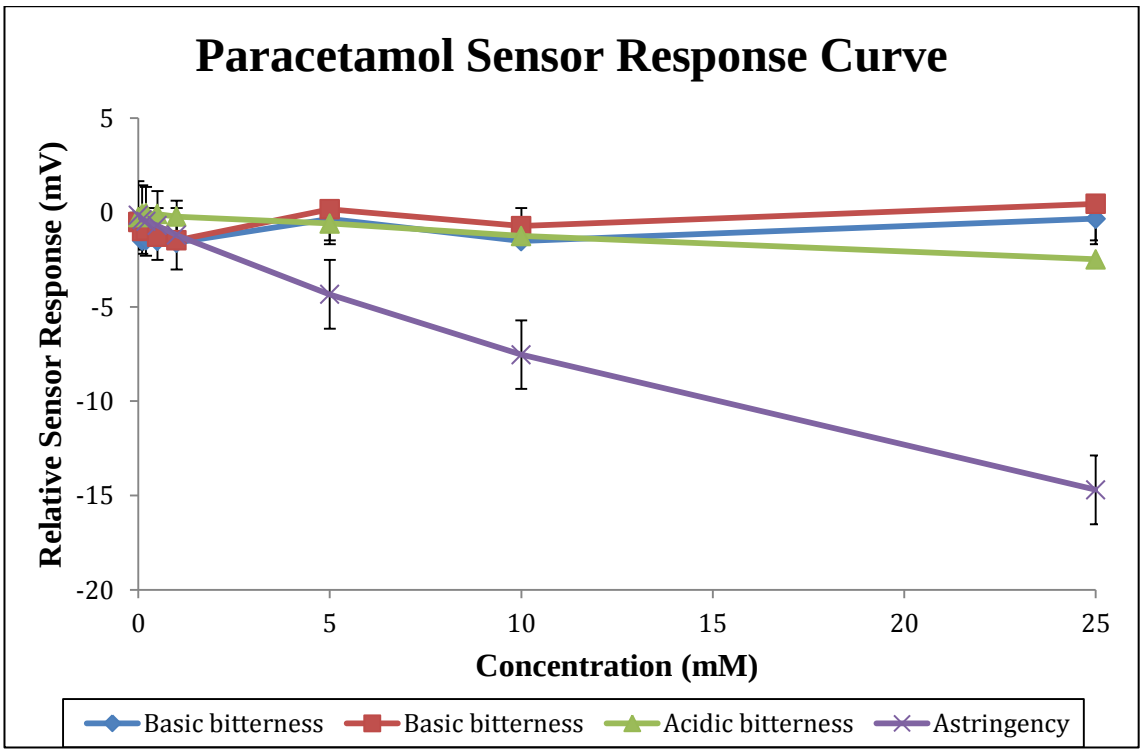


FIGURE 3. 18 RELATIVE SENSOR RESPONSE CURVE FOR PARACETAMOL DISSOLVED IN REFERENCE SOLUTION, SHOWING SENSOR RESPONSES AS A FUNCTION OF CONCENTRATION (N=6, $\bar{x}$±SD)

In Figure 3.19, which illustrates sensor responses to ibuprofen, both basic bitterness and acidic bitterness sensors show a slight variation with increases in concentration. However, the responsiveness appears to stabilise after 0.2mM. The astringency sensor does not show any significant different response with water, which may suggest that this sensor is not detecting the molecule or ibuprofen, does not have astringency as a taste attribute. Ibuprofen is practically insoluble in water hence for the concentrations above 0.5mM ibuprofen were suspended. Reports in the literature suggest that detection of ibuprofen is possible when drug is in suspension (Woertz *et al.* 2011b), however since a suspending agent was not used in this study, it is possible that ibuprofen particles gravitated to the bottom of the vessel and as such the readings obtained only show sensor response to ibuprofen in solution i.e. saturated solutions.

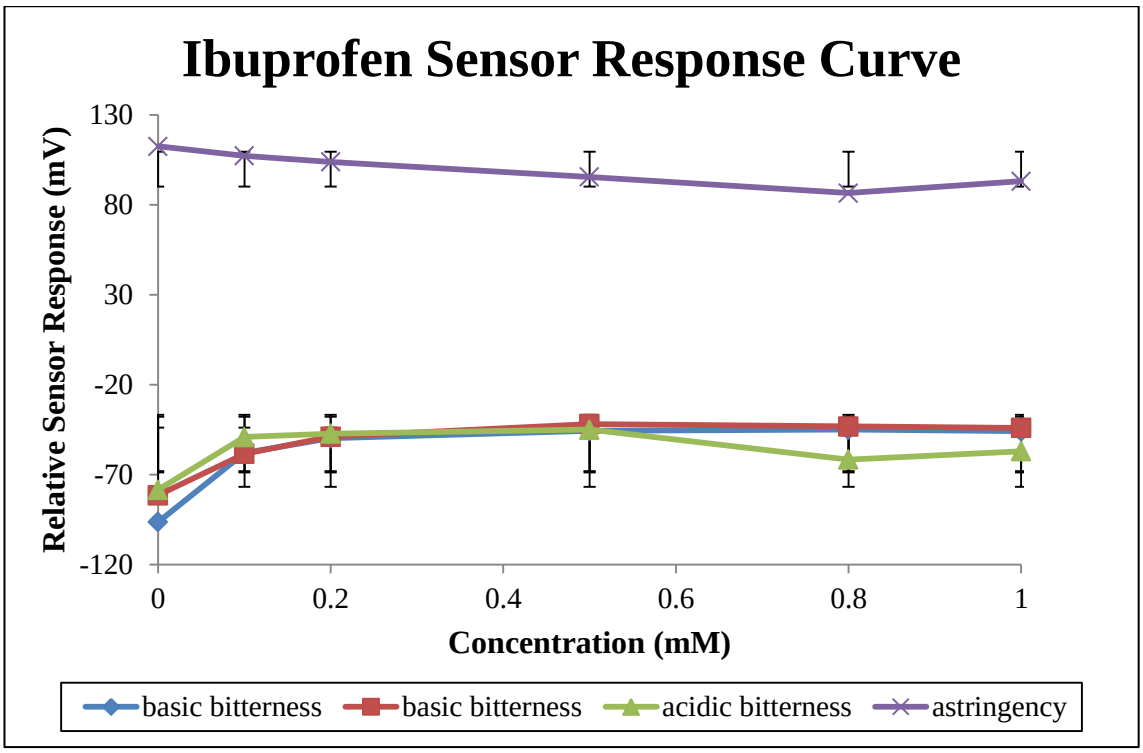


FIGURE 3. 19 RELATIVE SENSOR RESPONSE CURVE FOR IBUPROFEN, SHOWING SENSORS RESPONSE AS A FUNCTION OF CONCENTRATION (N=6, $\bar{x}$±SD)

The relative sensor response observed for metformin hydrochloride across all sensors indicates concentration dependence as shown in Figure 3.20. A one-way ANOVA ($p$= $1.06x10^{-12}$) revealed that there was a statistical difference between the sensor responses with increasing concentration of metformin hydrochloride. Another observation was that the two basic bitterness sensors respond in the same fashion; there was marked increase in response up to 1.0mM after which the rate of change in relative sensor response decreases. This sensor response pattern is similar to that observed for quinine hydrochloride and hydrochloric acid. The acidic bitterness sensor response pattern seems to decrease initially before a gradual increase after 1.0mM. This response appears inverted when compared to the same sensors' response to quinine hydrochloride and hydrochloric acid. The astringency sensors response also demonstrates concentration dependence. There is a gradual decrease in sensor response with increasing concentration of metformin. This pattern is similar to that observed with quinine hydrochloride. However, it is noteworthy that the magnitude of the relative sensor response differs between the two hydrochlorides.

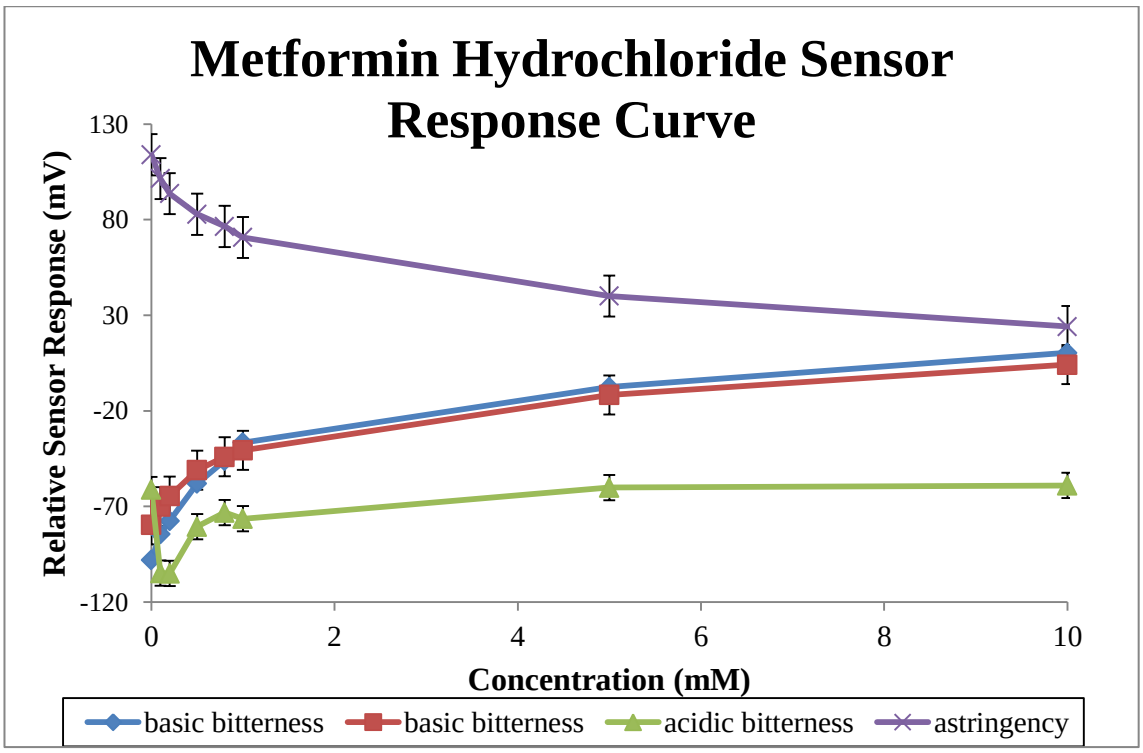


FIGURE 3. 20 RELATIVE SENSOR RESPONSE CURVE OF METFORMIN HYDROCHLORIDE, SHOWING SENSORS RESPONSE AS A FUNCTION OF CONCENTRATION, (N=$\bar{x}$±SD)

The relative sensor response values given in Table 3.3, paints a picture that paracetamol has the highest magnitude of response. However, it is noteworthy that the values observed for paracetamol have no statistical difference to those recorded for water (one-way ANOVA, $p$=2.28x10$^{-4}$.)

TABLE 3. 3 RELATIVE SENSOR RESPONSE VALUES OF PARACETAMOL, METFORMIN HYDROCHLORIDE AND IBUPROFEN

| Drug | Concentration (mM) | Sensor Response (mV) | | | |
|---|---|---|---|---|---|
| | | Basic bitterness (AN0) | Basic bitterness (AC0) | Acidic bitterness (C00) | Astringency (AE1) |
| **Paracetamol** | 1.0 | -116 | -86 | -76 | 111 |
| **Metformin hydrochloride** | 1.0 | -37 | -41 | -76 | 71 |
| **Ibuprofen** | 1.0 | -46 | -44 | -57 | 93 |

Principle component analysis (PCA) was performed on all drugs investigated in sections 3.3 and 3.4. Only the first two principle components have been used for the biplot. This is because, the cumulative values of the first principle component (PC1) and second principle component (PC2) account for approximately 97% of data variation (as shown in Table 3.4) therefore a two axis plot represents a statistically acceptable amount of data. It should also be noted that where significance level is greater than 0.05, there is no difference between principle components 2 and 3.

TABLE 3. 4 EIGENVALUES OF THE COVARIANCE MATRIX

| PCA | Eigenvalue | Percentage (%) of Variance | Cumulative (%) | χ2 | Degrees of Freedom | Significance level (p) |
|---|---|---|---|---|---|---|
| **1** | 13504.81 | 90.57 | 90.57 | 36.51 | 9 | $3.22 \times 10^{-5}$ |
| **2** | 953.53 | 6.39 | 96.96 | 7.74 | 5 | 0.17 |
| **3** | 377.24 | 2.53 | 99.49 | 3.40 | 2 | 0.18 |
| **4** | 76.10 | 0.51 | 100.00 | 0 | 0 | 0 |

The extraction eigenvectors give the contribution of each of the sensors to each principle component. These have been given in table 3.5. Essentially PC1 is primarily related to the basic bitterness1 sensor while PC2 is composed on basic bitterness 2 and 3. Therefore, the separation of the APIs is heavily influenced by the basic bitterness1 sensors on the *x*-axis and the basic bitterness and acidic bitterness sensors on the *y*-axis.

TABLE 3. 5 EXTRACTED EIGENVECTORS FOR PC1 AND PC2

| | Coefficient of PC1 | Coefficient of PC2 |
|---|---|---|
| **Basic bitterness1** | 0.78 | -0.67 |
| **Basic bitterness2** | 0.51 | 0.51 |
| **Acidic bitterness3** | 0.42 | 0.53 |
| **Astringency** | -0.10 | -0.03 |

The biplot illustrated in Figure 3.21, displays both the loading and the scores for the selected principle components. All the APIs under investigation are plotted as a scatter plot (in red dots). The APIs tested were at the same concentration i.e. 1mM. There is no significant difference between the predicted taste attributes between the quinine salts. The biplot shows that both quinine salts are close to the *x*-axis, which has loading of the basic bitterness1 sensor therefore suggesting basic bitterness for both quinine salts. In addition, the positioning of the two salts on the biplot overlap and therefore no separation between them. No significant difference was observed between hydrochloric acid and sulphuric acid. Interestingly, the biplot suggest both basic and acidic bitterness for the two acids. This is significantly different to the basic bitterness suggested for the quinine salts. The biplot also shows a significant difference between quinine and its salts. More importantly, the results suggest that the two salts are more bitter compared to quinine.

Paracetamol, ibuprofen, metformin lie in the loading direction of the astringency sensor which is in the opposite direction and of less magnitude than the bitterness sensors. For both principle components astringency has negative contribution, which suggests that it has no significant contribution. Therefore paracetamol, ibuprofen and metformin which are close to water display insignificant response with respect to the principle components observed.

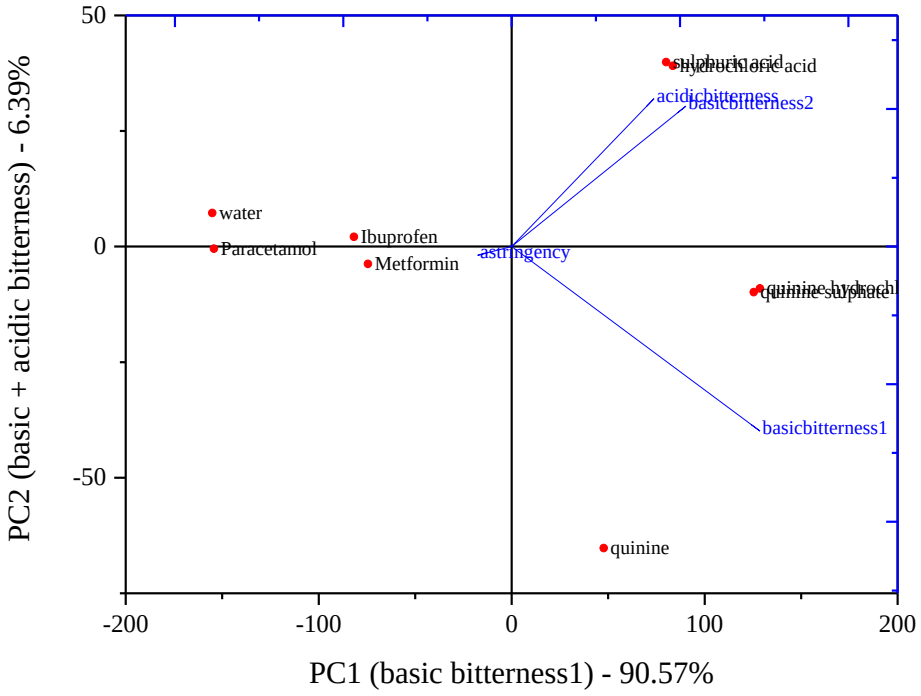


FIGURE 3. 21 A BIPLOT SHOWING PRINCIPLE COMPONENT ANALYSIS COMPARISON BETWEEN WATER AND PARACETAMOL, IBUPROFEN, METFORMIN, QUININE, QUININE SALTS, HYDROCHLORIC AND SULPHURIC ACIDS IN TERMS OF THEIR PREDICTED TASTE ATTRIBUTES TOGETHER WITH THE LOADING PLOT OF THE RESPONSIVE SENSORS.

## 3.5 DISCUSSION

There is no difference in sensor response to caffeine, theobromine and theophylline as compared to deionised water. This suggests that the methylxanthines are not being detected. Investigation of caffeine citrate revealed logarithmic concentration dependence between the relative sensor response and increase in concentration across all four sensors. The same relationship was observed when citric acid was investigated and therefore suggesting that the citrate was responsible for the relationship observed in caffeine citrate and this further demonstrates that caffeine was not being detected.

Quinine, quinine hydrochloride and quinine sulphate all demonstrate statistically significant differences when compared with de-ionised water, which suggests that all three molecules are being detected. Their sensor responses showed concentration dependence, particularly for both basic bitterness sensors. In all the cases, the basic

bitterness1 sensor and acidic bitterness sensors reveal an identical pattern. However, the magnitude of response differs for each molecule. With respect the basic bitterness2, quinine hydrochloride and sulphate have similar patterns which are different to that illustrated for quinine base. The astringency sensor results did not demonstrate conclusive concentration dependence. Astringency response to quinine hydrochloride appears to be concentration dependant, however this relationship is not observed for quinine or quinine sulphate. In fact, for the latter, the astringency sensor response is no different to de-ionised water. This therefore suggests that the astringency sensor has limited detection capability or quinine molecules have no astringency. Since this is the first time a study comparing the responsiveness of taste sensor to quinine and its salts has been reported, there were no reports in literature to compare with.

No significant sensor response was observed when paracetamol was compared with de-ionised water. This suggests that paracetamol is not being detected by taste sensor Woertz et al (2011) conducted the same study on paracetamol and reported a log linear relationship between sensor response and paracetamol. We have not found similar results. This may be due to the fact that our comparison was between paracetamol response and water, whereas Woertz et al (2011) only looked at paracetamol alone which therefore could have created a false positive reading. Further. It is also possible that different batches of sensors used could have given different readings.

Sensor response to ibuprofen does not demonstrate conclusive evidence to be different to de-ionised water. Furthermore no concentration dependence is observed. It can therefore be concluded that ibuprofen is possibly not being detected by the taste sensor. Woertz et al (2011) investigated ibuprofen in a similar fashion and suggested that a linear log relationship was observed but either a small slope was observed or only a few sensors demonstrated response. The results observed show some response at 0.1mM from both basic bitterness sensors, however no further response is

detected at concentrations higher than this. Furthermore, the astringency and acidic bitterness sensors do not show a difference to de-ionised water. Hence, there is inconclusive evidence to suggest that ibuprofen is being detected.

All four sensors show clear response to metformin hydrochloride as there is a statistically significant difference in relative sensor responses of metformin compare to de-ionised water. Additionally, sensor response also appears to be concentration dependant. The largest rate of change in relative sensor response is observed between the concentrations of 0.1 to 1.0mM. Interestingly, the general shape of the sensor response curves for metformin hydrochloride are similar to those observed for quinine hydrochloride; the magnitude of response is however different. This is the first time that metformin detection has been investigated using the TS; therefore we have no basis of comparison in the literature.

Three factors have been identified that could affect the detection of a drug by the taste sensor, namely:

- Interaction between detecting sensor and ions
- Extent of dissociation / ionisation of electrolyte
- Concentration
- Effect of solvent

### 3.5.1 INTERACTION BETWEEN DETECTING SENSOR AND IONS

The artificial lipid sensors on the taste sensor, are designed to detect different taste attributes. For the purposes of this study focus will be on bitterness and astringency taste detection. The composition of each of the sensors used in this study is given in Table 3.6 which describes the lipids and plasticisers used for each sensor type. The structures of each of the lipids as well as the plasticiser have been presented in **chapter 1**.

TABLE 3. 6 COMPOSITION OF SENSORS (BITTER DRUG SENSOR SET) ADAPTED FROM THE INSENT TASTE SENSING SYSTEM MANUAL (2010)

| | **Name of Taste Sensor** | **Characteristic** | **Composition (Artificial lipid + plastisicer** |
|---|---|---|---|
| **Positively charged membrane** | C00 | Evaluates bitterness and acidic bitterness | Tetradodecylammonium bromide + 2-Nitrophenyl octyl ether |
| | AE1 | Evaluates astringency and aftertaste from astringency | Tetradodecylammonium bromide + dioctyl phenylphosphonate |
| **Negatively charged membrane** | AC0 | Evaluates basic bitterness | hexadecanoic acid + dioctyl phenylphosphonate |
| | AN0 | Evaluates basic bitterness | phosphoric acid di-*n*-decyl ester + dioctyl phenylphosphonate |

The acidic bitterness sensor has a positively charged membrane, therefore it is expected that when immersed in aqueous solution the stern layer is composed primarily of anions while the diffuse layer will be comprised of cations. This is also true for the astringency sensor. The basic bitterness sensors however, are both negatively charged therefore it is expected that the stern layer will be predominately composed of cations while the diffuse layer will largely contain anions. Since the membranes are already charged, it is also expected that the drug either dissociate (if it is an ionic molecule) or be its ionised form in order to create a change in membrane potential.

To recap, the Gouy-Chapman- Stern theory states that when an artificial lipid based membrane is immersed in aqueous solution, an electrical double layer (stern and diffuse layer) is formed at the surface of the membrane. The double layer is a result of

the dissociation of the acid groups of lipid molecules hence causing a membrane potential. The stern layer either positive or negative comprises of ions adsorbed directly onto the membrane due to chemical interactions. The diffuse layer is composed of ions attracted to the surface charges via Coulomb force, electrically screening the stern layer. However, almost all the theoretical work on this theory has been based on the assumption that the cations and anions in question differ only in charge. In physical systems such as those investigated in this study, there is no reason to expect these symmetries. Ions are of varying dimensions and this alone can lead to different distances of approach. What is probably more important is that in order to approach the membrane surface, an ion has to penetrate the solvent. It is expected that different ions will behave differently in this matter. In particular, water interacts in an asymmetric way cations and anions so that a consistent bias is observed between cations and anions with regards to effective radii describing approach to the membrane surface.

Table 3.7 describes which cation / anion is theoretically expected to be in the stern layer of each sensor. Looking initially at the acidic bitterness sensor, for quinine hydrochloride, hydrochloric acid and metformin hydrochloride, the chloride ($Cl^-$) ion, is expected to be anion in the stern layer. However a closer look at the magnitude of sensor response at 1.0mM reveals that hydrochloric acid has the highest magnitude of response, followed by quinine hydrochloride and finally metformin. This relationship is also observed for the astringency sensor. Although, in all the three cases the stern layer is expected to have the same anion, the observed results demonstrate that the sensor response is not just due to the anion in the stern layer. Therefore, the cations in the diffuse layer could be affecting the overall response.

Expanding the Gouy-Chapman-Stern theory, the electrical distribution is equivalent to the double layer of charge i.e. stern and diffuse layers. The potential at the stern layer is the electro-thermodynamic (Nernst) potential (E), is defined as the difference in the

potential between the actual membrane surface and the electro-neutral region of the solution. The potential located at the shear plane (plane separating stern and diffuse layers), is known as the electro-kinetic or zeta (ζ). The zeta potential is defined as the difference in the potential between the shear plane and the electro-neutral region of the solution. Increasing the concentration of an electrolyte in this system increases the screening effect of the counter-ion thus resulting in a rapid fall in zeta potential. The distance of the electrical double layer decreases. It is the changes in both E and ζ potentials that are recorded as the sensor response.

The extent of dissociation of each of the drugs in solution could affect the magnitude of sensor response. In the case of the sulphate ion ($SO_4^{2-}$), the acidic and astringency sensors demonstrate highest response to $H_2SO_4$ as opposed to quinine sulphate. This again indicates that the anion in the stern layer is not solely responsible for the sensor response observed.

TABLE 3. 7 CATIONS AND ANIONS FORMING STERN LAYER FOR EACH SENSOR

| | QHD | QhS | HCl | Sulphuric acid | Metformin |
|---|---|---|---|---|---|
| **Acidic bitterness (C00)** | $Cl^-$ | $SO_4^{2-}$ | $Cl^-$ | $SO_4^{2-}$ | $Cl^-$ |
| **Astringency (AE1)** | $Cl^-$ | $SO_4^{2-}$ | $Cl^-$ | $SO_4^{2-}$ | $Cl^-$ |
| **Basic bitterness1 (AC0)** | $Qn^{2+}$ | $Qn^{2+}$ | $H^+$ | $H^+$ | $Mt^+$ |
| **Basic bitterness2 (AN0)** | $Qn^{2+}$ | $Qn^{2+}$ | $H^+$ | $H^+$ | $Mt^+$ |

Qn = Quinine, Mt = Metformin

The basic bitterness sensors are both negatively charged, therefore the stern layer is expected to be comprised of cations. In the case of quinine hydrochloride and quinine sulphate, the quinine ion is the cation. For both sensors the higher response value is observed for quinine hydrochloride. However, comparing these result to hydrochloric and sulphuric acid where the cation become $H^+$ revealed both acids to have a significantly higher response from the sensors. There are two possible explanations namely:1) The different radii of the cations means different distances of approach which in turn affects the change in membrane potential or 2) The molecules have different dissociation profiles which in turn affects the concentration of charges species in the system. The relative sensor response values for metformin hydrochloride at 1.0mM are higher than quinine salts but lower than the acids. .

### 3.5.2 EXTENT OF DISSOCIATION / IONISATION OF ELECTROLYTE

The Arrhenius theory of electrolytic dissociation defines strong electrolytes as those that dissociates into ions to a high degree, and a weak electrolyte as one that dissociates into ions to a low degree. In this study strong electrolyte refers to HCl and $H_2SO_4$, while weak electrolytes are quinine hydrochloride, quinine sulphate and metformin hydrochloride. It is noteworthy, that a strong electrolyte can be completely ionised and yet incompletely dissociated into free ions, thus the solution of a strong electrolyte has an “effective concentration”, a.k.a. activity. In general, the activity is less than the actual or stoichiometric concentration of the solute, not because the strong electrolyte is only partially ionised but because some of the ions are effectively “taken out of play” by the electrostatic forces of interaction between them. In solutions of weak electrolytes, regardless of concentration, the number of ions is small and the inter-ionic attractions are correspondingly insignificant. Hence, the Arrhenius theory and concept of degree of dissociation are valid for solutions for weak solutions but not for strong electrolytes unless they are in extremely dilute solutions like those used in this study. The results observed in this study show that the strong electrolytes have a higher magnitude of sensor response compared to the weak electrolytes. Although the solutions being compared are at the same concentration, it is apparent that the

difference in sensor response is linked to the difference in degree of dissociation. The strong electrolytes which are completely ionised and dissociated have more ions in solution which interact with the electronic tongue. The opposite is true for the weak electrolytes.

The degree dissociation of electrolytes depends on; the nature of the electrolyte; the degree of dilution and temperature. In this study, the degree of dilution (concentration) was varied to establish concentration dependence for each drug. However, in order to directly compare the drug a single concentration was used (1.0mM) as shown in Tables 3.2 and 3.3. Therefore, concentration and temperature were kept constant allowing any differences observed to be linked to the nature of the molecule i.e. degree of ionisation. The Henderson – Hasselbalch equation (Equation 3.2 and Equation 3.3) describes the link between pH, pKa and the degree of ionisation for a weak acid or weak base (Martin Alfred *et al.* 1973). It also shows that a drug is completely ionised or non- ionised (as appropriate) when two pH units away from its pKa.

$$pH = pK_a - log_{10}[A^-]/[HA]$$

EQUATION 3.10

$$pH = pK_a + log_{10}\left[\frac{[HA]}{[A^-]}\right]$$

EQUATION 3.11

If the $pK_a$ or $pK_b$ value of the drugs and the pH of the solutions are known then the degree of ionisation of the drugs can be calculated from the re-arranged Henderson-Hasselbalch equations for weak acids and bases (Equation 3.4 and Equation 3.5) respectively.

$$log_{10}\left[\frac{[HA]}{[A^-]}\right] = pK_a - pH$$

EQUATION 3.12

$$log_{10}\left[\frac{BH^+}{[B]}\right] = pK_b - pOH$$

EQUATION 3.13

As an example, the pKa for paracetamol is 9.38, the measures pH of the solution was 6.2, therefore from Equation 3.4:

$$log_{10}\left[\frac{[HA]}{[A^-]}\right] = 9.38 - 5.54$$

$$[HA]:[A^-] = 10^{3.18} = 1513.56:1$$

Therefore, at the measuring conditions in this study, paracetamol is largely non-ionised hence it is not easily detected by the electronic tongue. The ionised: non-ionised ratios of all the other APIs used in this study are calculated in a similar manner to paracetamol and presented in Table 3.8

Application of the Henderson-Hasselbalch equation in this study has revealed that where the drug is un-ionised, the molecule is not detected by the taste sensor. This is a significant finding as the degree of ionisation can be used as a predictor of detection capability by taste sensor. As shown in Table 3.8, quinine and quinine hydrochloride are ionised hence detectable. When considering metformin hydrochloride, it is ionised in both basic and acidic pH due to the presence of primary, secondary and tertiary amines on its structure which can either accept or donate a proton depending on pH. Therefore it is always detectable on the taste sensor. It is noteworthy that the biplot in Figure 3.21 illustrates that although metformin is detected, once compared to other APIs i.e. quinine and its salts, its detection is insignificant. No reports have been found in literature regarding the pKa values of caffeine citrate and quinine sulphate. However, both are ionic molecules therefore are both dissociated in solution and as such are detectable.

TABLE 3. 8 PKA, PH AND PREDICTION OF EXTENT OF IONISATION USING HENDERSON – HASSELBALCH EQUATION

| Drug | Literature pKa | Measured pH at [1.0mM] | Non-ionised : ionised ration ([HA]: [A-]) | Predominant form |
|---|---|---|---|---|
| **Hydrochloric acid** | < 1 | 2.54 | ----- | ionised |
| **Sulphuric acid** | < 1 | 2.54 | ----- | ionised |
| **Caffeine** | 10.4 | 7.01 | 2454.71 : 1 | un-ionised |
| **Theobromine** | 9.9 | 5.37 | 33884.4 : 1 | un-ionised |
| **Theophylline** | 8.62 | 5.41 | 1621.81 : 1 | un-ionised |
| **Caffeine citrate*** | ---- | 3.04 | ----- | |
| **Citric acid** | 3.08 | 4.40 | 0.05 : 1 | ionised |
| **Quinine** | 4.21 | 8.34 | 7.41 x 10-5 : 1 | ionised |
| **Quinine hydrochloride** | 4.33 | 5.74 | 0.04 :1 | ionised |
| **Quinine sulphate*** | ----- | 5.05 | ---- | ------ |
| **Paracetamol** | 9.38 | 5.54 | 6918.31 : 1 | un-ionised |
| **Ibuprofen** | 4.61 | 3.94 | 4.68 : 1 | un-ionised |
| **Metformin hydrochloride** | 12.4 | 5.92 | 3019951: 1 | ------ |

* no values quoted in literature.

### 3.5.3 CONCENTRATION

Investigating concentration dependence is vital for establishing sensor response. It begs to reason that different concentrations of the same drug should elicit different levels of sensor response. For quinine, quinine hydrochloride, quinine sulphate, HCl, $H_2SO_4$ and metformin hydrochloride all exhibited concentration dependence. With the

exception of metformin hydrochloride, the concentration dependence levelled off after 50mM. At this point we do not have enough evidence to generalise this observation to all API. However, it is important to note that concentration does affect sensor response and thus a concentration response curve should always be used to establish saturation concentration i.e. concentrations above which any further increases in concentration does not result in increases in sensor response. Sensor concentration curves are also important for establishing sensor response against a known standard. Based on the Gouy-Chapman-stern layer theory, a finite amount of cations/ anions can adhere to the membrane thus affecting a sensor response. This therefore implies that once the finite point has been reached, no further sensor response can be observed. The biplot displayed in Figure 3.21 suggests hydrochloric and sulphuric acid as having significant contribution from both basic bitterness1 and 2 and acidic bitterness sensors. This is in line with the magnitude values observed for the two acids in comparison with the other drugs. Quite rightly, PCA has identified the two acids as contributing to the most variation for the data observed. Variation of data in this case relates to magnitude of deviation from standard i.e. de-ionised water. However, reports in literature identify the detection of protons as the mechanism of detection for the sour taste attribute in humans (Breslin *et al.* 2006, Breslin *et al.* 2008). Therefore, it has been established in the literature that the presence of acids gives rise to sour taste, yet the taste sensor predicts highest magnitude of response from basic and acidic bitterness. The manufactures also have on sale a sour sensor which could have been used in this study. However, it is interesting that the sensors that are designed to detect basic bitterness and acidic bitterness respond more to HCl and $H_2SO_4$, molecules that are known to be sour, over quinine hydrochloride the molecule which the manufactures used as a bitterness standard. This discovery leads us to conclude that the mechanism of sensor response is highly dependent on dissociation / ionisation profile of the drug in question. Furthermore, it leads to the question- if detection and response are dependent on ionisation/ dissociation profile is the taste sensor measuring true taste attributes or the extent of dissociation/ ionisation in solution of the drug.

### 3.5.4 A NOTE OF SENSOR LONGEVITY

An issue that has not been discussed thus far is the lifespan of the sensors of the electronic tongue. This requires discussion because there is a significant financial implication in terms of overheads. More importantly, the longevity of the sensors impacts directly on the reliability of the measurement obtained. Table 6.1 gives a summary of the average number of cycles and days that each sensor had to be replaced throughout this study period. It is noteworthy that the acidic bitterness sensor was replaced almost twice as much as the basic bitterness sensors and three times as much as the astringency sensor. All sensors were stored and maintain as per manufactures' guidance with the exception of they were thoroughly rinsed with distilled water at the end of each experimental cycle. Only a single operator used the sensors in question therefore any operator error would have applied to all sensors. Therefore, the reasons for this difference in longevity remains unknown, however the manufacturers have been notified of this finding and are considering this data.

TABLE 3. 9 SUMMARY OF SENSOR USAGE THROUGHOUT THE STUDY

| **Sensor** | **Number of cycles before replacement ($\bar{x}$± SD)** | **Number of days before replacement ($\bar{x}$)** | **Number of times replaced** |
|---|---|---|---|
| **Basic bitterness (AC0)** | 293 | 88 | 5 |
| **Basic bitterness (AN0)** | 312 | 94 | 5 |
| **Acidic bitterness (C00)** | 156 | 51 | 9 |
| **Astringency (AE1)** | 399 | 123 | 3 |

## 3.6 CONCLUSIONS

This study has shown that caffeine, theophylline, theobromine, paracetamol and ibuprofen are not detected by the taste sensor as no difference is observed between de-ionised water and increasing concentrations of these drugs. Quinine and its salts, hydrochloric acid, sulphuric acid, caffeine citrate, citric acid and metformin hydrochloride all show concentration dependant sensor response. The latter molecules are detected by the taste sensor due to the fact that they are either ionised or dissociated in solution. Hydrochloric and sulphuric acid which are strong acids are fully dissociated in solution and therefore give the highest magnitude of sensor response.

The suggested mechanism of sensor response is based on the Gouy – Chapman – Stern theory, i.e. when a lipid membrane is placed in aqueous solution an electrical double layer is formed. It is the change in this electrical double layer, caused by the presence of drug that is being measured and amplified by taste sensor. However, the extent to which the drug affects the change in membrane potential is mostly due to dissociation or ionisation extent of the molecule at the given concentration. This study has shown that those molecules that dissociate to a greater extent i.e. hydrochloric and sulphuric acid give highest magnitude of response. It has also shown that use of the Henderson – Hasselbalch equations can be used to predict the extent of ionisation hence predict if the drug can be detected or not. Drugs that are either ionised or dissociated salt forms in solutions can be detected unlike those that are non-ionised. The extent of ionisation is dependent on the pH of the system, therefore in order to validate that proposed mechanism it is necessary to explore the effect of pH on the detection of ibuprofen. Literature reports ibuprofen pKa at 4.61, therefore at pH 5-7, ibuprofen will be ionised and should be detectable.

PCA reports hydrochloric and sulphuric acid having the most deviation from de-ionised water, when using a bitter drug sensor set i.e. sensors designed to detect bitterness and astringency. However, literature reports both acids to be sour and moreover it is well understood that sour taste perception in humans is innervated by hydrogen ions.

Quinine hydrochloride was used as a bitterness standard by the manufactures and it is reported to be bitter in literature yet its magnitude of response is lower than that of the two acids. This observation raises questions regarding the accuracy of each sensor response. Arguably, a bitterness sensor should respond more to a bitter drug than a sour drug. This study has shown that the sensor response is largely dependent on extent of ionisation / dissociation. Therefore, regardless of the "label" applied to the sensor i.e. bitter, astringent – sensors respond to highly ionised / dissociated molecules but this is not a true indicator of the taste of the molecule in question. We propose a further study to expose the sour sensor to hydrochloric acid, sulphuric acid and quinine hydrochloride, with the aim of comparing the magnitude of sensor response of the bitter sensors to the sour sensor. If our theory on sensor response is correct, then the order of magnitude of sensor response will be identical across the sensors.

It has also demonstrated in this study that for any taste assessment using taste sensor, it is necessary to initially conduct a concentration response curve and more importantly, to compare the sensor response of the unknown tastant molecule to a known reference i.e. de-ionised. It should be noted that the taste sensor will respond to the blank i.e. de-ionised water and therefore a comparison against the blank will allow the user to differentiate between the blank's response and a true response. The concentration response curve is also very useful for verifying the detection of the molecule in question.

# CHAPTER FOUR
# TASTE ASSESSMENT OF EXTEMPORANEOUSLY PREPARED AMLODIPINE FORMULATIONS

# CHAPTER 4- TASTE ASSESSMENT OF AMLODIPINE

In the biography on the life of his children, Charles Darwin astutely noted that children live in different sensory worlds compared to adults. They exhibit heightened preferences for sweet tasting substances and a greater rejection of bitter tasting substances. These preferences differ between the different paediatric age groups i.e. neonates (≤ 28 days), infant (1 month – 2 years), young children (2-6 years), children (6-12 years) and adolescence (12-18 years); with the adolescent taste preferences mirroring those of an adult. As the child grows the positive hedonistic responses to strong sweets seem to decline in late childhood and adolescence (Cowart 1981). Moreover taste perception also changes between health and disease (Schiffman 2007). This variation in taste preference in children of different ages presents a challenge in terms of taste masking strategies.

In recognising that “children are not small adults”, the European Medicines Agency (EMEA) published the paediatric regulation (EC No. 1901/2006), which came into effect in January 2007. This regulation requires the early submission of a pharmaceutical development plan for medicines: a paediatric investigation plan (PIP). The applicant is required to provide an overview of planned measures / performed studies of which taste masking and assessment are of particular relevance. The applicant is expected to demonstrate paediatric acceptability of the product. However, debates are still ongoing as to the definition of acceptability. Questions are still being raised that, if the product is presented to children, what percentage of these children giving positive affirmation is deemed acceptable. Furthermore, other questions revolve around whether acceptability referring to the type of formulation, ease of dose adjustment for the different paediatric populations, mouth feel, taste or all of the above. Nonetheless, it is clear that taste masking and taste assessment during development of paediatric oral formulations is undisputed. In addition, it is expected that human taste panels for paediatric formulations should as far as ethically possible be made up of

children and not adults. To this end, more and more taste testing studies of medicines for children is expected even for medicines already on the adult market.

Over the past decade, the prevalence of childhood arterial hypertension in the paediatric population has increased due to increases in children's excess body weight. Unfortunately from 1970 to 1990, the prevalence of overweight children and adolescents in the UK has increased from 5-11% (Hughes *et al.* 1997, Stamatakis *et al.* 2005). The European Society of Hypertension (ESH) and European Society of Cardiology (ESC) recommend the use of calcium channel blockers in the treatment of hypertension, in particular amlodipine (Lurbe *et al.* 2009). However, only 5mg and 10mg tablets are available on the UK market. These are available generically as amlodipine besilate, amlodipine maleate and amlodipine mesilate. In younger children that are unable to swallow tablets, parents and / or clinicians are encouraged to crush tablets and disperse them in water. In this form the taste of the amlodipine salt becomes apparent. In a recent study comparing the palatability of calcium channel blockers, it was reported that from the perspective of the child, the taste of pulverised amlodipine besilate was less preferred to that of lernacadipine (Milani *et al.* 2010). There are no reports in the literature describing the taste of amlodipine maleate and amlodipine mesilate.

In Japan, amlodipine orally disintegrating tablets (ODT) are popular and have been recently evaluated using a taste sensor SA501C equipped with a bitterness sensor AN0. However, it is important to point out that the main focus of this study was developing the method to evaluate the disintegration of ten ODTs thus identifying the main factors influencing the palatability of ODTs (Uchida *et al.* 2013). In the UK, in order to make amlodipine acceptable to children, generic tablets are extemporaneously prepared into two formulations. These two formulations have been shown to be stable for over 90 days when stored in the fridge and 56 days at room temperature (Nahata *et al.* 1999). The assessment of these two formulations in terms of palatability

has not been reported in the literature. The structure of the amlodipine has already been shown in **Figure 2.9.** The corresponding salts namely besilate, mesilate and maleate are shown in Figures 4.1, 4.2 and 4.3 respectively.

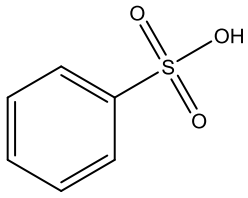


FIGURE 4. 1 STRUCTURE OF BESILATE

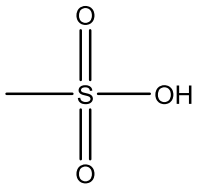


FIGURE 4. 2 STRUCTURE OF MESILATE

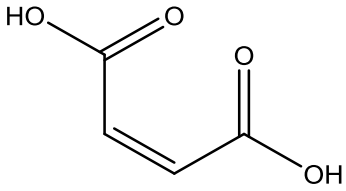


FIGURE 4. 3 STRUCTURE OF MALEATE

## 4.1 STUDY OBJECTIVES

The overarching question addressed in this chapter was whether the taste sensor could be used to predict which salt of amlodipine was superior in terms of taste. In addition, the taste masking efficiency of two commonly used extemporaneous vehicles is investigated using the electronic tongue. Finally, the results from the electronic tongue are compared to an untrained human taste panel study with a view to draw correlations between the two methods of taste assessment. The responsiveness of the sensors (**detailed in Section 4.2**) to amlodipine (base) is compared to its salts with a view of establishing which salt demonstrates best palatability. Furthermore, in keeping with methodology established in **chapter 3**, amlodipine besilate, maleate are compared to benzene sulphonic acid, sodium maleate respectively in order to establish the sensitivity of the sensors to different salts of the same molecule.

## 4.2 METHODOLOGY

The bitter drug sensor set i.e. AC0 (basic bitterness1), AN0 (basic bitterness2), C00 (acidic bitterness) and AE1 (astringency) were used to evaluate increasing concentrations of amlodipine and its salts. Solutions of amlodipine (0.25mg/ml, 0.5mg/ml, 0.75mg/ml and 1mg/ml) were prepared by the addition of the required quantity of amlodipine, amlodipine besilate, and amlodipine maleate into the vortex created by the action of a magnetic stirrer. A 30% v/v aqueous ethanol was used as solvent. The stirring was continued for 30 minutes. All solutions were prepared at room temperature on the day of testing.

Suspensions of amlodipine with similar concentrations to solutions were prepared using the schematic illustrated in Figure 4.6. Essentially, amlodipine tablets were pulverised using a pestle and mortar before being suspended in the different vehicles i.e. water (**F1**), 50:50 1% methylcellulose and simple syrup (**F2**) and 50:50 Ora sweet® and Ora plus® (**F3**). The suspension was stirred in the respective vehicle using a magnetic stirrer for 30 minutes. Schematics for the preparation of F1 and F2 are given in **Appendix A2**. All suspensions were prepared on the day of testing. Each of the different salts was prepared into three different formulations. The suspensions were tested on the taste sensor with no further agitation as the testing cycle was running.

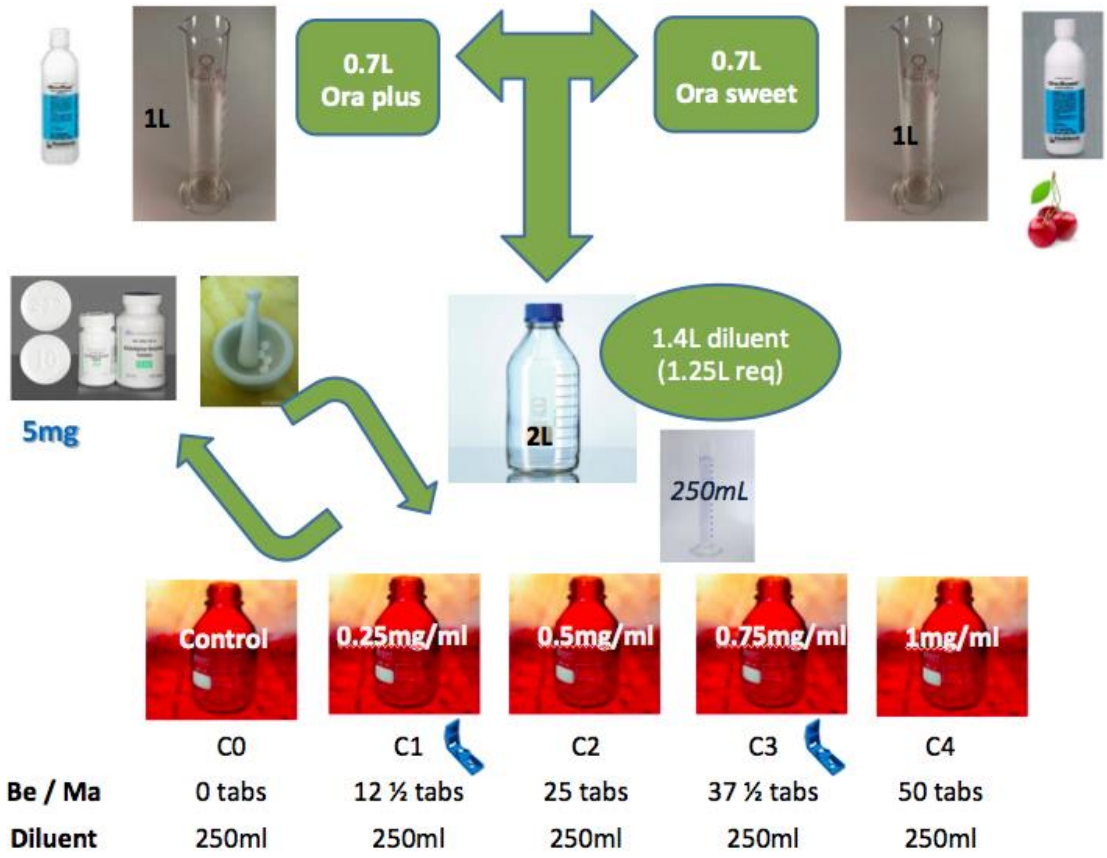


FIGURE 4. 4 SCHEMATIC OF PREPARATION OF AMLODIPINE SUSPENSIONS FOR F3 FORMULATIONS.

### 4.2.1 DATA ANALYSIS

Each solution / suspension was tested 4 times in order to ensure reliability. The average sensor response reading (μ) was calculated from the last three readings for every sensor response recorded for each sample tested. In order to analyse the reading directly from the API under investigation, the placebo value was subtracted from each sensor response reading. Sensor response curves and principal component analysis was performed as described in **chapter 2** and **Chapter 3, section 3.4.3**. In addition, hierarchical cluster analysis was performed using the method described in **Section 4.3.2**. Data management and analysis was performed using Originpro® 9.0 (OriginLab, Northampton, USA).

### 4.2.2 HUMAN TASTE PANEL STUDY

A single, blinded, cross over human taste assessment study was conducted in collaboration with J. Marbay, M.Orlu Gul, F. Olanipekun, S. Ranmal, J.Soto and C. Tuleu at the University College London (UCL), School of Pharmacy Policy and Practice

Unit. Ethical approval was sought from and granted by the UCL Research Ethics Committee (Project ID number 4612/001, **Appendix A3**). Twenty four healthy untrained participants (13 female, 11 male) were recruited. Their mean age was 23years and all participants completed the study. Each panellist attended four sessions, with each session lasting no more than two hours to prevent taste fatigue. The sessions were timetabled one week apart to allow for a washout period. The terminal elimination half-life of amlodipine is approximately 35- 50 hours (Faulkner *et al.* 1986) therefore, it was necessary to have a 7 day washout period gives sufficient time for the elimination of amlodipine from systemic circulation should any of the participants accidentally swallow instead of spitting amlodipine samples. To control for bias, the formulations were coded with random three digit codes and presented to the participants in random order.

Participants were asked to swirl 5ml of each sample in their mouth for 20s. The swirling time was minimised to 20s in order to reduce the risk of oromucosal absorption. Following the swirling the participants had to spit the sample in the container provided. The participants were asked to pay particular attention to the whether the formulation was pleasant or unpleasant and annotate this on a 10cm visual analogue scale (VAS), illustrated in Figure 4.7.

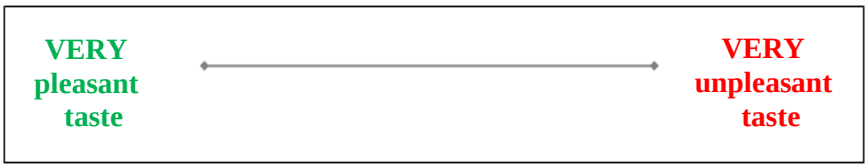


FIGURE 4. 5 VISUAL ANALOGUE SCALE (NOT TO SCALE), USED BY PARTICIPANTS TO ASSESS PALATABILITY OF F1, F2 AND F3 FORMULATIONS

Before and after each sample, the participants were given an unsalted cracker and bottled water to cleanse the palate and rinse their mouth. A ten minute washout period was observed between each sample to allow panellists sensor recovery and also to minimise risk of sensor fatigue. Each participant tasted ten samples per session

including two controls namely; bottled water (positive control) and 1mg/ml amlodipine salt (negative control). The samples to be tasted were presented to each panellist in the order described in Table 4.1.

TABLE 4. 1 ORDER OF PRESENTATION OF SAMPLES TO PANELLISTS ON EACH VISIT

| Visit number | Formulation | Presentation order of concentrations (mg/ml) | | | | |
|---|---|---|---|---|---|---|
| **1st visit** | amlodipine besilate API | 1 | 0.5 | 0 | 0.25 | 0.75 |
| | amlodipine besilate F1 | 0.25 | 0.5 | 0 | 0.75 | 1 |
| **2nd visit** | amlodipine mesilate F1 | 0.75 | 0.5 | 0 | 0.25 | 1 |
| | amlodipine maleate F1 | 0.75 | 0.25 | 0 | 1 | 0.5 |
| **3rd visit** | amlodipine besilate F2 | 1 | 0.25 | 0 | 0.75 | 0.5 |
| | amlodipine besilate F3 | 1 | 0.25 | 0 | 0.5 | 0.75 |
| **4th visit** | amlodipine maleate F2 | 0.5 | 0.75 | 0 | 1 | 0.25 |
| | amlodipine maleate F3 | 0.5 | 0.25 | 0 | 1 | 0.75 |

Data management and analysis was performed using Microsoft Excel® 2010.

## 4.3 RESULTS

### *4.3.1 AMLODIPINE AND ITS SALTS CONCENTRATION CURVES*

In keeping with methodology established in **chapter 3**, the responsiveness of the taste sensor to increasing concentrations of amlodipine and its salts i.e. mesilate, besilate and maleate was investigated. In light of issues identified in **chapter 3**, de-ionised water was used as a negative control. Figure 4.8 illustrates the sensor responses to

increasing concentrations of amlodipine. The reading (mV) at concentration 0mg/ml is that for de-ionised water. The basic bitterness2 and acidic bitterness sensors both show variation to increasing concentrations of amlodipine. However, basic bitterness 1 and astringency sensors do not illustrate responsiveness to increases in concentration of amlodipine. It is therefore important to note this response differs from water. Overall a one-way ANOVA showed no statistical difference between the sensor response and increasing concentrations of amlodipine ($p= 1.97 \times 10^{-6}$)

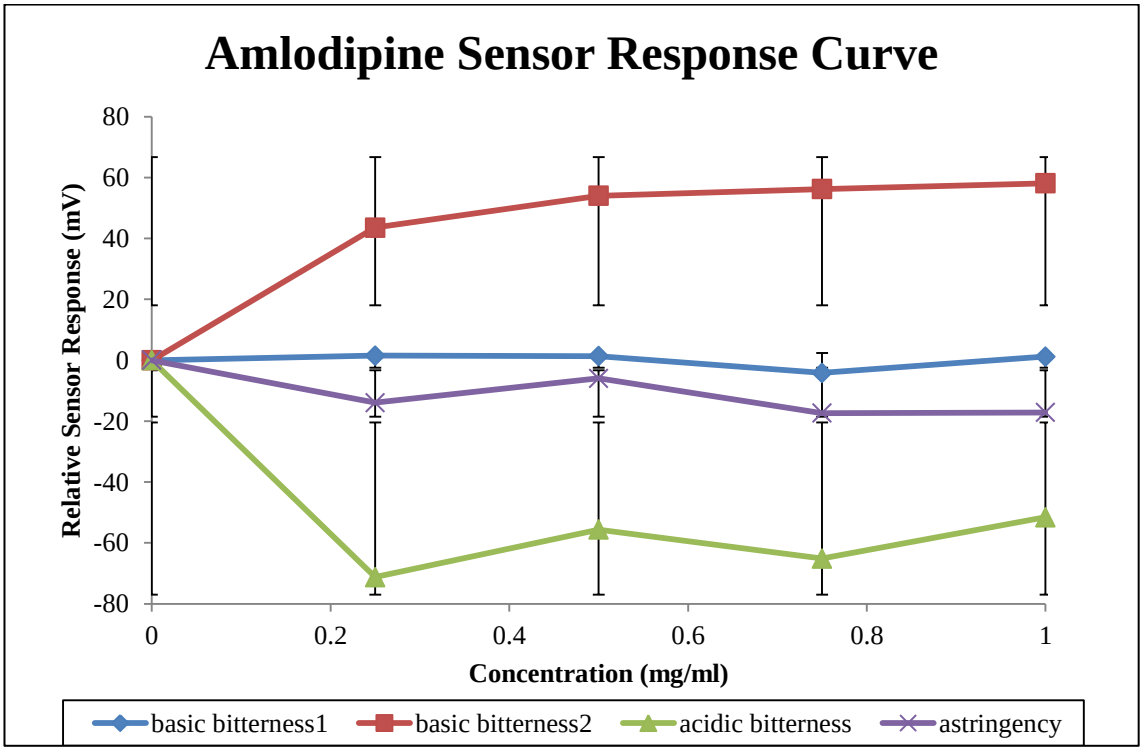


FIGURE 4. 6 RELATIVE SENSOR RESPONSE CURVE FOR AMLODIPINE, SHOWING THE RESPONSES OF FOUR SENSORS WHICH CORRESPOND TO DIFFERENT TASTE SPECIFICATIONS, AS A FUNCTION OF CONCENTRATION (N=3, $\bar{x}$±SD)

The responsiveness of the sensors to amlodipine besilate is illustrated in Figure 4.9. Both the acidic bitterness and astringency sensors show an increase in responsiveness with increase in concentration. It is also noteworthy, that the standard deviation error bars for these two sensors overlap therefore there is no statistical difference in response between the two sensors. The basic bitterness sensors show a difference in sensor response to solvent however, there is no concentration

dependence across the four concentrations explored in this study. A one-way ANOVA shows no statistical difference ($p= 1.49\ x10^{-5}$).

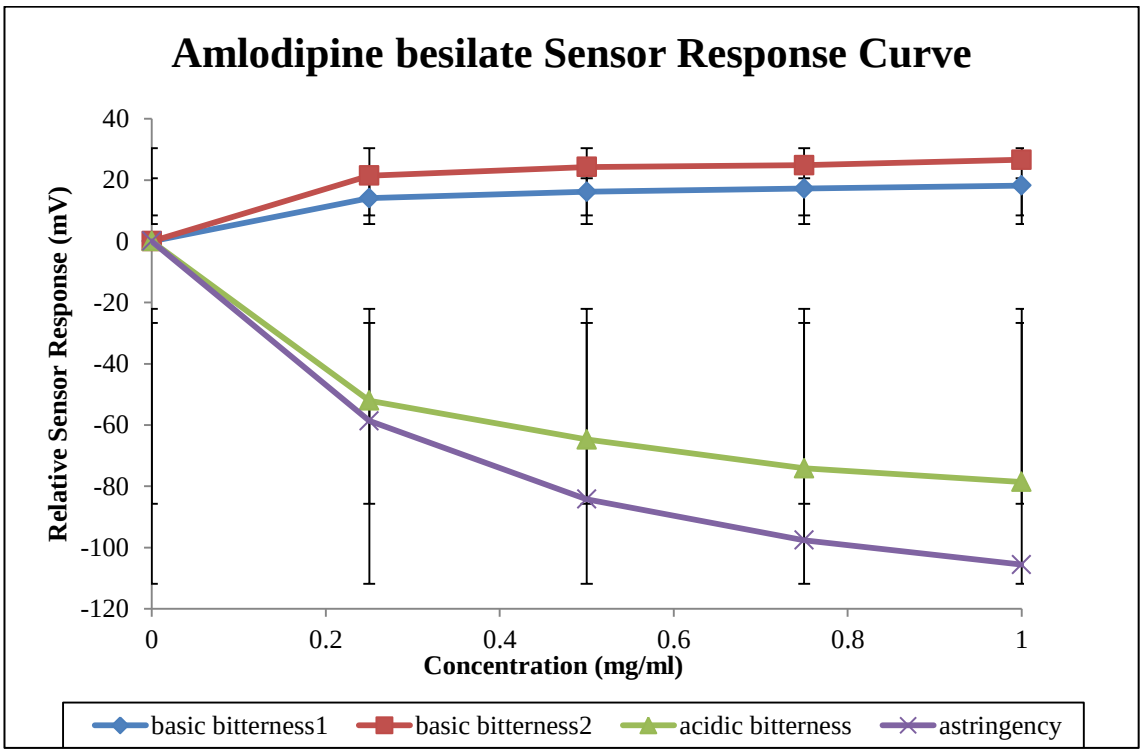


FIGURE 4. 7 RELATIVE SENSOR RESPONSE CURVE FOR AMLODIPINE FOR AMLODIPINE BESILATE, SHOWING THE RESPONSES OF FOUR SENSORS AS A FUNCTION OF CONCENTRATION (N=3, $\bar{x}$±SD)

Amlodipine besilate (Figure 4.1) is composed of amlodipine and benzene sulphonic acid therefore in order to appreciate which species in solution was responsible for the sensor response observed; the sensors response to benzene sulphonic acid is illustrated in Figure 4.10. The acidic bitterness and astringency sensors show a change in response with increasing concentrations of benzene sulphonic acid. Both basic bitterness sensors show no difference with solvent and no difference in response between them. It is noteworthy that the pattern of response observed for benzene sulphonic acid is similar to that observed for amlodipine besilate. Once again, a one-way ANOVA shows no statistical difference ($p= 3.05\ x10^{-5}$).

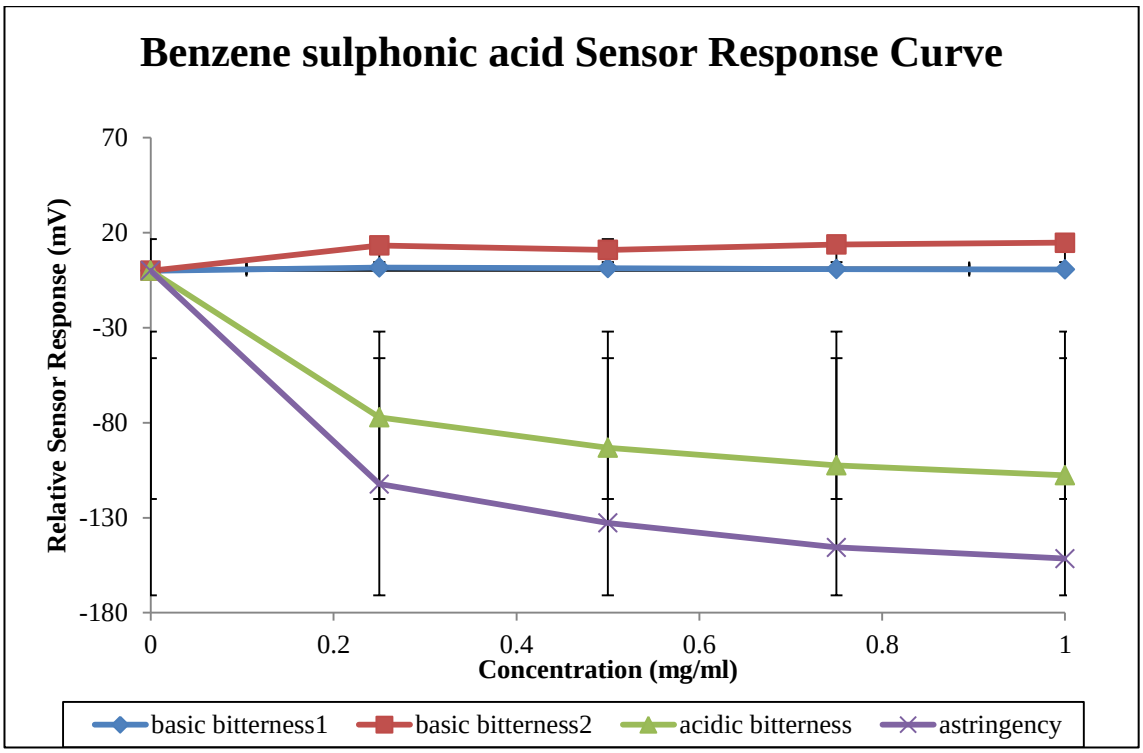


FIGURE 4. 8 RELATIVE SENSOR RESPONSE CURVE FOR BENZENE SULPHONIC ACID, SHOWING BITTER DRUG SENSOR SET RESPONSES AS A FUNCTION OF CONCENTRATION (N=3, $\bar{x}$±SD)

The responsiveness of the sensors to amlodipine maleate is given in Figure 4.11. Consistent with results observed for amlodipine besilate, the acidic bitterness and astringency sensors both show a clear concentration dependant response. The standard deviation error bars for both sensors overlap suggesting that there is no statistical difference in sensor response between the two sensors. The basic bitterness sensors illustrate a difference between solvent and solutions containing amlodipine maleate, however, no change in response is observed with increasing concentration of amlodipine maleate. This is confirmed using a one-way ANOVA which showed no statistical difference ($p= 1.28\ x10^{-5}$).

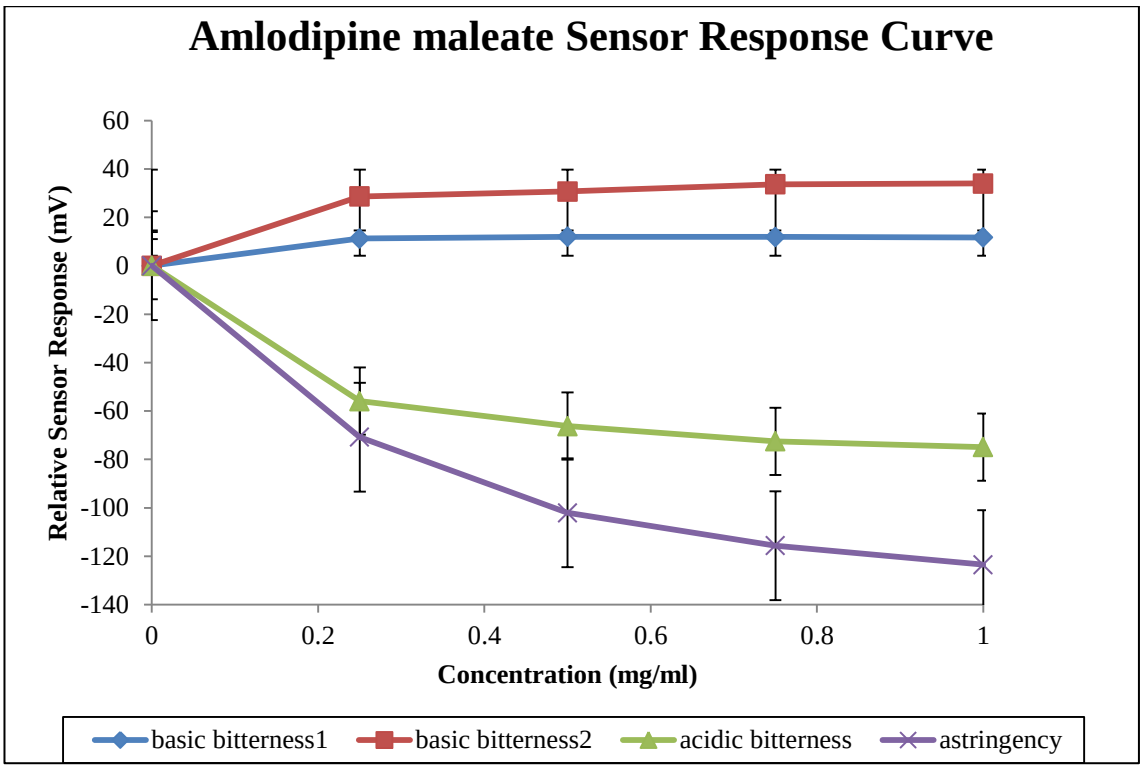


FIGURE 4. 9 RELATIVE SENSOR RESPONSE CURVE FOR AMLODIPINE MALEATE, SHOWING THE RESPONSIVENESS OF FOUR SENSORS CODING FOR A TASTE ATTRIBUTES, AS A FUNCTION OF CONCENTRATION (N=3, $\boldsymbol{x}$±SD)

Similar to the strategy applied for amlodipine besilate and benzene sulphonic acid, sodium maleate, structure of which is given in Figure 4.5 was compared to amlodipine maleate. The responsiveness of sensors to sodium maleate is shown in Figure 4.12. In this case, a clear response is observed between solvent and solutions of sodium maleate were observed for the acidic bitterness and astringency sensors. Interestingly, there is no concentration dependence observed with increasing concentrations of sodium maleate for all four sensors. A one-way ANOVA confirms that there is no statistical difference ($p= 2.56\ x10^{-5}$).

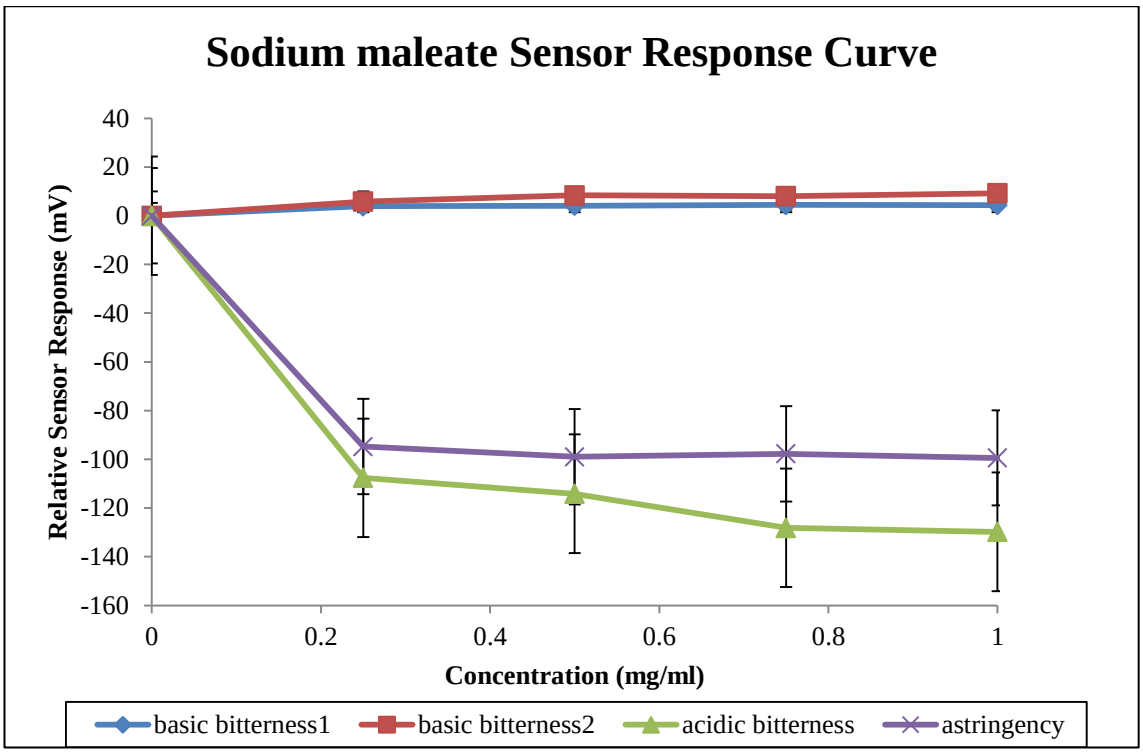


FIGURE 4. 10 RELATIVE SENSOR RESPONSE CURVE FOR SODIUM MALEATE, SHOWING THE RESPONSIVENESS OF FOUR SENSORS CODING FOR A TASTE ATTRIBUTES, AS A FUNCTION OF CONCENTRATION (N=3, $\bar{x}$±SD)

#### 4.3.1.1 SUMMARY OF RESULTS

The present study set out to investigate the responsiveness of sensors to pure amlodipine, its salts besilate and maleate. De-ionised water was used as negative control. It is apparent that there is a difference in sensor response patterns between amlodipine and its salts i.e. besilate and maleate. With respect to amlodipine base, only the basic bitterness 2 and acidic bitterness sensors show a response, while the salts show astringency and acidic bitterness being the predominant responses. This is supported by the fact that benzene sulphonic acid and sodium maleate also have same sensor response as amlodipine besilate and amlodipine maleate respectively. Therefore, it appears that in salt form, the sensor response switches from basic and acidic bitterness to astringency and acidic bitterness.

### 4.3.2 AMLODIPINE F1 FORMULATIONS

Sensor response curve for pulverised amlodipine besilate tablets suspended in water (**F1**) is illustrated in Figure 4.13. Concentration dependent sensor response is observed with the astringency sensor, while this is absent for the other three sensors. Interestingly, the acidic sensor shows a response when solutions were made with 30%v/v aqueous ethanol but this response is absent when water alone is used. However, overall, a one-way ANOVA shows that there is no statistical difference in senor response with increasing concentrations of amlodipine besilate ($p= 2.71\ x10^{-6}$).

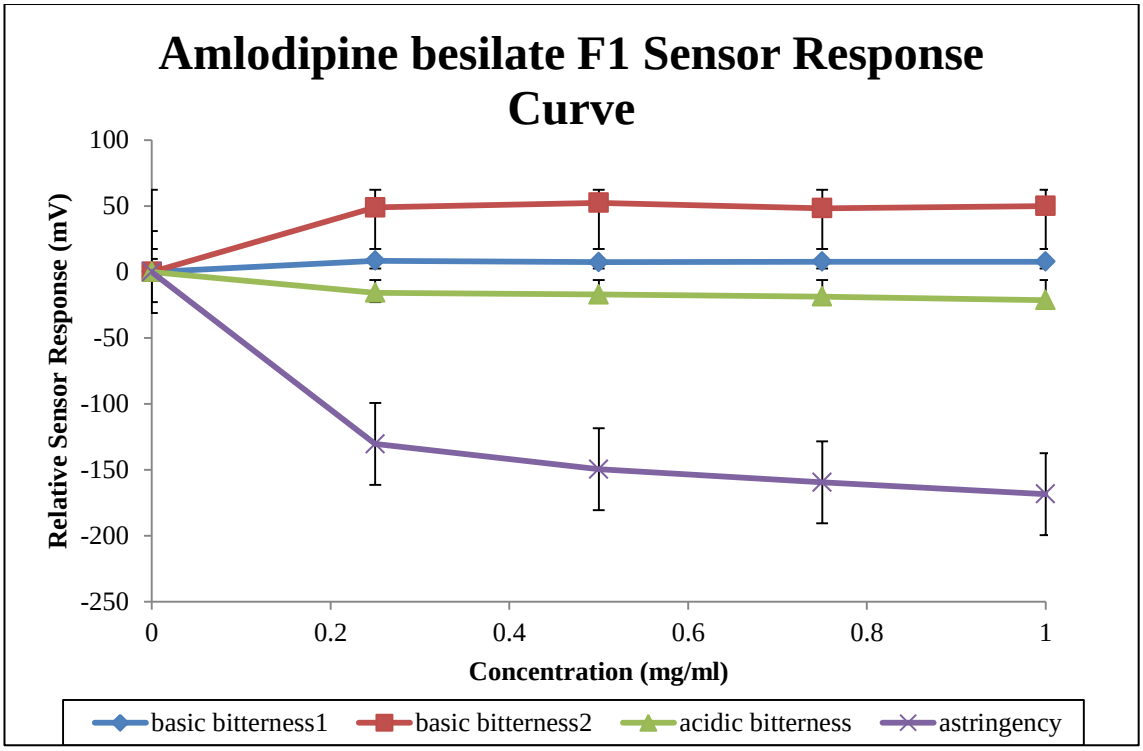


FIGURE 4. 11 RELATIVE SENSOR RESPONSE CURVE FOR AMLODIPINE BESILATE F1 FORMULATIONS, SHOWING THE RESPONSIVENESS OF FOUR SENSORS CODING FOR DIFFERENT TASTE ATTRIBUTES, AS A FUNCTION OF CONCENTRATION (N=3, $\bar{x}$±SD)

The sensor responses to amlodipine maleate tablets crushed and dispersed in water (F1) is illustrated in Figure 4.14. A clear concentration dependent response is observed with the astringency and acidic bitterness sensors. Conversely, there is no difference in response between water and formulations containing crushed amlodipine maleate tablets when considering the basic bitterness sensors. Interestingly, the sensor responses for the basic bitterness sensors are diminished in F1 compared to 30% aqueous ethanol. However, overall, a one-way ANOVA show that there is no statistical difference in sensor response with increasing concentration ($p= 2.12\ x10^{-5}$).

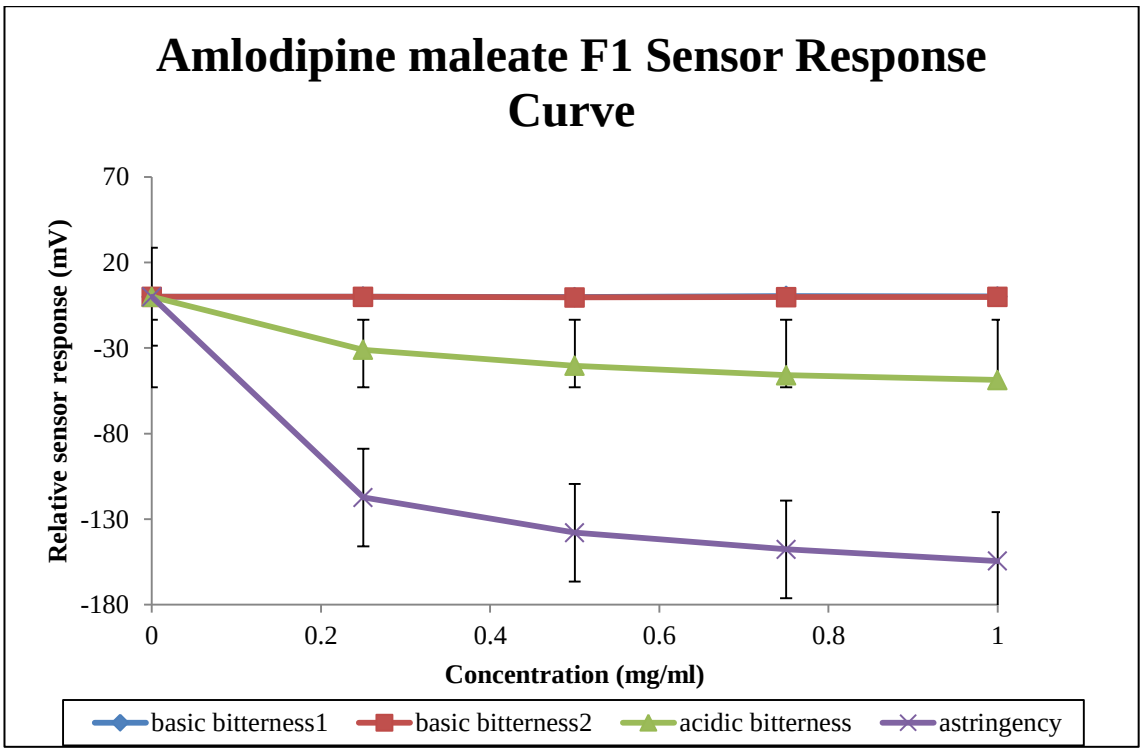


FIGURE 4. 12 RELATIVE SENSOR RESPONSE CURVE FOR AMLODIPINE MALEATE F1 FORMULATIONS, SHOWING THE RESPONSIVENESS OF FOUR SENSORS CODING FOR A TASTE ATTRIBUTES, AS A FUNCTION OF CONCENTRATION (N=3, $\bar{x}$±SD)

F1 formulations of amlodipine mesilate were investigated using the taste sensor. The responsiveness of the sensors is shown in Figure 4.15. The astringency sensor shows significant changes in sensor response with increasing concentration, which is not apparent for the other three sensors. Interestingly, the acidic sensor response is showing positive values (mV) as opposed to negative values which have been observed thus far on amlodipine and its salts besilate and maleate. However, overall, a one-way ANOVA show that there is no statistical difference in sensor response with increasing concentration ($p$= *3.82* $x10^{-6}$).

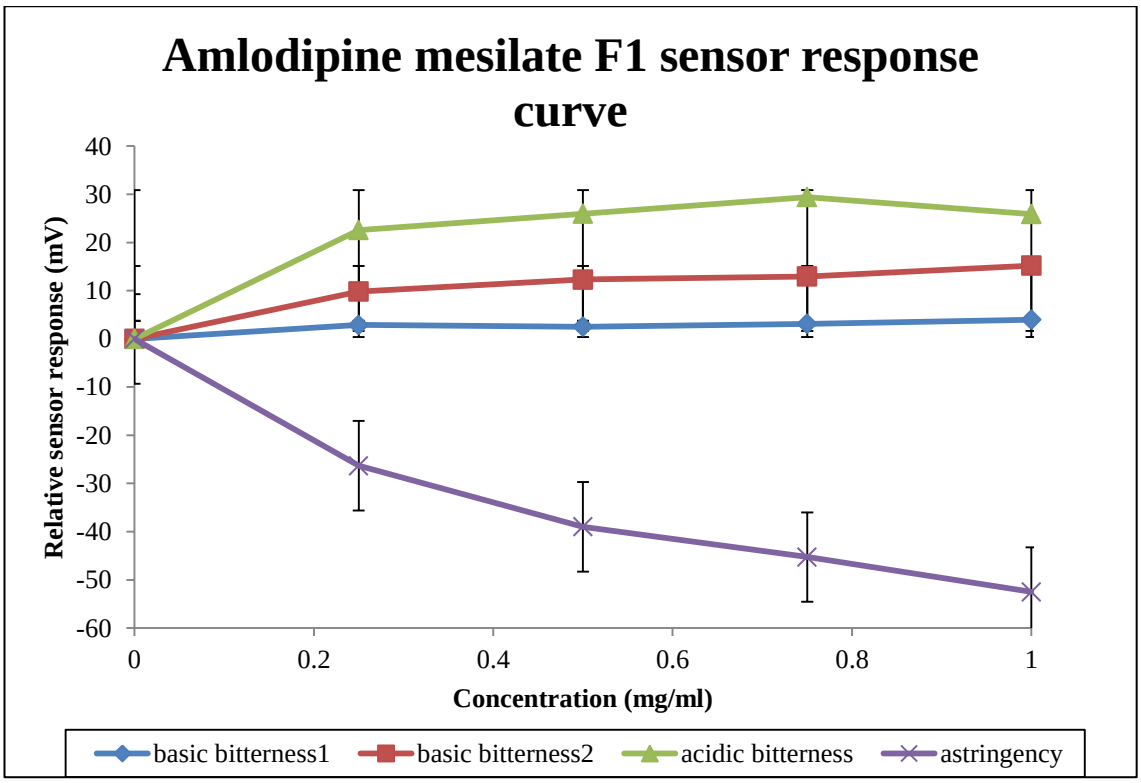


FIGURE 4. 13 RELATIVE SENSOR RESPONSE CURVE FOR AMLODIPINE MALEATE F1 FORMULATIONS, SHOWING THE RESPONSIVENESS OF FOUR SENSORS CODING FOR A TASTE ATTRIBUTES, AS A FUNCTION OF CONCENTRATION (N=3, $\bar{x}$±SD)

Principle component analysis was performed in order to establish taste differentiation between F1 formulations of the amlodipine salts. The eigenvalues of the covariance matrix shown in Table 4.2, show the percentage of variance (spread of data) apportioned to each principal component. It is apparent that the first and second principle components (PC1 and PC2), have the highest eigenvalues and proportionally account for 98% of variance observed. Therefore a two axis plot would represent a statistically significant amount of data. It should be noted that low *p* values for PC1 and PC2 indicate a greater confidence that there is statistical difference between the observations for both principal components. A similar argument applies to the third principle component (PC3) even though it has not been used in this analysis as it was not necessary.

TABLE 4. 2 EIGENVALUES OF THE COVARIANCE MATRIX SHOWING CONTRIBUTION AND SIGNIFICANCE OF EACH PRINCIPLE COMPONENT

| PCA | Eigenvalue | Percentage (%) of Variance | Cumulative (%) | χ2 | Degrees of Freedom | Significance level (p) |
|---|---|---|---|---|---|---|
| **1** | 4918.35 | 88.63 | 88.63 | 102.79 | 9 | $4.28 \times 10^{-18}$ |
| **2** | 556.23 | 10.02 | 98.65 | 59.59 | 5 | $1.47 \times 10^{-11}$ |
| **3** | 74.38 | 1.34 | 99.99 | 35.20 | 2 | $2.26 \times 10^{-8}$ |
| **4** | 0.52 | 0.01 | 100.00 | 0 | 0 | 0 |

The extracted eigenvectors give the contribution of each of the sensors to the first and second principal components. These are given in Table 4.3. Essentially, the astringency sensor has highest contribution to PC1, while the basic bitterness2 sensor is the predominant signal for PC2. Therefore, the separation of the amlodipine F1 formulations is influenced by astringency on the *x*-axis and basic bitterness2 on the *y*-axis.

TABLE 4. 3 EXTRACTED EIGENVECTORS FOR PC1 AND PC2 AND CORRESPONDING SENSOR ALLOCATION

| | Coefficient of PC1 | Coefficient of PC2 |
|---|---|---|
| **Basic bitterness1** | -0.01 | 0.12 |
| **Basic bitterness2** | -0.11 | 0.76 |
| **Acidic bitterness** | 0.41 | 0.61 |
| **Astringency** | 0.90 | -0.18 |

The biplot shown in Figure 4.16 displays both the loadings and the scores for principal components 1 and 2. The raw data under investigation are plotted as a scatter plot (in red dots). All four concentrations of each of the amlodipine salts are shown on the

biplot. There is a significant difference between the amlodipine salts and placebo (de-ionised water). As already illustrated with the extracted eigenvectors the astringency sensor is closely linked with the *x*-axis while the basic bitterness2 sensor is aligned to the *y*-axis. The acidic bitterness is located between the *x* and *y* axes. The loading for basic bitterness1 is insignificant. The amlodipine mesilate formulations (designated AMme) on the biplot are all aligned with the x-axis signifying astringency. As the concentration of amlodipine mesilate increases an element of acidic bitterness increases. The amlodipine besilate formulations (designated AMbe) are clustered together and closely associated with basic bitterness2. Interestingly, at low concentration i.e. 0.25mg/ml, amlodipine besilate is clustered with amlodipine mesilate.

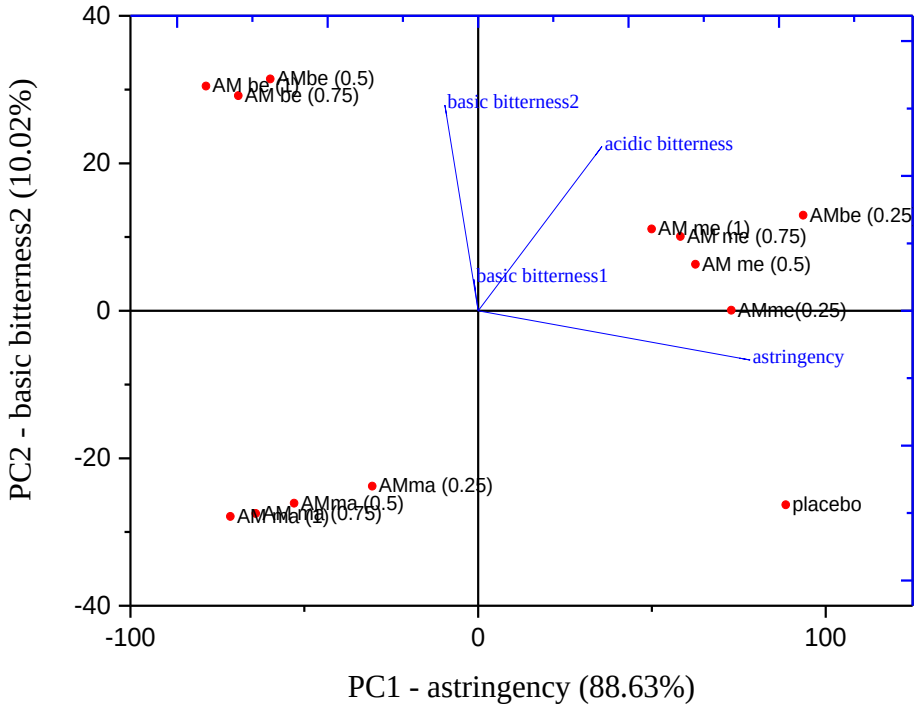


FIGURE 4. 14 A BIPLOT SHOWING PRINCIPAL COMPONENT ANALYSIS AND LOADING PLOTS OF AMLODIPINE BESILATE, MALEATE AND MESILATE F1 FORMULATIONS IN TERMS OF THEIR PREDICTED TASTE ATTRIBUTES.

Hierarchical clustering is one of the most straight forward methods of grouping heterogeneous data into homogenous data sets. It can either be agglomerative or divisive. In agglomerative clustering it begins with every data set being a cluster unto

itself. At successive steps, similar clusters are merged (Kaufman *et al.* 2009). In this case, the average relative sensor response readings (mV) for each sensor per concentration of each amlodipine salt were a cluster. At the next step, the two sensor readings which have largest similarity are joined into a single cluster. For example, amlodipine ma (0.25) and amlodipine ma 0.5 have a small difference between them and as such are merged into one cluster. At every step, individual data are added to existing clusters, two individual clusters are combined or two existing clusters are combined. The algorithm ends with the whole data set merged into one cluster. In other words agglomerative hierarchical clustering is a bottom up approach to grouping data. In this type of clustering once the cluster is formed it cannot be split. In this study, agglomerative cluster analysis was used to determine the distances between each of the clusters observed in the principal component analysis. A visual representation of the distance at which the clusters are combined is shown in a dendrogram illustrated in Figure 4.17. The dendrogram illustrates that the higher concentrations of amlodipine formulations are very similar. This is exemplified by the fact the first observations to be merged are 7:10, 9:12 and 8:11. As shown in Table 4.2, these observations represent the higher concentration of the amlodipine mesilate, amlodipine maleate and amlodipine besilate F1 formulations respectively.

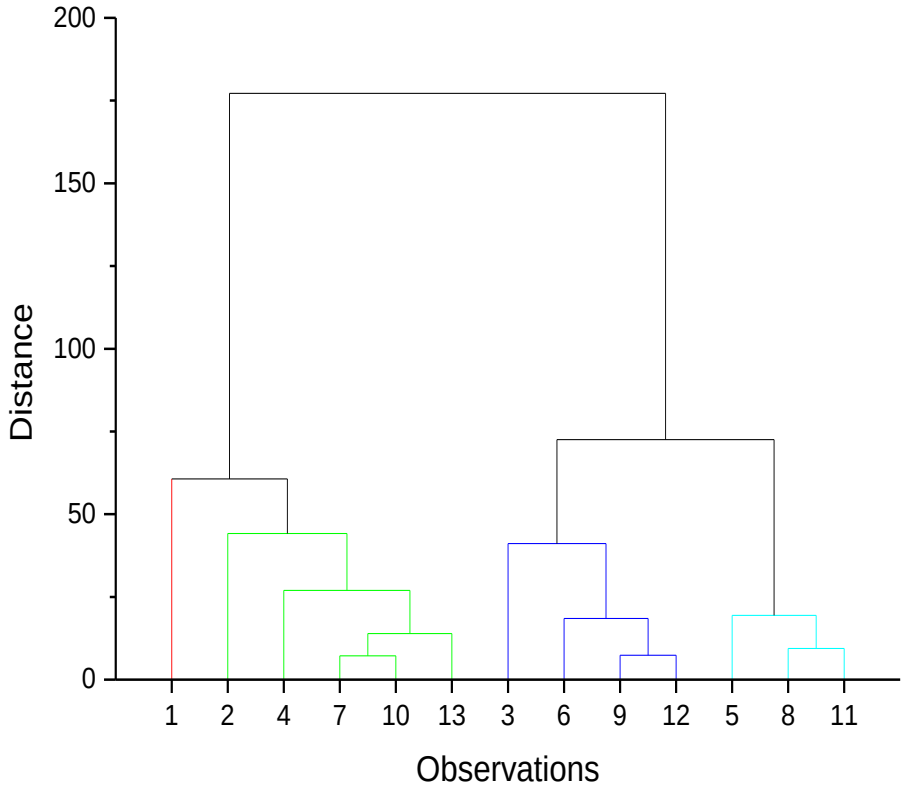


FIGURE 4. 15 A DENDROGRAM SHOWING CLUSTER ANALYSIS OF AMLODIPINE BESILATE, MALEATE AND MESILATE F1 FORMULATIONS, SHOWING FOUR CLUSTERS OF THE OBSERVED VARIABLES.

The composition of each of the clusters is given in Table 4.4, to support the results shown by the principal analysis biplot, each of the amlodipine salts are clustered closely together.

TABLE 4. 4 CLUSTER MEMBERSHIP TABLE SHOWING THE OBSERVATION NUMBER AND SAMPLE NAME OF EACH SAMPLE IN THE FOUR DIFFERENT CLUSTERS IDENTIFIED

| Cluster | Membership (observation number and sample name) | |
|---|---|---|
| **1** | 1 - placebo | |
| **2** | 2- amlodipine besilate 0.25<br>4- amlodipine mesilate 0.25<br>7- amlodipine mesilate 0.5 | 10- amlodipine mesilate 0.75<br>13 – amlodipine mesilate 1 |
| **3** | 3- amlodipine maleate 0.25<br>6- amlodipine maleate 0.5 | 9 - amlodipine maleate 0.75<br>12- amlodipine maleate 1 |
| **4** | 5- amlodipine besilate 0.5<br>8- amlodipine besilate 0.75 | 11- amlodipine besilate 1 |

The distances between the clusters were calculated using the Euclidean equation below.

$$d: (x: y) = \sqrt{\sum_{i=1}^{n} (y_i - x_i)^2}$$

EQUATION 4.14

The distances between the clusters is given in Table 4.5, which shows that cluster 4 i.e. amlodipine besilate is furthest deviation from placebo therefore indicating that it has poor palatability in comparison to placebo. The distances were calculated using coordinates (*x:y*) at an imaginary centre point of the cluster, which is also known as cluster centre.

TABLE 4. 5 EUCLIDEAN DISTANCES BETWEEN CLUSTER CENTRES

| | Cluster 1 | Cluster 2 | Cluster 3 | Cluster 4 |
|---|---|---|---|---|
| **Cluster 1** | 0 | 48.56 | 154.43 | 168.21 |
| **Cluster 2** | 48.56 | 0 | 126.81 | 138.21 |
| **Cluster 3** | 154.43 | 126.81 | 0 | 59.12 |
| **Cluster 4** | 168.21 | 138.21 | 59.12 | 0 |

#### 4.3.2.1 SUMMARY OF RESULTS

The findings from this section suggest that in general, all the F1 formulations are detectable on the taste sensor with the astringency sensor exhibiting the most response (89%). The basic bitterness2 demonstrates the next prominent response, accounting for 10% of data variation observed. Cluster analysis revealed four distinct clusters. Cluster 2 was associated with astringency, while cluster 4 was linked to basic bitterness2. The results suggest that amlodipine besilate of concentrations 0.5, 0.75 and 1mg/ml show the largest deviation from placebo (cluster 1), whilst cluster 2 (consisting predominantly of amlodipine mesilate) shows closest distance to placebo. Therefore when considering F1 formulations, amlodipine besilate is least palatable while amlodipine mesilate has the best palatability. In the next section a similar comparison is reported for F2 formulations of amlodipine salts.

### *4.3.3 AMLODIPINE F2 FORMULATIONS*

To recap, F2 formulations were prepared using 1:1 mixture of 1% methylcellulose and simple syrup before suspending pulverised amlodipine besilate, maleate and mesilate tablets. The responsiveness of the sensors AN0 (basic bitterness1), AC0 (basic bitterness2), C00 (acidic bitterness) and AE1 (astringency) was investigated using increasing concentrations of each amlodipine salt. Figure 4.18 reveals that there is change in sensor response (mV) with increasing concentrations of amlodipine besilate when considering the astringency sensor. With respect to the bitterness sensors, although a significant change is observed between placebo (0mg/ml) and 0.25mg/ml

no further changes in response are observed with increases in concentration of amlodipine besilate. A one-way ANOVA shows that there is no statistical difference in the sensor responses ($p= 1.15\ x10^{-5}$)

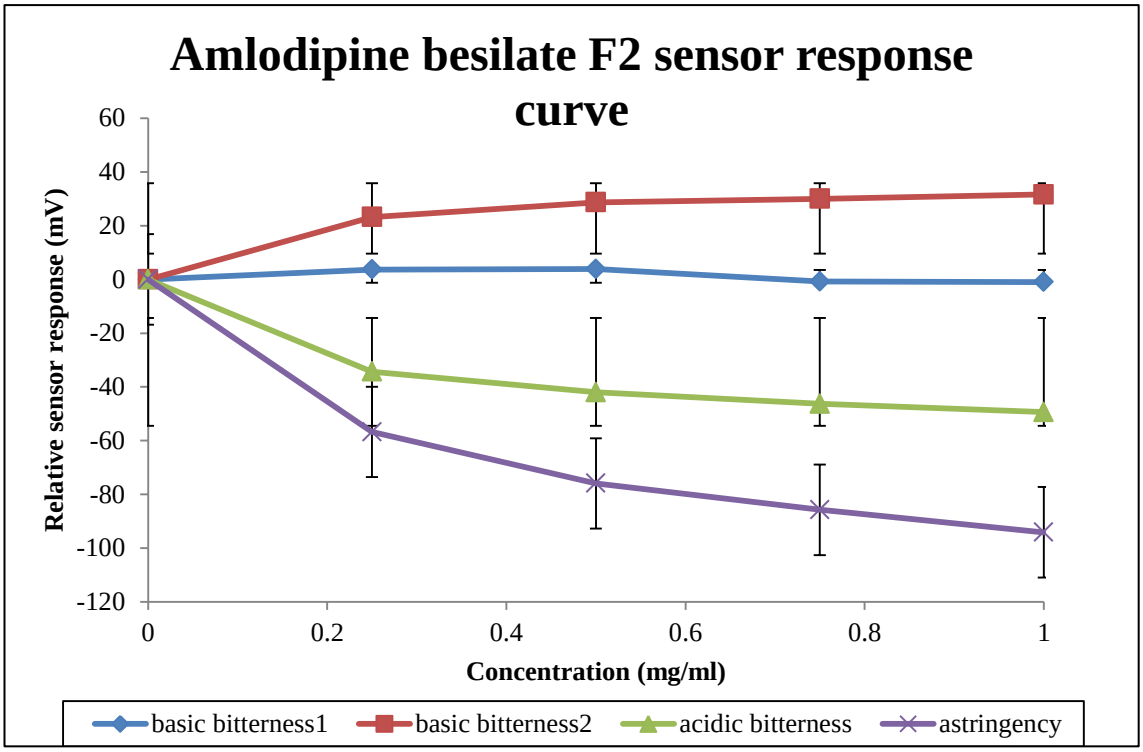


FIGURE 4. 16 RELATIVE SENSOR RESPONSE OF AMLODIPINE BESILATE F2, SHOWING SENSOR RESPONSES AS A FUNCTION OF CONCENTRATION ((N=3, $\bar{x}$±SD)

The graph shown in Figure 4.19 reveals similar trends to those observed in Figure 4.18. The astringency sensor shows a concentration dependant change in sensor response. The other bitterness sensors however, demonstrate a change in response to placebo but no change with increasing concentrations of amlodipine maleate. A one-way ANOVA shows that there is no statistical difference between sensor response and increasing concentrations of amlodipine besilate ($p= 5.61x10^{-6}$).

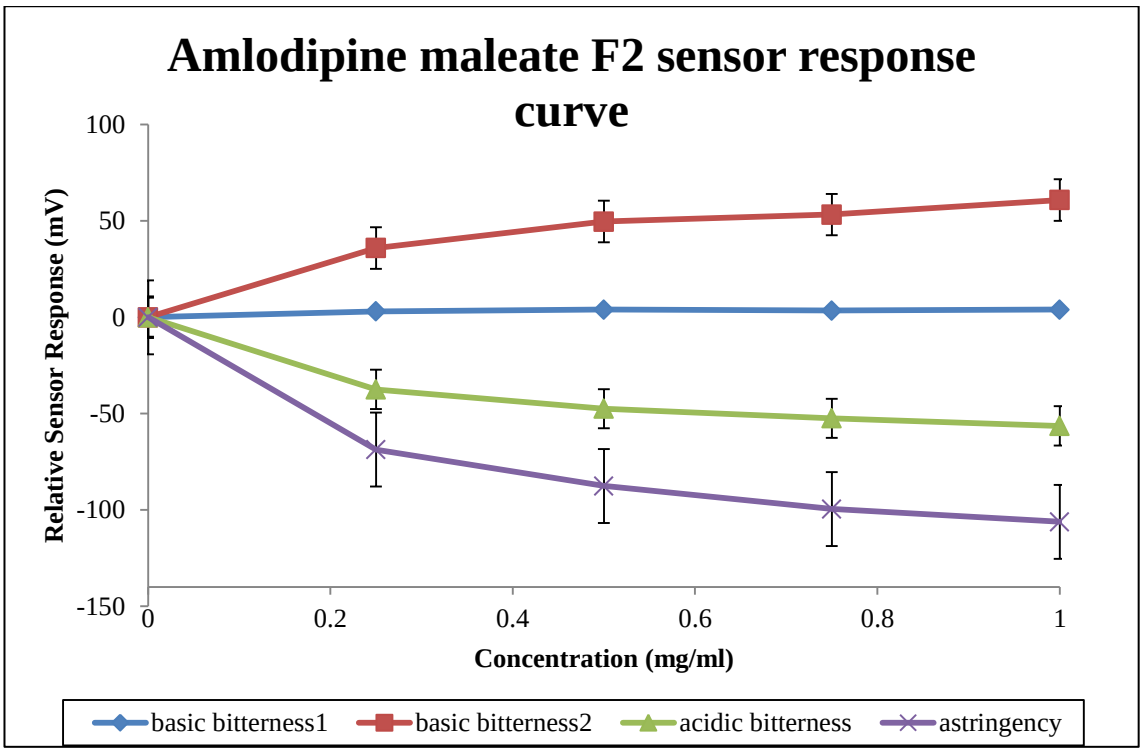


FIGURE 4. 17 RELATIVE SENSOR RESPONSE CURVE OF AMLODIPINE MALEATE F2, SHOWING SENSOR RESPONSES AS A FUNCTION OF CONCENTRATION (N=3, $\bar{x}$±SD)

In contrast to sensor responses observed in Figures 4.18 and 4.19, Figure 4.20 reveals that the basic bitterness 2 sensor shows a definite change in sensor response with increases in concentrations of amlodipine mesilate. The other three sensors i.e. basic bitterness 1, acidic bitterness and astringency do not show any significant deviation from placebo. A statistical analysis using one-way ANOVA showed that there was no difference between sensor response and increases in concentration of amlodipine mesilate ($p= 1.43x10^{-5}$).

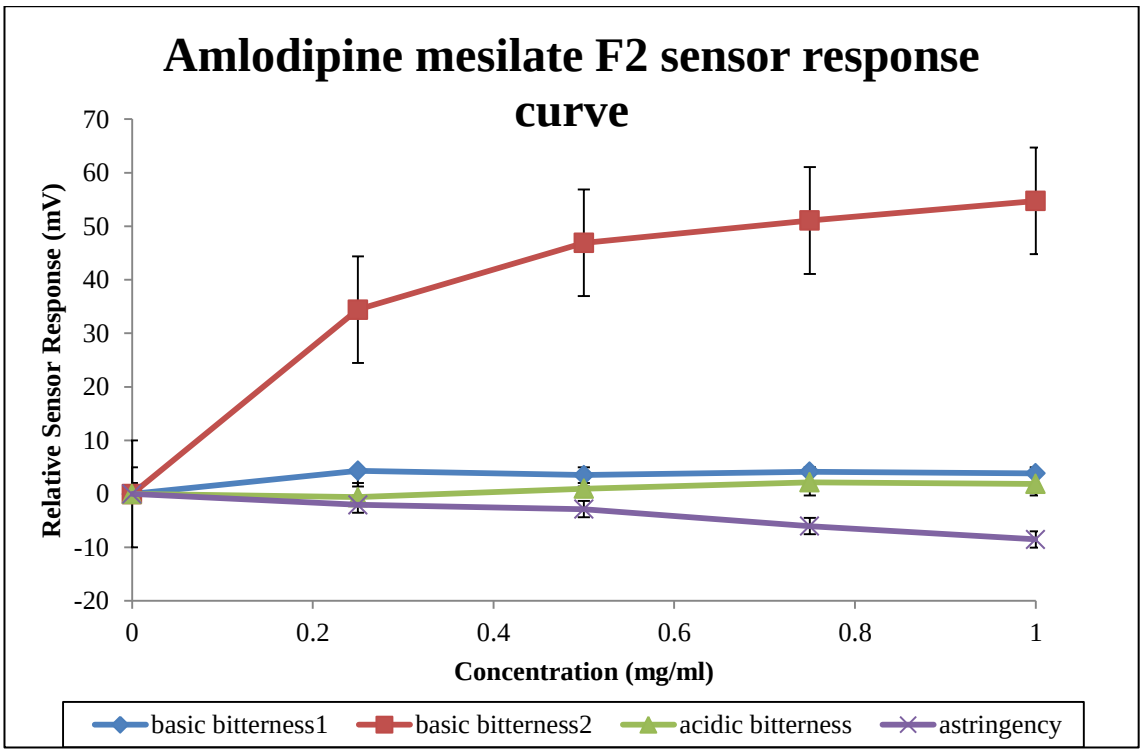


FIGURE 4. 18 RELATIVE SENSOR RESPONSE CURVE OF AMLODIPINE MESILATE F2, SHOWING SENSOR RESPONSES AS A FUNCTION OF CONCENTRATION (N=3, $\bar{x}$±SD)

The eigenvalues of the covariance matrix shown in Table 4.6 show the percentage of variance apportioned to each principal component. It is apparent that PC1 and PC2 have the highest eigenvalues and proportionally account for 99% of variance observed. Therefore a two axis plot would represent a statistically significant amount of data. It should be noted that low *p* values (i.e. > 0.05) for PC1 and PC2 indicate a greater confidence that there is statistical difference between the observations for both principal components. A similar argument applies to PC3 even though it has not been used in this analysis as it was not necessary.

TABLE 4. 6 EIGENVALUES OF THE COVARIANCE MATRIX SHOWING CONTRIBUTION AND SIGNIFICANCE OF EACH PRINCIPLE COMPONENT

| PCA | Eigenvalue | Percentage (%) of Variance | Cumulative (%) | χ2 | Degrees of Freedom | Significance level (p) |
|---|---|---|---|---|---|---|
| **1** | 2419.48 | 89.99 | 89.99 | 118.69 | 9 | $2.48 \times 10^{-21}$ |
| **2** | 264.96 | 99.84 | 99.84 | 71.88 | 5 | $4.17 \times 10^{-14}$ |
| **3** | 3.68 | 99.98 | 99.98 | 8.57 | 2 | 0.01 |
| **4** | 0.50 | 0.02 | 100 | 0 | 0 | 0 |

After looking at the value of the spread as given by the eigenvalues, the extracted eigenvectors show the direction of the spread. In other words the eigenvectors quantitatively demonstrate which sensor(s) are responsible for the variation observed. In this case, it is clear that the astringency sensor contributes heavily on the variation observed for the first principal component while basic bitterness 2 dominates response in PC2. It is worth pointing out that where the coefficient eigenvector takes a negative value, this suggests that that particular vector has no significance.

TABLE 4. 7 EXTRACTED EIGENVECTORS FOR PC1 AND PC2, SHOWING THE CONTRIBUTION OF EACH SENSOR TO THE FIRST AND SECOND PRINCIPAL COMPONENTS

| | Coefficient of PC1 | Coefficient of PC2 |
|---|---|---|
| **Basic bitterness1** | 0.01 | 0.08 |
| **Basic bitterness2** | -0.08 | 0.99 |
| **Acidic bitterness** | 0.49 | 0.12 |
| **Astringency** | 0.86 | 0.02 |

The results of the principal component analysis biplot are presented in Figure 4.21.The loading plot (illustrated in blue) shows the magnitude (in length) and the direction of the contribution of each sensor to each principal component. In this case, astringency has the highest magnitude in the direction of the first principal component PC1 while basic

bitterness2 has close association with the second principal component. The amlodipine mesilate formulations show close association with astringency. So much so, that at 0.25mg/ml amlodipine mesilate (shown on plot as AMMe 0.25) is in line with *x*-axis and astringency loading. Surprisingly, increasing the concentration of amlodipine mesilate appears to reduce the association with astringency. Amlodipine maleate suspensions (shown as AMMa0.25, AMMa0.5, AMMa0.75 and AMMa1) show some association with basic bitterness2 while amlodipine besilate suspensions (shown as AMBe0.25, AMBe0.5, AMBe0.75 and AMBe1) have no clear association with any of the sensors. Equally so the placebo does not show association with any of the sensors.

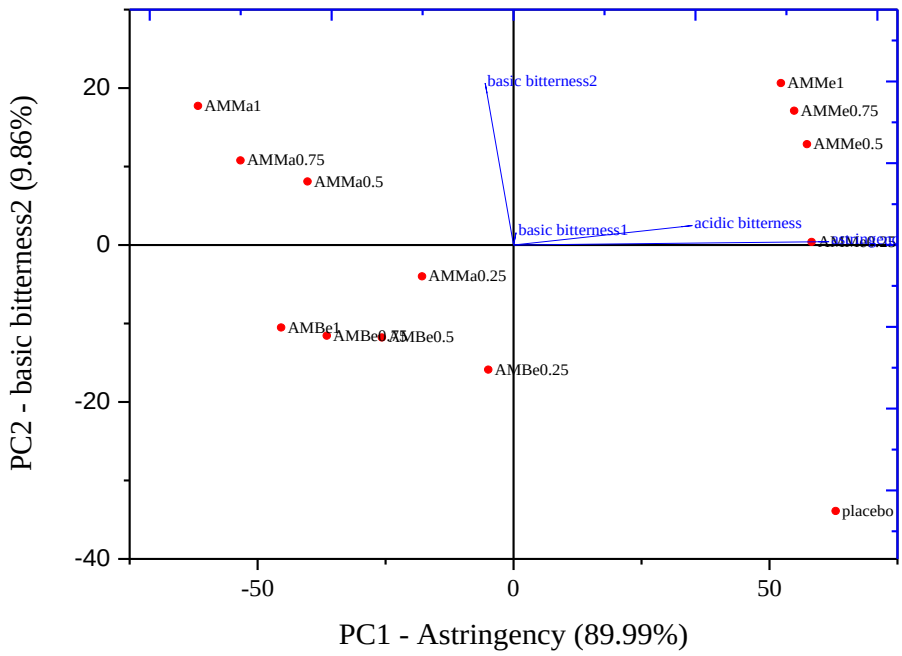


FIGURE 4. 19 A BIPLOT SHOWING PRINCIPAL COMPONENT ANALYSIS TOGETHER WITH LOADING PLOT OF EACH OF THE FOUR SENSORS SHOWING THE PREDICTED TASTE SPECIFICATION OF F2 AMLODIPINE BESILATE (AMBE), AMLODIPINE MALEATE (AMMA) AND AMLODIPINE MESILATE (AMME).

Figure 4.21 presents a dendrogram (produced using agglomerative hierarchical clustering), shows the breakdown of the amlodipine formulations in groups based on their taste attributes. 4 groups have been identified. These are distinguished by their colour. The observations on the *x*-axis refer to the sample under investigation while the distance given on the *y*-axis is the Euclidean distance between the samples.

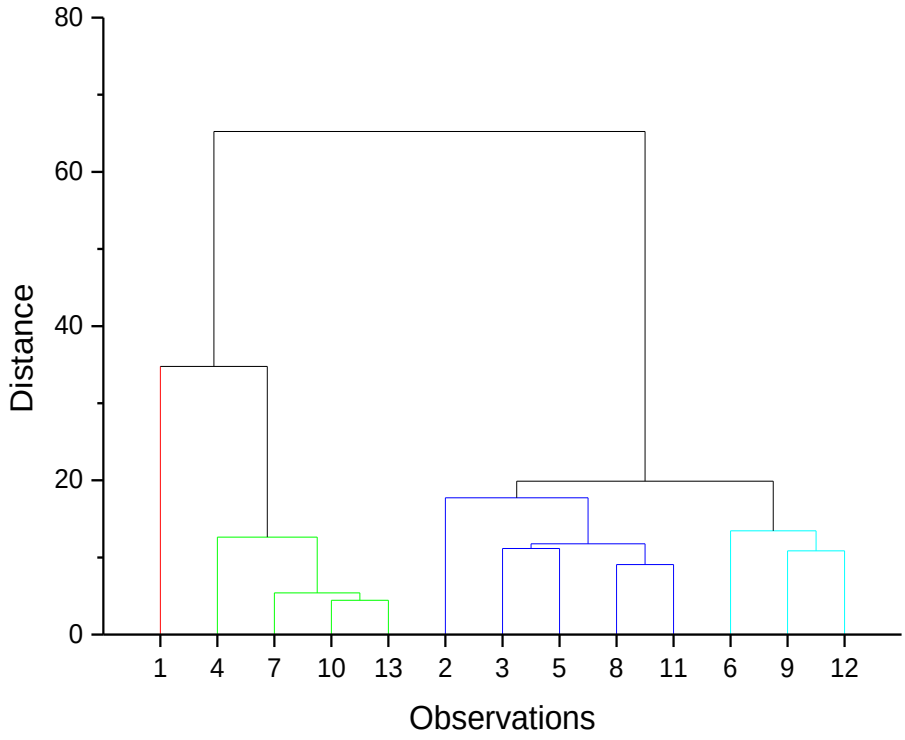


FIGURE 4. 20 A DENDROGRAM USING THE CLUSTERING OF THE AMLODIPINE F2 SUSPENSIONS.

Table 4.8 shows the breakdown of the clusters and their membership. What is interesting but expected in this data is the fact that all the samples are grouped according to their salt forms, i.e. all the amlodipine mesilate samples are in the same group. The exception to this observation is amlodipine maleate 0.25, which is grouped together with the amlodipine besilate suspensions.

TABLE 4. 8 CLUSTER MEMBERSHIP, SHOWING WHICH OBSERVATIONS ARE SIMILAR HENCE GROUPED TOGETHER

| Cluster | Membership (observation number and sample name) | |
|---|---|---|
| **1** | 1 - placebo | |
| **2** | 4- amlodipine mesilate(0.25)<br>7- amlodipine mesilate (0.50 | 10- amlodipine mesilate (0.75)<br>13 – amlodipine mesilate (1) |
| **3** | 2- amlodipine besilate (0.25)<br>3- amlodipine maleate (0.25)<br>5 – amlodipine besilate (0.5) | 8 – amlodipine besilate (0.75)<br>11 – amlodipine besilate )1) |
| **4** | 6- amlodipine maleate (0.5)<br>9- amlodipine maleate (0.75) | 12- amlodipine maleate (1) |

The Euclidean distances between the imaginary centre of the clusters is given in Table 4.8. Interestingly the largest difference is observed between placebo (cluster 1) and amlodipine maleate (cluster 4). Another interesting observation is that amlodipine mesilate (cluster 2) has the smallest separation from placebo.

TABLE 4. 9 EUCLIDEAN DISTANCES BETWEEN THE CLUSTER CENTRES OF THE FOUR CLUSTERS

| | Cluster 1 | Cluster 2 | Cluster 3 | Cluster 4 |
|---|---|---|---|---|
| **Cluster 1** | 0 | 47.22 | 91.99 | 123.61 |
| **Cluster 2** | 47.22 | 0 | 85.04 | 107.40 |
| **Cluster 3** | 91.99 | 85.04 | 0 | 34.43 |
| **Cluster 4** | 123.61 | 107.40 | 34.43 | 0 |

#### 4.3.3.1 SUMMARY OF RESULTS

The results in this section indicate that, all the F2 formulations are detectable on the taste sensor with the astringency sensor exhibiting the most response (89%). The basic bitterness2 demonstrates the next prominent response, accounting for 10% of data variation observed. Cluster analysis revealed four distinct clusters. The association between the clustering and the PCA loading is unclear for the F2 formulations. Amlodipine maleate of concentrations 0.5, 0.75 and 1mg/ml show the largest deviation from placebo (cluster 1), whilst cluster 2 (consisting predominantly of amlodipine mesilate) shows closest distance to placebo. Therefore when considering F2 formulations, amlodipine maleate is least palatable while amlodipine mesilate has the best palatability. It is noteworthy that amlodipine mesilate F1 and F2 formulations have been identified to have the least separation from water thus far. The next section, therefore, will move on to explore F3 formulations of the three different salts.

### *4.3.4 AMLODIPINE F3 FORMULATIONS*

The sensor response patterns of amlodipine besilate F3 formulation is shown in Figure 4.23. This figure reveals a gradual change in sensor response with increases in concentration for acidic bitterness and astringency. The changes for the basic bitterness sensors are not readily obvious. There is no change observed at lower concentrations i.e. 0.25 and 0.5mg/ml, however for the basic bitterness1 sensor, a step change is observed between 0.5mg/ml and 0.75mg/ml. In general, a statistical anaylsis using a one-way ANOVA showed that there was no significant difference ($p= 4.94x10^{-5}$).

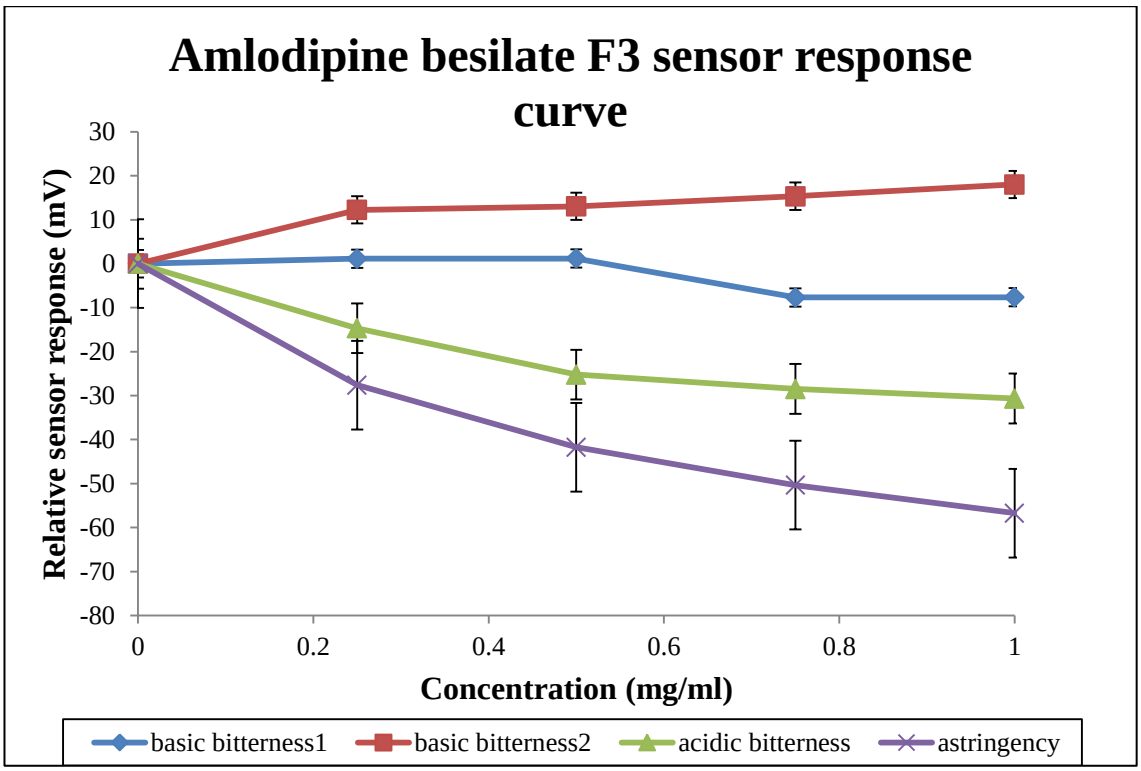


FIGURE 4. 21 RELATIVE SENSOR RESPONSE CURVE FOR AMLODIPINE BESILATE F3 FORMULATION, SHOWING THE RESPONSES OF FOUR SENSORS WHICH CORRESPOND TO DIFFERENT TASTE SPECIFICATIONS, AS A FUNCTION OF CONCENTRATION (N-3, $\bar{x}$±SD)

The responsiveness of the sensors to amlodipine maleate F3 formulations is shown in Figure 4.24. The most striking result to emerge from this data is that the response pattern for amlodipine F3 is similar to that observed in amlodipine F2 formulations. Both the astringency and acidic bitterness sensors show a concentration dependant response. The basic bitterness 1 sensors shows no difference in response to placebo, while basic bitterness 2 sensors shows a difference between placebo and 0.25mg/ml concentration, however no further changes in response are observed as concentrations continued to increase. This was confirmed by a one-way ANOVA which showed that there no statistically significant difference ($p= 4.59x10^{-5}$).

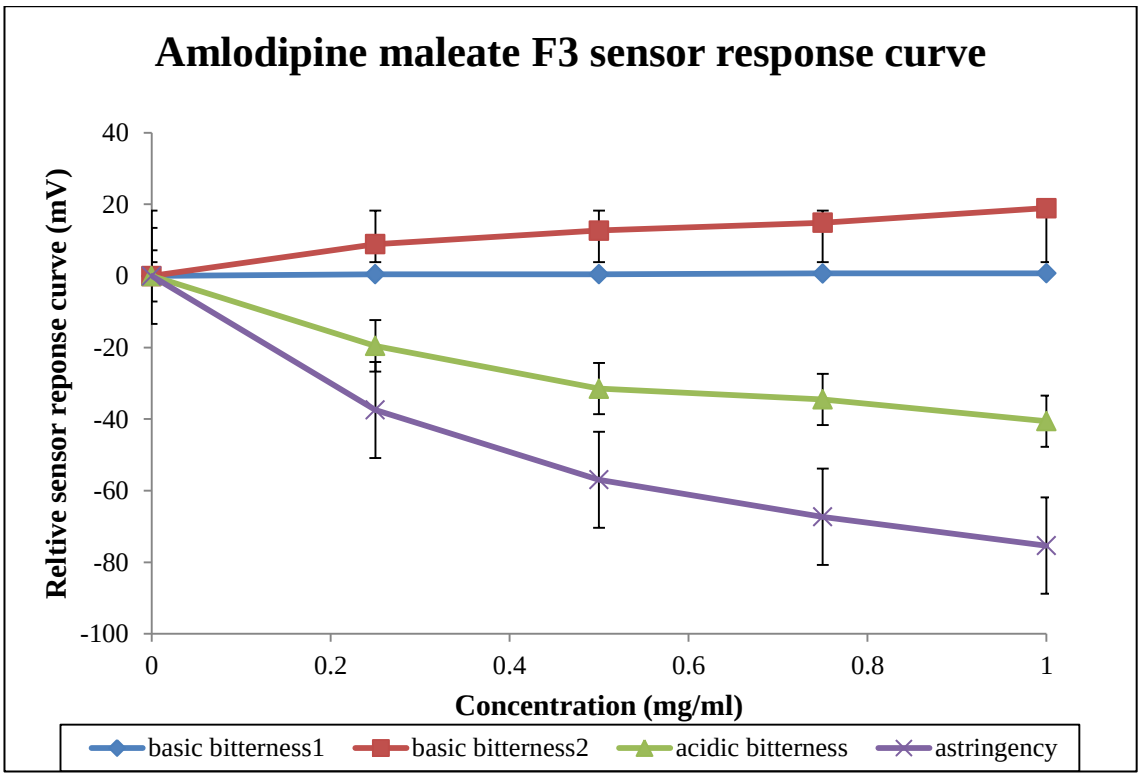


FIGURE 4. 22 RELATIVE SENSOR RESPONSE CURVE FOR AMLODIPINE MALEATE F3 FORMULATION, SHOWING THE RESPONSES OF FOUR SENSORS WHICH CORRESPOND TO DIFFERENT TASTE SPECIFICATIONS, AS A FUNCTION OF CONCENTRATION (N-3, $\bar{x}$±SD)

Contrary to the results reported for amlodipine maleate, amlodipine mesilate shows a different pattern of response between the F2 and F3 formulations. With the exception of the basic bitterness1 sensor which shows no concentration dependent response, all the other sensors exhibit that trait. Interestingly the acidic bitterness sensor shows no concentration dependence when comparing the higher concentrations. A one-way ANOVA showed that there was no statistically significant difference in the sensor response patterns ($p= 2.15x10^{-5}$).

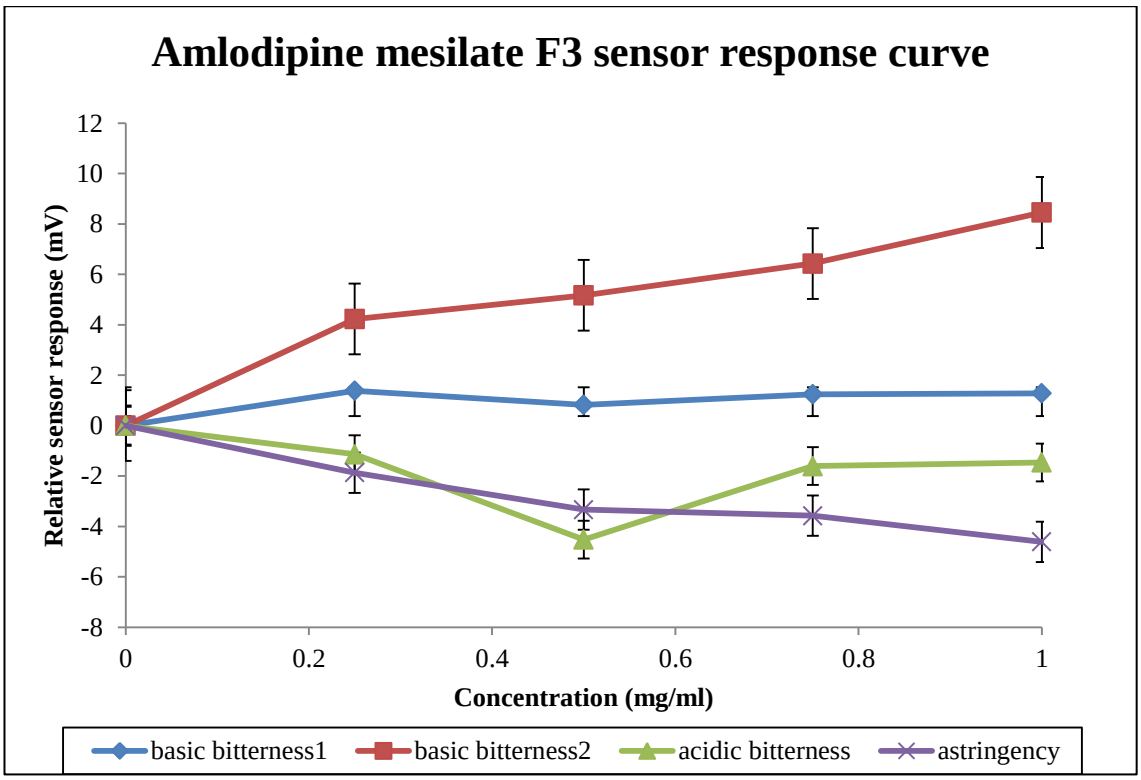


FIGURE 4. 23 RELATIVE SENSOR RESPONSE CURVE FOR AMLODIPINE MESILATE F3 FORMULATION, SHOWING THE RESPONSES OF FOUR SENSORS WHICH CORRESPOND TO DIFFERENT TASTE SPECIFICATIONS, AS A FUNCTION OF CONCENTRATION (N-3, $\bar{x}$±SD)

The eigenvalues and corresponding variance for each of the principal components are shown in Table 4.10. The cumulative percentage shows that the first and second principal components (PC1) and (PC2) respectively, account for approximately 99% of the variance. To this end, only PC1 and PC2 are used in further analysis of the data. It is noteworthy that the significance levels of PC1 and PC2 are both low ($p<0.05$), therefore suggesting that there is a statistically significant difference between them.

TABLE 4. 10 EIGENVALUES OF THE COVARIANCE MATRIX ILLUSTRATING THE CONTRIBUTION AND SIGNIFICANCE OF EACH PRINCIPLE COMPONENT

| PCA | Eigenvalue | Percentage of Variance (%) | Cumulative (%) | χ2 | Degrees of Freedom | Significance level (p) |
|---|---|---|---|---|---|---|
| **1** | 2432.34 | 96.84 | 96.84 | 110.4 | 9 | $1.22 \times 10^{-19}$ |
| **2** | 66.48 | 2.65 | 99.48 | 22.19 | 5 | $4.81 \times 10^{-4}$ |
| **3** | 8.98 | 0.36 | 99.84 | 1.71 | 2 | 0.42 |
| **4** | 4.01 | 0.16 | 100 | 0 | 0 | 0 |

Similar to the results reported in **Section 4.3.3**, the extracted eigenvalues are shown in Table 4.11. It is clear that the highest contribution to PC1 is predominantly astringency, while PC2 has major influence from acidic bitterness.

TABLE 4. 11 EXTRACTED EIGENVECTORS FOR PC1 AND PC2, SHOWING THE CONTRIBUTION OF EACH SENSOR TO THE FIRST AND SECOND PRINCIPAL COMPONENTS.

| | Coefficient of PC1 | Coefficient of PC2 |
|---|---|---|
| **Basic bitterness1** | 0.02 | 0.12 |
| **Basic bitterness2** | -0.14 | -0.15 |
| **Acidic bitterness** | 0.27 | 0.93 |
| **Astringency** | 0.95 | -0.29 |

The results of the principal component analysis scores and loadings are set out in Figure 4.26. The biplot is revealing in several ways. In the first instance, the amlodipine mesilate (AMMe) samples are clustered together with the placebo (1:1 mixture of ora-sweet® and ora- plus®). Secondly, none of the samples under investigation are aligned with astringency. Thirdly, the amlodipine mesilate samples are associated with acidic bitterness; however caution is needed when interpreting this observation as acidic bitterness only accounts for approximately 3% of the variance. Lastly, significant and expected differentiation is observed between F3 formulations and water.

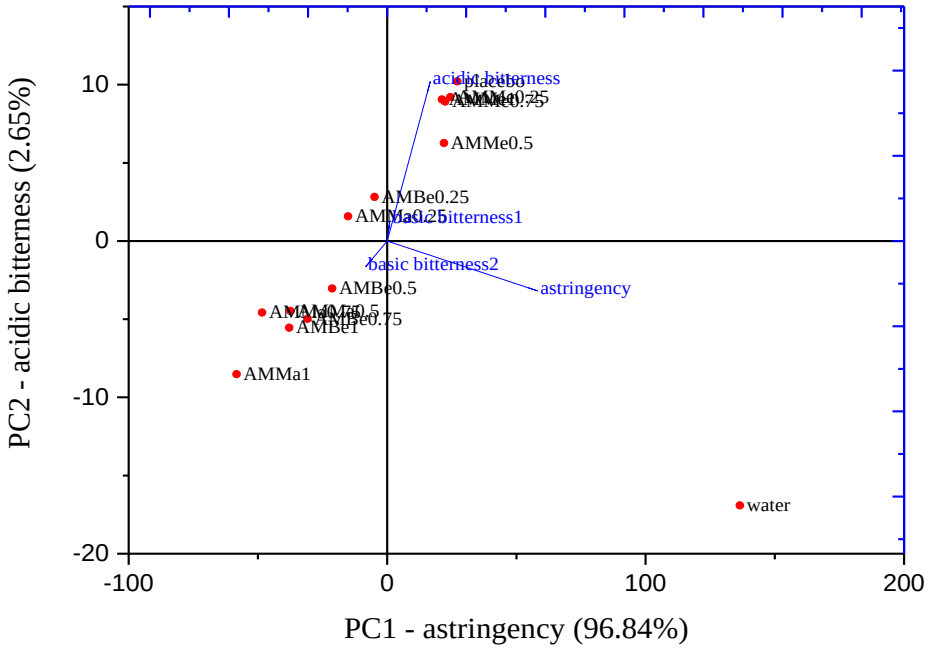


FIGURE 4. 24 A BIPLOT SHOWING PRINCIPAL COMPONENT ANALYSIS TOGETHER WITH LOADING PLOT OF EACH OF THE FOUR SENSORS SHOWING THE PREDICTED TASTE SPECIFICATION OF AMLODIPINE BESILATE (AMBE), AMLODIPINE MALEATE (AMMA) AND AMLODIPINE MESILATE (AMME) WHEN PRESENTED AS F3 FORMULATION.

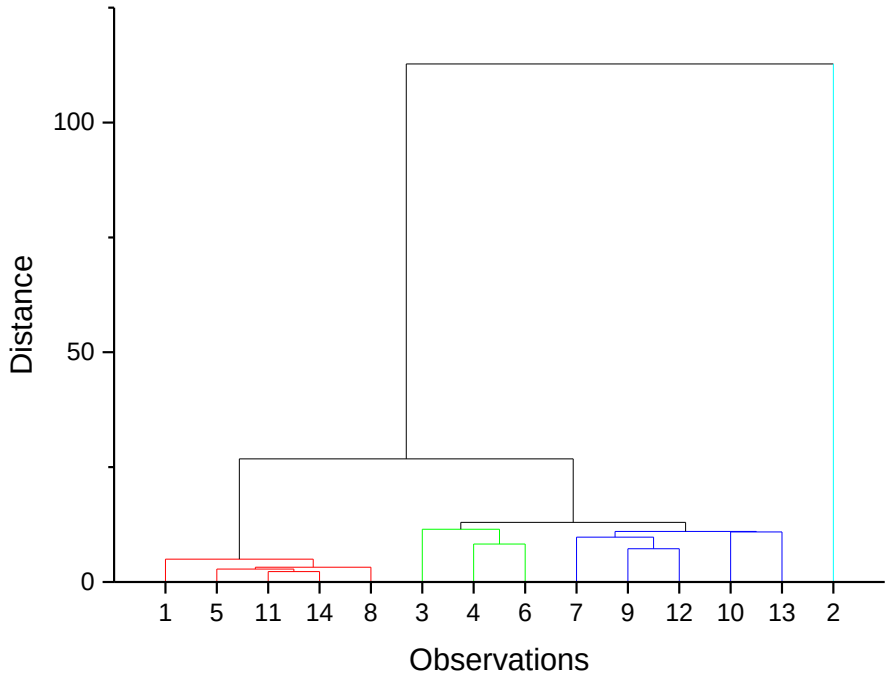


FIGURE 4. 25 DENDROGRAM FOR AMLODIPINE F3 FORMUALTIONS, SHOWING FOUR CLUSTERS

The clusters identified from the sensor responses are presented in Table 4.11 and the Euclidean distances between the clusters is given in Table 4.12. As can been seen from the biplot (Figure 4.26) and dendrogram (Figure 4.27), the amlodipine mesilate F3 formulations are similar to placebo hence in the same cluster. It is somewhat surprising that the separation between amlodipine besilate and maleate is unclear. It appears the lower concentrations of both salts are clustered together and the same is true for the higher concentrations.

TABLE 4. 12 CLUSTER MEMBERSHIPS, SHOWING WHICH OBSERVATIONS ARE SIMILAR HENCE GROUPED TOGETHER

| Cluster | Membership (observation number and sample name ( concentration)) | |
|---|---|---|
| **1** | 1- placebo<br>5- amlodipine mesilate (0.25)<br>8 – amlodipine mesilate (0.5) | 11- amlodipine mesilate (0.75)<br>14 – amlodipine mesilate (1) |
| **2** | 3- amlodipine besilate (0.25)<br>4- amlodipine maleate (0.25) | 6 – amlodipine besilate (0.5) |
| **3** | 7- amlodipine maleate (0.5)<br>9 – amlodipine besilate (0.75)<br>10 – amlodipine maleate (0.75) | 12- amlodipine besilate (1)<br>13 amlodipine maleate (1) |
| **4** | 2 - water | |

The Euclidean distances between the imaginary centres of the four clusters are given in Table 4.12. Unsurprisingly, clusters 3 and 4 show the largest separation

TABLE 4. 13 EUCLIDEAN DISTANCES BETWEEN THE CLUSTER CENTRES OF THE FOUR CLUSTERS

| | Cluster 1 | Cluster 2 | Cluster 3 | Cluster 4 |
|---|---|---|---|---|
| **Cluster 1** | 0 | 38.11 | 67.54 | 115.90 |
| **Cluster 2** | 38.11 | 0 | 29.56 | 151.20 |
| **Cluster 3** | 67.55 | 29.56 | 0 | 179.39 |
| **Cluster 4** | 115.90 | 151.20 | 179.39 | 0 |

#### 4.3.4.1 SUMMARY OF RESULTS

The findings from this section suggest that all the F3 formulations are detectable on the taste sensor with the astringency sensor exhibiting the most response (97%). The acidic bitterness demonstrates the next prominent response, accounting for 3% of data variation observed. Cluster analysis revealed four distinct clusters. Unlike the previous reported results in **Section 4.32 and 4.3.3**, in these results the cluster and sensors association is not evidently obvious. Furthermore, there is no significant separation between the clustering of amlodipine maleate and amlodipine besilate. However, it is clear that these two amlodipine salts exhibit the largest Euclidean distance from water. Again, amlodipine mesilate has the smallest separation from water in terms of the Euclidean distance. Therefore when considering F3 formulations amlodipine mesilate has the best palatability, a result which has been consistent in observations thus far. The next section reports a comparison of amlodipine besilate salt in the three different formulations.

### *4.3.5 AMLODIPINE BESILATE F1, F2, F3*

It can be seen from the data presented in Table 4.14 that the cumulative percentage of variance for PC1 and PC2 is approximately 99%, therefore this suggests that only the first two principal components were necessary to display data on a biplot. The significance level of both principal components 1 and 2 are less than 0.05 therefore these principal components are statistically significant.

TABLE 4. 14 EIGENVALUES OF THE COVARIANCE MATRIX FOR AMLODIPINE BESILATE F1, F2 AND F3 FORMULATIONS

| PCA | Eigenvalue | Percentage of Variance (%) | Cumulative (%) | χ2 | Degrees of Freedom | Significance level (p) |
|---|---|---|---|---|---|---|
| **1** | 5729.12 | 95.89 | 95.89 | 98.75 | 9 | $2.82 \times 10^{-17}$ |
| **2** | 212.63 | 3.56 | 99.45 | 26.29 | 5 | $7.83 \times 10^{-5}$ |
| **3** | 26.10 | 0.44 | 99.89 | 4.13 | 2 | 0.13 |
| **4** | 6.82 | 0.11 | 100.00 | 0 | 0 | 0 |

The data presented in Table 4.15 shows that the astringency sensor has the highest contribution to PC1. The major contributor for PC2 is acidic bitterness.

TABLE 4. 15 EXTRACTED EIGENVECTORS FOR PC1 AND PC2, SHOWING THE CONTRIBUTION OF EACH SENSOR TO THE FIRST AND SECOND PRINCIPAL COMPONENTS

| | Coefficient of PC1 | Coefficient of PC2 |
|---|---|---|
| **Basic bitterness1** | -0.04 | 0.21 |
| **Basic bitterness2** | -0.23 | 0.21 |
| **Acidic bitterness** | 0.06 | 0.95 |
| **Astringency** | 0.97 | -0.01 |

The biplot shown in Figure 4.27 unsurprisingly shows the separation between F1 formulations and the rest of the samples. From the biplot, the separation between F2 and F3 formulations is not as clear. As previously highlighted the F1 formulations are closely associated with acidic bitterness while F2 and F3 formulations as clustered around astringency. However, it is also clear than none of the formulations are associated with water which is removed from the loadings of the sensors.

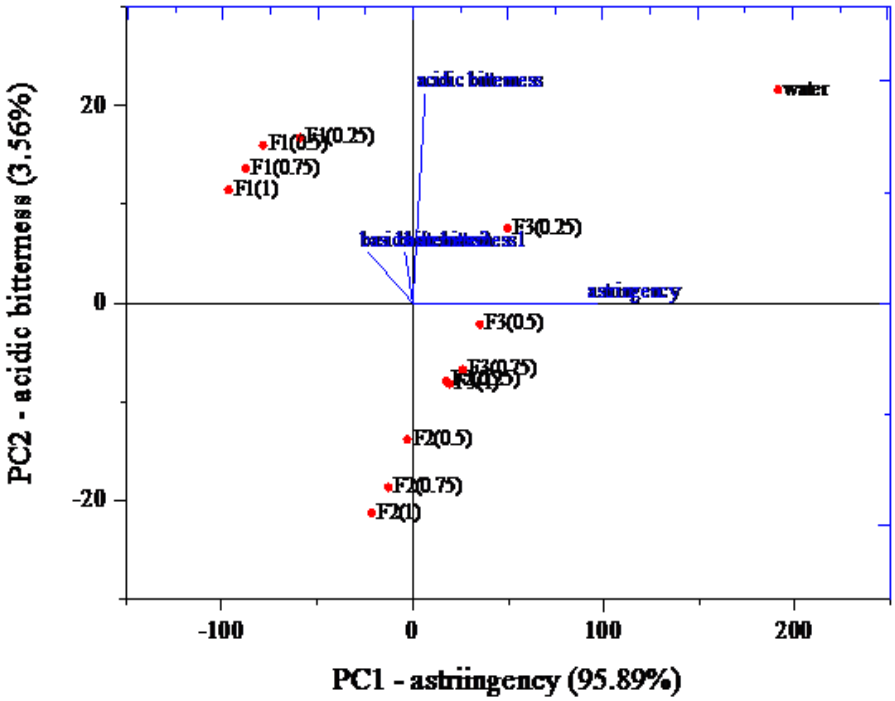


FIGURE 4. 26 A BIPLOT SHOWING PRINCIPAL COMPONENT ANALYSIS TOGETHER WITH LOADING PLOT OF EACH OF THE FOUR SENSORS SHOWING THE PREDICTED TASTE SPECIFICATION OF AMLODIPINE BESILATE F1, F2 AND F3 FORMULATIONS.

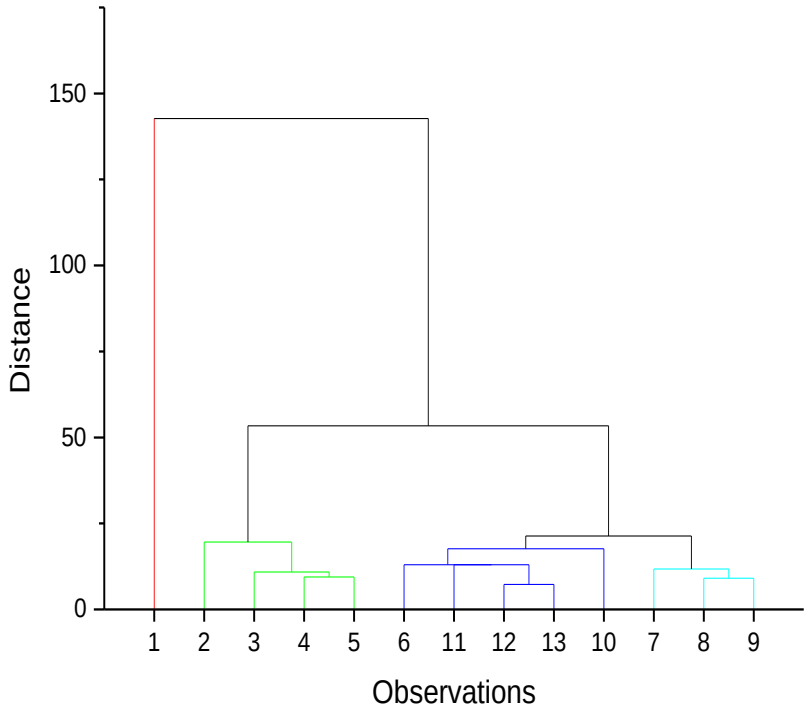


FIGURE 4. 27 DENDROGRAM FOR AMLODIPINE BESILATE F1, F2 AND F3 FORMULATIONS, SHOWING FOUR CLUSTERS DIFFERENTIATED BY COLOURS.

The data presented in Table 4.16 supports the observations reported on the biplot. From this data, it is apparent that cluster analysis has shown separation between F2 and F3 formulations. It appears that only F2 0.25mg/ml is clustered with the F3 formulations. The significance of the separation is given in Table 4.16 in the form of Euclidean distances.

TABLE 4. 16 CLUSTER MEMBERSHIP, SHOWING WHICH OBSERVATIONS ARE SIMILAR HENCE GROUPED TOGETHER

| Cluster | Membership (observation number and sample name ( concentration)) | |
|---|---|---|
| **1** | 1-water | |
| **2** | 2- F1(0.25)<br>3- F1 (0.5) | 4- F1 (0.75<br>5- F1 (1) |
| **3** | 6- F2 (0.25)<br>10- F3 (0.25)<br>11-F3 (0.5) | 12- F3 (0.75)<br>13- F3 (1) |
| **4** | 7- F2 (0.5)<br>8- F2 (0.75) | 9- F2 (1) |

Clusters 1 and 2 (water and F1 formulations) exhibit the biggest separation represented by the Euclidean distance between them, as illustrated in Table 4.17. The smallest separation is observed between clusters 1 and 3 (F3 formulations), suggesting that the F3 formulations have better palatability when compared to the other formulations. It can therefore be concluded that the ordering of separation of the samples from water is as follows: F1>F2>F3.

TABLE 4. 17 EUCLIDEAN DISTANCES BETWEEN THE CLUSTER CENTRES OF THE FOUR CLUSTERS OF AMLODIPINE BESILATE F1, F2 AND F3 FORMULATIONS

| | Cluster 1 | Cluster 2 | Cluster 3 | Cluster 4 |
|---|---|---|---|---|
| **Cluster 1** | 0 | 271.58 | 163.86 | 207.43 |
| **Cluster 2** | 271.58 | 0 | 111.35 | 75.32 |
| **Cluster 3** | 163.86 | 111.35 | 0 | 45.31 |
| **Cluster 4** | 207.43 | 75.32 | 45.32 | 0 |

#### 4.3.5.1 SUMMARY OF RESULTS

The findings in this section show that the astringency (96%) and acidic bitterness (4%) sensors are the major contributors to responses observed. Unsurprisingly, the largest separation in terms of Euclidean distances is observed between water and the F1 formulations. However, cluster analysis does not show a significant difference between the F2 and F3 formulations.

### *4.3.6 AMLODIPINE MALEATE F1, F2 AND F3*

The data presented in Table 4.18 shows that the first and second principal components account for over 99% of the variation observed, therefore only these principal components are considered when plotting the biplot shown in Figure 4:30.

TABLE 4. 18 EIGENVALUES OF THE COVARIANCE MATRIX FOR AMLODIPINE MALEATE F1, F2 AND F3 FORMULATIONS

| PCA | Eigenvalue | Percentage of Variance (%) | Cumulative (%) | χ2 | Degrees of Freedom | Significance level (p) |
|---|---|---|---|---|---|---|
| **1** | 4853.35 | 89.19 | 89.19 | 131.88 | 9 | $4.88 \times 10^{-24}$ |
| **2** | 577.33 | 10.61 | 99.80 | 87.24 | 5 | $2.55 \times 10^{-17}$ |
| **3** | 10.73 | 0.20 | 100 | 27.40 | 2 | $1.12 \times 10^{-6}$ |
| **4** | 0.17 | 0 | 100 | 0 | 0 | 0 |

The extracted eigenvectors of PC1 and PC2 are given in Table 4.19. They show that the astringency sensor has the highest coefficient of PC1 (0.98). The basic bitterness2 sensor has the highest coefficient of PC2 (0.95).

TABLE 4. 19 EXTRACTED EIGENVECTORS FOR PC1 AND PC2, SHOWING THE CONTRIBUTION OF EACH SENSOR TO THE FIRST AND SECOND PRINCIPAL COMPONENTS

| | Coefficient of PC1 | Coefficient of PC2 |
|---|---|---|
| **Basic bitterness1** | -0.00 | 0.06 |
| **Basic bitterness2** | -0.06 | 0.95 |
| **Acidic bitterness** | 0.02 | -0.29 |
| **Astringency** | 0.98 | 0.12 |

The biplot given in Figure 4:30, shows the principal components 1 and 2 together with the loadings of the sensors. The F2 formulations are closely associated with the basic bitterness 2 while the F3 formulations are associated with astringency and acidic bitterness. It is also apparent that there is clear separation between all three formulations.

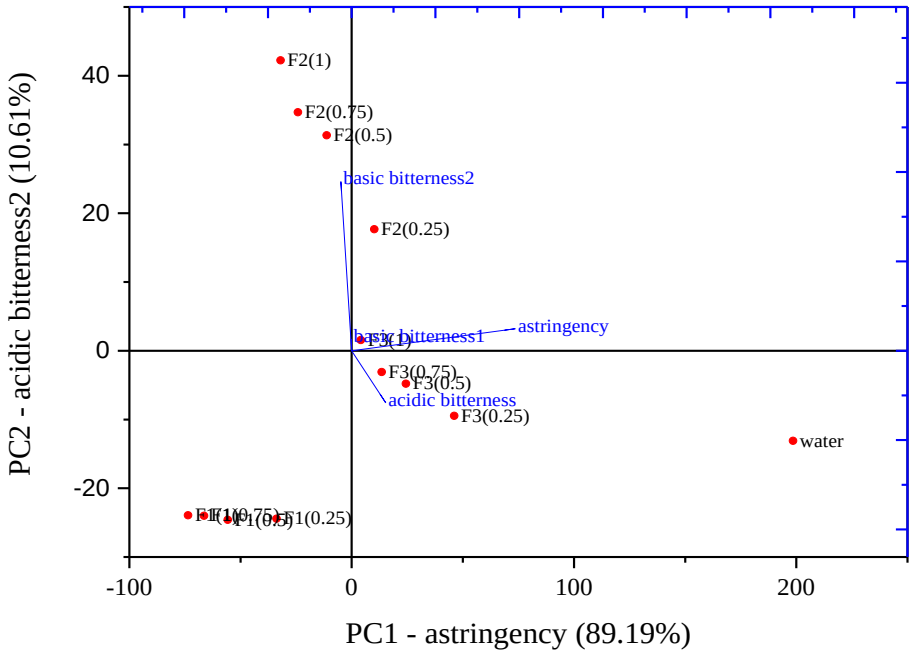


FIGURE 4. 28 A BIPLOT SHOWING PRINCIPAL COMPONENT ANALYSIS TOGETHER WITH LOADING PLOT OF EACH OF THE FOUR SENSORS SHOWING THE PREDICTED TASTE SPECIFICATION OF AMLODIPINE MALEATE F1, F2 AND F3 FORMULATIONS

The dendrogram illustrated in Figure 4.31 produced following agglomerative hierarchical cluster analysis shows the grouping of formulations (*x*-axis) which are similar in terms of principal component analysis. The *y* axis shows the Euclidean distances separating the imaginary centres of each cluster. Table 4.20 details which formulations make up each cluster. Interestingly, the lowest concentration of F2 i.e. F2 (0.25), is grouped together with the F3 formulations. Although the biplot appears to demonstrate separation between all the formulation groups cluster analysis has revealed that there no clear separation between F2 and F3 formulations of amlodipine maleate.

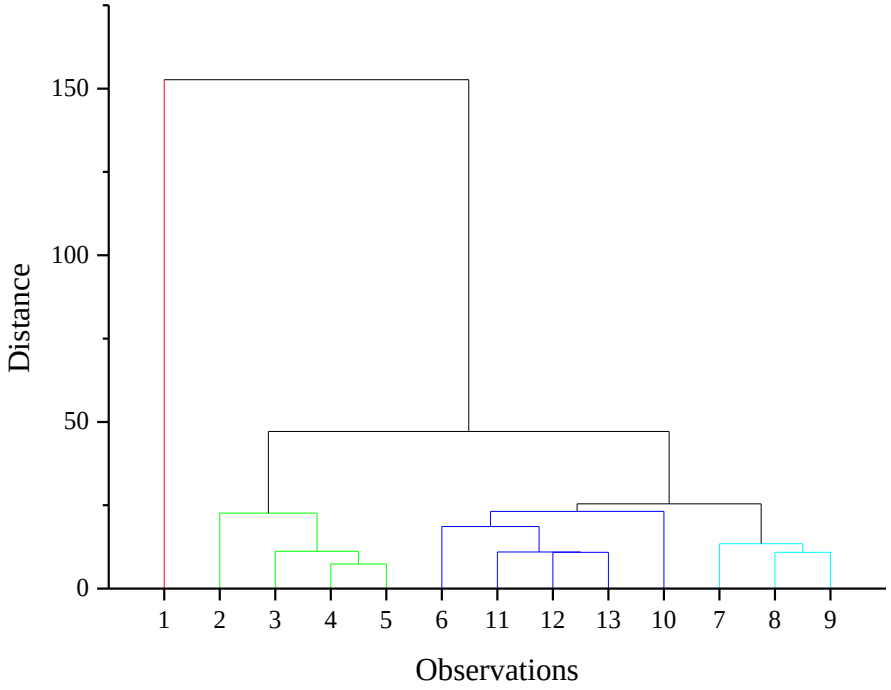


FIGURE 4. 29 DENDROGRAM FOR AMLODIPINE MALEATE F1, F2 AND F3 FORMULATIONS, SHOWING FOUR CLUSTERS DIFFERENTIATED BY FOUR COLOURS.

TABLE 4. 20 CLUSTER MEMBERSHIP, SHOWING THE GROUPING OF FORMULATIONS BY SIMILARITY

| Cluster | Membership (observation number and sample name ( concentration)) | |
|---|---|---|
| **1** | Water | |
| **2** | 1- F1 (0.25)<br>2- F1(0.5) | 3- F1 (0.75)<br>4- F1 (1) |
| **3** | 5- F2 (0.25)<br>10 – F3 (0.25)<br>11- F3 (0.5) | 12- F3 (0.75)<br>13 – F3 (1) |
| **4** | 6- F2 (0.5)<br>7- F2 (0.75) | F2 (1) |

The Euclidean distances between the imaginary centres of the four clusters are given in Table 4.21. Unsurprisingly, the largest separation distance is observed between

water (cluster 1) and the F1 formulations in cluster 2. Assuming that water has good palatability, this implies that F1 formulations are furthest away from the same palatability as water. Equally of note, is that fact that the shortest Euclidean distance is observed between clusters 1 and 3. This suggests that F3 formulations are closest to water in terms of taste therefore suggesting better palatability than the other formulation clusters. The ordering of the formulations with respect to their separation from water is as follows: F1>F2>F3. This observation is similar to that already shown for amlodipine besilate reported in **Section 4.3.5**.

TABLE 4. 21 CLUSTER MEMBERSHIPS, SHOWING WHICH OBSERVATIONS ARE SIMILAR HENCE GROUPED TOGETHER

| | **Cluster 1** | **Cluster 2** | **Cluster 3** | **Cluster 4** |
|---|---|---|---|---|
| **Cluster 1** | 0 | 256.16 | 179.40 | 226.41 |
| **Cluster 2** | 256.16 | 0 | 80.87 | 60.70 |
| **Cluster 3** | 179.40 | 80.87 | 0 | 55.22 |
| **Cluster 4** | 226.41 | 69.70 | 55.22 | 0 |

### *4.3.7 AMLODIPINE MESILATE F1, F2 AND F3*

The eigenvalues and corresponding variance for each of the principal components are shown in Table 4.22. The cumulative percentage shows that the first and second principal components (PC1) and (PC2) respectively, account for approximately 95% of the variance. To this end, only PC1 and PC2 are used in further analysis of the data. It is noteworthy that the significance levels of PC1 and PC2 are both low (<0.05), therefore suggesting that there a statistically significant difference between them.

TABLE 4. 22 EIGENVALUES OF THE COVARIANCE MATRIX FOR AMLODIPINE MESILATE F1, F2 AND F3 FORMULATIONS

| PCA | Eigenvalue | Percentage (%) of Variance | Cumulative (%) | χ2 | Degrees of Freedom | Significance level (p) |
|---|---|---|---|---|---|---|
| **1** | 1678.68 | 77.16 | 77.16 | 84.51 | 9 | $2.04 \times 10^{-24}$ |
| **2** | 400.95 | 18.43 | 95.59 | 60.52 | 5 | $9.48 \times 10^{-12}$ |
| **3** | 95.70 | 4.40 | 99.99 | 44.85 | 2 | $1.83 \times 10^{-10}$ |
| **4** | 0.25 | 0.01 | 0.01 | 0 | 0 | 0 |

The extracted eigenvectors for the first and second principal components are given in Table 4.23. It is clear that the astringency sensor with a coefficient of 0.98 is the only contributor to PC1 and the basic bitterness2 sensor which has a coefficient of 0.98 is the major contributor for PC2. With this in mind it can be inferred that the *x*-axis on the biplot illustrates astringency while the *y*- axis illustrates basic bitterness.

TABLE 4. 23 EXTRACTED EIGENVECTORS FOR PC1 AND PC2, SHOWING THE CONTRIBUTION OF EACH SENSOR TO THE FIRST AND SECOND PRINCIPAL COMPONENTS

| | Coefficient of PC1 | Coefficient of PC2 |
|---|---|---|
| **Basic bitterness1** | -0.02 | 0.04 |
| **Basic bitterness2** | -0.14 | 0.98 |
| **Acidic bitterness** | -0.16 | -0.29 |
| **Astringency** | 0.98 | 0.09 |

The biplot shown in Figure 4.32 gives the first and second principal components plotted on the *x* and *y*- axes respectively, with the sample plotted as a scatter plot. The sensors loadings (shown in blue) are also plotted. As already illustrated via the extracted eigenvalues, the astringency sensor is closely associated with the *x*- axis, while the basic bitterness 2 sensor is associated with the *y*- axis. It is clear from this biplot that there is separation between F1, F2, F3 formulations and water.

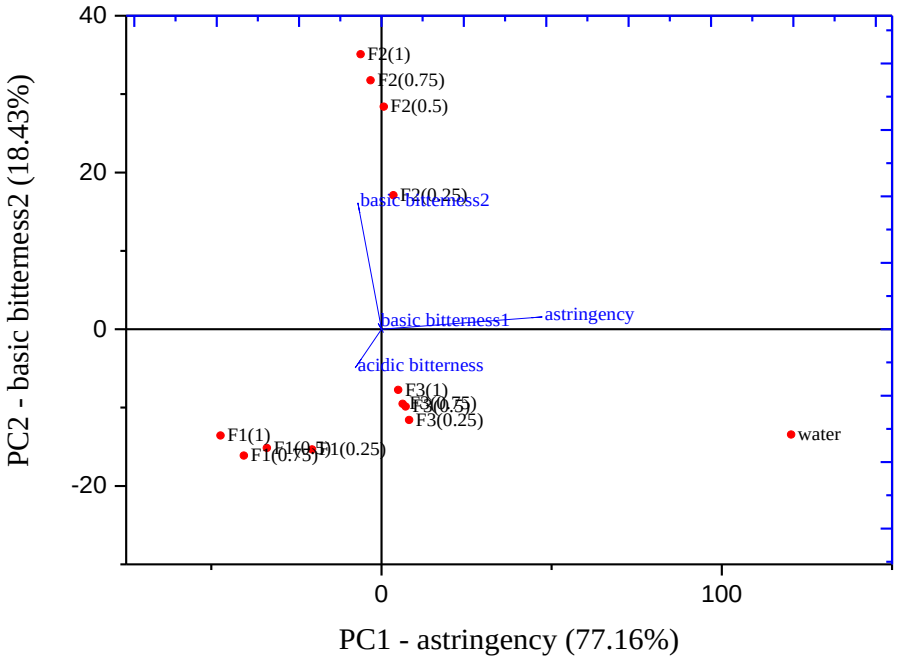


FIGURE 4. 30 A BIPLOT SHOWING PRINCIPAL COMPONENT ANALYSIS TOGETHER WITH LOADING PLOT OF EACH OF THE FOUR SENSORS SHOWING THE PREDICTED TASTE SPECIFICATION OF AMLODIPINE MESILATE F1, F2 AND F3 FORMULATIONS

The dendrogram shown in Figure 4.33 illustrates hierarchical agglomerative cluster analysis which groups the samples according to their similarities. Four clusters are identified as predicted by the biplot shown the in Figure 4.32.

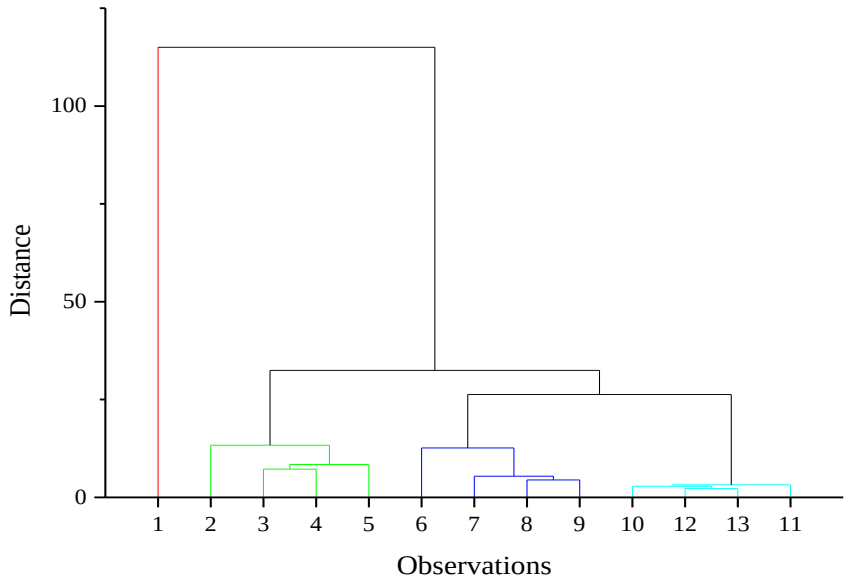


FIGURE 4. 31 DENDROGRAM FOR AMLODIPINE MESILATE F1, F2 AND F3 FORMULATIONS, SHOWING FOUR CLUSTERS DIFFERENTIATED BY FOUR COLOURS.

The membership of each cluster is given in Table 4.24. It is noteworthy that unlike in the case of the previous salts i.e. besilate and maleate, the mesilate formulations are homogenous in each cluster.

TABLE 4. 24 CLUSTER MEMBERSHIP, SHOWING WHICH OBSERVATIONS ARE SIMILAR HENCE GROUPED TOGETHER

| Cluster | Membership (observation number and sample name ( concentration)) | |
|---|---|---|
| **1** | 1 - water | |
| **2** | 2- F1 (0.25)<br>3- F1 (0.5) | 4- F1 (0.75)<br>5 – F1 (1) |
| **3** | 6 – F2 (0.25)<br>7 – F2(0.5) | 8 – F2 (0.75)<br>9 – F2 (1) |
| **4** | 10 – F3 (0.25)<br>11 – F3(0.5) | 12 – F3 (0.75)<br>13- F3 (1) |

The extent of separation of the four clusters is shown in Table 4.25, which gives the Euclidean distances between each cluster. It is evident that the largest separation is observed between water and the F1 formulations. The F3 formulations are closest to water. Therefore, the separation of the formulations from water is as follows: F1>F2>F3.

TABLE 4. 25 CLUSTER MEMBERSHIP, SHOWING WHICH OBSERVATIONS ARE SIMILAR HENCE GROUPED TOGETHER

| | Cluster 1 | Cluster 2 | Cluster 3 | Cluster 4 |
|---|---|---|---|---|
| **Cluster 1** | 0 | 155.88 | 129.10 | 116.72 |
| **Cluster 2** | 155.88 | 0 | 55.50 | 47.33 |
| **Cluster 3** | 129.10 | 55.50 | 0 | 40.97 |
| **Cluster 4** | 116.72 | 47.33 | 40.97 | 0 |

### *4.3.8 HUMAN TASTE PANEL*

#### 4.3.8.1 AMLODIPINE F1 FORMULATIONS

The taste scores from the participants for the amlodipine are given in Table 4.24. In general, for all three salts, there is an increase in taste scores with increasing concentrations. The highest taste scores were recorded for amlodipine besilate suggesting that this salt was associated with highest unpleasantness.

TABLE 4. 26 AVERAGE TASTE SCORES FOR AMLODIPINE F1 FORMULATIONS

| **Concentrations (mg/ml)** | **0** | **0.25** | **0.5** | **0.75** | **1.0** |
|---|---|---|---|---|---|
| **Amlodipine** besilate **average score ± SD** | 2.8 ± 2.4 | 6.9± 2.4 | 7.7±2.0 | 8.4±1.9 | 8.9±1.8 |
| **Amlodipine** maleate **average score ± SD** | 2.6± 2.3 | 5.8±2.4 | 7.3± 1.8 | 8.2±1.6 | 8.6±1.4 |
| **Amlodipine** mesilate **average score ± SD** | 2.9±2.4 | 5.6±2.2 | 5.9±2.4 | 5.8±2.4 | 8.2±1.5 |

A graphical representation of the taste scores of the F1 formulations of the amlodipine salts is shown in Figure 4.34. It is apparent that there is taste scores of amlodipine besilate and maleate increase with increasing concentration. This is not the case with amlodipine mesilate where no significant difference is observed between 0.25mg/ml – 0.75mg/ml. In all three cases, there is statistically significant difference between placebo and the tastant concentrations.

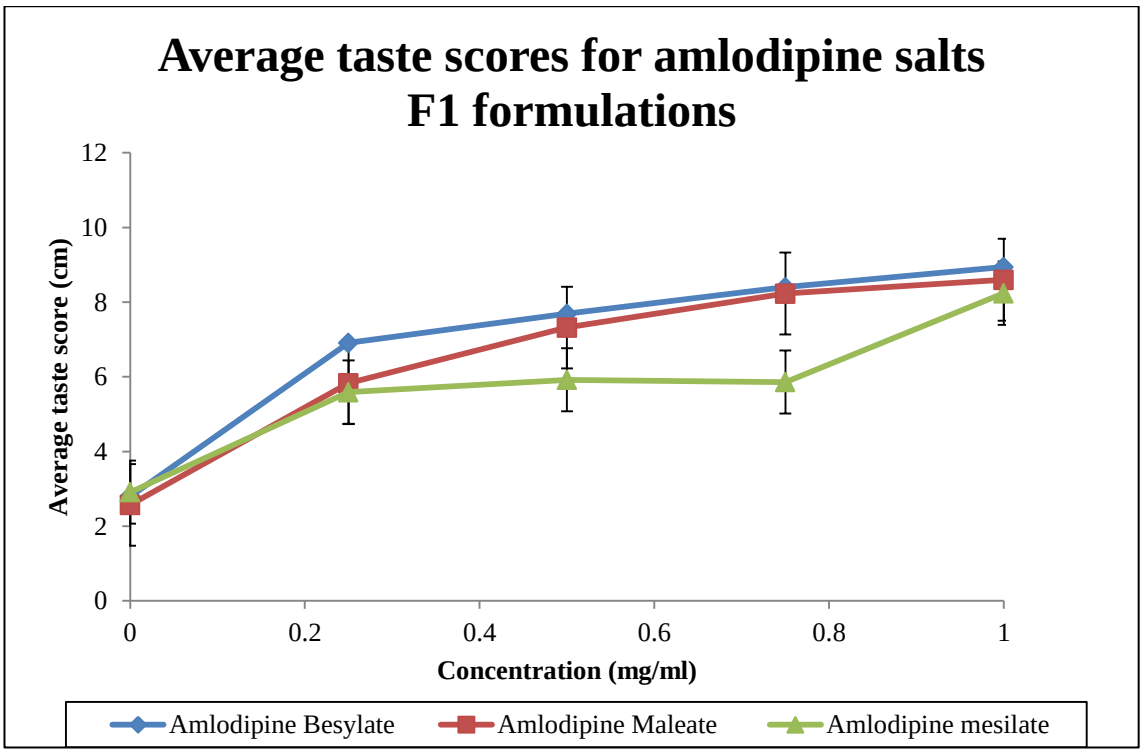


FIGURE 4. 32 AVERAGE TASTE SCORES OF AMLODIPINE F1 FORMULATIONS SHOWING AN INCREASE IN UNPLEASANTNESS WITH INCREASING CONCENTRATION OF EACH SALT (N= 24, $\bar{x}$±SD).

### 4.3.8.2 AMLODIPINE F2 FORMULATIONS

In view of results obtained in section 4.3.8.1, which showed that amlodipine mesilate had the least taste score, it was therefore prudent to only investigate amlodipine besilate and maleate in relation to the taste masking efficiency of F2 formulation. This was necessary to limit the number of samples presented to the participants in order to minimise the risk of taste fatigue. Figure 4.35 illustrates a comparison of taste scores between amlodipine besilate F1 and F2 formulations in conjunction with amlodipine maleate F1 and F2 formulations. It is clear that the addition of simple syrup and 1% methylcellulose reduces the unpleasantness of amlodipine salts. Of interest is the observation that the highest concentration (1mg/ml) appears to have lower taste scores than the proceeding concentration. However, this is not statistically significant in view of the overlapping standard deviation. Also of note is the fact that for the F2 formulations the difference in taste scores between placebo and 0.25mg/ml concentration is negligible. While in contrast, for the F1 concentrations the difference in taste scores between aforementioned concentrations is more evident.

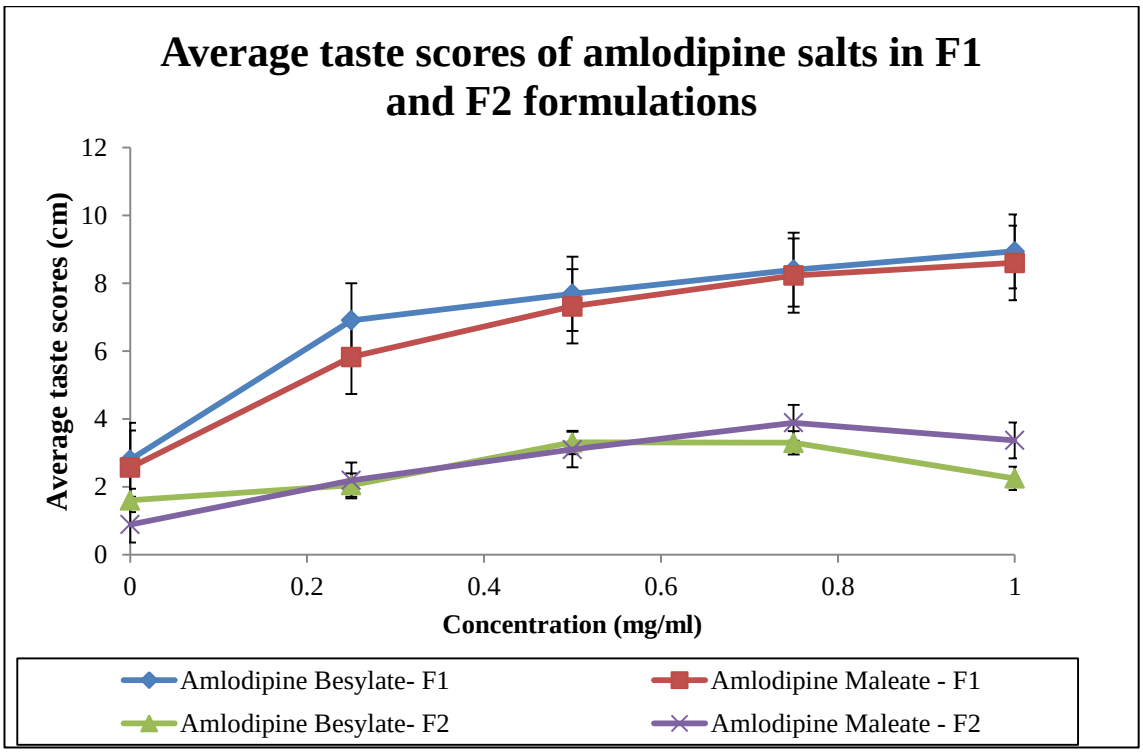


FIGURE 4. 33 AVERAGE TASTE SCORES COMPARING THE DIFFERENCES IN TASTE PERCEPTIONS BETWEEN F1 AND F2 FORMULATIONS FOR AMLODIPINE MALEATE AND BESILATE SALTS (N= 24 $\bar{x}$±SD).

#### 4.3.8.3 AMLODIPINE F3 FORMULATIONS

Similar to the comparison already made in section 4.3.8.2, amlodipine F3 formulations were compared to amlodipine F1 formulations. Similar to the previous comparison to F2 formulations, there is a clear difference in taste scores between the F1 and F3 formulations. Unsurprisingly, the F3 formulations appear to be more pleasant than the F1 formulations. Interestingly, the separation between the amlodipine besilate and maleate formulations is not clear, a theme that is observed throughout the results thus far.

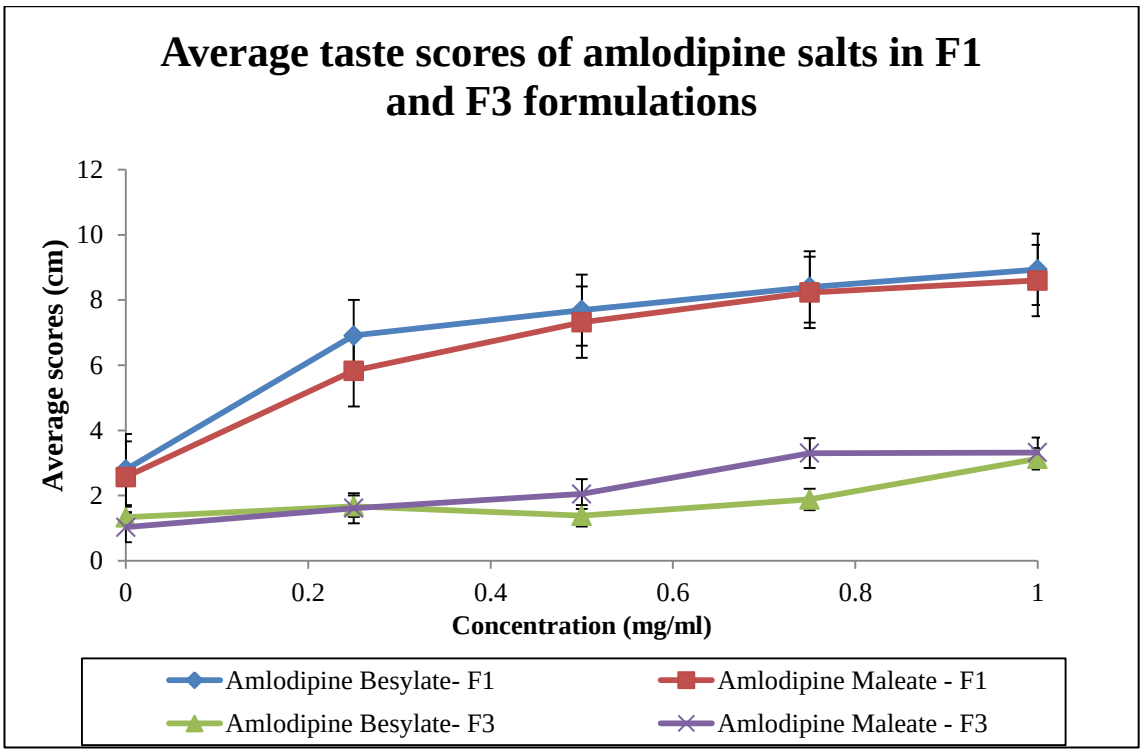


FIGURE 4. 34 AVERAGE TASTE SCORES COMPARING THE DIFFERENCES IN TASTE PERCEPTIONS BETWEEN F1 AND F2 FORMULATIONS FOR AMLODIPINE MALEATE AND BESILATE SALTS (N= 24 $\bar{x}$±SD).

A comparison of the taste scores for F2 and F3 formulations is shown in Figure 4.37. Although, a general increase in unpleasantness is reported with increase concentrations of amlodipine, the separation between the F2 and F3 formulations for each salt is not as clear. This therefore points to the conclusion that it is not possible to separate F2 and F3 formulations in terms of taste, an observation already suggested via the electronic tongue experiments reported.

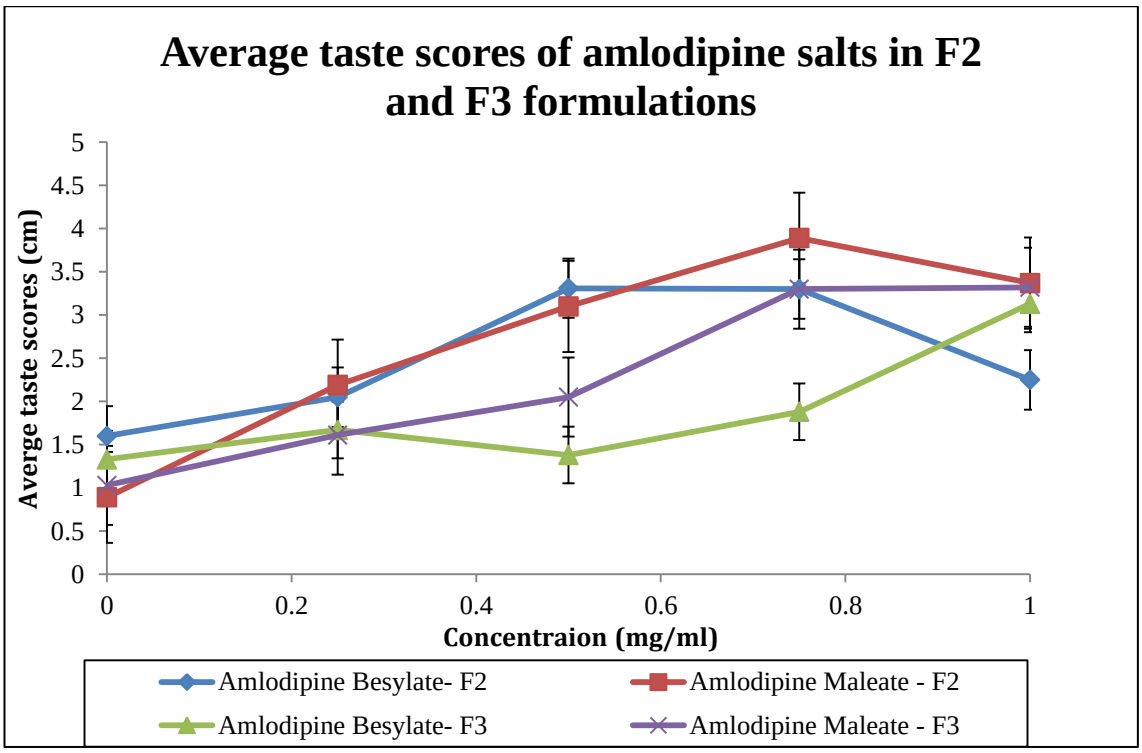


FIGURE 4. 35 HUMAN TASTE PANEL SCORES COMPARING AMLODIPINE BESILATE AND AMLODIPINE MALEATE F2 AND F3 FORMULATIONS (N= 24 $\bar{x}$±SD)..

### *4.3.9 HUMAN, ELECTRONIC TONGUE CORRELATION*

Thus far results have been reported separately; in the section the correlation between the electronic tongue results and the scores from the human panel is highlighted. The findings highlighted in **sections 4.3.2, 4.3.3** and **4.3.4**, show that astringency sensor accounts for 89- 92% of sensor responses observed. Therefore astringency sensor responses from the electronic tongue were compared to taste scores from the human taste panel **Figure 4.38** shows positive correlation between the electronic tongue and human panel for all three salts in F1 formulations. Amlodipine besilate and maleate show stronger correlation i.e. $R^2$ values are 0.96 and 0.99 respectively.

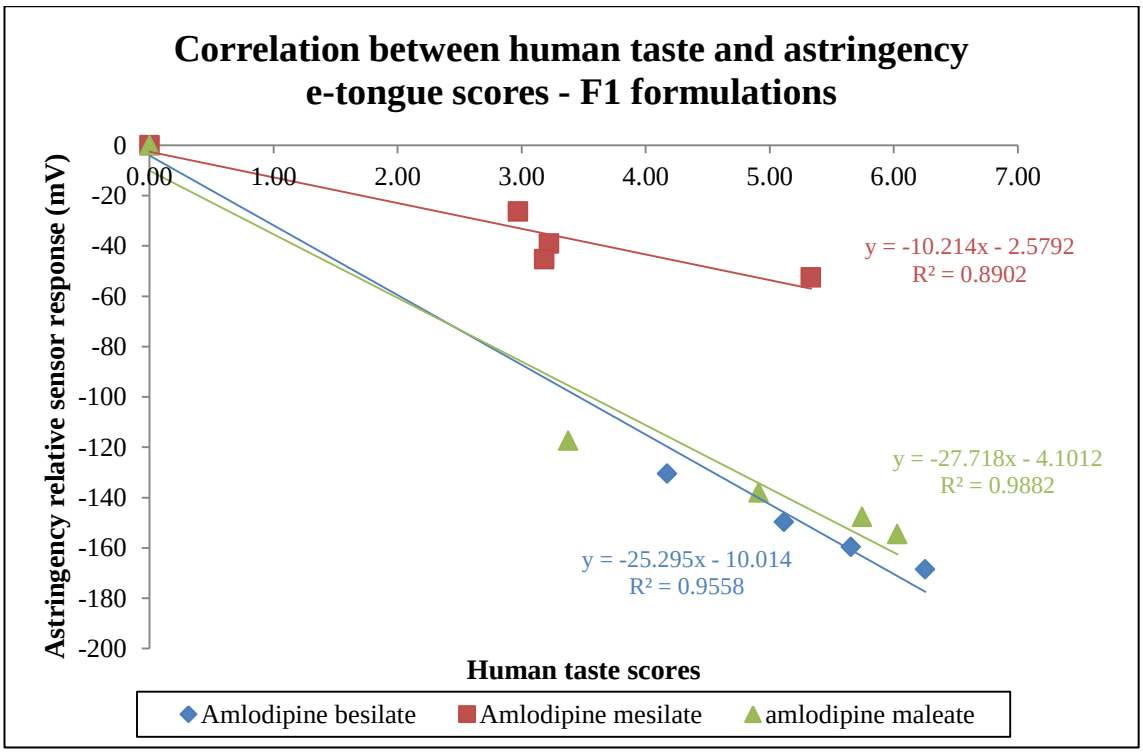


FIGURE 4. 36 CORRELATION BETWEEN HUMAN TASTE SCORES AND ELECTRONIC TONGUE FOR AMLODIPINE SALTS DISSOLVED IN WATER (F1)

Figure 4.39 shows the correlation between human taste scores and electronic tongue in relation to F2 formulations. Similar to results reported for F1 formulations, positive correlation is realised for the F2 samples.

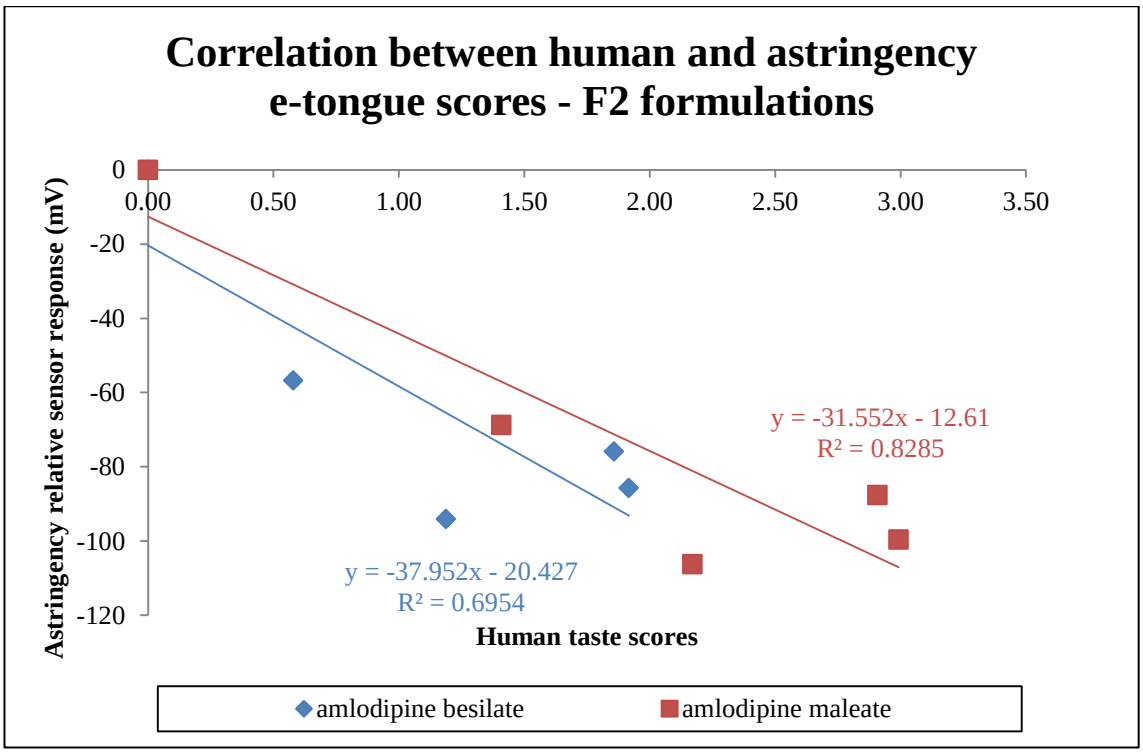


FIGURE 4. 37 CORRELATION BETWEEN HUMAN TASTE SCORES AND ELECTRONIC TONGUE PREDICTIONS FOR AMLODIPINE MALEATE AND BESILATE SUSPENDED IN F2 FORMULATIONS.

Correlation analysis of F3 formulations are illustrated in Figure 4.40. Positive correlation was found between the human panel taste scores and those recorded on the electronic tongue. The correlation coefficients reported are similar to those for F2 formulations. The significance of these findings will become apparent in the **section 4.4.3**.

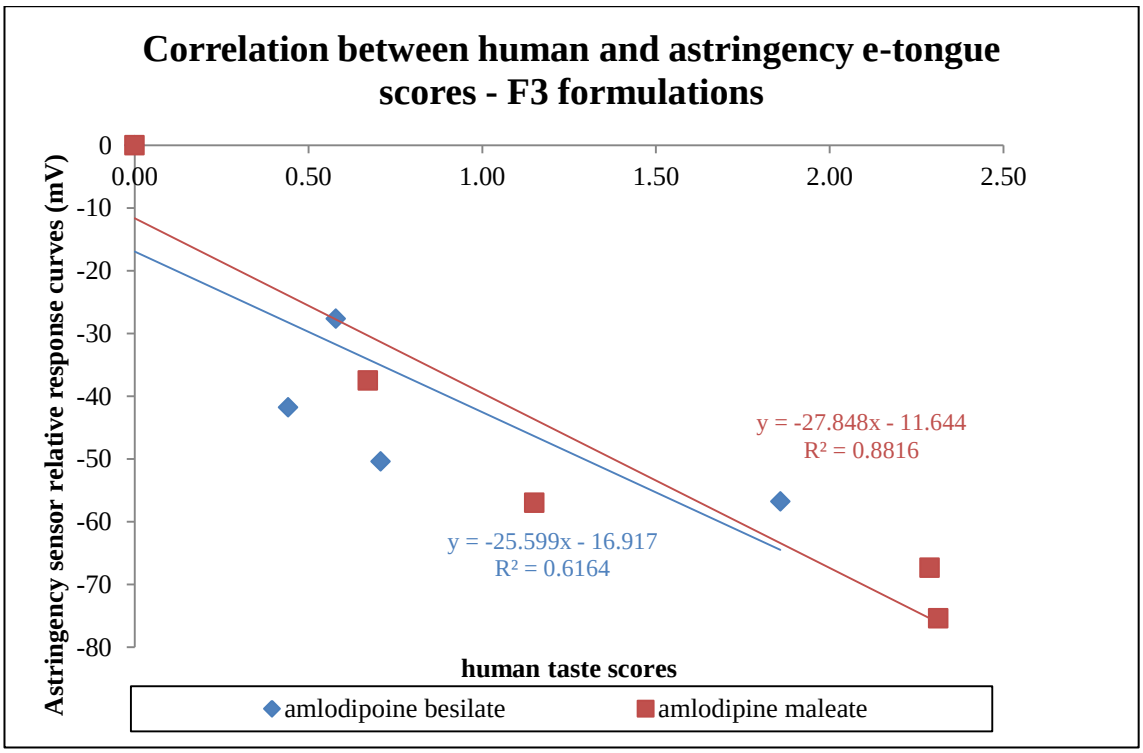


FIGURE 4. 38 CORRELATION BETWEEN HUMAN TASTE SCORES AND ELECTRONIC TONGUE FOR AMLODIPINE MALEATE AND BESISLATE SUSPENDED IN F3 FORMULATIONS.

## 4.4 DISCUSSION

### 4.4.1 ELECTRONIC TONGUE

The first question in this study sought to establish the responsiveness of the sensors: basic bitterness1 (AC0), basic bitterness2 (AN0), acidic bitter (C00) and astringency (AE1) to different salts of amlodipine. Amlodipine base (AM), amlodipine besilate (AMB) and amlodipine maleate (AMM) were investigated. A summary of the responding sensor is given in Table 4.26. In brief, the basic bitterness2 and acidic bitterness sensors show concentration response to amlodipine base when compared to negative control (de-ionised water). It is somewhat surprising that there is a difference in response between the basic bitterness1 and basic bitterness2 sensors. This result has not been previously reported. In all other experimental work carried out thus far in **chapters 3 and 4**, both the negatively charged sensors have responded in an identical fashion. Woertz et al (2010) showed similar response patterns between the two negatively charged sensors when looking at different salts of ibuprofen. Equally, Guhman et al 2012 also reported identical response patterns for the both negatively

charged sensors when comparing diclofenac sodium and potassium salts. It is therefore surprising that only one of the sensors would respond. In **chapter 3**, it was postulated that the mechanism of sensor response was dependent on both nature and extent of dissociation. Based on this hypothesis, it was therefore expected that amlodipine which is positively charged, would produce an identical reaction to both bitterness sensors that are negatively charged. It is important to note that this behaviour is only reported with amlodipine (free base). At present it is difficult to explain this result but it may be related to the fact that when in physiological membranes, it is suggested that the nonpolar ring system of amlodipine adopts the same orientation as the hydrophobic part of the membrane. The long molecular axis extends parallel to the hydrocarbon chains. The dihydropyridine ring of the drug is positioned with the –NH end pointing towards the aqueous phase, while the aromatic system is buried in the hydrocarbon core (Baeuerle *et al.* 1991). The difficulty lies in the fact that the orientation of the lipids on the artificial membrane of the sensor is unknown as it is commercially protected, therefore this orientation could affect the response of the sensors in question.

In salt form i.e. amlodipine besilate and maleate, concentration dependant response is observed from the astringency and acidic bitterness sensors. This response pattern is also observed for benzene sulphonic acid and sodium maleate. These findings therefore suggest that in their salt forms, the sensor response switches from basic and acidic bitterness to astringency and acidic bitterness. In essence this translates to a reversal of the predominant species being detected. In the former case, the positively charged amlodipine is being detected by negatively charges sensors whereas in the latter the besilate and maleate anion are being detected by the positively charged sensors. It could be suggested that due to the steric size of the amlodipine cation, proportionally fewer of these cations interact with the sensor membrane in comparison with the relatively smaller besilate and maleate anions. As such based on a concentration dependant effect a larger response is observed for the positively charged

response. This suggestion is quashed by the fact that in benzene sulphonic acid and sodium maleate the predominant response is also from the astringency and basic bitterness sensors. In these two molecules, the besilate and maleate anions are larger molecules than the $H^+$ and $Na^+$ cations, which would imply that the negatively charged membranes would have larger response. But this is not the case. However, it should be noted that since benzene sulphonic acid and sodium maleate were dissolved in 30% aqueous ethanol, the cations $H^+$ and $Na^+$ both react with OH- groups from the ethanol hence are "taken out" and do not interact with the sensors, which leaves the cationic amlodipine (which will effectively be at a higher concentration as a result), to interact with the sensors hence giving the results observed. Of course, the implications of this result should be taken with caution because most biological membranes are negatively charged which therefore begs the question whether the mechanism suggested could be translated to human beings.

TABLE 4. 27 SUMMARY TABLE, SHOWING PRE-DOMINANT SENSOR RESPONSE FOR EACH MOLECULE

| Drug / molecule | Sensors showing concentration dependant response |
|---|---|
| **Amlodipine** | Basic bitterness2 and acidic bitterness |
| **Amlodipine besilate** | Acidic bitterness and astringency |
| **Amlodipine maleate** | Acidic bitterness and astringency |
| **Benzene sulphonic acid** | Acidic bitterness and astringency |
| **Sodium maleate** | Acidic bitterness and astringency |

*A NOTE ON EXCIPIENTS*

A question that remains to be addressed pertains to the contribution of the excipients to the overall taste quality described by the electronic tongue. The excipients used for the amlodipine salts are given in Table 4.26. Amlodipine besilate and mesilate both have identical excipients albeit concentrations of these excipients remain a commercial secret for each tablet. This therefore implies that the taste differentiation observed between these two tablets is either due to intrinsic bitterness or a function of concentrations of the excipients.

TABLE 4. 28 LIST OF EXCIPIENTS IN EACH AMLODIPINE TABLET

| Drug | Manufacturer | Excipients |
|---|---|---|
| **amlodipine besilate** | Teva®, UK | Microcrystalline cellulose, calcium hydrogen phosphate, sodium starch glycolate and magnesium stearate |
| **amlodipine maleate** | Dr Reddy's ® Laboratories, UK | Microcrystalline cellulose, sodium starch glycolate, **colloidal anhydrous silica** and magnesium stearate |
| **amlodipine mesilate** | Actavis®, UK | Microcrystalline cellulose, anhydrous calcium hydrogen phosphate, sodium starch gylcollate type A, magnesium stearate |

Microcrystalline cellulose is used primarily used as a binder / diluent in tablets. It is purified, partially depolymerised cellulose that occurs as a white, odourless, tasteless powder. It is practically insoluble in water, dilute acids and most organic solvents but slightly soluble in 5% w/v sodium hydroxide. In light of this information, it can be assumed that microcrystalline cellulose does not contribute to the overall taste perception on the electronic tongue.

Magnesium stearate is a very fine, light white, precipitate or milled, impalpable powder of low bulk density having a faint odour of stearic acid and a characteristic taste. It is practically insoluble in ethanol, ethanol (95%), ether and water whilst slightly soluble in warm benzene and warm ethanol (95%). Although magnesium stearate is described as having a characteristic taste, its insolubility in water or ethanol implies that in this study it was suspended rather than solubilised. Since the electronic tongue requires substances to be in solution in order to be detected it therefore be concluded that magnesium stearate is not detected and therefore can be discounted as contributing to taste specification recorded on the electronic tongue.

Calcium hydrogen phosphate is a white odourless, tasteless powder used both as an excipient and a source of calcium in nutritional supplements. During the tableting process, it is used for its compaction and good flow properties of course grade material. Similar to the other excipients discussed thus far, it is also practically insoluble in ether, ethanol and water but soluble in dilute acids. To this end, it can also be concluded that calcium hydrogen phosphate provides no bearing on the taste attributes recorded on the electronic tongue.

Sodium starch glycolate is used as a disintegrant in tablet formulations prepared either via direct compression or wet granulation processes. The usual concentration employed in such formulations is between 2% and 8%. It occurs as a white or almost white free flowing very hygroscopic powder. It is practically insoluble in methylene chloride and gives a translucent suspension in water. Although, the taste of sodium starch glycolate is not readily described in the literature, since it forms a suspension in water and it can be concluded that it has no significant addition to taste attributes described by the electronic tongue.

Colloidal anhydrous silica has nano-sized primary particles and a large specific surface area which provided desirable flow characteristics in dry powders used for tableting. Hence, it is used as an anticaking, emulsion stabilising, suspending, viscosity increasing agent and glidant. It is soluble in 1 in 6.7 parts of water, practically insoluble in organic solvents and acids except hydrofluoric acid. It is soluble in hot solutions of alkali hydroxide. The taste of silica is not directly documented in the literature, however, a formulation containing silica was used to sufficiently taste mask roxithromycin (Gao *et al.* 2006). Based on these facts, it is unlikely that colloidal silica could contribute to taste information obtained from the electronic tongue.

Therefore with respect to the excipients that are present in the amlodipine tablets used in this study, due to their poor water solubility none of the excipients can be regarded to contribute to the taste information described by the electronic tongue.

### 4.4.2 HUMAN TASTE PANEL

The initial objective of this study was to ascertain taste differences between the amlodipine besilate, maleate and mesilate tablets when they were crushed and dispersed in water (F1). The results of the study point towards amlodipine besilate being identified as being unpleasant by the panel of untrained participants. This was particularly obvious at the lower concentrations where amlodipine besilate averages scores were higher than those of the other two salts. More importantly, with the increase in concentration of amlodipine besilate the taste scores also increased. Amlodipine maleate follows the same trend as amlodipine besilate. Surprisingly, there is no increase in taste scores with increasing concentration of amlodipine mesilate. This therefore suggested that the unpleasantness of amlodipine mesilate was related to intrinsic unpleasantness rather than concentration dependant, while the other two salts exhibit both intrinsic and concentration dependant unpleasantness. It is worth noting that a limitation of the study design was the use of the terms “pleasant” and “unpleasant” as descriptors. With respect to palatability, the term unpleasant could describe bitterness and / or grittiness i.e. bad taste or bad mouthfeel. In this study, all three amlodipine salts tablets were pulverised using the same method i.e. pestle and mortar therefore an assumption was made that the participants were scoring samples in terms of their taste. Therefore, based on the participants’ scores, it can be concluded that amlodipine mesilate had the least bitterness. This result in itself is significant as there are no studies in the literature comparing the taste of different salts on the same API. However, these findings do not explain why amlodipine mesilate is described as more pleasant in comparison to the other two salts. Therefore, caution must be applied, as these results might not be transferrable to all APIs in their different salt forms.

Following the establishment of amlodipine mesilate having the least bitterness, it was necessary to continue the study using only amlodipine besilate and maleate. This is because, the second question of this study sought to assess the taste masking effect of using a 1:1 mixture of 1% methylcellulose and simple syrup (F2) and 1:1 mixture of Ora-sweet® and Ora-plus® (F3) on the bitter amlodipine salts. The results of this study showed a clear difference in scores between the F1 and F2 formulation containing amlodipine besilate or amlodipine maleate: with the F2 formulations scoring lower i.e. more palatable. In fact, all the taste scores recorded for both F2 formulations were no greater than 4, a score which has no statistical difference with scores recorded for the F1 placebo. This is to say that the F2 formulations scores were similar to water. Also to note, was that there was no difference in scores for the F2 formulations between amlodipine besilate and maleate. At 1mg/ml concentration, there is a 60% reduction taste scores between the F1 and F2 formulations. The results from this study unsurprisingly illustrate that the use of a 1:1 mixture of simple syrup and 1% methylcellulose was sufficient as a taste masking medium. The mechanism of the bitter-masking strategy remains unknown. Historically it was thought that the high concentrations of sucrose in simple syrup saturates the taste receptor cells thereby reducing the contact of API with taste receptor cells which in turn translates to reduced taste detection therefore taste masking. However, the elucidations of the mechanisms of taste transduction of bitter and sweet molecules which both utilise G-protein coupled receptors (GPRC) have disproved this line of thinking. It has currently been suggested that the taste masking activities are mostly caused by the psychophysical effects of using a strong flavour to overcome another i.e. off-taste by camouflage. Unfortunately, the use of strong flavours or tastant is not acceptable in a lot of applications. If anything, this is growing unpopular particular in the paediatric population where dental practitioners are raising concerns with increasing dental carries amongst children with chronic illnesses who need long term treatment.

The taste scores recorded for the comparison of F1 and F3 formulations present a similar pattern to those described between F1 and F2. Essentially, at 1mg/ml concentration, there is a 70% reduction in bitterness between F1 and F3 formulations. Interestingly, a one way ANOVA showed that there was no statistical difference between placebo and F3 formulations containing amlodipine salts ($p > 0.05$). Another interesting observation is that no difference was observed between amlodipine besilate and amlodipine maleate in relation to their taste scores. In similar fashion to analysis of the F2 formulations, the mechanism behind the bitter-taste masking remains unknown but can be postulated as psychophysical.

Another noteworthy observation was that this study did not find a significant difference between F2 and F3 formulations. A possible explanation for this result is that in both F2 and F3 formulations, the sweetening agent; sucrose was sufficient to achieve taste masking. It should be noted that sweet and bitter taste transduction in humans occurs via T1R and T2R G-protein coupled receptors respectively (chapter one). In both cases, the taste receptor cells secrete the same neurotransmitter substance i.e. ATP onto afferent fibres (Breslin *et al.* 2006). Discrete synapses are lacking that might couple receptor cells with sensory afferent fibres to transmit a single taste quality. Although some taste cells and sensory afferent neurons are tightly tuned, while others are responsive to multiple taste qualities (Chaudhari *et al.* 2010). Therefore, the question remains as to exactly how information gathered by taste receptor cells in taste buds is "coded" for the eventual perception of distinct taste qualities. This question remains to be addressed in the literature and has fundamental importance in understanding the reduction in bitterness perception in the presence of heightened sweetness perception. In addition, other questions remain i.e. is the ATP production from T1R and T2R cells dependant on cell activation which may be dependent on concentration of ligands or is ATP production dependent on T1R and T2R cell density. Also to note, is that comparison of F1 formulations in water did not reveal a distinct difference between the two salts. Therefore, it can be suggested that seeing as the two salts have similar

score before taste masking, they exhibit similar scores with suspended in F2 and F3 vehicles.

### 4.4.3 HUMAN PANEL – E-TONGUE CORRELATION

Despite various reports in the literature illustrating the utility of electronic tongues as a method of taste assessment, questions still remain as to whether this technology can be used in place of human panels. Recently, Eckert el al (2013) compared the detection of herbal products in lozenges using HPLC, an electronic tongue and a human panel. The study concluded that electronic tongues although useful they cannot replace human panels (Eckert *et al.* 2013). Therefore, the most significant question in this study relates to whether the electronic tongue could be used as a predictor of taste in human beings.

The findings from electronic tongue reported in sections 4.3.1 – 7, showed that the astringency sensor response was the predominant sensor response, therefore in this section; correlation between the predominant sensors responses were compared to human panel scores. In all cases investigated, there is a strong positive correlation between the astringency sensor responses and the human panel taste scores. Although, these findings are significant, they should be treated with caution. In the first instance only one group of molecules was investigated therefore these results may not be transferrable to other APIs. In the second incidence, a small sample size was used therefore in order to allow for broad strokes to be used, the studies will need to be modified with power calculations and multicentre in order to ensure that results are transferrable to different populations.

## 4.5 CONCLUSION

This chapter has investigated the taste assessment of amlodipine (base), amlodipine besilate, maleate and mesilate using the electronic tongue. One of the more significant findings to emerge from this study is that the electronic tongue predominantly and consistently identifies astringency as the major descriptor of all the amlodipine salts. It

would appear that amlodipine free base can be described in terms of basic and acidic bitterness while its salts are all described in terms of astringency. These findings are unique for several reasons. Firstly, this study has shown a difference in response patterns between amlodipine free base and its salts. It is clear the presence of cationic amlodipine and anionic besilate and maleate ions affects the detection profile, which further cements mechanism described in chapter 3. Secondly, this study has also shown that in addition to considering the dissociation profile of the salt forms, it is also important to consider the size of the resulting moieties. In the case where the cation is considerably larger than the corresponding anion, then more anions interact with the sensors therefore showing large response. Of course, this observation should be treated with caution because the interaction between the positively charged sensor and anions is an unusual occurrence in nature. Thirdly, this study has also shown a difference in response patterns between the two negatively charged sensors, particularly when considering amlodipine free base. A clear reason could not be identified for this phenomenon which has not been reported this far. However, it is possible that the possibly different orientation of the lipids on the two sensors could be attributed to the difference in sensor response. With respect to the electronic tongue, the amlodipine besilate salt was identified as having the least palatability in comparison to the other amlodipine salts. Results from the electronic tongue showed that F1 formulations were the least palatable formulations, however, it was not possible to statistically distinguish between F2 and F3 formulations. Finally, a strong positive correlation was observed between the electronic tongue scores and those from the human taste panel. However, these results need to be treated with caution as only amlodipine salts were investigated and furthermore a small sample size was used. Therefore, further research is required on different APIs and larger sample sizes in the human panels.

# CHAPTER FIVE
# TASTE ASSESSMENT OF HOT MELT EXTRUDED QUININE

# CHAPTER 5 – TASTE ASSESSMENT OF QUININE HYDROCHLORIDE

In **Chapter 4**, the taste masking efficiency of sweeteners and flavours was investigated using the TS500Z electronic tongue and a human taste panel. Broadly speaking, this approach to taste masking uses strong flavours to overpower the bitter API or to reduce contact between API and taste buds or to reduce the release of API in the oral cavity (Sohi *et al.* 2004). Whilst flavours and sweeteners provide a straight forward taste masking strategy, they are not without limitations. Many excipients are subject to regulatory restrictions which limit their use particularly in paediatric setting. For example, it is well understood that sucrose, a common sweetener can contribute to dental disease (Roberts *et al.* 1979), whilst flavours have been associated with hypersensitivity, toxicity or allergy reactions and as such their use has been kept to a minimum (Kanny *et al.* 1994). In addition, they may not sufficiently mask the taste of extremely bitter APIs.

There are numerous taste masking strategies and these have already been highlighted in **chapter 1, section 1.5**. Reports in the literature have indicated that the formation of solid dispersions provide a framework for taste masking. As highlighted in **chapter 1**, **section 1.5**, there are a limited number of studies that use recognised taste assessment methods to validate taste masking using solid dispersions. Therefore, this chapter describes the production of hot melt extruded quinine hydrochloride dihydrate with Eudragit® EPO, with a view of assessing the taste masking efficacy of this formulation using the Insent® TS5000Z electronic tongue.

## 5.1 STUDY OBJECTIVES

The work detailed in this chapter takes on a two pronged approach. The first arm focuses on the characterisation of quinine and its salts i.e. quinine hydrochloride

dihydrate and quinine hemisulphate dihydrate with a view to highlight the similarities and differences between the salts. This characterisation aided the choice of which quinine salt was used for the Eudragit® EPO melt extrudates. In addition, the analysis also provided baseline characteristics which formed the basis of comparison with hot melt extrudates. Quinine hydrochloride dihydrate was selected following this analysis; therefore an attempt was made to describe the form of quinine hydrochloride dihydrate salt that was present following hot melt extrusion. The reasoning behind the selection of quinine hydrochloride dihydrate will become apparent in **section 5.4.1**. An investigation into the stability of the melt extrudates form is also reported. The second half describes the taste masking capability of hot melt extruded quinine hydrochloride dihydrate with Eudragit®EPO. This analysis was carried out using a modified dissolution apparatus in combination with spectrophotochemical analysis together with a comparison on the electronic tongue. Modification to the dissolution apparatus have been discussed in **chapter 2** while the rationale for the modification is detailed in **chapter 1**.

## 5.2 METHODOLOGY

### 5.2.1 HOT MELT EXTRUSION

Quinine hydrochloride dihydrate (QHD) formulations with Eudragit® EPO (EPO) were mixed using a pestle and mortar in 30g batches for five minutes. The extrusion of all quinine hydrochloride blends were performed using Thermo Scientific Process 11 twin screw extruder (Thermo Scientific UK) with co-rotating screws. The drug/polymer composition consisted of QHD/ EPO at a ratio of **1**) 10/90, **2**) 30/70, **3**) 50/50 and **4**) 70/30 (%w/w). The process parameters of the HME barrel are shown in Table 5.1 These parameters were used for formulations 1-3.

TABLE 5 1 PROCESS PARAMETERS FOR HOT MELT EXTRUSION FOR FORMULATIONS 1, 2 AND 3

| **Zone** | **1 (feed)** | **2(mixing)** | **3** | **4** | **5** | **6** | **7** | **8 (die)** |
|---|---|---|---|---|---|---|---|---|
| **Temp $^{o}$C** | 120 | 120 | 140 | 140 | 140 | 140 | 140 | 140 |

The temperature profile for formulation 4 is given in Table 5.2. The screw speed was set to 50rpm. An explanation of the difference in the process parameters will be given in **section 5.4.1**.

TABLE 5 2 PROCESS PARAMETERS FOR HOT MELT EXTRUSION FOR FORMULATION 4

| Zone | 1 (feed) | 2(mixing) | 3 | 4 | 5 | 6 | 7 | 8 (die) |
|---|---|---|---|---|---|---|---|---|
| | 120 | 120 | 140 | 140 | 140 | 140 | 160 | 160 |

The produced extrudates (strands) were approximately 1.5mm in diameter allowed to cool at room temperature before being milled using the methods described in **chapter 2, section 2.4.3**. The powders obtained were sieved manually using an 180µm sieve and stored in the following conditions: **a**) 25$^{o}$C, 0% relative humidity **b**) 4$^{o}$C, and 50% relative humidity and **c**) 40$^{o}$C, 75% relative humidity. The extrudates were characterised using a number of thermal and analytical techniques namely, DSC (**chapter 2.4.4**), PXRD (**chapter 2.4.5**), SEM (**chapter 2.4.6**), HSM (**chapter 2.4.7**), TGA (**chapter 2.4.8**).

### 5.2.3 DISSOLUTION TESTING

The solubility of the QHD-EPO extrudates powder was assessed after adding required amount of melt extrudate powder (milled as described in **chapter 2, section 2.4.9**) to 90ml of de-ionised water in a beaker. This was then shaken using the Incu shaker, the resulting solution was filtered using a 0.22µm filter and assessed spectrophotochemically. In order to avoid duplication, the reader is referred back to **chapter 2, section 2.4.11** for full descriptions of methods.

## 5.3 RESULTS

The objective of the work detailed in this section focuses on the characterisation of the raw materials i.e. unprocessed quinine, quinine hydrochloride dihydrate, quinine hemisulphate and Eudragit® EPO. This was necessary in order to recognise the differences between the salts and more importantly to establish baseline characteristics from which comparisons will be made against the hot melt extrudates.

### 5.3.1 POWDER X-RAY DIFFRACTION (PXRD) ANALYSIS OF RAW MATERIALS

PXRD diffractograms of quinine hydrochloride dihydrate, quinine and quinine hemisulphate are shown in Figures 5.1, 5.2 and 5.3 respectively. All three diffractograms display spectra characteristic of crystalline materials with numerous diffraction peaks. The three peaks of highest intensity for quinine hydrochloride dihydrate are observed at 8.8$^{o}$, 17.2$^{o}$ and 12.2$^{o}$.Quinine's three highest peaks are recorded at 15.8$^{o}$, 16.5$^{o}$ and 5.1$^{o}$. The diffraction peaks for quinine hydrochloride dihydrate and quinine recorded in this study correspond to those reported in the literature (Jones *et al.* 2014). The diffractogram for quinine hemisulphate dihydrate also has numerous peaks with the two highest observed at 18.8$^{o}$ and 8.2$^{o}$. This is consistent with predominant form reported in the literature (Karan *et al.* 2012).

As expected the diffractograms have distinct difference. These are mainly related to the intensity of peaks approximately 8$^{o}$ and 18$^{o}$. Quinine hydrochloride dihydrate exhibits peak intensity at 8$^{o}$ and closely followed by peak at 18$^{o}$. In contrast, quinine only has one major peak at 18$^{o}$, while the one at 8$^{o}$ is significantly diminished. Similar to quinine hydrochloride dihydrate, quinine hemisulphate dihydrate shows two distinct peaks at 8$^{o}$ and 18$^{o}$. However the intensities for these peaks are reversed with respect to quinine hemisulphate dihydrate. This is to say that the highest peak is observed 18$^{o}$ then closely followed by the peak at 8$^{o}$.

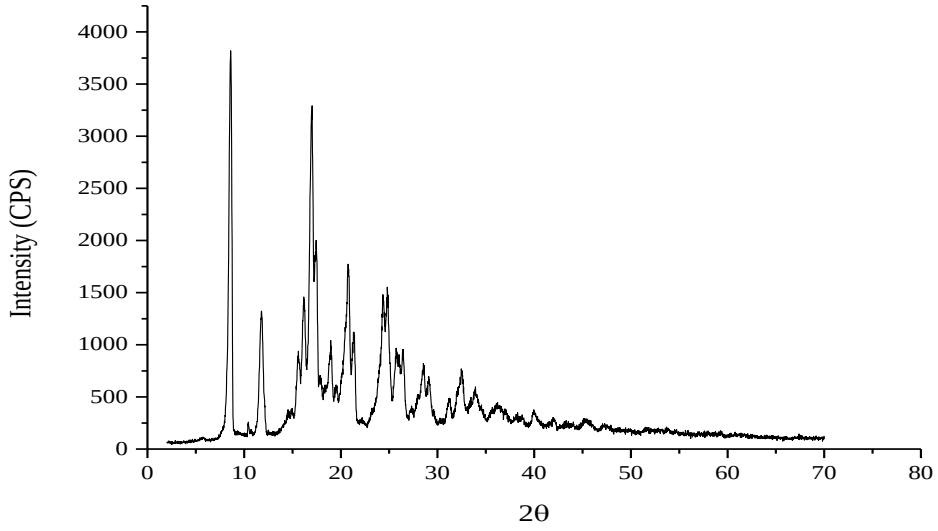


.

FIGURE 5. 1 PXRD DIFFRACTOGRAM OF QUININE HYDROCHLORIDE DIHYDRATE

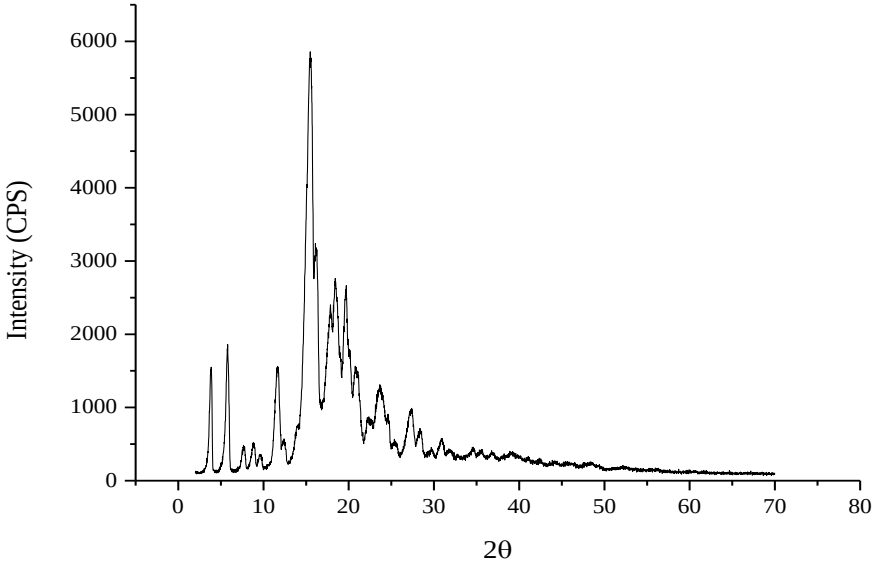


FIGURE 5. 2 PXRD DIFFRACTOGRAM OF QUININE (QN)

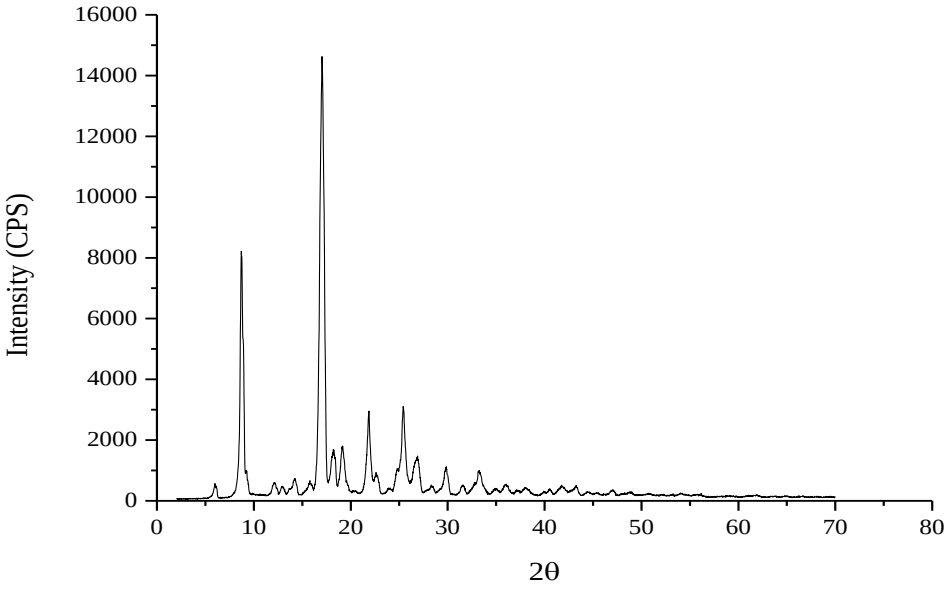


FIGURE 5. 3 PXRD DIFFRACTOGRAM OF QUININE HEMISULPHATE (QHS)

The PXRD diffractogram of Eudragit® EPO is shown in Figure 5.4. Eudragit®EPO showed an “amorphous halo” pattern showing no sign of peaks, indicating the absence of crystallinity (within the instrument detection limits). The observed “amorphous halo” pattern occurs as a result of relative random arrangements of molecules within the amorphous material. PXRD results for both amorphous and crystalline materials highlight the distinct differences in molecular arrangements between the two states. The “amorphous halo” exhibited by Eudragit® EPO is expected as it is described as an amorphous polymer in the literature (Kojima *et al.* 2012).

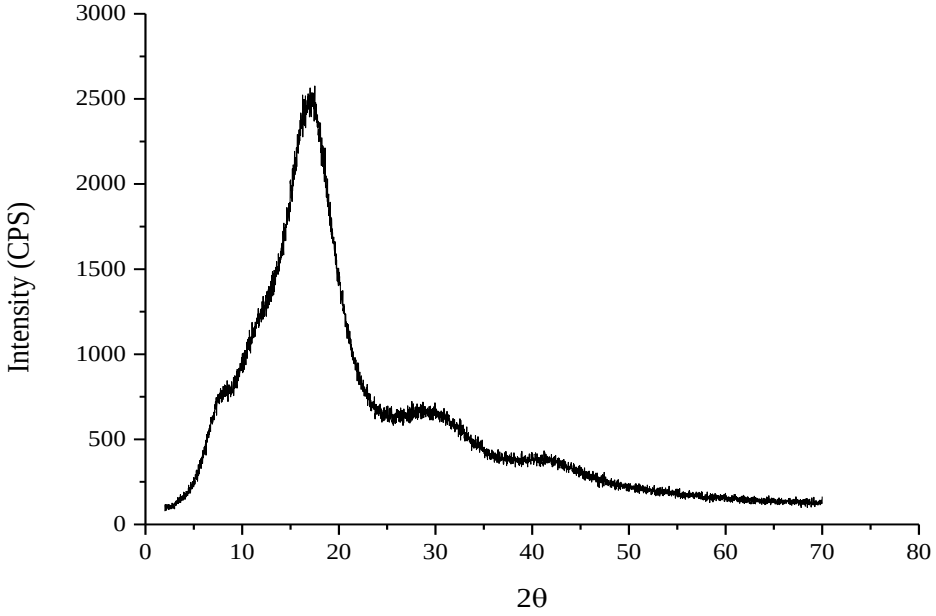


FIGURE 5. 4 PXRD DIFFRACTOGRAM OF EUDRAGIT® EPO

### 5.3.2 THERMAL ANALYSIS OF RAW MATERIALS

In this section the characterisation of the thermal properties of quinine hydrochloride dihydrate (QHD), quinine (Qn), quinine hemisulphate dihydrate (QhS) and Eudragit® EPO using conventional differential scanning calorimetry (DSC), thermogravimmetric analysis (TGA) and hot stage microscopy (HSM) was reported. DSC experiments were performed using open pans at 10$^{o}$C/min from 25$^{o}$C to 250$^{o}$C to study the sample thermal transitions. HSM and TGA experiments were used in conjunction with DSC (using the same heating parameters) to capture visual images of the samples to aid interpretation of the observed thermal events. Details of these techniques are fully discussed in **Chapter 2**.

Figures 5.5, 5.10 and 5.11 show the DSC (in green) and corresponding TGA (in blue) traces for quinine hydrochloride dihydrochloride (QHD), quinine (Qn) and quinine hemisulphate dihydrate (QhS) respectively. The DSC heat flow for QHD (Figure 5.5) shows a broad temperature endotherm (***a***) at onset 48$^{o}$C with no presence of noise in

the baseline. Another smaller endotherm (***b***) is observed at onset 135°C. This is followed by a temperature exotherm (***c***) at onset 171°C. The final transition observed is a sharp low endotherm at onset 221°C (***d***). This is interesting because it implies that quinine hydrochloride dihydrate initially get dehydrated into an unstable form (***a***) which melts (***b***) and crystallises (***c***) into a stable form which eventually melts (***d***) (Margetson *et al.* 2008). The corresponding measured water content (TGA) was 9.01%. This was within the expected water content values of QHD of 9.07%.

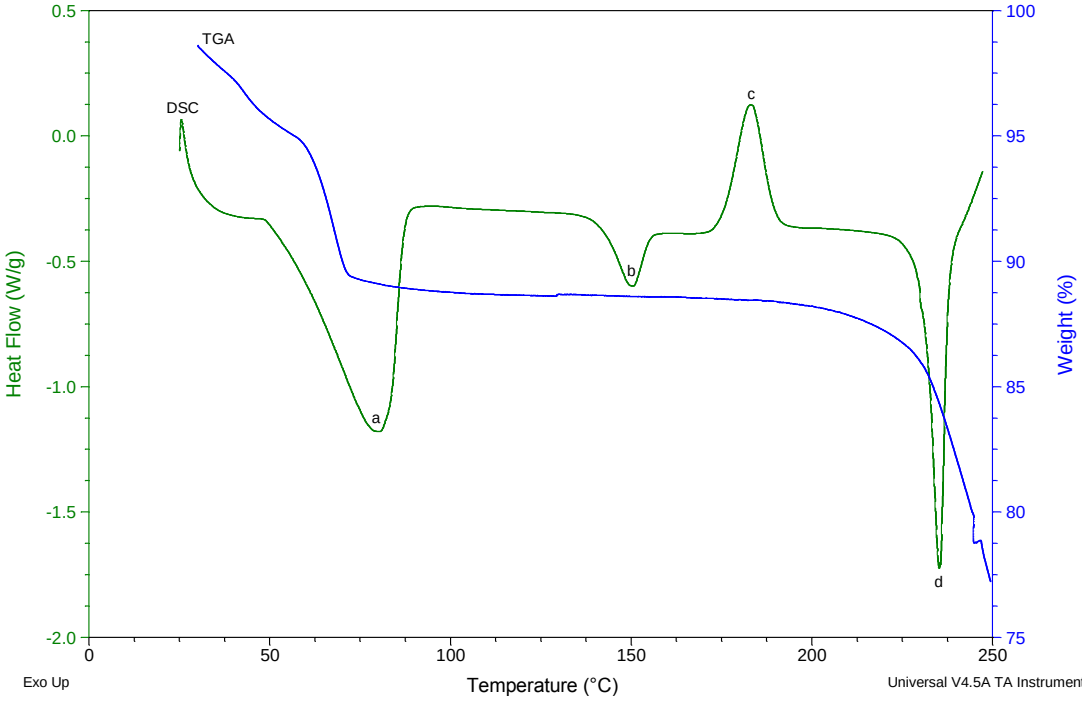


FIGURE 5. 5 TYPICAL TGA AND DSC HEAT FLOW SIGNAL FOR QUININE HYDROCHLORIDE DIHYDRATE (QHD) AT 10OC/MIN USING AN OPEN PAN.

The objective of the thermal analysis was to elucidate what form of quinine hydrochloride would be present in the final quinine hydrochloride dihydrate – Eudragit® EPO; therefore since three endotherms were observed (Figure 5.5), further analysis was necessary. Initially, quinine hydrochloride dihydrate was heated to 100°C, cooled to 25°C then reheated to 250°C. The DSC heating and cooling rates were 10°C/min. Open pans were used and the DSC thermograph is shown in Figure 5.6. The transition initially observed between 53°C and 95°C during the first heating cycle is not observed during the second heating cycle. This may point towards water being lost during the 1st

cycle therefore once it is lost the transition is not observed during the 2nd heating cycle. However, the melt, re-crystallisation and melt are observed consistent with initial standard heating of quinine hydrochloride dihydrate. Curiously, there appears to be a second exotherm starting after 240°C, therefore further investigation is required to ascertain is this is indeed another thermal event, however it is almost certainly the degradation of the material.

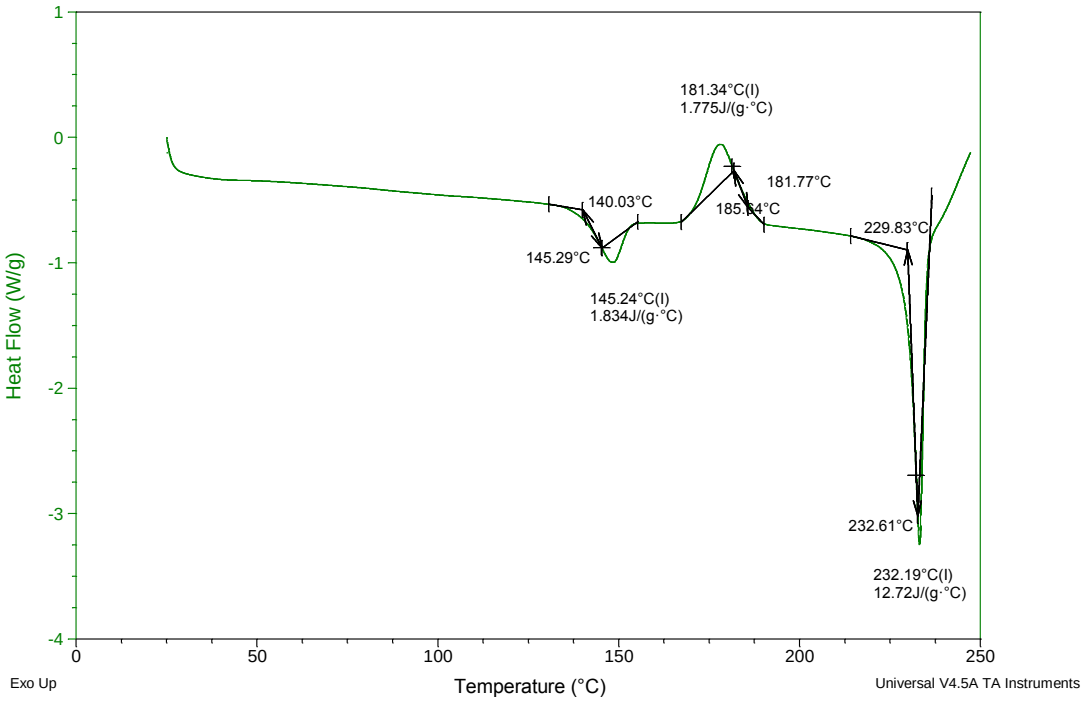


FIGURE 5. 6 TYPICAL DSC HEAT FLOW SIGNAL OF QUININE HYDROCHLORIDE DIHYDRATE FOLLOWING HEATING TO 100°C, THEN COOLING TO 25°C AND REHEATING TO 250°C. HEATING RATE WAS 10°C/MIN USING OPEN PAN.

DSC thermograph for quinine hydrochloride dihydrate following heating to 156°C at 10°C/min, cooling to 25°C then reheating to 250°C at the same rate is shown in Figure 5.7. Similar to the thermograph shown in Figure 5.6, the initial transition which could possibly be ascribed as water loss is also not observed when sample is heated to 156°C. Interestingly, the second heat shows a $T_g$ at 127°C followed by a recrystallisation peak at 175°C then the subsequent melt at with onset at 235°C.

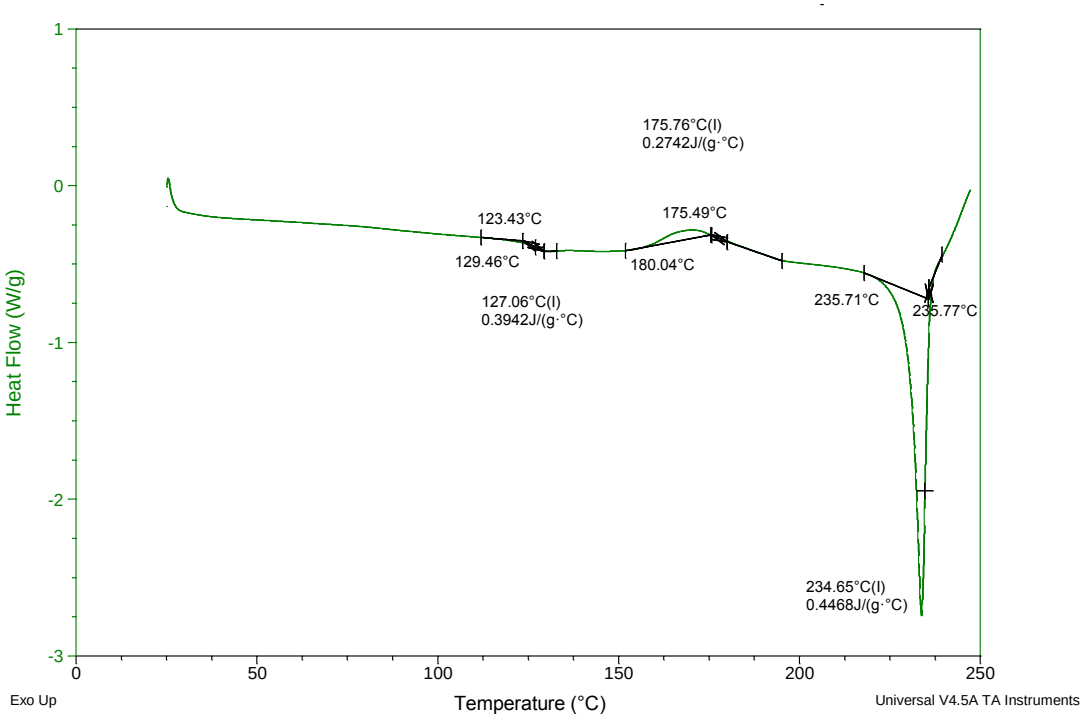


FIGURE 5. 7 TYPICAL DSC HEAT FLOW SIGNAL OF QUININE HYDROCHLORIDE DIHYDRATE FOLLOWING HEATING TO 156°C, THEN COOLING TO 25°C AND REHEATING TO 250°C. HEATING AND COOLING RATE WAS 10°C/MIN USING OPEN PAN.

DSC thermograph for quinine hydrochloride dihydrate following heating to 180°C at 10°C/min, cooling to 25°C then reheating to 250°C at the same rate is shown in Figure 5.8. Unsurprisingly, the initial endotherms reported for quinine hydrochloride dihydrate (Figure 5.5) are not observed on the second heating. Furthermore, the melt observed at 232°C was consistent despite the heating and cooling of quinine hydrochloride dihydrate.

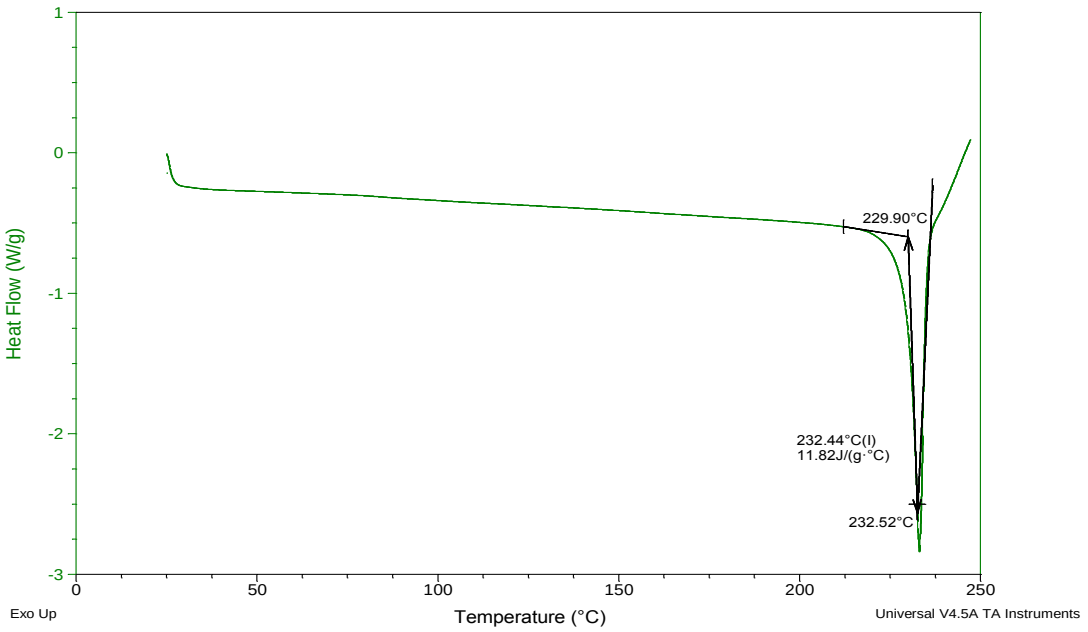


FIGURE 5. 8 TYPICAL DSC HEAT FLOW SIGNAL OF QUININE HYDROCHLORIDE DIHYDRATE FOLLOWING HEATING TO 180°C, THEN COOLING TO 25°C AND REHEATING TO 250°C. HEATING RATE WAS 10°C/MIN USING OPEN PAN.

Figure 5.9 gives a summary of the three heat– cool- heat cycles described individually in Figures 5.6, 5.7 and 5.8. All three traces are of the second heating. To recap, the first DSC trace (when describing top to bottom), shows the second heating cycle following heating of quinine hydrochloride dihydrate to 100°C, then cooling to 25°C before reheating to 250°C. The second (shown in red) and third (shown in blue) traces were heated to 156°C and 180°C respectively before being cooled to 25°C and then reheated to 250°C. It is noteworthy that a downward shift in endotherms and reduced peaks between heating to 100°C and heating to 156°C. However the final melt was consistent across all three heating cycles.

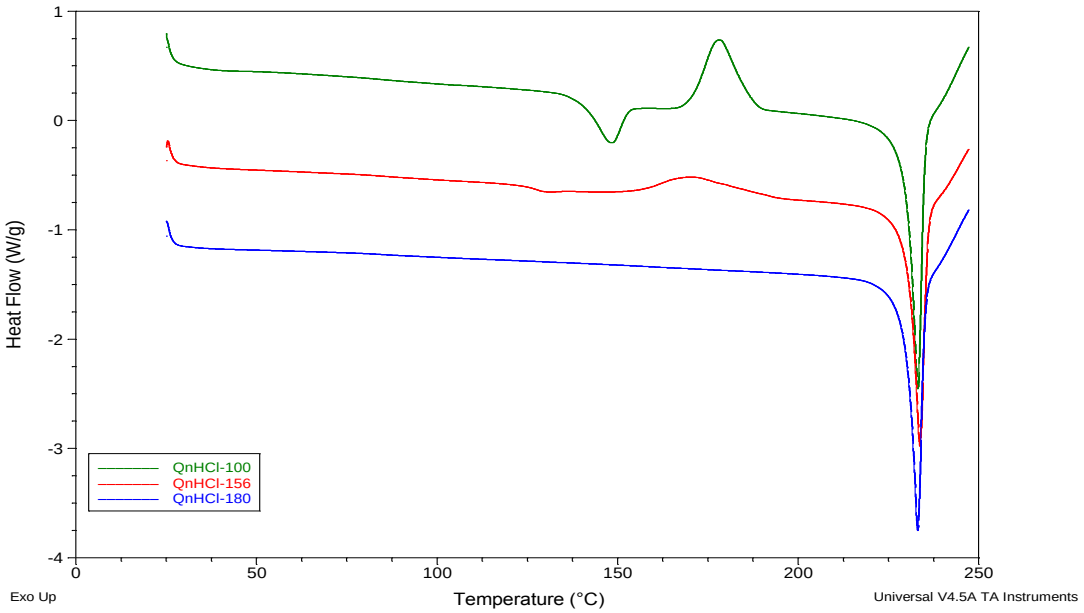


FIGURE 5. 9 TYPICAL DSC HEAT FLOW SIGNAL OF QUININE HYDROCHLORIDE DIHYDRATE FOLLOWING HEATING TO 100°C (GREEN), HEATING TO 156°C (RED) OR HEATING TO 180°C (BLUE), THEN COOLING TO 25°C AND REHEATING TO 250°C. HEATING RATE WAS 10°C/MIN USING OPEN PAN.

The DSC heat flow of quinine (Figure 5.10) shows a temperature endotherm at 177°C. Notably unlike quinine hydrochloride dihydrate, there are no other transitions observed for quinine.

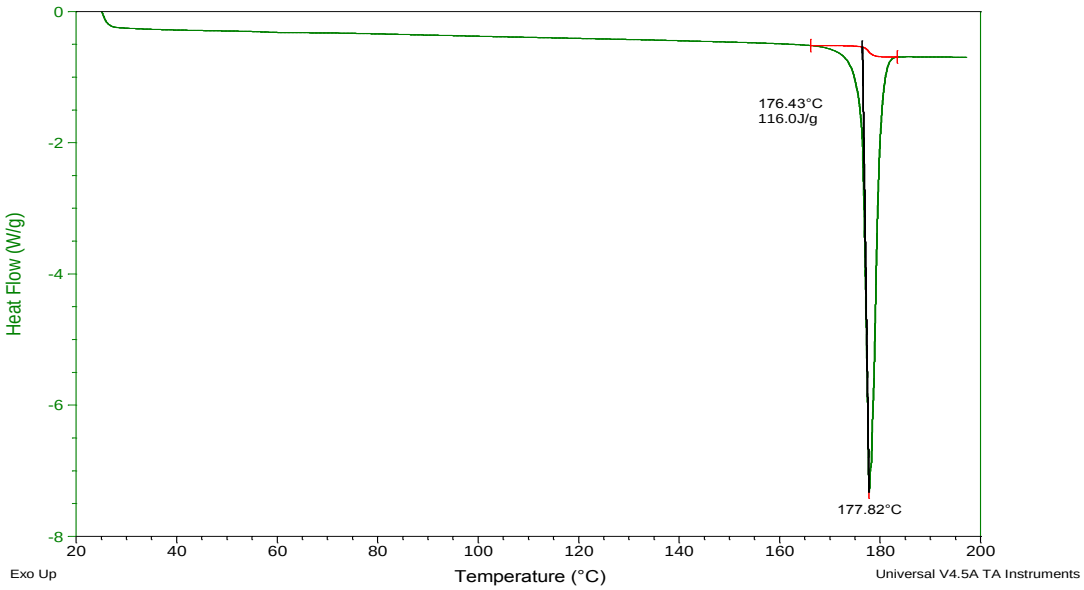


FIGURE 5. 10 TYPICAL DSC HEAT FLOW SIGNAL OF QUININE FOLLOWING HEATING TO 250°C. HEATING RATE WAS 10°C/MIN USING OPEN PAN

The DSC heat flow of quinine hemisulphate dihydrate illustrated in Figure 5.11 shows a broad temperature endotherm at onset 42°C. The shape and size of this endotherm is similar to the one observed for quinine hydrochloride dihydrate. A sharp endotherm with onset temperature 221°C was observed. Interestingly, this endotherm is also similar to the one observed for QHD. The measured water content (TGA) for quinine hemisulphate dihydrochloride was 9.30% which is within the expected water content value of 9.20%. The DSC trace recorded for QhS has also been described in the literature (Karan *et al.* 2012).

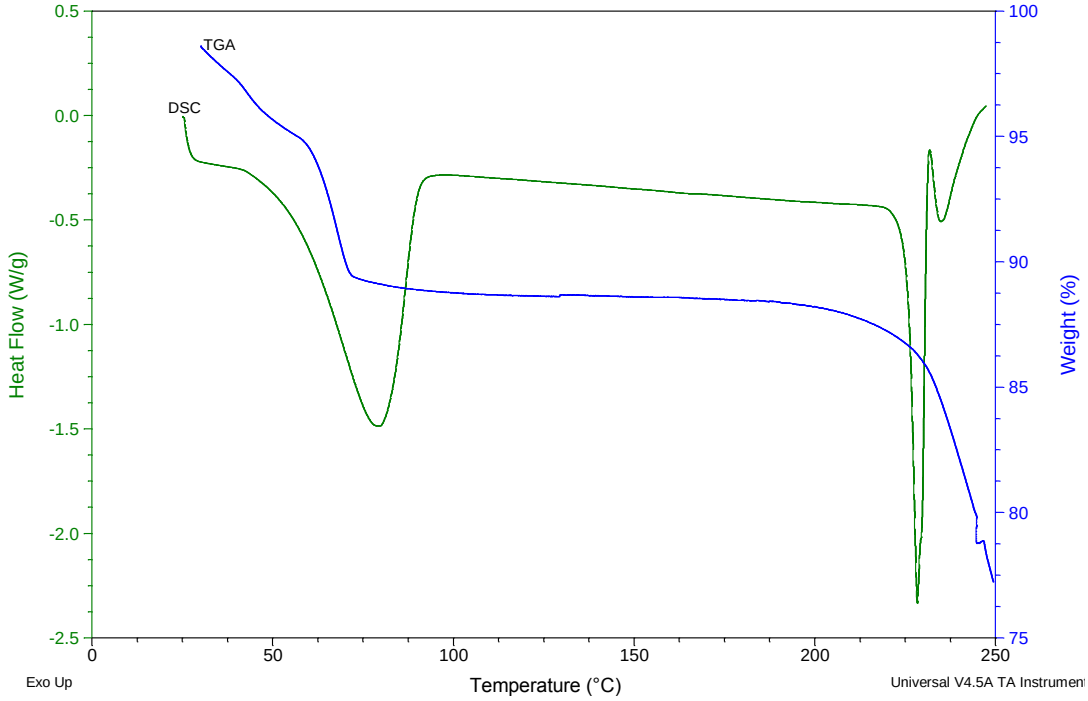


FIGURE 5. 11 TYPICAL TGA AND DSC HEAT FLOW SIGNAL OF QUININE HEMISULPHATE DIHYDRATE (QHS) RECORDED AT HEATING RATE 10°C/MIN USING ON OPEN PAN.

Figure 5.12 shows comparative DSC traces of the quinine salts i.e. quinine hydrochloride dihydrate (red), quinine hemisulphate dihydrate (black) and quinine (blue). It is clear that both the dihydrates exhibit endotherms which correspond to water loss and feature not displayed by quinine. Recrystallisation is shown for quinine hydrochloride dihydrate while the other two salts only show a final melt. The melting temperatures of the three salts are 177°C, 228°C and 232°C for quinine, quinine hemisulphate dihydrate and quinine hydrochloride dihydrate respectively.

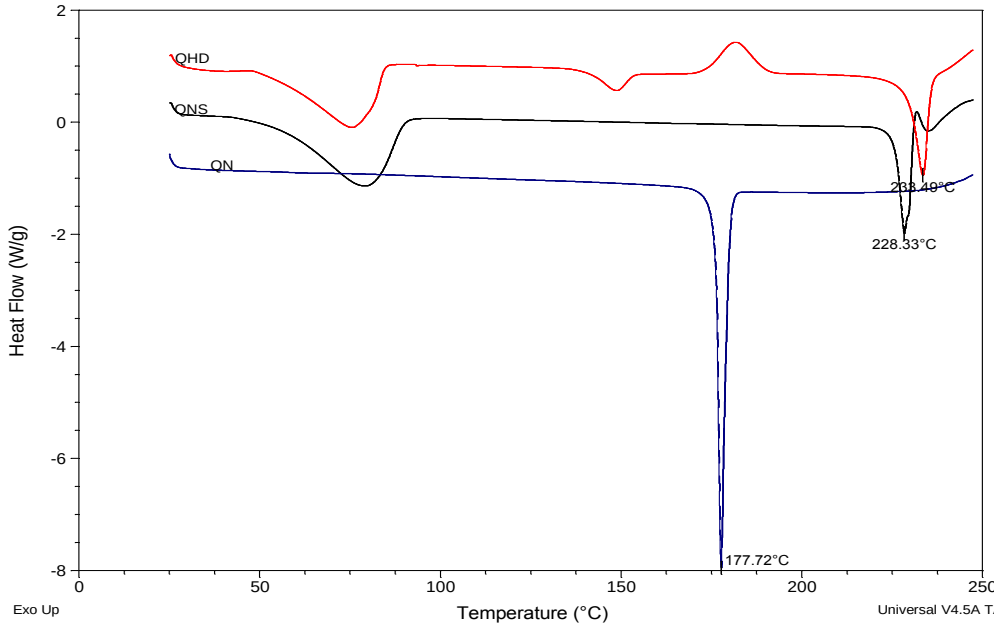


FIGURE 5. 12 TYPICAL DSC HEAT FLOW SIGNAL OF QUININE HYDROCHLORIDE DIHYDRATE (QHD), QUININE HEMISULPHATE DIHYDRATE (QHS) AND QUININE RECORDED AT HEATING RATE 10°C/MIN USING AN OPEN PAN

The DSC heat flow of Eudragit® EPO illustrated in Figure 5.11 shows a broad temperature endotherm at onset 45°C. Since, Eudragit®EPO is an amorphous copolymer, this endotherm is consistent with a glass transition ($T_g$). Reports in the literature suggest that the $T_g$ value observed at 48°C is accompanied by an endothermic relaxation over the $T_g$ region when analysed using modulated temperature DSC (MTDSC) (Qi *et al.* 2008c, Moffat *et al.* 2014).

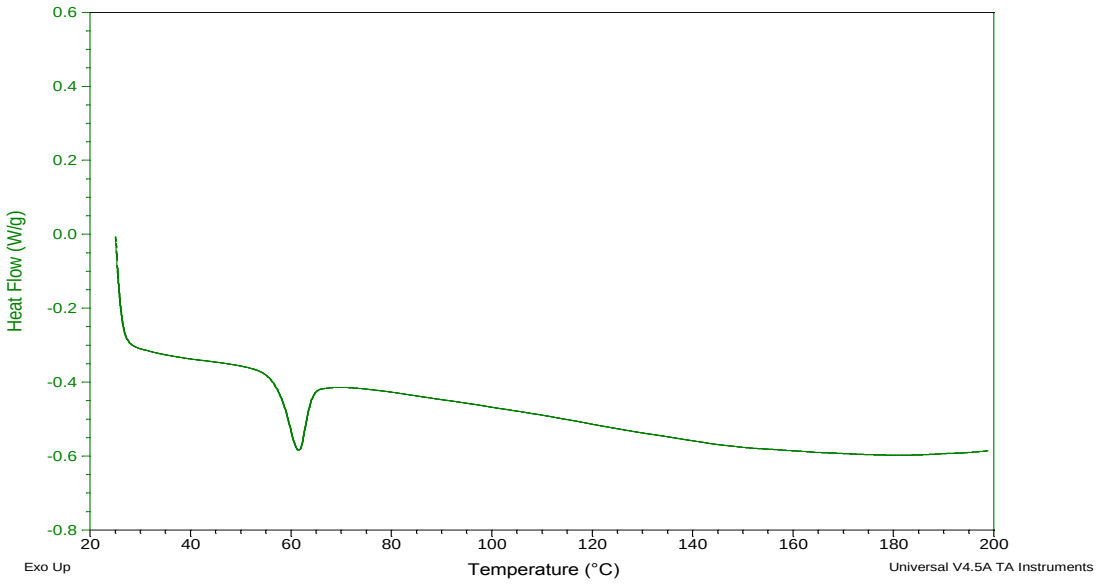


FIGURE 5. 13 TYPICAL DSC HEAT FLOW SIGNAL OF EUDRAGIT® EPO RECORDED AT HEATING RATE 10°C/MIN USING ON OPEN PAN.

Slow heating rates result in good resolution of thermal events, but unfortunately this is coupled with poor sensitivity, whilst fast heating rates result in poor resolution but good sensitivity of thermal events. Various reports in the literature have identified that the dehydration process is dependent on the heating rate. Increasing heating rates from 0.5$^{o}$C – 50$^{o}$C/min were used. Higher heating rates were used to eliminate kinetic events on the observed thermal transitions. Figure 5.14 shows a typical DSC heat flow signal for quinine hydrochloride dihydrate at 0.5, 1, 2, 5, 10, 20 and 50$^{o}$C/min using an open pan. There is an upward shift for the onset of the endotherms with increasing heating rates for all endothermic and exothermic peaks. For example the recrystallisation peaks occurs at 152.1$^{o}$C at 0.5$^{o}$C/min heating rate while the same exotherm occurs at 203.9$^{o}$C when 50$^{o}$C/min heating rate is used. Transitions such as crystallisation are kinetic events and therefore are a function of both time and temperature. This means that the transition will shift to a higher temperature when heated at a higher rate because it has less time at any specific temperature. Although, these endothermic- and exothermic peaks are not pronounced for the lower heating rates there is still a visible shift from baseline which suggests that these are indeed kinetic events.

It was evident from Figure 5.14 that the recrystallisation of the melt was dependant on the heating rates. As the heating rate increased the peak recrystallisation temperature increased. At the fast heating rates the total thermal energy that the sample was exposed to at any particular time was smaller, thus a higher temperature was required before the thermal energy quota to activate the recrystallisation process is obtained. The same is true for the subsequent final melt.

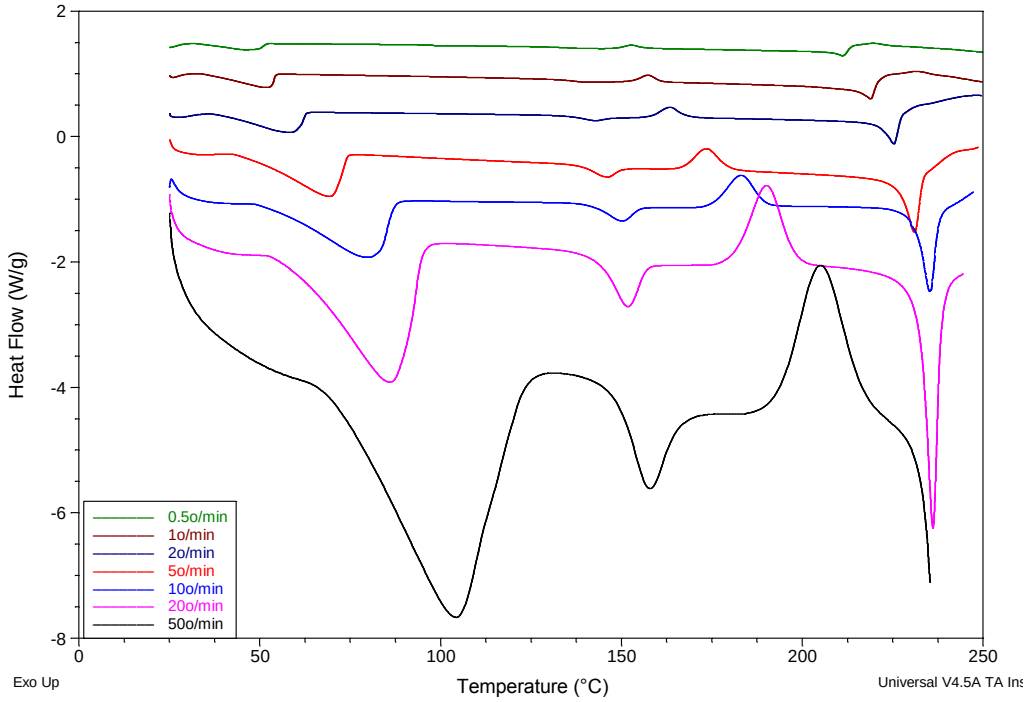


FIGURE 5. 14 TYPICAL DSC HEAT FLOW SIGNAL FOR QUININE HYDROCHLORIDE DIHYDRATE AT 0.5, 1, 2, 5, 10, 20, AND 50°C/MIN USING AN OPEN PAN.

HSM was conducted on all three quinine molecules; all were cohesive, agglomerated, coloured. Quinine hydrochloride dihydrate and quinine sulphate both showed birefringence at 30°C (Figure 5.15 and Figure 5.16) while quinine did not. Although not conclusive, some studies have suggested that birefringence is observed for the hydrate forms of local anaesthetics while their anhydrous forms did not (Schmidt *et al.* 2005). Birefringence results from the refractive index of a sample, which is derived from the ratio between the speed of light within a vacuum and the speed of light within the sample. It refers to colour produced when polarised light passes through a crystal. A sample is deemed to be birefringent when a light ray splits into two beams when passing through it having the effect of birefringence (or double refraction). Figure 5.15 shows HSM images captured at specific temperatures for quinine hydrochloride dihydrate on heating samples at 10°C/min. On heating, no change in birefringence is observed until 141.5°C where birefringence is lost as the crystals melt. It is noteworthy that there is no complete melting of the crystals. Crystallisation started at 149.8°C resulting in fully formed crystals at 206.5°C with their consequent melt at 226.1°C.

Figure 5.16 shows HSM images of quinine captured at 30.2°C and 176.9°C. Essentially on heating, the quinine crystals do not show any changes until the complete melting of the crystals at 176.9°C. Figure 5.17 shows HSM images of quinine hemisulphate dihydrate. In contrast to quinine hydrochloride dihydrate, heating of quinine sulphate did not change birefringence; in fact the only change observed was the dissolution of the crystals which started at 167.0°C with complete melt at 225.3°C.

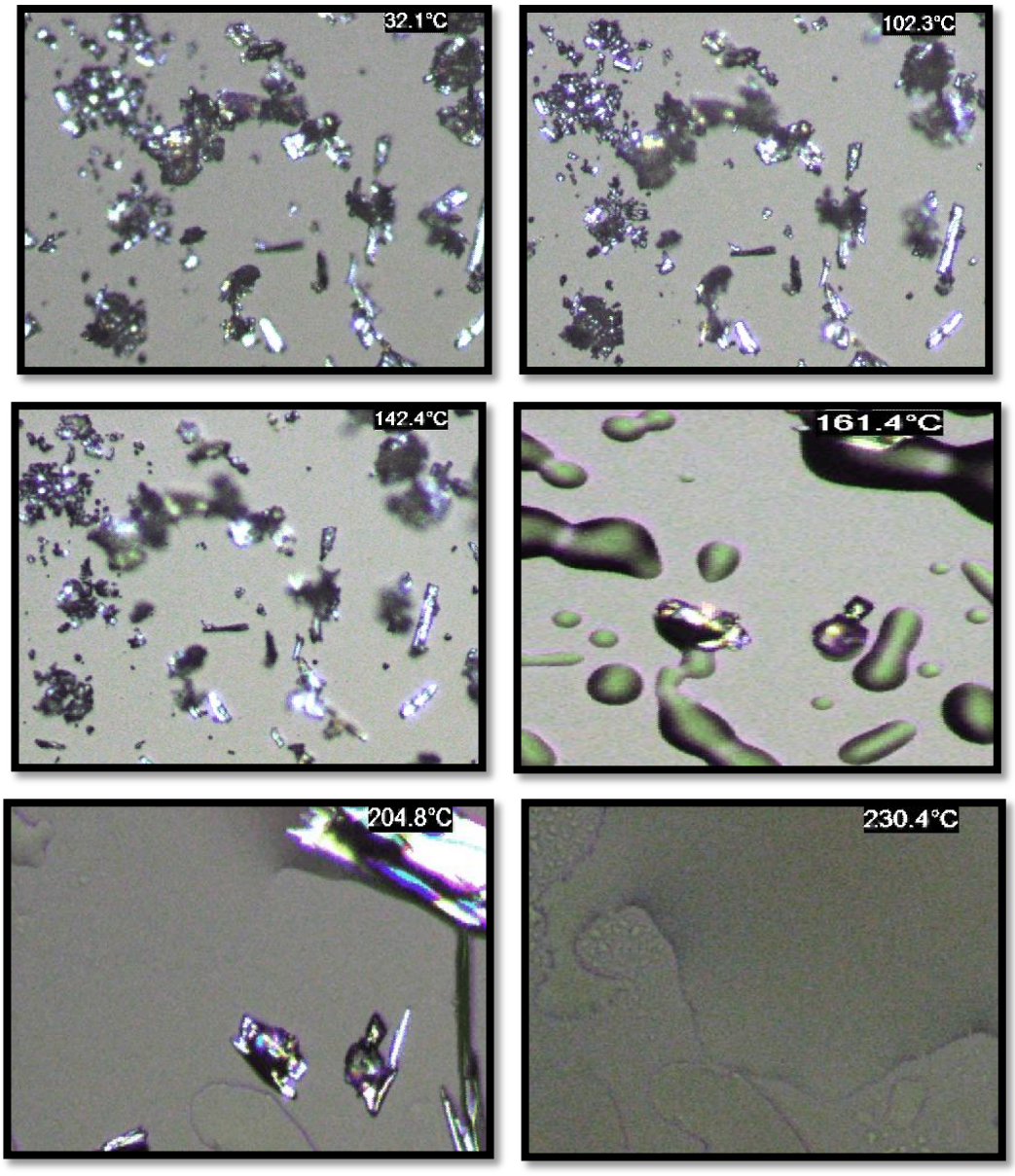


FIGURE 5. 15 HOT STAGE MICROSCOPE IMAGES CAPTURING THE RECRYSTALLISATION OF QUININE HYDROCHLORIDE FROM THE DEHYDRATE FORM. SAMPLES WERE HEATED AT 10°C/MIN

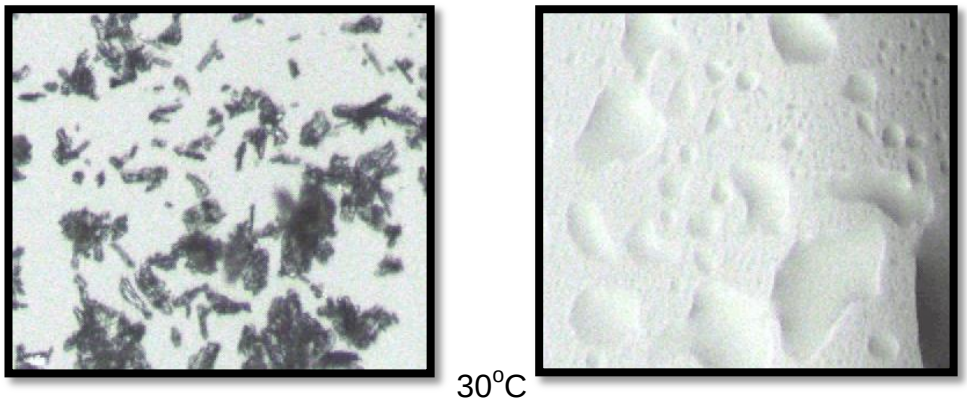


FIGURE 5. 16 HOT STAGE MICROSCOPY IMAGES CAPTURING THE MELTING OF QUININE CRYSTALS. SAMPLES WERE HEATED AT 10°C/MIN

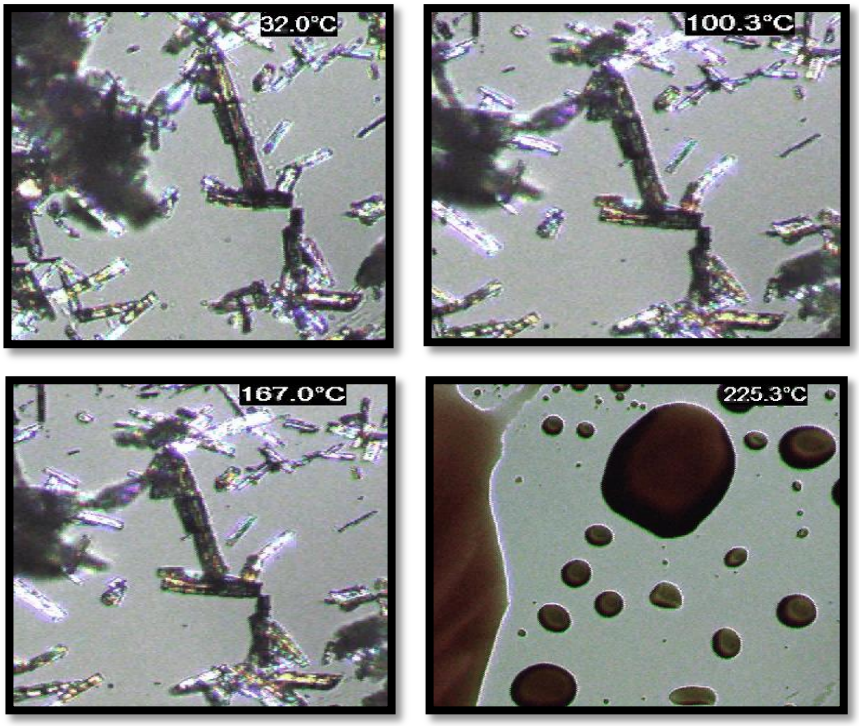


FIGURE 5. 17 HOT STAGE MICROSCOPY IMAGES CAPTURED AT SPECIFIC TEMPERATURES FOR QUININE SULPHATE SAMPLE HEATED AT 10°C/MIN

### 5.3.3 PARTICLE MORPHOLOGY OF RAW MATERIALS

SEM images of quinine hydrochloride dihydrate (Figure 5.18), quinine hemisulphate dihydrate (Figure 5.19) and Eudragit® EPO (Figure 5.20). The quinine particles appear to be crystalline in nature.

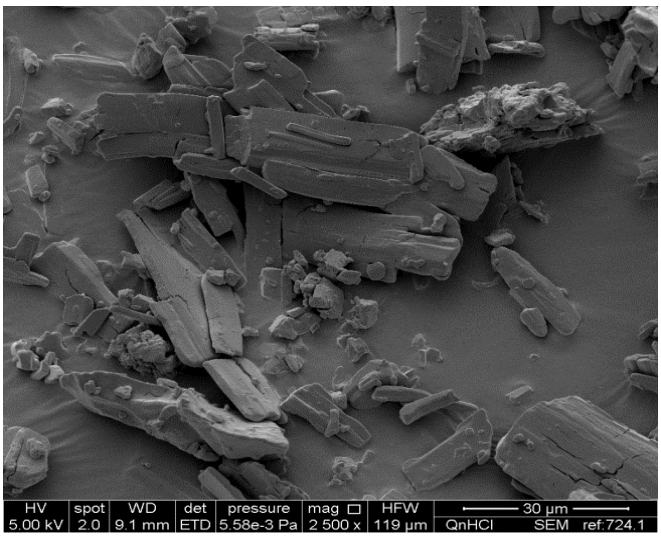


FIGURE 5. 18 SEM IMAGE OF CRYSTALLINE QUININE HYDROCHLORIDE DIHYDRATE. SCALE BAR CORRESPONDS TO 30µM

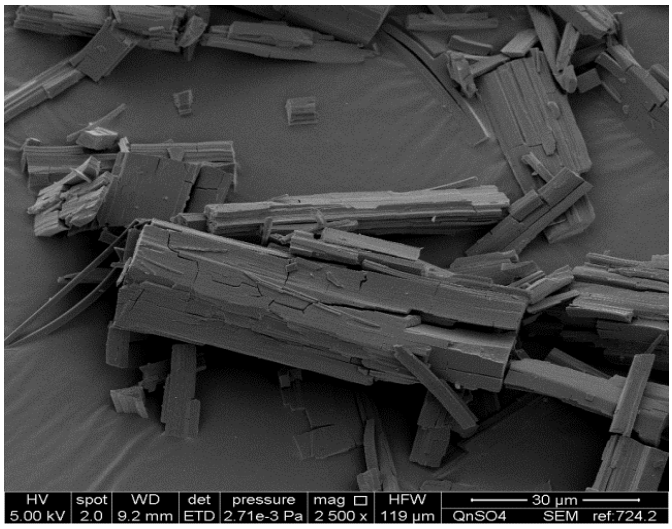


FIGURE 5. 19 SEM IMAGE OF CRYSTALLINE QUININE HEMISULPHATE DIHYDRATE. SCALE BAR CORRESPONDS TO 30µM

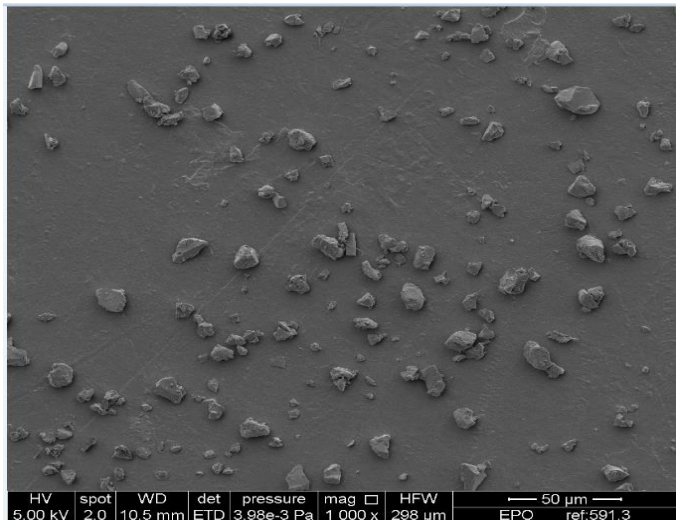


FIGURE 5. 20 SEM IMAGE OF EUDRAGIT® EPO. SCALE BAR CORRESPONDS TO 50µM

### 5.3.4 CHARACTERISATION OF HOT MELT EXTRUDED SAMPLES OF QUININE HYDROCHLORIDE DIHYDRATE AND EUDRAGIT® EPO

In section 5.3.2., the thermal characteristics of quinine hydrochloride dihydrate and Eudragit® EPO were reported. To recap, quinine hydrochloride dihydrate shows four transitions from baseline. The first endotherm is broad and has onset at 48$^{o}$C. The TGA trace suggests that this endotherm corresponds to water loss. Therefore, this implies that at the point of the next transition whose onset was 135$^{o}$C, quinine hydrochloride exists in the anhydrous form. This form undergoes a melt followed by a re-crystallisation which is shown in Figure 5.11. In the next section, the Eudragit® EPO – quinine hydrochloride (EPO-QHD) extrudates are characterised. As previously described in **chapter 2**, the extrudates are milled before being analysed.

#### *5.3.4.1 POWDER X-RAY DIFFRACTION OF EUDRGIT® EPO – QUININE HYDROCHLORIDE MELT EXTRUDATES*

In section 5.3.1 the crystallinity of quinine hydrochloride is described using PXRD. In addition, the “amorphous halo” of Eudragit®EPO (EPO) is also described. This section was concerned with reporting the effect of hot melt extrusion on the materials in question with a view of understanding whether the drug remained crystalline following hot melt extrusion with the amorphous polymer. In addition, an investigation into the miscibility of the two materials is described. The thermal stability of the Eudragit®EPO-QHD extrudates was also investigated and finally the release profile of quinine hydrochloride dihydrate from the Eudragit® EPO–QHD extrudate was compared to the corresponding physical mixtures with a view to describe the taste masking efficacy of the extrudates. To this end, increasing concentrations of quinine hydrochloride dihydrate i.e. 30%, 50% and 70% w/w Eudragit® EPO extrudates and their corresponding physical mixtures were investigated.

Figure 5.21 shows a comparative PXRD diffractograms of untreated quinine hydrochloride dihydrate and Eudragit® EPO together with Eudragit®EPO 30% quinine

hydrochloride dihydrate (EPO30% QHD), Eudragit®EPO 50% quinine hydrochloride dihydrate (EPO50% QHD), Eudragit®EPO 70% quinine hydrochloride dihydrate (EPO70% QHD). It is clear from the diffractograms that at all three drug loading, quinine remains crystalline. Interestingly, at 70% drug loading, two peaks are recorded at $38^{o}$ and $45^{o}$. These peaks are both not observed for pure quinine hydrochloride dihydrate. This suggests that the crystal habit of the quinine in EPO70%QHD is different from that of QHD. The significance of this observation will become apparent in **section 5.4.3**. The simplest explanation could be that the dehydration process which the drug undergoes during the HME process produces the anhydrous form of QHD which has different crystal habit when compared to the hydrate form. It can be postulated that the presence of this crystallinity could indicate that the saturation solubility has been exceeded such that crystalline material does not undergo a melt (Qi *et al.* 2008c). In addition, noticeable changes were observed on viscosity/torque during processing of EPO 70% QHD extrudates, indicating that at this concentration of QHD, there was a lack of intermolecular interaction between drug and polymer (Wu *et al.* 1999). To this end processing parameters were altered as described in Table 5.2.

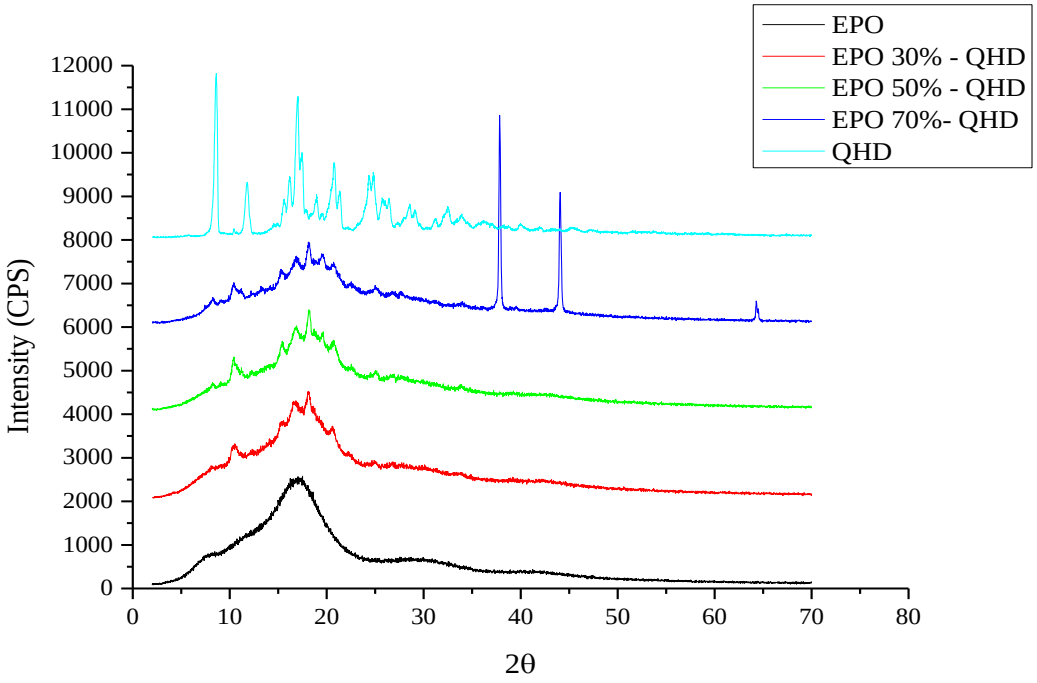


FIGURE 5. 21 PXRD DIFFRACTOGRAM OF QUININE HYDROCHLORIDE DIHYDRATE, EUDRAGIT® EPO AND QUININE HYDROCHLORIDE DIHYDRATE – EUDRAGIT® EPO MELT EXTRUDATES AT 30%, 50% AND 70% W/W RECORDED ON DAY ZERO

Although the crystallinity of the EPO-QHD melt extrudates had been compared to untreated quinine hydrochloride dihydrate and Eudragit®EPO, it was also necessary to compare these diffractograms to physical mixtures of quinine hydrochloride dihydrate and Eudragit®EPO at similar drug loading concentration. This was done to ascertain whether the diffractograms observed differed from those of the physical mixtures. Figure 5.22 shows the PXRD diffractograms of the EPO-QHD physical mixtures. This figure illustrates that the physical mixtures retain crystallinity and lack the “amorphous halo” of Eudragit® EPO. A distinctive peak is observed at $8^{o}$, although the intensity of the peak is reduced with decreasing concentrations of quinine hydrochloride dihydrate. Also to note, is the absence of two peaks at $38^{o}$ and $45^{o}$, for the EPO 70%QHD physical mixture, whereas they were observed for the same concentrate of extrudate.

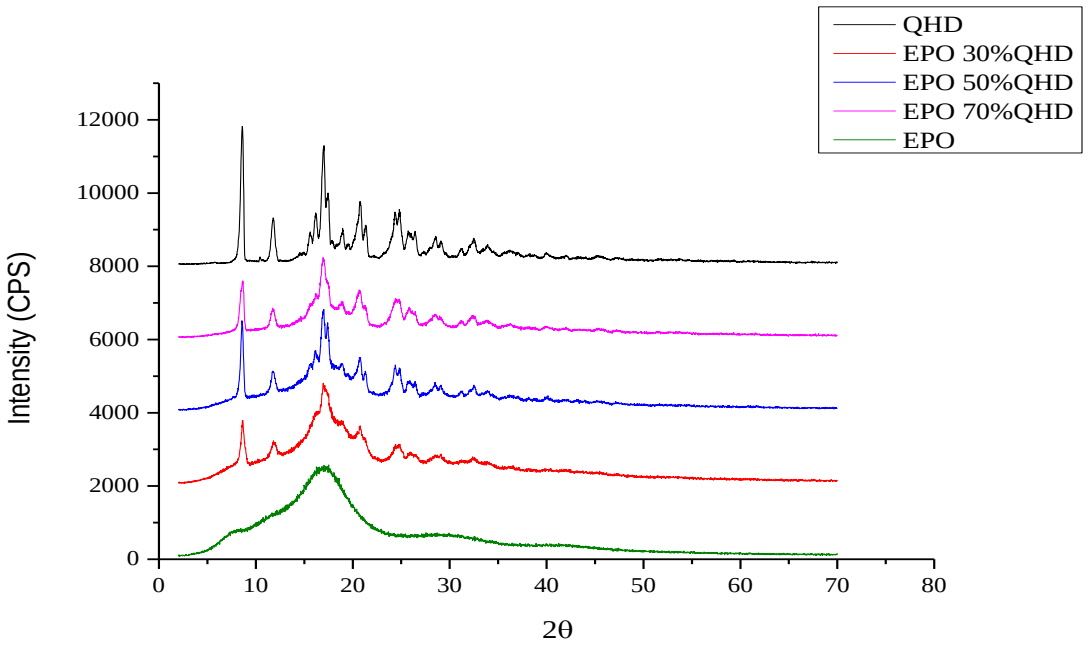


FIGURE 5. 22 PXRD DIFFRACTOGRAM OF QUININE HYDROCHLORIDE DIHYDRATE, EUDRAGIT® EPO AND QUININE HYDROCHLORIDE DIHYDRATE – EUDRAGIT® EPO PHYSICAL MIXTURES AT 30%, 50% AND 70% W/W RECORDED ON DAY ZERO

### EFFECT OF TEMPERATURE, HUMIDITY AND TIME.

In the previous section, the crystallinity of 30, 50% and 70% w/w EPO-QHD melt extrudates when the samples were fresh is reported. However, in order to understand the stability of the EPO-QHD melt extrudates, the samples were exposed to stresses of temperature and humidity over twenty eight days with the view to describe changes to the crystal character of the melt extrudates. The samples were exposed to 0% relative humidity, 25$^{o}$C and 50% relative humidity, 4$^{o}$C.

Tables 5.3 and 5.4 gives a summary of the PXRD diffractograms of EPO 30% QHD, EPO 50% QHD and EPO 70% QHD melt extrudates after ageing for seven, fourteen and twenty eight days in two different conditions i.e. 0% relative humidity, 25$^{o}$C and 50% relative humidity, 4$^{o}$C. It is clear that after seven days, there is a peak of highest intensity at 12.2$^{o}$. This signifies that the drug is crystalline. In addition, the crystal habit remains the same across the different storage conditions. After fourteen days, the samples retain crystallinity and the diffractograms are similar to those of the fresh sample, hence suggesting that the drug is crystalline. The different stress conditions do

not affect the results observed It is clear from the diffractograms that there is no change in the crystallinity of the melt extrudates after twenty eight days

Similar analysis was conducted for EPO50%QHD melt extrudates. Tables 5.3 and 5.4 shows PXRD diffractograms of EPO 50%QHD melt extrudates after storing for seven days at same condition as those described for EPO 30% QHD. The aged samples show crystallinity which is similar to fresh samples and different to the amorphous halo of Eudragit®EPO **(Figure 5.4).** After fourteen and twenty eight day ageing of Eudragit®EPO 50%QHD samples, It is apparent from this diffractogram that the melt extrudate stored at 50% relative humidity and 4$^{o}$C remains crystalline. A noticeable observation is that the sample stored at 50%RH and 4$^{o}$C shows an amorphous halo suggesting that this sample is amorphous. An explanation for this observation is that this sample congealed into a solid mass and despite efforts to load onto sampling pan, it is conceivable that the detection of this sample was impaired and as such is appears to be amorphous. Further discussions on this issue will be made in **section 5.4.2.**

Following on from investigating the 30% and 50% EPO-QHD melt extrudates, the EPO 70% QHD melt extrudates were also investigated. The PXRD diffractograms are shown also shown in Tables 5.3 and 5.4 ageing for seven, fourteen and twenty eight days respectively. On all three occasions, there is no difference in the patterns between the fresh and aged samples. What is also noteworthy is the presence of two peaks at 38$^{o}$ and 45$^{o}$, which are characteristic peaks only observed for EPO 70% QHD, again suggesting a different crystal habit in these samples. It would appear that at these conditions did not affect the crystallinity of the EPO70% QHD melt extrudates when stored at 0% relative humidity and 25$^{o}$C. It would appear that at 50% relative humidity and 4$^{o}$C the PXRD trace is parallel to the x-axis. This could be ascribed to that fact that after storage for twenty eight days the powder extrudate congealed into a solid mass. Even though an attempt was made to mount this sample on the PXRD sample

holders the resultant diffractogram suggests that the sample was not detected. Further discussions on this issue will be made in **section 5.4.2.**

The corresponding diffractograms of Eudragit® EPO 30% QHD and EPO 50% QHD for the physical mixtures have been summarised in Table 5.3 after seven days of stress conditions. Unremarkably, there are no changes in the diffractograms with time or stress conditions. This trend also continues after fourteen and twenty eight days of storage. What is apparent is that the three peaks of highest intensity at $8.8^{o}$, $12.2^{o}$ and $17.2^{o}$ reported in Figure 5.1 are also shown in the diffractograms of the physical mixtures shown in Table 5.3 which is expected because the quinine hydrochloride in the physical mixtures is unprocessed

TABLE 5 3 SUMMARY OF PXRD DIFFRACTOGRAMS OF EPOQHD MELT EXTRUDATES AFTER EXPOSURE TO STRESS CONDITION OF 0% RELATIVE HUMIDITY, 25$^{O}$C AND 50% RELATIVE HUMIDITY, 4$^{O}$C .

| Day | EPO30% QHD | EPO50% QHD | EPO70% QHD |
|---|---|---|---|
| Seven | 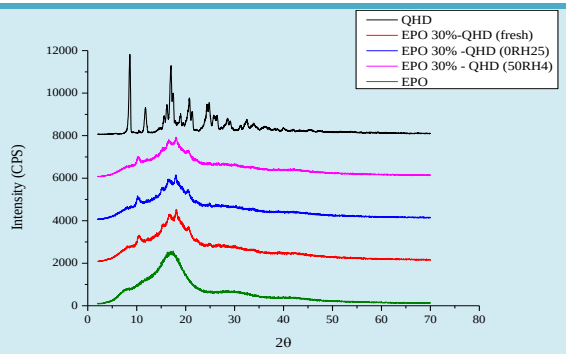 | 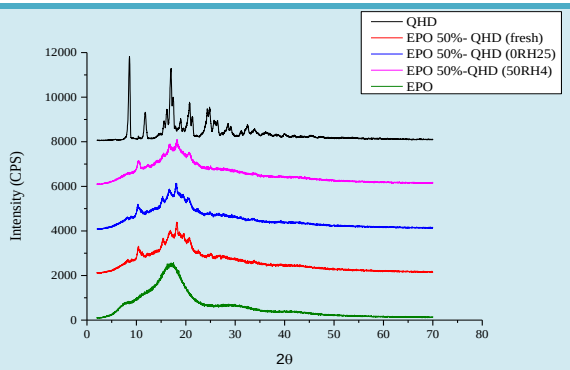 | 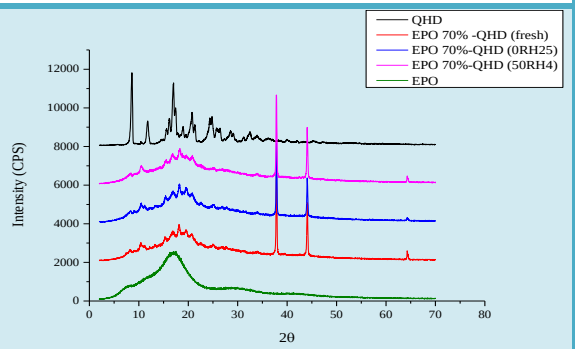 |

TABLE 5 4 SUMMARY OF PXRD DIFFRACTOGRAMS OF EPOQHD MELT EXTRUDATES AFTER EXPOSURE TO STRESS CONDITION OF 0% RELATIVE HUMIDITY, 25°C AND 50% RELATIVE HUMIDITY, 4°C .

| | | | |
|---|---|---|---|
| **Fourteen** | 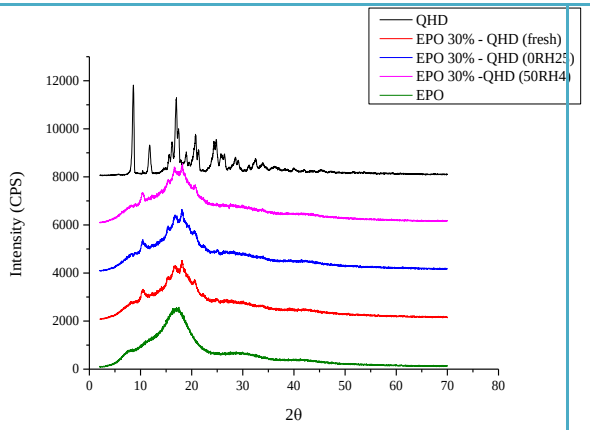 | 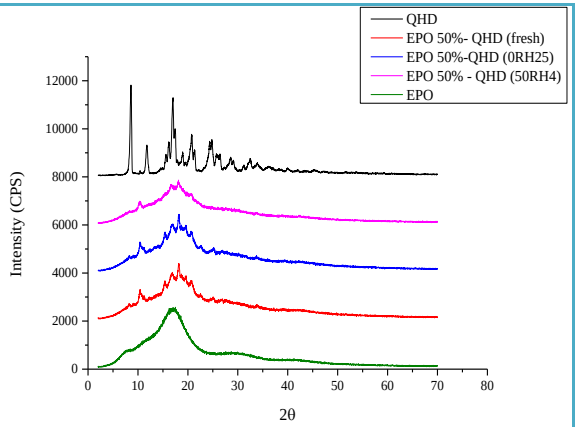 | 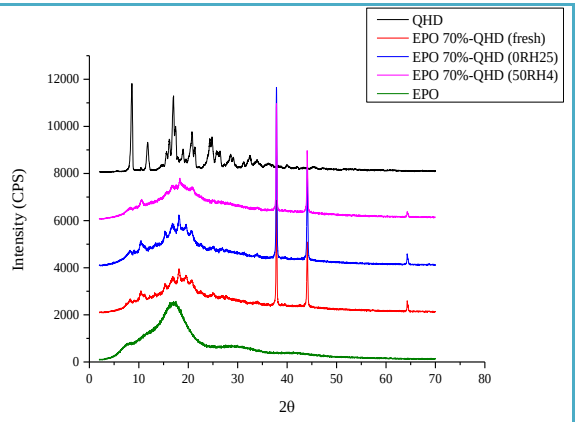 |
| **Twenty eight** | 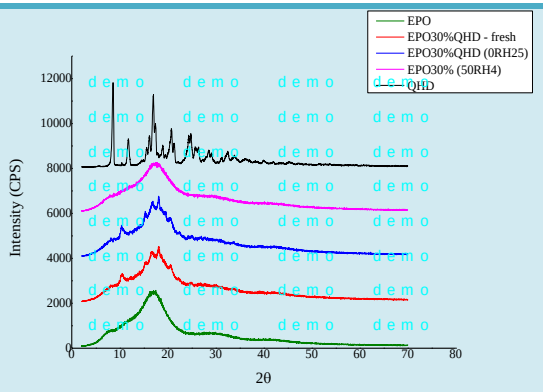 | 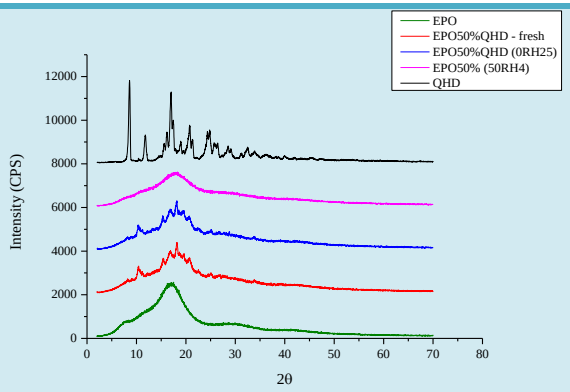 | 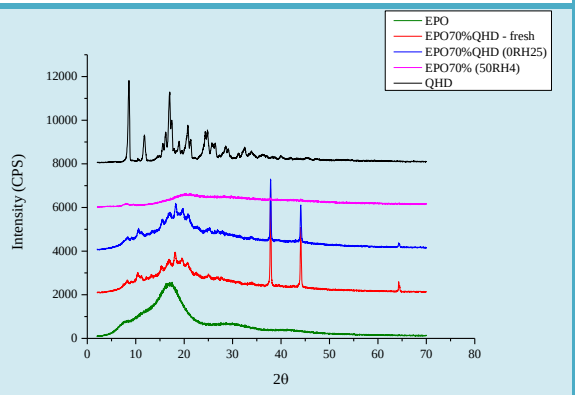 |

TABLE 5 5 SUMMARY OF PXRD DIFFRACTOGRAMS OF EPOQHD PHYSICAL MIXTURES AFTER EXPOSURE TO STRESS CONDITION OF 0% RELATIVE HUMIDITY, 25$^{O}$C AND 50% RELATIVE HUMIDITY, 4$^{O}$C.

| Day | EPO 30%QHD | EPO50%QHD |
|---|---|---|
| seven | 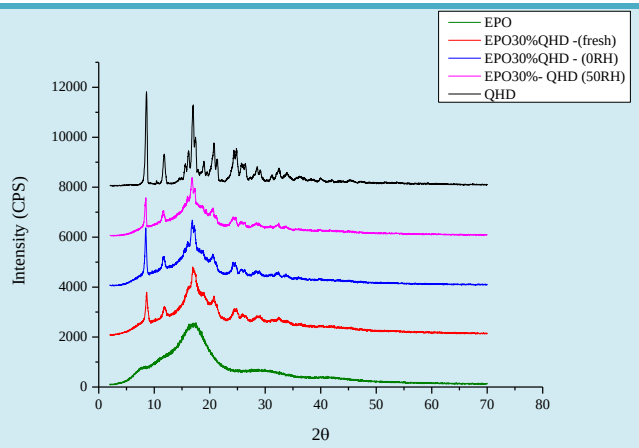 | 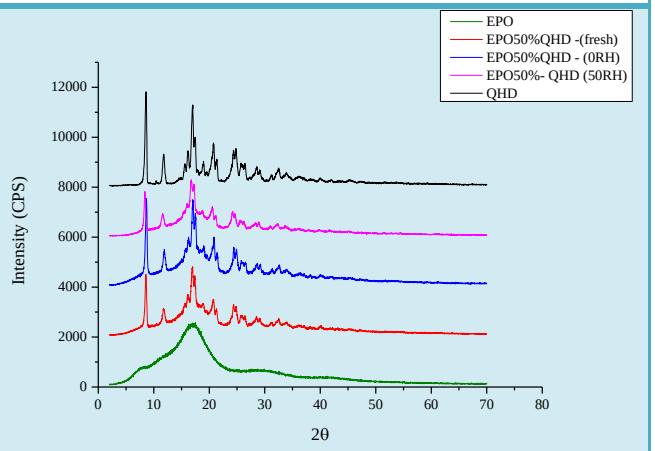 |

**SUMMARY OF RESULTS**

Before proceeding to the next section where thermal analysis of the melt extrudate is described, it is worth pointing out that so far PXRD has shown that EPO30%QHD and EPO50%QHD both crystalline when fresh. This is also true for EPO70%QHD which shows sharp peaks at $38^{o}$ and $45^{o}$ indicative of crystallinity. These two peaks are absent on the diffractogram for untreated quinine hydrochloride dihydrate. At the temperatures at which melt extrusion was carried out. After storing EPO 50%QHD and EPO70%QHD for twenty eight days at 50% relative humidity and $4^{o}$C PXRD diffractograms show an amorphous halo. In both cases, due to the samples being a solid mass, hence it was not in powder form when mounted onto the sample holders. Therefore, it is possible that the detection was impaired hence an erroneous result. This significance of these findings will be discussed in **section 5.4.2** in conjunction with findings from the next section which look at thermal analysis of the samples. Unsurprisingly there is no change in crystallinity observed for the physical mixtures of Eudragit® EPO QHD.

### *5.3.4.2 THERMAL ANALYSIS OF EUDRAGIT® EPO –QUININE HYDROCHLORIDE SAMPLES*

In **section 5.3.2**, the DSC thermographs of quinine hydrochloride dihydrate and Eudragit® EPO are shown in Figures 5.5 and Figure 5.10 respectively. In this section, these thermographs will be compared with those obtained from Eudragit® EPO-quinine hydrochloride (EPO QHD). The EPOQHD extrudates analysed were in increasing concentrations of quinine hydrochloride dihydrate i.e. 10%, 30%, 50% and 70% w/w. In addition, the EPOQHD extrudates were compared with physical mixtures of the same concentrations.

Figure 5.23 shows the DSC thermographs of the EPOQHD extrudates. Unsurprisingly, the increasing concentrations of quinine hydrochloride dihydrate (top to bottom) translated to the DSC thermograph matching that of quinine hydrochloride dihydrate.

Interestingly, QHD has a melt at 232$^{o}$C however EPO 70%QHD shows a downward shift in this melt to 222$^{o}$C. The significance of this finding will be discussed in **section 5.4**. In addition the other transitions reported for QHD are not pronounced for the other EPO-QHD melt extrudates. This can be possibly explained by the fact that in order for crystal growth to occur after melting, secondary nucleation (crystal growth generated in the vicinity of other crystalline matter present in the melt) needs to occur. Strickland-Constable (1968) described several possible mechanisms of secondary nucleation of which “collision” breeding (a complex process resulting from interaction of crystals with one another) seems particularly significant in this instance. HSM studies showed that secondary crystal growth was more prolific with increasing concentrations of quinine hydrochloride in the melt extrudates. As such the DSC traces also show that increasing concentrations of quinine in the melt extrudates results in the DSC trace resembling that of pure quinine hydrochloride dihydrate. Another point to note is that EPO 50%QHD shows a broad endotherm with onset at 205$^{o}$C. At this stage it is unclear as to what this endotherm represents, however it could be suggested that crystal growth is ongoing though this was not visible under HSM.

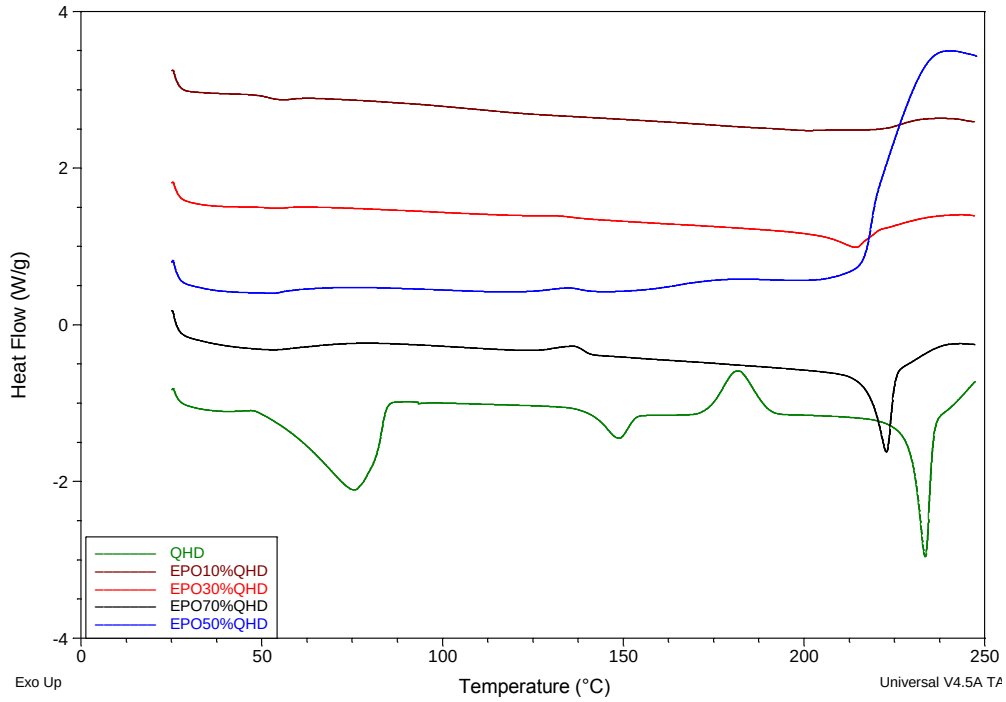


FIGURE 5. 23 TYPICAL DSC HEAT FLOW SIGNAL OF QUININE HYDROCHLORIDE DIHYDRATE (QHD), EUDRAGIT® EPO 70% QUININE HYDROCHLORIDE DIHYDRATE EXTRUDATE (EPO70%QHD), EUDRAGIT® EPO 50% QUININE HYDROCHLORIDE DIHYDRATE EXTRUDATE (EPO 50% QHD), EUDRAGIT® EPO 30% QUININE HYDROCHLORIDE DIHYDRATE EXTRUDATE (EPO 30% QHD) AND EUDRAGIT® EPO 10% QUININE HYDROCHLORIDE DIHYDRATE EXTRUDATE (EPO10% QHD) RECORDED AT HEATING RATE 10°C/MIN USING AN OPEN PAN

In order to understand the effect of the hot melt extrusion process on the thermal characteristic of the EPOQHD extrudates, it was necessary to compare the extrudates with their physical mixture counterparts. Figure 5.24 shows the DSC thermographs of 10, 30, 50, 70% w/w Eudragit®EPO – quinine hydrochloride dihydrate (EPOQHD) physical mixtures. It is safe to say that the inclusion of the polymer to quinine causes a downward shift in the water loss endotherm reported in Figure 5.5. Furthermore, the subsequent transitions also show a downward shift albeit they are not pronounced for 30, 50 and 70% w/w EPOQHD physical mixtures. The significance of this downward shift will become apparent in **section 5.4**. The same transition are relatively non-existent for the EPO 10%QHD physical mixture.

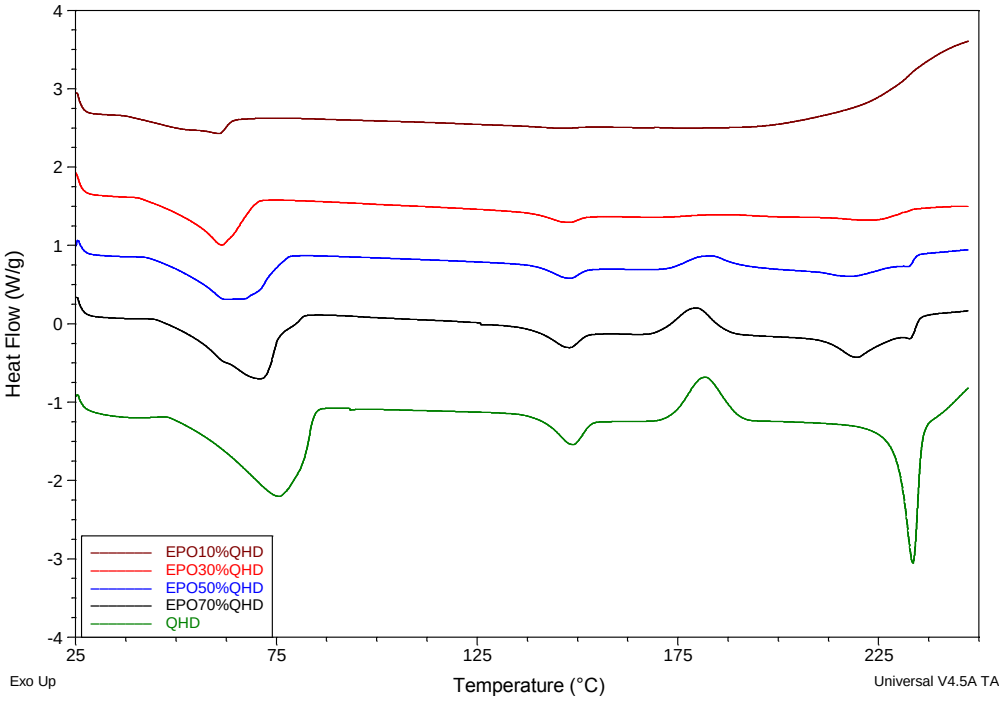


FIGURE 5. 24 TYPICAL DSC HEAT FLOW SIGNAL OF QUININE HYDROCHLORIDE DIHYDRATE (QHD), EUDRAGIT® EPO 70% QUININE HYDROCHLORIDE DIHYDRATE PHYSICAL MIXTURE (EPO 70% QHD), EUDRAGIT® EPO 50% QUININE HYDROCHLORIDE DIHYDRATE PHYSICAL MIXTURE (EPO 50% QHD), EUDRAGIT® EPO 30% QUININE HYDROCHLORIDE DIHYDRATE PHYSICAL MIXTURE (EPO 30% QHD) AND EUDRAGIT® EPO 10% QUININE HYDROCHLORIDE DIHYDRATE PHYSICAL MIXTURE (EPO10% QHD) RECORDED AT HEATING RATE 10$^{o}$C/MIN USING OPEN PANS

### EFFECT OF TEMPERATURE, HUMIDITY AND TIME

The characterisation of EPOQHD extrudates has been described in **section 5.3.4**. This analysis focussed on freshly prepared samples. However, as already eluded to, anhydrous quinine hydrochloride is formed during the extrusion process therefore it was necessary to investigate the stability of this form by exposing it to extreme stresses of temperature and humidity. In addition, the samples stability was investigated as a function of time. EPO 10%QHD did not exhibit any interesting behaviour therefore has not been reported here. Further analysis in terms of temperature, humidity and time was conducted on the EPO 30%, 50% and 70% QHD samples.

Table 5.5 shows the DSC (green) and the overlaid TGA (blue) for Eudragit®EPO 30% quinine hydrochloride dihydrate (EPO 30% QHD) after storing for seven, fourteen and twenty eight days at 0% relative humidity and 25$^{o}$C together with 50% relative humidity

The DSC heat flow shows a small endotherm between 48$^{o}$C and 55$^{o}$C with no presence of noise in the baseline. In comparison to untreated QHD shown in **Figure 5.3** this endotherm can be ascribed to $T_g$ of Eudragit® EPO. In addition, it is clear that the overarching water loss endotherm observed for untreated quinine hydrochloride dihydrate (Figure 5.5) is clearly absent in this DSC trace. This is expected as water loss occurs during the HME process. An exotherm is also observed between 122$^{o}$C and 138$^{o}$C (re-crystallisation) which is followed by a broad endotherm with onset at 202$^{o}$C (melt). Of note, is there are a downward shift both the re-crystallisation and melt temperatures. The corresponding measured weight change was 12.08%. Initially it appears that this weight change is attributed to water loss. However, on closer inspection, this weight loss could also include the degradation of Eudragit®EPO. A typical TGA trace for Eudragit® EPO is given in Figure 5.25 as a basis for comparison.

The EPO30% QHD extrudates which were stored for seven, fourteen and twenty eight days at 50% relative humidity and 4$^{o}$C and the DSC (green) and corresponding TGA (blue) also shown in the summary Table 5.5. It is apparent that the DSC trace is similar to that described for EPO 30%QHD which had been stored at 0% relative humidity and 25$^{o}$C. It would appear that after seven days of different storage conditions the thermal behaviour of Eudragit®EPO remains unchanged and is in still the anhydrous form of quinine hydrochloride. No further changes are observed in the DSC traces with increasing storage time.

TABLE 5 6 SUMMARY TABLE OF DSC AND TGA TRACES OF EPO 30% QHD EXTRUDATES AFTER STORAGE AT 0RH, 25°C, 50RH AND 4°C FOR SEVEN, FOURTEEN AND TWENTY EIGHT DAYS

| Day | Stored at 0RH, 25°C | Stored at 50RH, 4°C |
|---|---|---|
| seven | 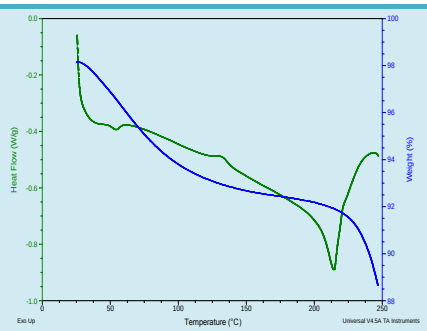 | 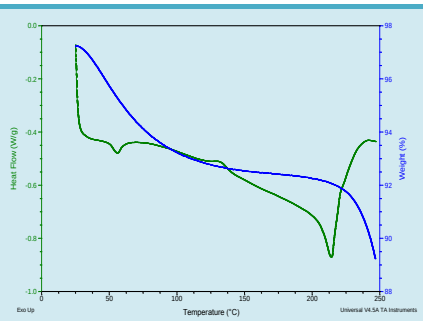 |
| fourteen | 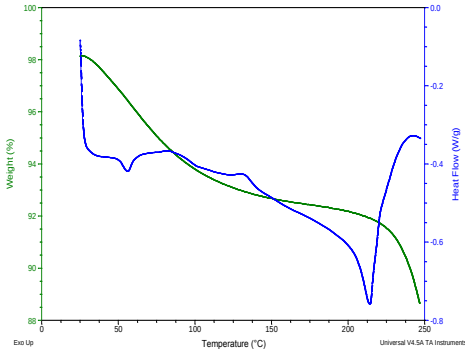 | 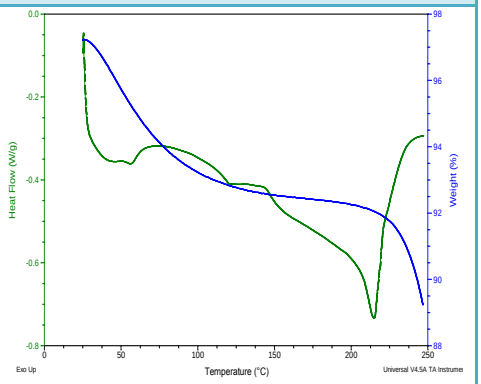 |
| twenty eight | 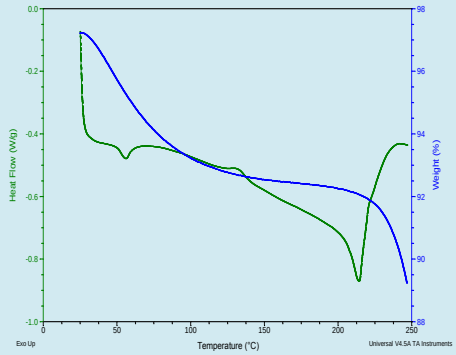 | 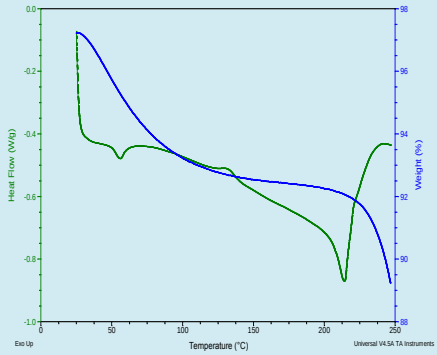 |

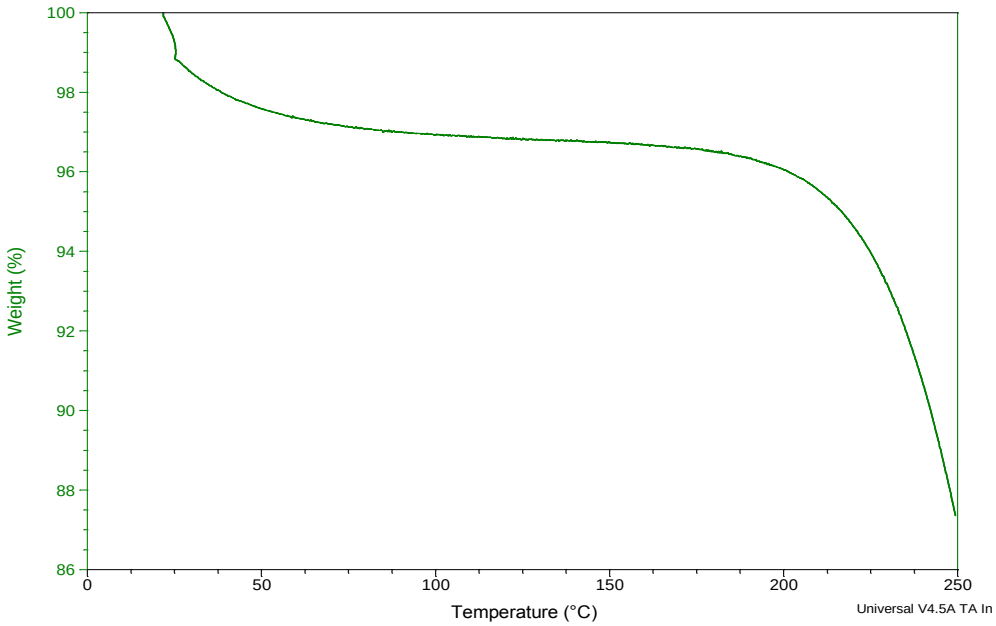


FIGURE 5. 25 TYPICAL TGA TRACE FOR EUDRAGIT®EPO, HEATING RATE 10$^{o}$C/MIN USING AN OPEN PAN

Table 5.6 focuses on the physical mixture of EPO 30% QHD after storing for seven days at 0% relative humidity and 25$^{o}$C. The DSC (green) heat flow shows a broad endotherm with onset at 46$^{o}$C. Another smaller endotherm is observed with onset temperature 148$^{o}$C. This is quickly followed by an exotherm with onset temperature 162$^{o}$C then a broad endotherm with onset temperature 208$^{o}$C. What is interesting about the physical mixture is the absence of an obvious melt endotherm which was prominent in all previous DSC traces of QHD. A possible explanation for this lies in the fact that like many solid state reaction, recrystallisation occurs through the processes of nucleation and growth. The lack of other crystals to aid the nucleation and growth process results in diminished recrystallisation hence the absence of the melt endothermic peak. The corresponding measured weight change (TGA) shown in blue, was 9.02%. This weight change can be attributed to both water loss from the 30% quinine hydrochloride and 70%Eudragit®EPO.

Table 5.6 also shows DSC and TGA traces of the physical mixture of Eudragit ®EPO 30% QHD stored at 50% relative humidity and 4$^{o}$C for seven days. Unsurprisingly, the DSC (green) and the TGA traces (blue) remain unchanged in comparison to that of the

physical mixture stored at 0% relative humidity and 25°C shown in the same table. Unsurprisingly, the DSC and TGA traces remain unchanged over the twenty eight day storage time.

TABLE 5 7 SUMMARY TABLE OF DSC AND TGA TRACES OF EPO 30% QHD PHYSICAL MIXTURES AFTER STORAGE AT 0RH, 25°C, 50RH AND 4°C FOR SEVEN DAYS

| Day | Stored at 0%RH, 25°C | Stored at 50%RH,4°C |
|---|---|---|
| Seven | 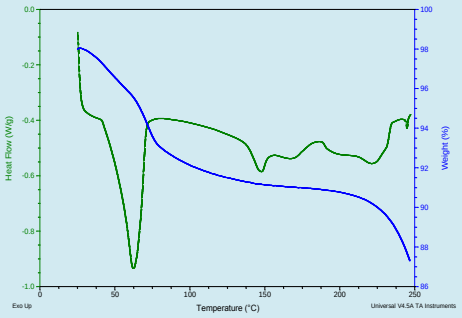 | 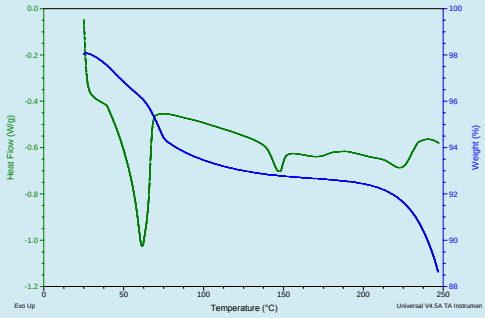 |

EPO 50% QHD extrudates were stored at 0% relative humidity, and temperature of 25°C for seven days and the corresponding DSC (green) and TGA (blue) traces are shown in Table 5.7. In contrast to EPO 30% QHD extrudates, the DSC trace shows a broad endotherm with onset 48°C. This endotherm is similar to the endotherm observed for quinine hydrochloride dihydrate and is attributed to water loss. In addition, the other two transitions at 142°C and 162°C are more pronounced when compared to EPO30% QHD. A possible explanation for this observation is that at 50% drug loading there are more “seeds” allowing nucleation and crystal growth. This DSC trace resembles that of pure quinine hydrochloride dihydrate which could also suggest that under these conditions EPO50%QHD, the anhydrous form reverts back to resemble pure quinine hydrochloride. The weight change measured was 10.02%, which can be ascribed to both water losses from quinine hydrochloride dihydrate and degradation of EPO.

Table 5.7 also shows the DSC (green) and overlaid TGA (blue) traces of EPO 50% QHD physical mixture after storing for seven days at 0% relative humidity, 25°C.

Interestingly, this DSC and corresponding TGA traces are similar to those for EPO 50%QHD stored at 0% relative humidity and 25°C. Therefore this implies that after seven days, the stress conditions applied do not seem to affect the thermal behaviour of EPO 50%QHD. This suggests that this extrudate is thermally stable under these stress conditions.

TABLE 5 8 SUMMARY TABLE OF DSC AND TGA TRACES OF EPO 50% QHD EXTRUDATES AFTER STORAGE AT 0RH, 25°C, 50RH AND 4°C FOR SEVEN DAYS

| Day | 0%RH, 25°C | 50%RH,4°C |
|---|---|---|
| Seven | 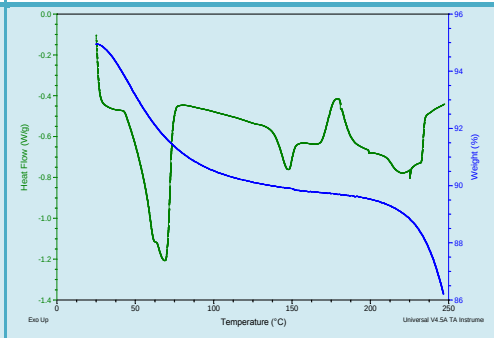 | 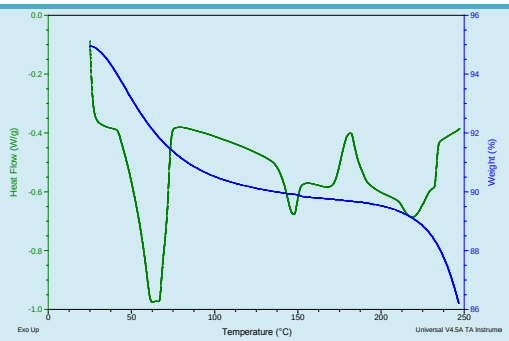 |



The DSC (green) and TGA (blue) traces of the physical mixture of EPO 50% QHD after storing for seven days at 0% relative humidity and 25°C are shown in Table 5.8. What is apparent from the DSC trace is that it exhibits similar endotherms and exotherm to those observed for quinine hydrochloride dihydrate (Figure 5.5). Also to note, albeit unremarkable is the fact that the physical mixture remains unchanged in terms of thermal properties. The measured weight changed was 10.4% which can be ascribed to water loss. The physical mixture of EPO50% QHD were also stored at 50% relative humidity and 4°C and the overlaid DSC and TGA traces are reported in Table 5.8. Unsurprisingly, the traces reported do not deviate from those previously reported for those stored at 0% relative humidity and 25°C

TABLE 5 9 SUMMARY TABLE OF DSC AND TGA TRACES OF EPO 50% QHD PHYSICAL MIXTURES AFTER STORAGE AT 0RH, 25°C, 50RH AND 4°C FOR SEVEN DAYS

| Day | Stored at %RH, 25°C | Stored at 50%RH, 4°C |
|---|---|---|
| seven | 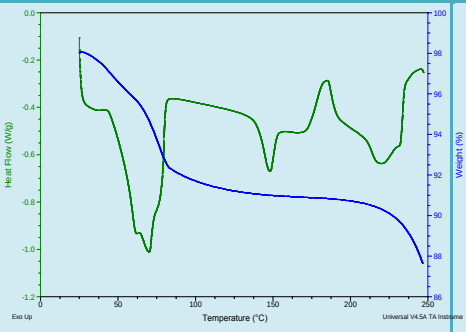 | 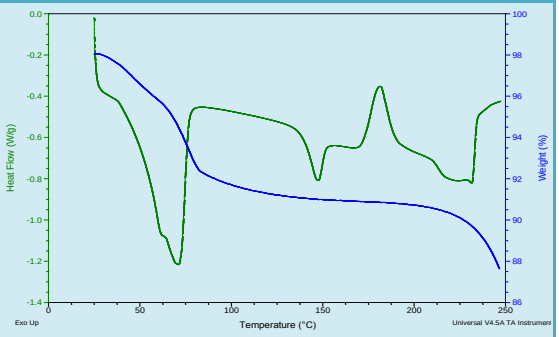 |



Figure 5.26 gives a comparative summary of the DSC traces of EPO30%QHD stored at the different stress conditions for seven days. This suggests that the thermal behaviour of this extrudate is not affected by the storage conditions to which it is exposed. Quinine hydrochloride remains in its dehydrated form. In all cases, an endothermic step change from baseline is observed with onset 48°C. This step change denotes the $T_g$ of Eudragit® EPO. The next transition is an exothermic peak with onset 128°C which is the recrystallisation of quinine hydrochloride. The final endotherm with onset at 218°C represents the melt of the recrystallized quinine hydrochloride. What is significant is that there is a major downward shift of the recrystallisation exotherm.

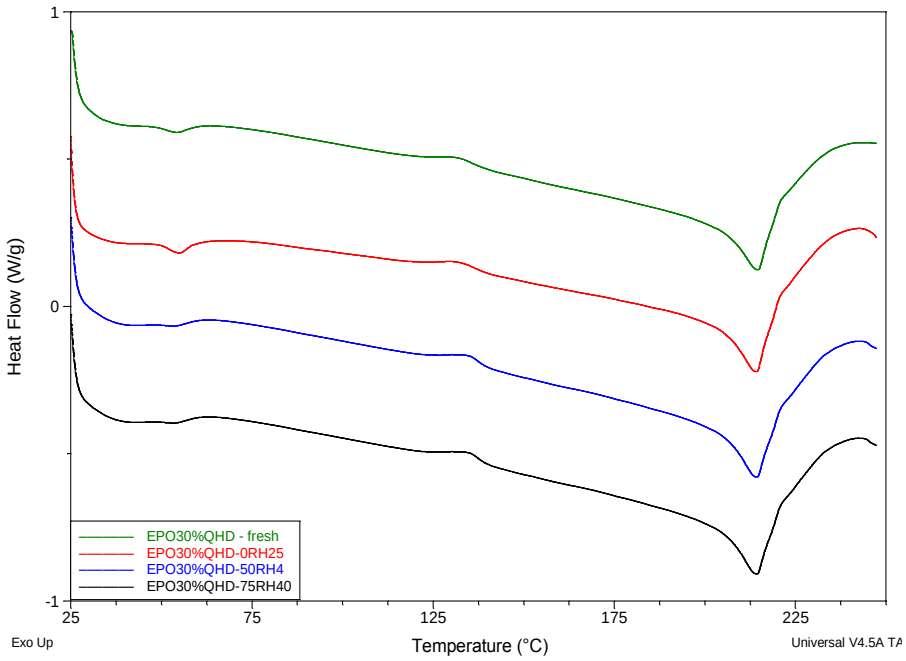


FIGURE 5. 26 TYPICAL DSC HEAT FLOW SIGNAL OF EUDRAGIT®EPO30% QUININE HYDROCHLORIDE DIHYDRATE MELT EXTRUDATES FOLLOWING STORAGE AT 0% RELATIVE HUMIDITY, 25$^{O}$C (0RH, 25$^{O}$C), 50% RELATIVE HUMIDITY, 4$^{O}$C (50RH,4$^{O}$C) AND 75% RELATIVE HUMIDITY, 40$^{O}$C (75RH,40$^{O}$C) FOR SEVEN DAYS. HEATING RATE WAS 10$^{O}$C/MIN USING OPEN PANS

On examination of the same samples i.e. EPO 30% QHD after they had been stored for fourteen days (Figure 5.27), it is apparent that similar to results reported after seven days, there are no differences between the fresh sample and the other three which had been exposed to temperature and humidity stresses. In addition, the different stress conditions appear to have not altered the thermal properties of the EPO30% QHD samples. What is also apparent is the exothermic and endothermic peaks reported for after seven days (Figure 5.47) are less pronounced after fourteen days. This suggests that quinine hydrochloride is still in the anhydrous form and in addition the nucleation and growth of the crystals following melt is somewhat diminished.

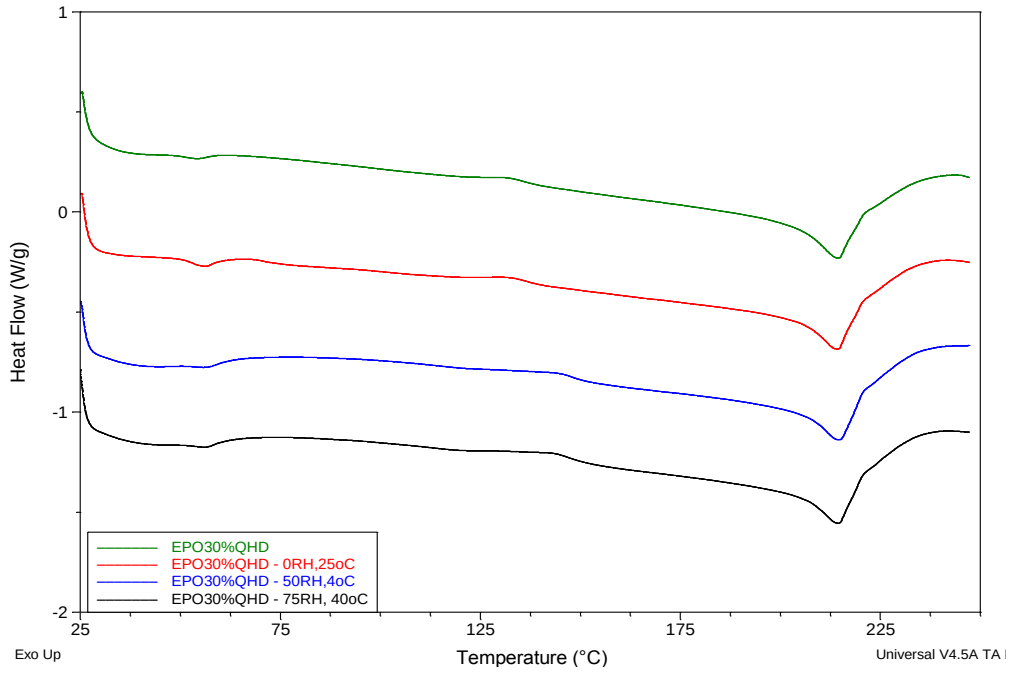


FIGURE 5. 27 TYPICAL DSC HEAT FLOW SIGNAL OF EUDRAGIT®EPO 30% QUININE HYDROCHLORIDE DIHYDRATE MELT EXTRUDATES FOLLOWING STORAGE AT 0% RELATIVE HUMIDITY, 25$^{O}$C (0RH, 25$^{O}$C), 50% RELATIVE HUMIDITY, 4$^{O}$C (50RH,4$^{O}$C) AND 75% RELATIVE HUMIDITY, 40$^{O}$C (75RH,40$^{O}$C) FOR FOURTEEN DAYS. HEATING RATE WAS 10$^{O}$C/MIN USING AN OPEN PAN

Finally, the EPO30%extrudates are analysed again after twenty days and a comparative summary is given in Figure 5.28 It is also apparent from this figure that there is no difference in the thermal behaviour of the fresh samples and those that have been stored for twenty eight days. This is to say that quinine hydrochloride remains in its dehydrated form hence the endothermic peak at 48$^{o}$C denoted the $T_g$ of Eudragit®EPO while to exothermic peak at 128$^{o}$C shows recrystallisation followed by an endothermic peak at 218$^{o}$C

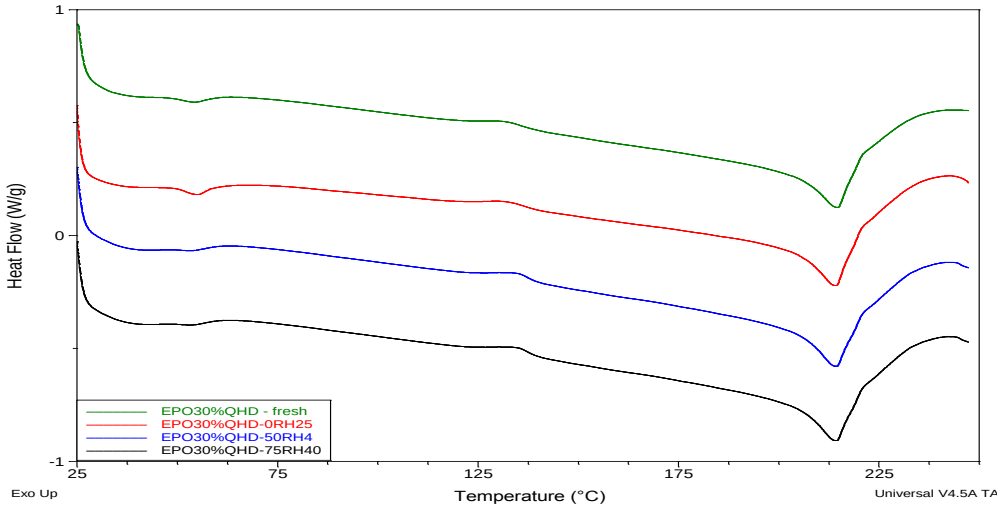


FIGURE 5. 28 TYPICAL DSC HEAT FLOW SIGNAL OF EUDRAGIT®EPO 30% QUININE HYDROCHLORIDE DIHYDRATE MELT EXTRUDATES FOLLOWING STORAGE AT 0% RELATIVE HUMIDITY, 25°C (0RH, 25°C), 50% RELATIVE HUMIDITY, 4°C (50RH,4°C) AND 75% RELATIVE HUMIDITY, 40°C (75RH,40°C) FOR TWENTY EIGHT DAYS. HEATING RATE WAS 10°C/MIN USING AN OPEN PAN.

In similar fashion to EPO30%QHD extrudate thermographs shown in Figure 5.29, the DSC traces of the EPO 30%QHD physical mixtures are shown in Table 5.9. A marked difference is observed in terms of the transitions. Unsurprisingly the physical mixtures exhibit the broad endotherm with onset 45°C, which can be ascribed to both water losses from the quinine hydrochloride dihydrate and the $T_g$ of Eudragit® EPO. It is also essential to point out is that after the broad endotherm attributed to water loss, the next transition observed is similar to that observed for QHD (Figure 5.5), however the recrystallisation and subsequent melt are not as pronounced for the physical mixtures. A possible explanation for this is that the presence of the polymer means that quinine hydrochloride crystals are separated therefore nucleation and subsequent crystal growth from melt is reduced as demonstrated by the DSC trace.

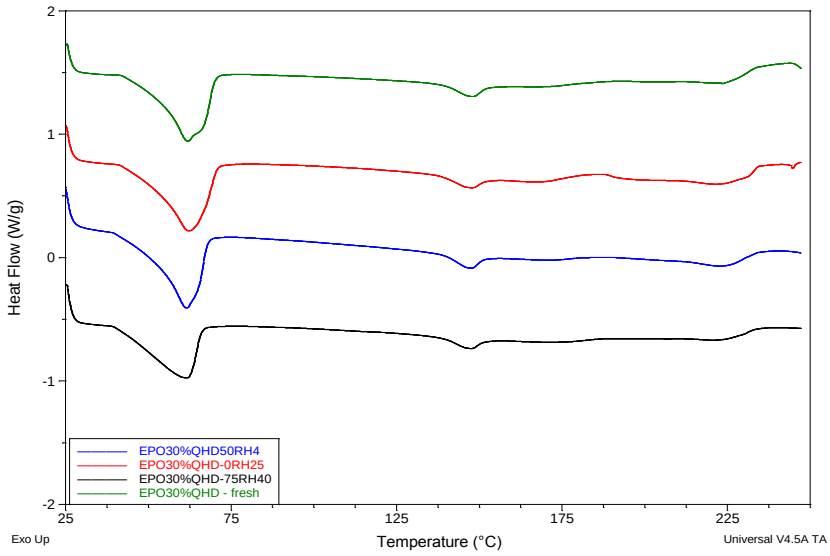


FIGURE 5. 29 TYPICAL DSC HEAT FLOW SIGNAL OF EUDRAGIT®EPO 30% QUININE HYDROCHLORIDE DIHYDRATE PHYSICAL MIXTURES FOLLOWING STORAGE AT 0% RELATIVE HUMIDITY, 25$^{O}$C (0RH, 25$^{O}$C), 50% RELATIVE HUMIDITY, 4$^{O}$C (50RH,4$^{O}$C) AND 75% RELATIVE HUMIDITY, 40$^{O}$C (75RH,40$^{O}$C) FOR SEVEN DAYS. HEATING RATE WAS 10$^{O}$C/MIN USING AN OPEN PAN

The differences between the fresh Eudragit® EPO 50% quinine hydrochloride dihydrate (EPO 50% QHD) and the same sample having been exposed to stresses of temperature and humidity is highlighted in Figure 5.30. It is clear that when fresh, there is only one transition, however after seven days each of the samples of EPO 50% QHD DSC thermographs begins to resemble the original QHD thermograph shown in Figure 5.5. This therefore suggests that after storing the anhydrous form of quinine gets hydrated and as such the DSC trace resembles that of quinine hydrochloride dihydrate. Interestingly, EPO 50%QHD milled melt extrudate stored at 75% relative humidity and 40$^{o}$C appear to have made the most change towards resembling unprocessed QHD.

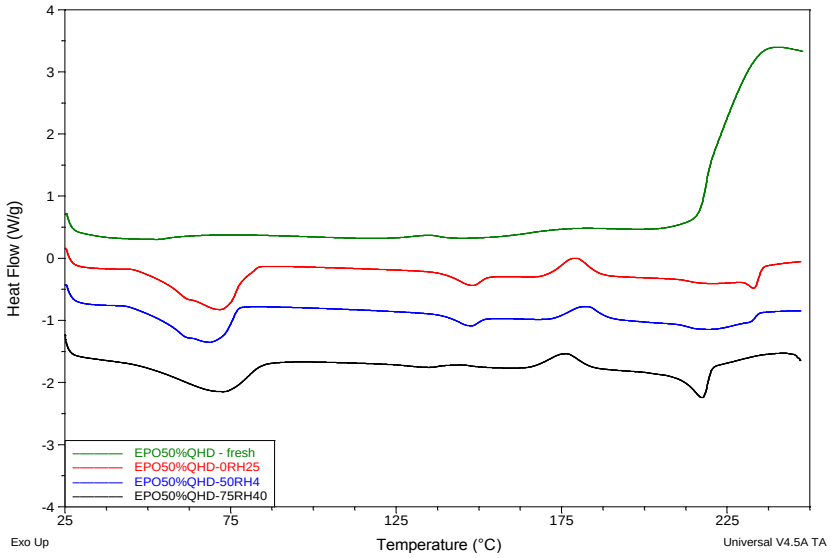


FIGURE 5. 30 TYPICAL DSC HEAT FLOW SIGNAL OF EUDRAGIT®EPO 50% QUININE HYDROCHLORIDE DIHYDRATE EXTRUDATES FOLLOWING STORAGE AT 0% RELATIVE HUMIDITY, 25$^{O}$C ( 0RH, 25$^{O}$C), 50% RELATIVE HUMIDITY, 4OC (50RH,4$^{O}$C) AND 75% RELATIVE HUMIDITY, 40$^{O}$C (75RH,40$^{O}$C) FOR SEVEN DAYS. HEATING RATE WAS 10$^{O}$C/MIN USING AN OPEN PAN.

The DSC analysis of the EPO 50% QHD physical mixtures are illustrated in Figure 5.31. It is apparent that the physical mixtures thermographs resemble those of the fresh samples. In essence, the stresses of humidity and temperature do not appear to change the thermal properties of the physical mixtures. This is not surprising because there is no chemical interaction between the polymer and quinine hydrochloride dihydrate and as such each individual component remains in the same state as it would be unprocessed.

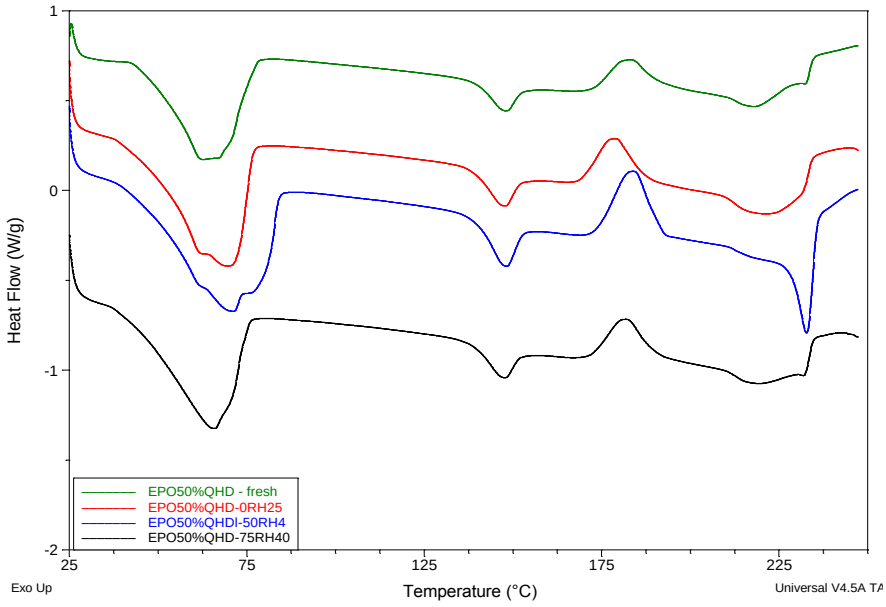


FIGURE 5. 31 TYPICAL DSC HEAT FLOW SIGNAL OF EUDRAGIT®EPO 50% QUININE HYDROCHLORIDE DIHYDRATE PHYSICAL MIXTURES FOLLOWING STORAGE AT 0% RELATIVE HUMIDITY, 25°C (0RH, 25°C), 50% RELATIVE HUMIDITY, 4°C (50RH,4°C) AND 75% RELATIVE HUMIDITY, 40°C (75RH,40°C) FOR SEVEN DAYS. HEATING RATE WAS 10°C/MIN USING AN OPEN PAN.

The DSC trace which examines the thermal behaviour of EPO50% melt extrudates after fourteen days of stress conditions of 0% relative humidity, 25°C is presented in Figure 5.32. The thermal behaviour of the melt extrudates does not deviate from that observed after seven days. It would appear that this anhydrous form of QHD is stable under these stress conditions at fourteen days.

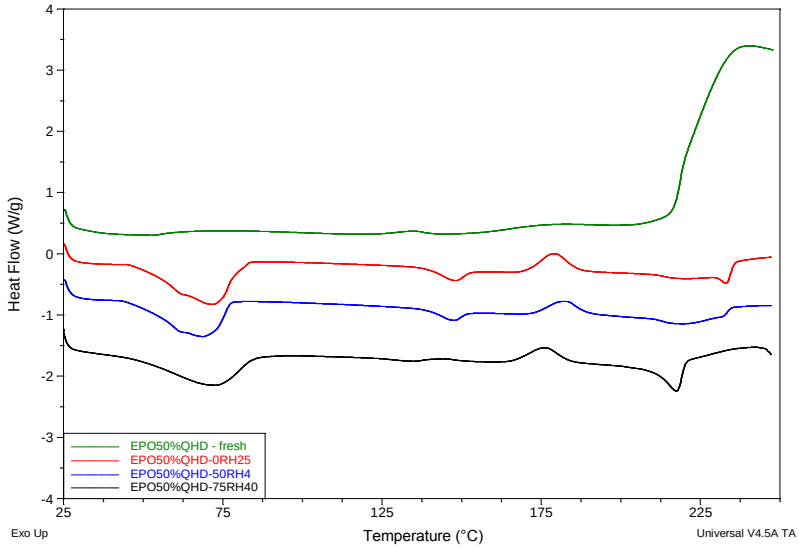


FIGURE 5. 32 TYPICAL DSC HEAT FLOW SIGNAL OF EUDRAGIT®EPO 50% QUININE HYDROCHLORIDE DIHYDRATE EXTRUDATES FOLLOWING STORAGE AT 0% RELATIVE HUMIDITY, 25°C ( 0RH, 25°C), 50% RELATIVE HUMIDITY, 4°C (50RH,4°C) AND 75% RELATIVE HUMIDITY, 40°C (75RH,40°C) FOR FOURTEEN DAYS. HEATING RATE WAS 10°C/MIN USING AN OPEN PAN.

A further thermal analysis using DSC was conducted on EPO50%QHD after twenty eight days of storage. The resultant DSC thermograph is shown in Figure 5.33. What is evident from these traces is that the EPO50%QHD exposed to stress conditions of 75% relative humidity and 40$^{o}$C shows a DSC trace similar to that of unprocessed quinine hydrochloride dihydrate with a distinguished melt endotherm with onset 208$^{o}$C.

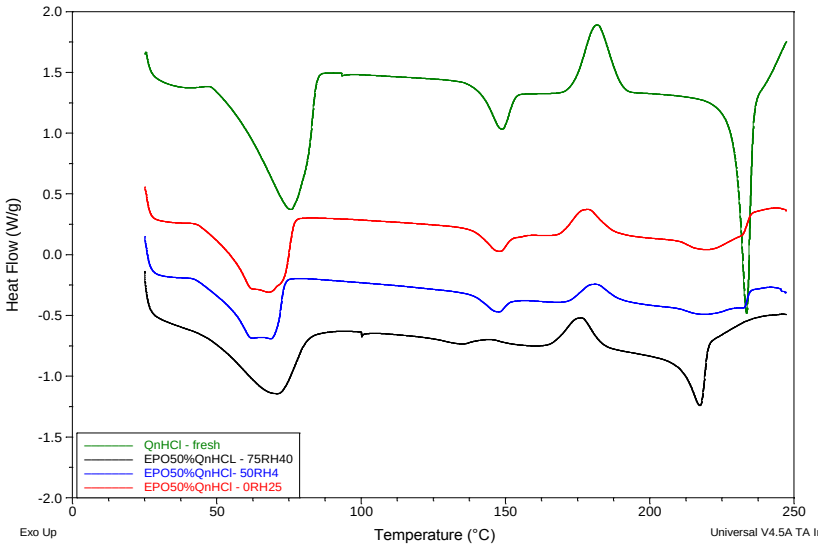


FIGURE 5. 33 TYPICAL DSC HEAT FLOW SIGNAL OF EUDRAGIT®EPO 50% QUININE HYDROCHLORIDE DIHYDRATE EXTRUDATES FOLLOWING STORAGE AT 0% RELATIVE HUMIDITY, 25$^{o}$C ( 0RH, 25$^{o}$C), 50% RELATIVE HUMIDITY, 4$^{o}$C (50RH,4$^{o}$C) AND 75% RELATIVE HUMIDITY, 40$^{o}$C (75RH,40$^{o}$C) FOR TWENTY DAYS. HEATING RATE WAS 10$^{o}$C/MIN USING AN OPEN PAN

The DSC thermographs of EPO 70%QHD melt extrudates after seven days of stresses of humidity and temperature are shown in Figure 5.34. It is clear that the exception of the sample exposed to 50% relative humidity, 4$^{o}$C, all the other retain an endotherm with onset 222$^{o}$C. However, sample that is exposed to 75% relative humidity and 40$^{o}$C temperature, shows an endotherm with onset temperature 102$^{o}$C, which has not been observed in any of the samples so far. In addition, the same sample shows an exothermic peak with onset temperature 158$^{o}$C. This endothermic peak corresponds to the exothermic peak observed for raw quinine hydrochloride dihydrate (Figure 5.5). Therefore, the sample exposed to 75% relative humidity, 40$^{o}$C reverts back to resemble untreated quinine hydrochloride.

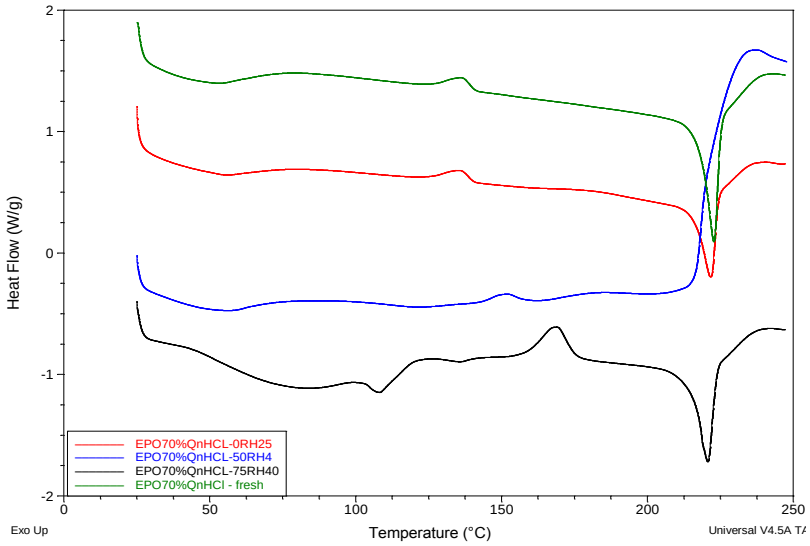


FIGURE 5. 34 TYPICAL DSC HEAT FLOW SIGNAL OF EUDRAGIT®EPO 70% QUININE HYDROCHLORIDE DIHYDRATE EXTRUDATES FOLLOWING STORAGE AT 0% RELATIVE HUMIDITY, 25°C ( 0RH, 25°C), 50% RELATIVE HUMIDITY, 4°C (50RH,4°C) AND 75% RELATIVE HUMIDITY, 40°C (75RH,40°C) FOR SEVEN DAYS. HEATING RATE WAS 10°C/MIN USING AN OPEN PAN

The corresponding DSC traces for EPO70%QHD physical mixtures after storage for seven days are shown in Figure 5.35. In short, the different stress conditions do not affect the thermal behaviour of QHD.

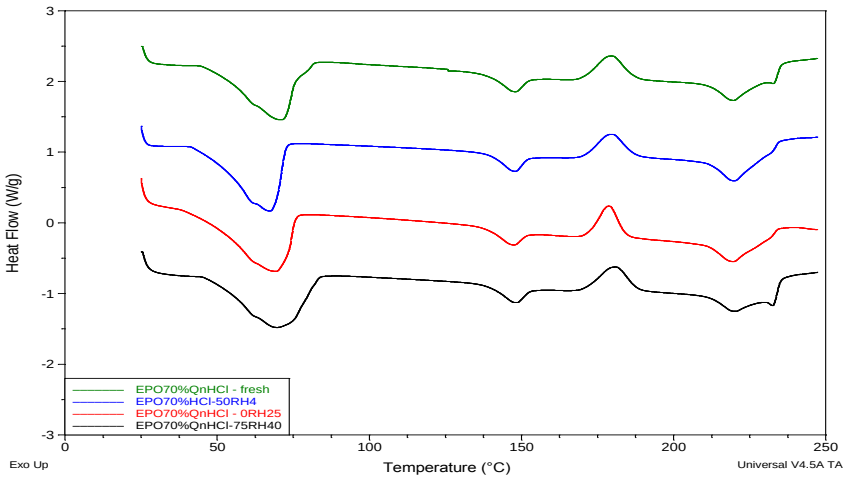


FIGURE 5. 35 TYPICAL DSC HEAT FLOW SIGNAL OF EUDRAGIT®EPO 70% QUININE HYDROCHLORIDE DIHYDRATE PHYSICAL MIXTURES FOLLOWING STORAGE AT 0% RELATIVE HUMIDITY, 25°C (0RH, 25°C), 50% RELATIVE HUMIDITY, 4°C (50RH,4°C) AND 75% RELATIVE HUMIDITY, 40°C (75RH,40°C) FOR SEVEN DAYS. HEATING RATE WAS 10°C/MIN USING AN OPEN PAN.

After fourteen and twenty eight days of storage, the EPO70% QHD melt extrudates DSC traces are shown in Figures 5.36 and 5.37 respectively. Both these figures serve

to illustrate that there is no change in thermal behaviour of QHD between fourteen and twenty eight days storage.

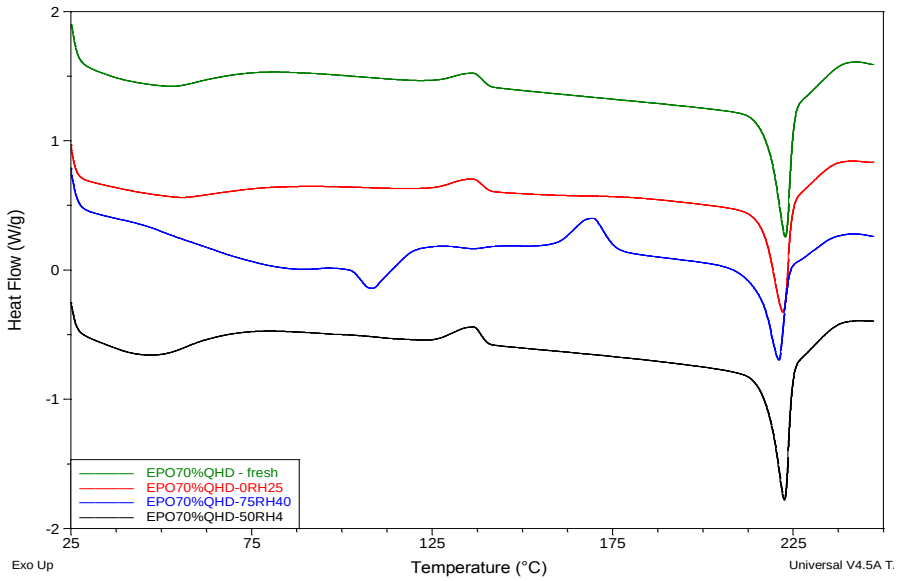


FIGURE 5. 36 TYPICAL DSC HEAT FLOW SIGNAL OF EUDRAGIT®EPO 70% QUININE HYDROCHLORIDE DIHYDRATE EXTRUDATES FOLLOWING STORAGE AT 0% RELATIVE HUMIDITY, 25°C ( 0RH, 25°C), 50% RELATIVE HUMIDITY, 4°C (50RH,4°C) AND 75% RELATIVE HUMIDITY, 40°C (75RH,40°C) FOR FOURTEEN DAYS. HEATING RATE WAS 10°C/MIN USING AN OPEN PAN.

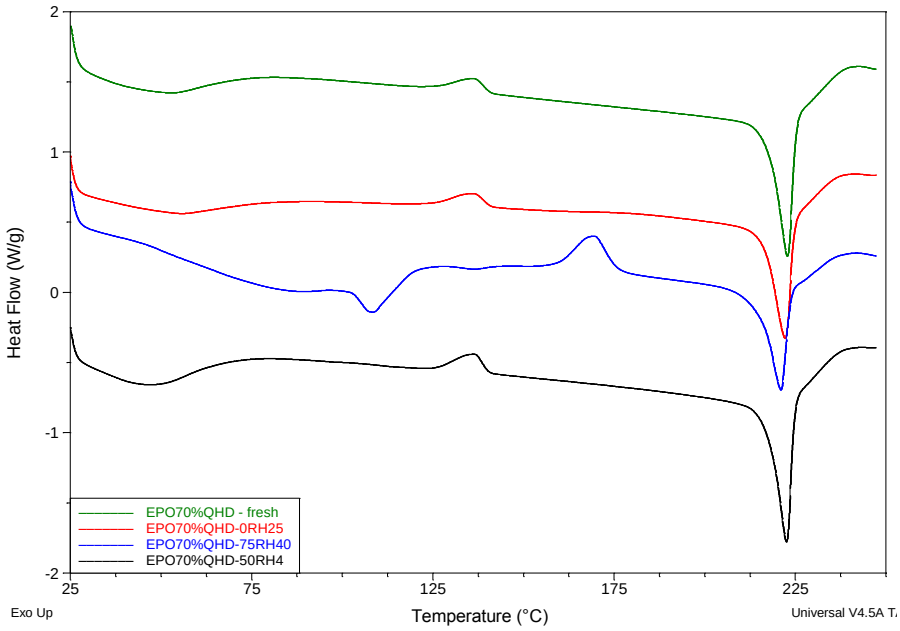


FIGURE 5. 37 TYPICAL DSC HEAT FLOW SIGNAL OF EUDRAGIT®EPO 70% QUININE HYDROCHLORIDE DIHYDRATE EXTRUDATES FOLLOWING STORAGE AT 0% RELATIVE HUMIDITY, 25°C (0RH, 25°C), 50% RELATIVE HUMIDITY, 4°C (50RH,4°C) AND 75% RELATIVE HUMIDITY, 40°C (75RH,40°C) FOR TWENTY EIGHT DAYS. HEATING RATE WAS 10°C/MIN USING AN OPEN PAN

## SUMMARY OF RESULTS

This section began by describing the DSC thermographs of Eudragit® EPO-QHD melt extrudates. Unsurprisingly, as the content of quinine hydrochloride increased in the melt extrudates the DSC traces begin to resemble that of pure quinine hydrochloride dihydrate. Just highlighting EPO70%QHD melt extrudates which shows a downward shift in the melt endotherm from 232$^{o}$C (pure quinine hydrochloride) to 222$^{o}$C. EPO30%QHD and EPO50%QHD also have a similar phenomenon both with melt endotherms at 205$^{o}$C. It is worth noting that the DSC traces of the melt extrudates differ remarkably from their corresponding physical mixtures. This is evidenced by the absence of the broad endotherm with onset 48$^{o}$C which signifies water loss. This analysis has shown that quinine hydrochloride exists as the anhydrous form after HME.

This section also investigated the effect of temperature, humidity and time on the melt extrudate powders with a view of assessing the stability of quinine hydrochloride in this formulation. The thermal analysis has revealed that at 30% drug loading there is no change in the thermal behaviour of quinine hydrochloride over twenty eight days despite exposure to different stress conditions. EPO50%QHD has a somewhat different behaviour in that when fresh, there is a marked absence of broad endotherm (onset 45$^{o}$C), which is ascribed to water loss. This is to say when fresh the anhydrous form of quinine hydrochloride is predominant in the melt extrudates. However, after seven days of exposure to stress conditions the quinine hydrochloride rehydrates and as such the broad endotherm (onset 45$^{o}$C) can be observed. In addition, after seven days the melt extrudate stored at 75% relative humidity and 40$^{o}$C shows a melt with onset 220$^{o}$C, which is not as apparent for the other stress conditions. This suggests that this stress condition seems to hasten the rehydration of quinine hydrochloride in the melt extrudate powders. Interestingly EPO70%QHD melt extrudate powders which were stored at 50% relative humidity and 4$^{o}$C, show a broad exotherm (onset 205$^{o}$C) and no subsequent melt endotherm. This would suggest that this sample is undergoing recrystallisation. When this sample was analysed after fourteen days, the absence of this broad endotherm is noted. It is instead replaced with an endotherm (onset 130$^{o}$C)

and a subsequent melt endotherm at 222°C which is in keeping with transitions that are observed for the samples stored at the other stress conditions. The analysis of the corresponding physical mixtures showed no changes with time, temperature or humidity

### 5.3.4.3 TASTE ASSESSMENT OF EUDRAGIT®EPO – QUININE HYDROCHLORIDE DIHYDRATE EXTRUDATES.

The third objective in this chapter was to assess the taste masking ability of the newly formulated EPO-QHD melt extrudates; this was assessed following method described in **chapter 2**. The release of quinine hydrochloride from the EPO-QHD melt extrudates in illustrated in Figure 5.38. There are a number of observations to note. Firstly, across of three drug-loading concentrations of EPO-QHD melt extrudates, there is less than 10% drug released in the first three minutes. In contrast, almost 90% of drug is detected in the absence of polymer. Secondly, there is no difference in the release profiles of the three drug loading EPO-QHD extrudates. Lastly, after two hours, only 60% of the drug is released. The significance of these findings will become apparent in **section 5.4.3**.

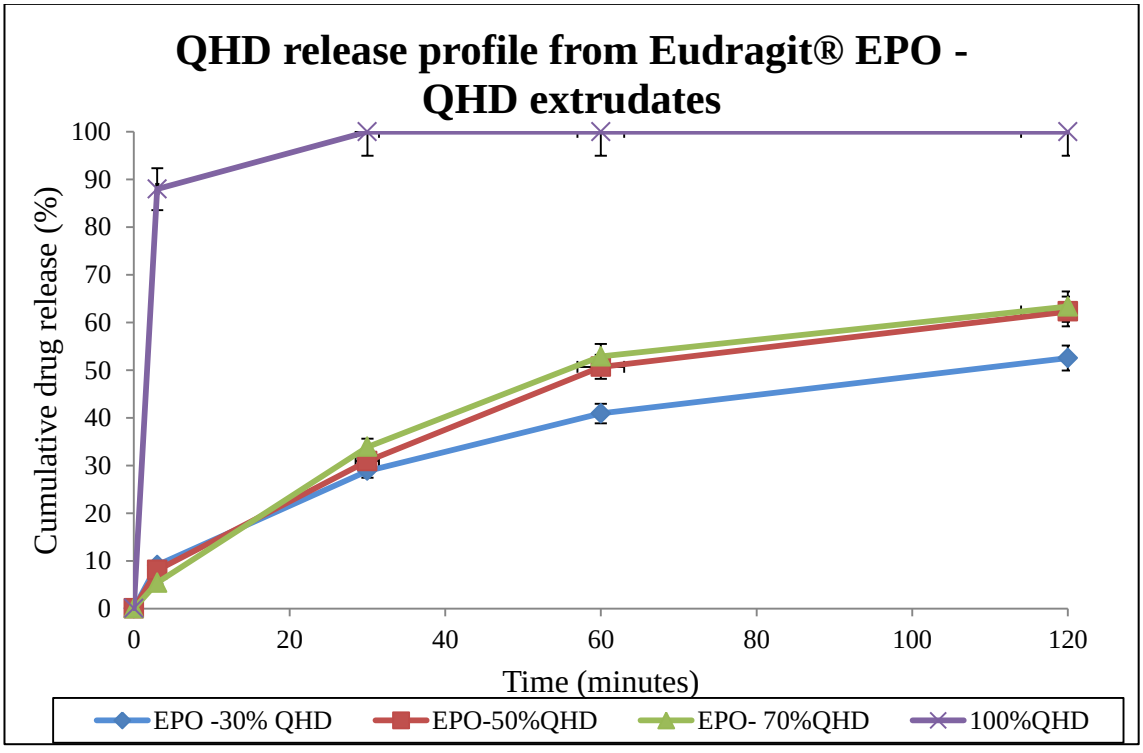


FIGURE 5. 38 HINDERED RELEASE OF QUININE HYDROCHLORIDE FROM TASTE MASKED EPO®-QHD MELT EXTRUDATES WITH DIFFERENT CONCENTRATION OF DRUG LOADING, 30, 50 AND 70% W/W.(N=3, $\bar{x}$±SD)

The detection of the quinine hydrochloride released from the melt extrudate was analysed using the Insent® TS5000Z electronic tongue. It is worth making it clear that the maximum concentration of quinine hydrochloride that could be released from the extrudates was set at 0.5mM (a concentration that has been shown is detectable on the electronic tongue and also measureable on the UV spectrometer). Sensor response curves for the increasing concentrations of QHD are shown in Figure 5.39. These reading were recorded after three minutes of shaking. The mark 0 in the *x*-axis represents de-ionised water. The concentration increase on the *x*-axis is that of quinine hydrochloride in the melt extrudates. Surprisingly, there is no statistical difference in sensor response curves with increasing concentrations of QHD i.e. 10, 30, 50 and 70% (one-way ANOVA, p=0.05). This suggests that the released quinine hydrochloride is not detectable on the electronic tongue. Since in **chapter 3**, it has already been shown that this molecule is detectable on the electronic tongue, the drug released is in concentration that are below the detection concentration of the electronic tongue.

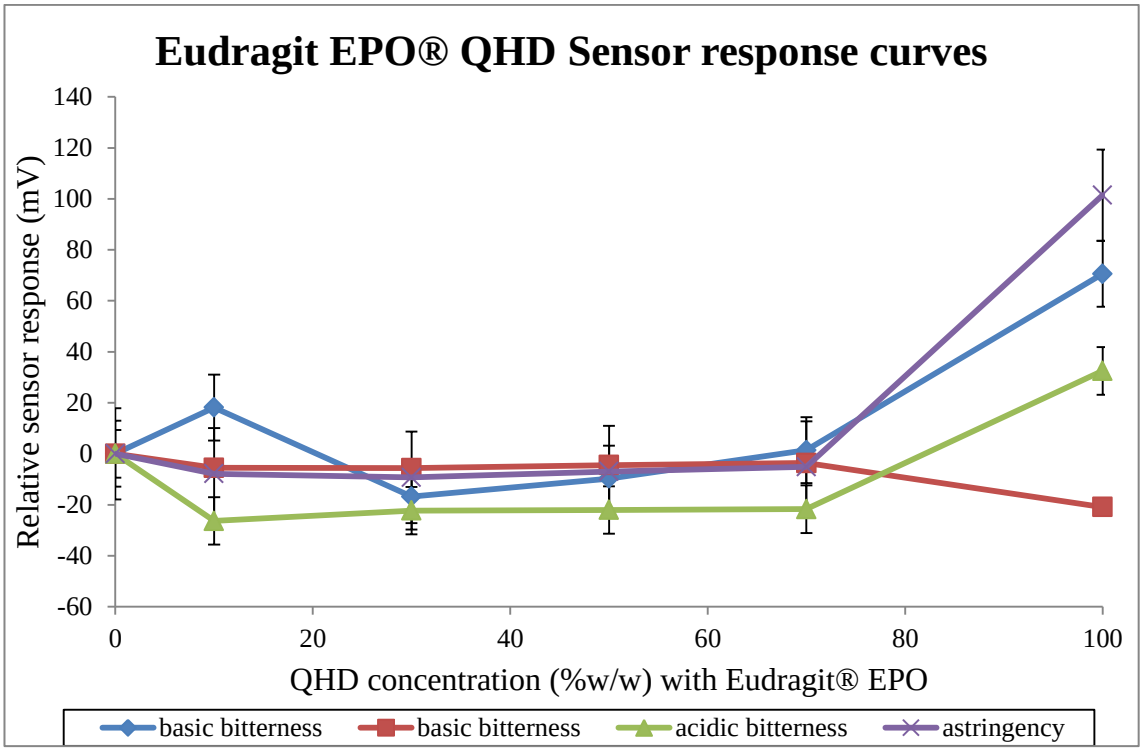


FIGURE 5. 39 RELATIVE SENSOR RESPONSE CURVE OF EPO50%QHD EXTRUDATES DISSOLVED IN DE-IONISED WATER, SHOWING SENSOR RESPONSES AS A FUNCTION OF CONCENTRATION (N=3, $\bar{x}$±SD).

In order to ascertain the taste masking effect of the extrusion process, it was necessary to investigate the release of quinine hydrochloride dihydrate from physical mixtures of Eudragit® EPO and quinine hydrochloride dihydrate. The drug release profiles are illustrated in Figure 5.40. Notably, the cumulative percentage release of drug in the first two minutes ranged from 10% to 20%. This was not statistically significant as illustrated by a one-way ANOVA (p= 0.97). However, after sixty minutes 90% of the QHD is released and detectable. This observation is statistically different, shown by a one-way ANOVA ($p = 4.96x\ 10^{-3}$) when compared to the melt extrudates.

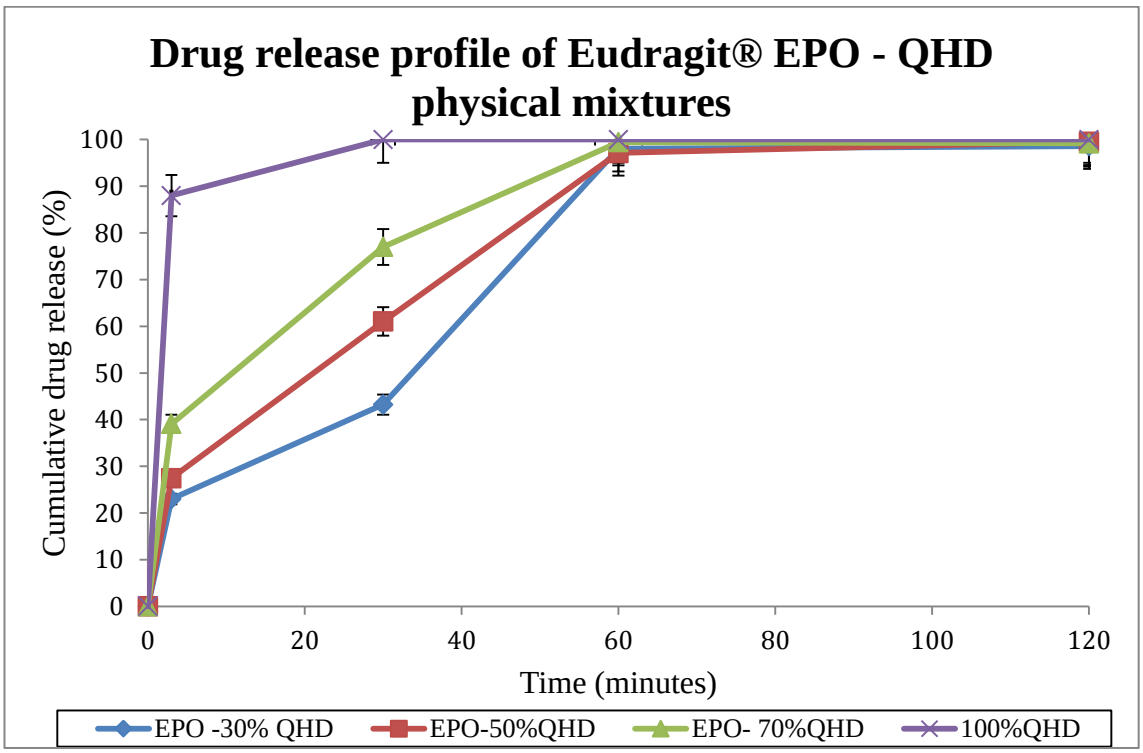


FIGURE 5. 40 RELEASE OF QUININE HYDROCHLORIDE FROM TASTE MASKED EPO®-QHD PHYSICAL MIXTURES WITH DIFFERENT CONCENTRATION OF DRUG LOADING, 30, 50 AND 70% W/W (N=3, $\bar{x}$±SD).

The EPO30%QHD extrudates were exposed to 0% relative humidity and 25°C for seven, fourteen and twenty eight days and the release profiles of the QHD from the extrudate powders is shown in Figure 5.41. The graph shows that there is no difference in the release profile of quinine hydrochloride from the melt extrudates. The stress condition and the ageing process appear not to affect the drug release profile.

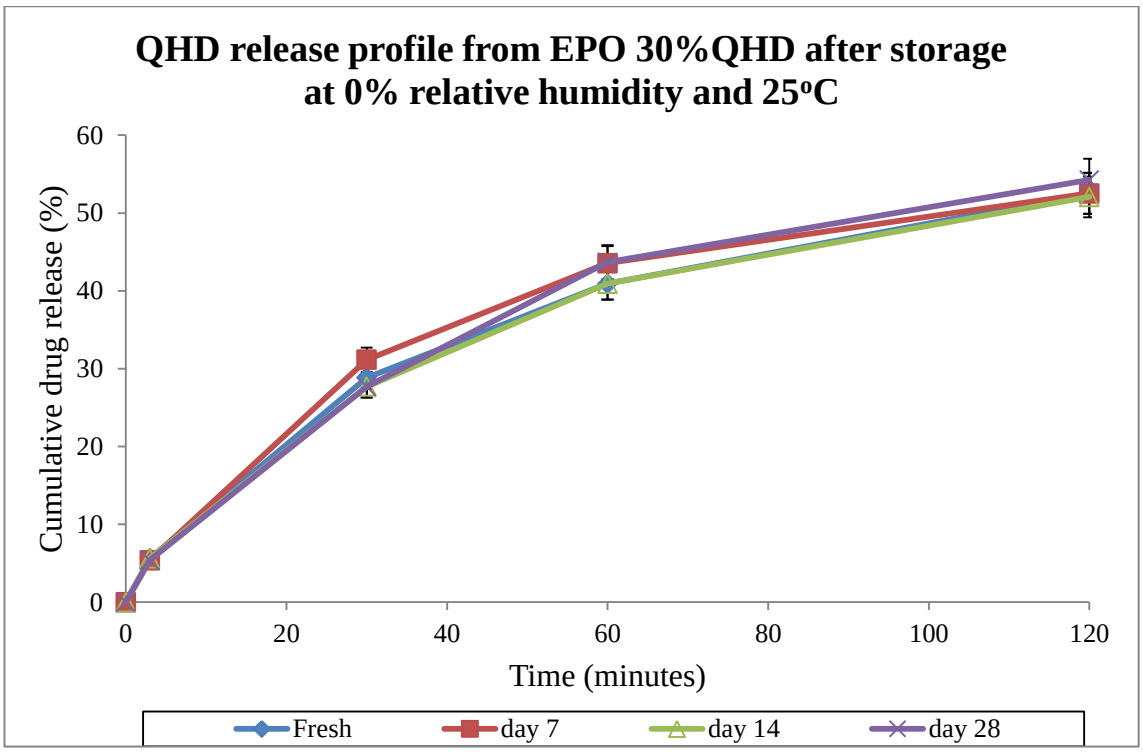


FIGURE 5. 41 RELEASE OF QUININE HYDROCHLORIDE FROM TASTE MASKED EPO® 30%QHD MELT EXTRUDATES AFTER STORAGE AT 0% RELATIVE HUMIDITY AND 25°C FOR SEVEN, FOURTEEN AND TWENTY EIGHT DAYS (N=3, $\bar{x}$±SD).

Eudragit®EPO 30%QHD melt extrudate were also stored at 50% relative humidity and 4°C and the release profile after seven, fourteen and twenty eight days is shown in Figure 5.42. What is clear from this graph is that under these stress conditions, the release profile of quinine from the melt extrudate also remains unchanged.

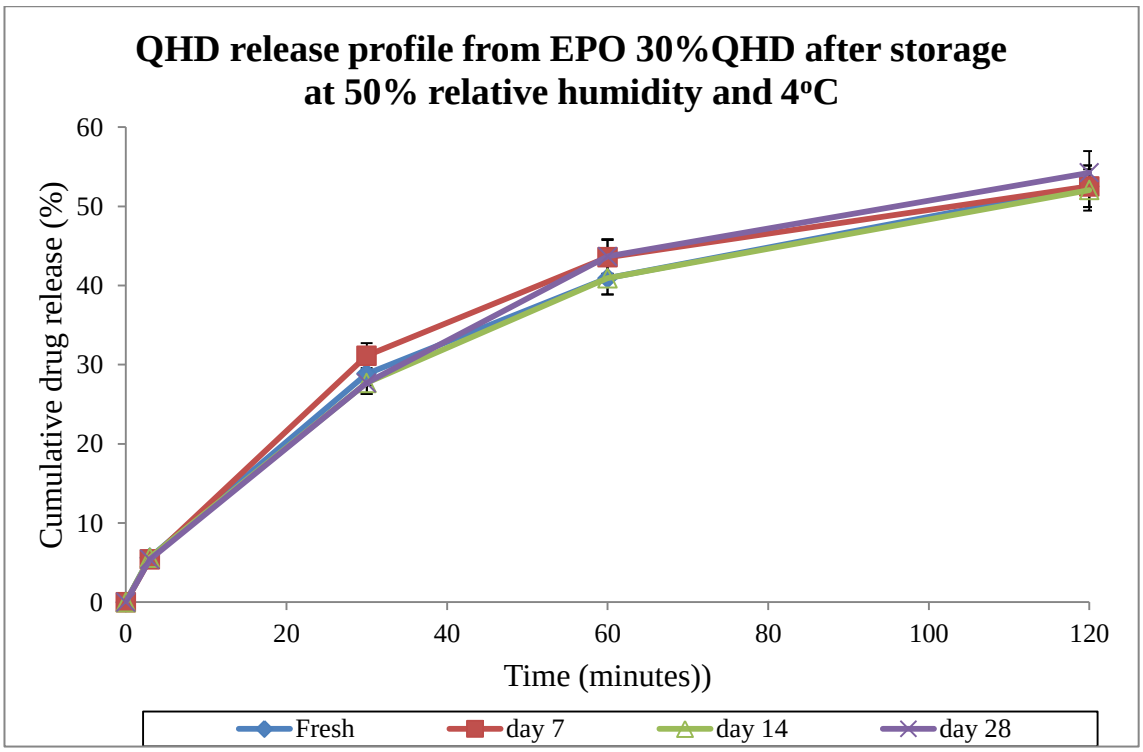


FIGURE 5. 42 RELEASE OF QUININE HYDROCHLORIDE FROM TASTE MASKED EPO® 30%QHD MELT EXTRUDATES AFTER STORAGE AT 50% RELATIVE HUMIDITY AND 4°C FOR SEVEN, FOURTEEN AND TWENTY EIGHT DAYS (N=3, $\bar{x}$±SD)

A similar analysis was conducted for EPO50%QHD melt extrudate powders after storing them under two stress conditions i.e. 0% relative humidity,25°C and 50% relative humidity,4°C for seven, fourteen and twenty eight days. Figure 5.43 shows the release profile of quinine hydrochloride when EPO50%QHD melt extrudate powders were exposed to 0% relative humidity, 25°C, while Figure 5.44 shows release after storage at 50% relative humidity, 4°C. In both cases the release profile of quinine hydrochloride remains unchanged across both time and stress condition hence suggesting that the EPO50%QHD melt extrudate remain stable for up to twenty eight days. This is in line with results shown from the thermal properties.

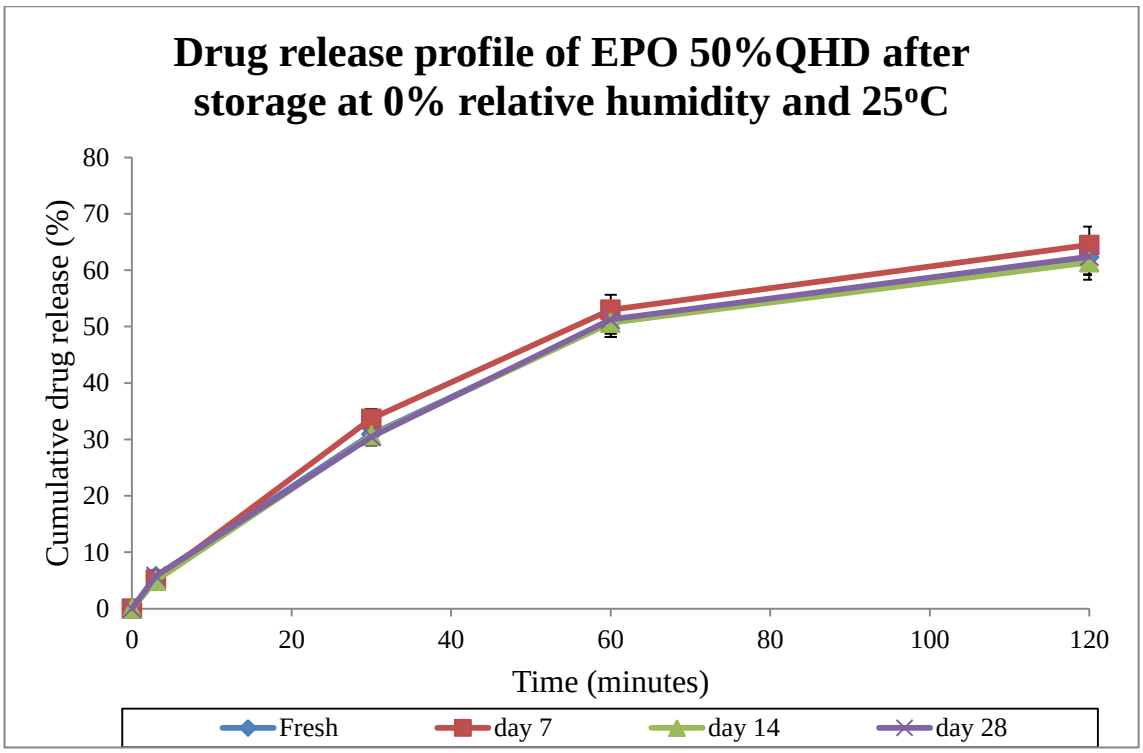


FIGURE 5. 43 RELEASE OF QUININE HYDROCHLORIDE FROM TASTE MASKED EPO® 50%QHD MELT EXTRUDATES AFTER STORAGE AT 0% RELATIVE HUMIDITY AND 25°C FOR SEVEN, FOURTEEN AND TWENTY EIGHT DAYS (N=3, $\bar{x}$±SD).

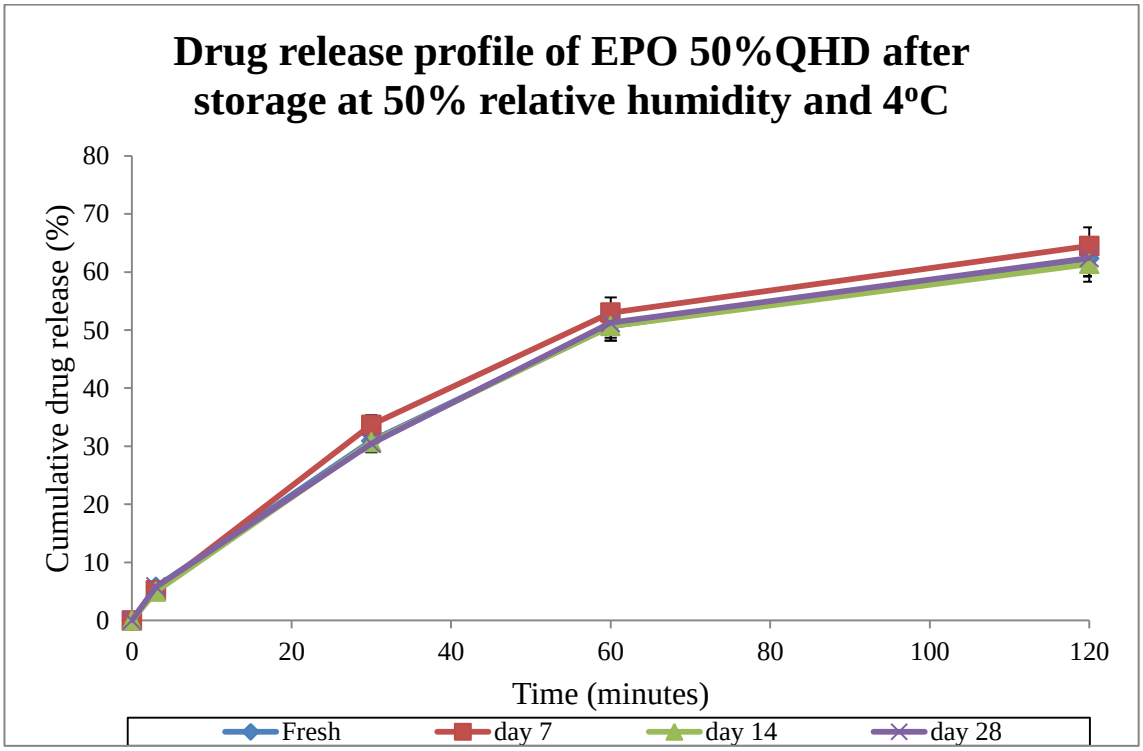


FIGURE 5. 44 RELEASE OF QUININE HYDROCHLORIDE FROM TASTE MASKED EPO® 50%QHD MELT EXTRUDATES AFTER STORAGE AT 50% RELATIVE HUMIDITY AND 4°C FOR SEVEN, FOURTEEN AND TWENTY EIGHT DAYS (N=3, $\bar{x}$±SD).

Figure 5.45 shows the release profile of quinine hydrochloride from EPO70%QHD melt extrudate powders after exposure to ageing conditions of time, temperature and humidity i.e. 0% relative humidity and 25°C. Notably, there is a 50% increase in the release of QHD after seven days, and expectedly this release rate continues through to twenty eight days. This is consistent with thermal analysis which showed that after seven days the thermal behaviour of EPO70%QHD largely mirrors that of unprocessed QHD. This difference is confirmed by a *one-way ANOVA* (*p= 8.28*).

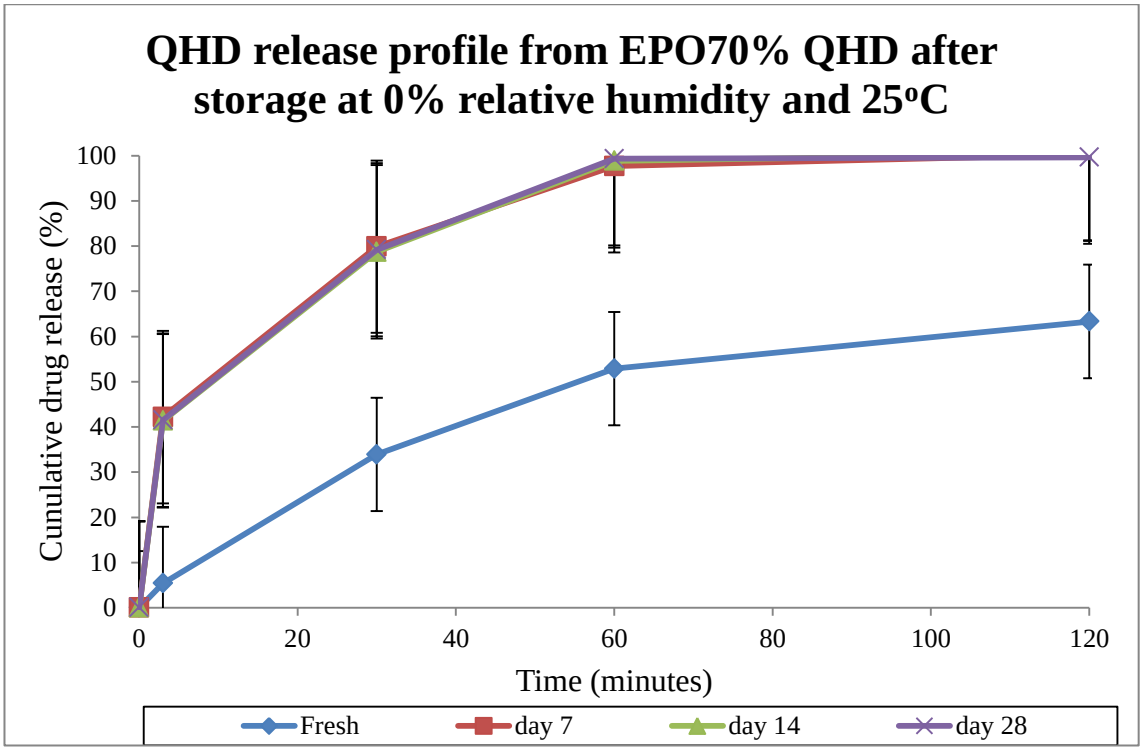


FIGURE 5. 45 RELEASE OF QUININE HYDROCHLORIDE FROM TASTE MASKED EPO® 50%QHD MELT EXTRUDATES AFTER STORAGE AT 0% RELATIVE HUMIDITY AND 25°C FOR SEVEN, FOURTEEN AND TWENTY EIGHT DAYS (N=3, $\bar{x}$±SD).

Similarly, the release profiles of quinine hydrochloride dihydrate from EPO70%QHD melt extrudates were analysed after they were stored at 50% relative humidity and 4°C for seven, fourteen and twenty eight days. The results of these release profiles are given in Figure 5.46. Interestingly, there is an approximate 50% increase in the release of QHD at day fourteen and twenty days in comparison to the fresh samples. At seven days, the release rate is similar to that of the fresh samples. This difference is statistically significant as evidenced by a *one-way ANOVA* (*p= 7.29*). What is even

more interesting is that in Table 5.6 DSC thermograph of EPO70%QHD stored at 50% relative humidity and 4°C suggests that QHD in this form is undergoing recrystallisation. In addition, it would appear at these conditions the relaxation of quinine hydrochloride is somewhat retarded. This is not evident in the release profile. An explanation for this observation is suggested in **section 5.4.3**.

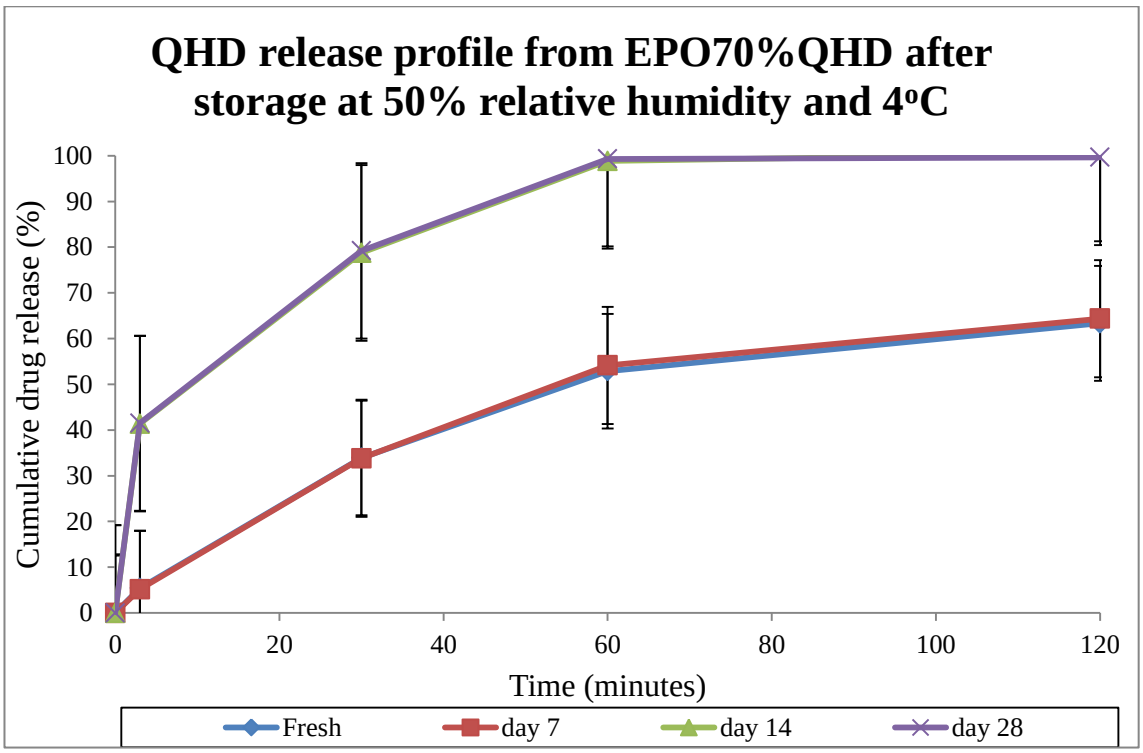


FIGURE 5. 46 RELEASE OF QUININE HYDROCHLORIDE FROM TASTE MASKED EPO® 50%QHD MELT EXTRUDATES AFTER STORAGE AT 50% RELATIVE HUMIDITY AND 4°C FOR SEVEN, FOURTEEN AND TWENTY EIGHT DAYS (N=3, $\bar{x}$±SD).

After 120 minutes, the solutions from EPO30%QHD and EPO50%QHD were then tested on the Insent TS500Z electronic tongue and the results are shown the Figures 5.47 and Figure 5.48 respectively. These figures show sensor response for each of the melt extrudates under the different stress conditions. What is worth noting is that a *one-way ANOVA* showed there is no statistically significant difference in sensor responses as samples were aged ($p= 1.11x10^{-15}$ and $p = 1.14x10^{-15}$ respectively).

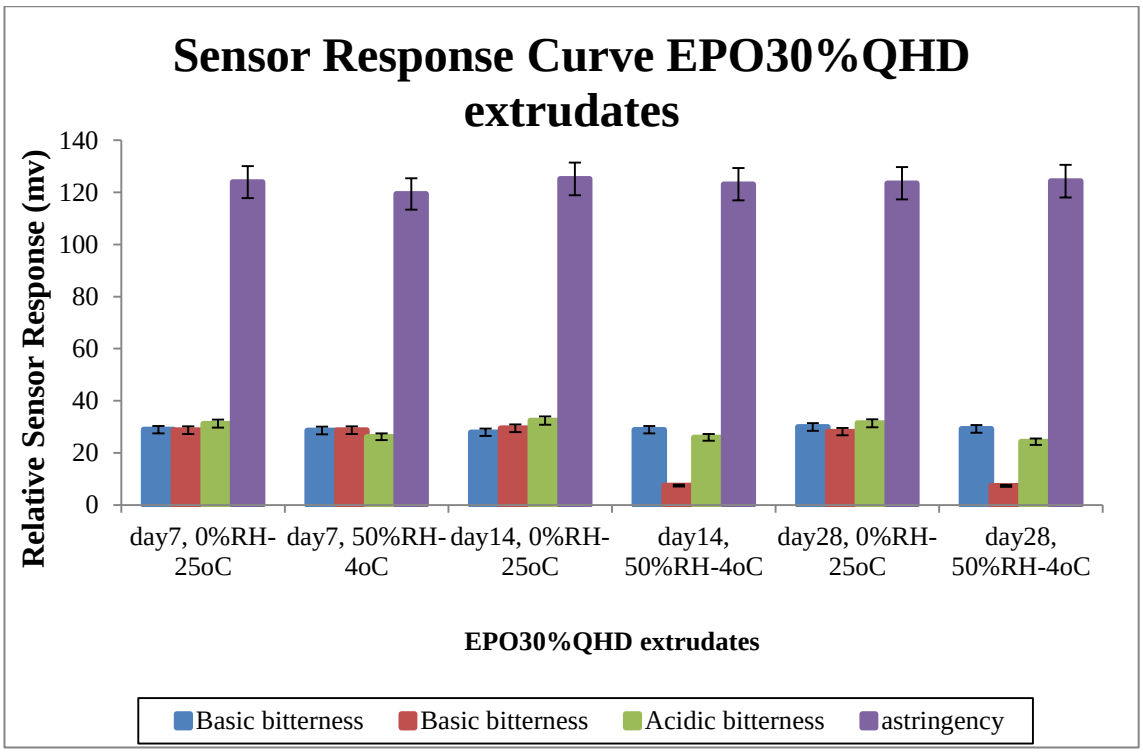


FIGURE 5. 47 RELATIVE SENSOR RESPONSE CURVE OF EPO50%QHD EXTRUDATES DISSOLVED IN DE-IONISED WATER, SHOWING SENSOR RESPONSES AS A FUNCTION OF CONCENTRATION (N=3, $\bar{x}$±SD).

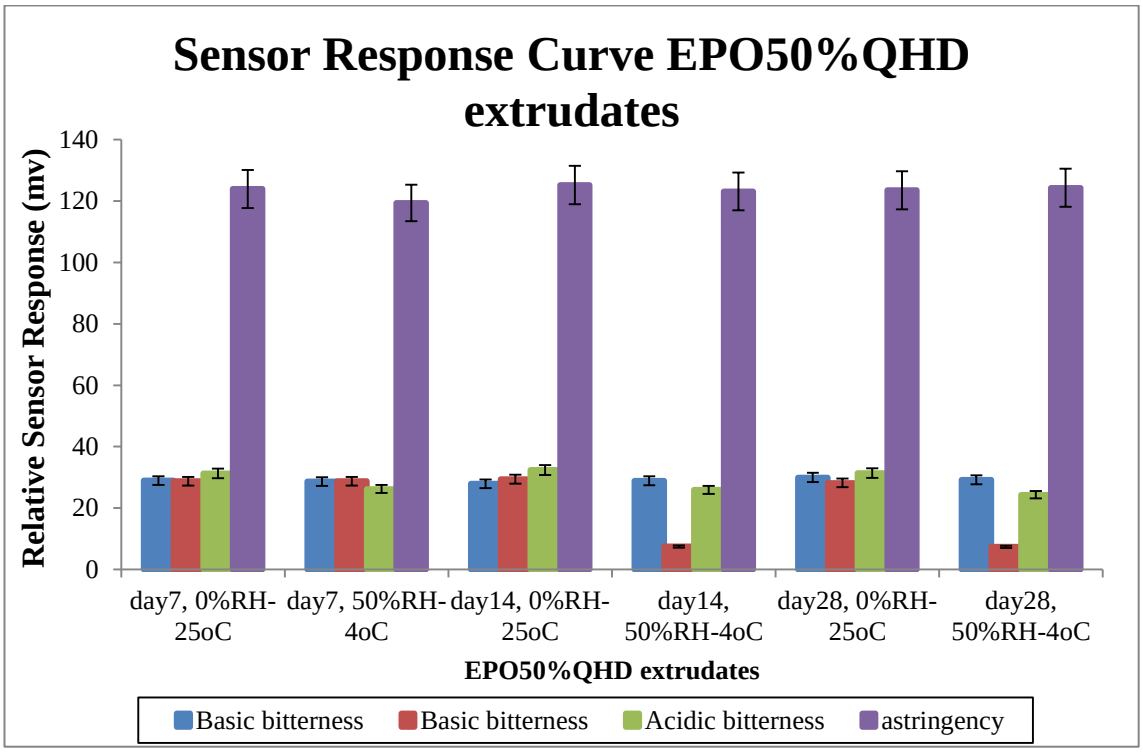


FIGURE 5. 48 RELATIVE SENSOR RESPONSE CURVE OF EPO50%QHD EXTRUDATES DISSOLVED IN DE-IONISED WATER, SHOWING SENSOR RESPONSES AS A FUNCTION OF CONCENTRATION (N=3, $\bar{x}$±SD).

The sensor response curve of EPO70%QHD melt extrudates after testing on the electronic tongue is shown in Figure 5.49. What is evident from this graph is that there is a clear dose response observed with the ageing of the samples. This is confirmed via a *one-way ANOVA* (*p= 0.73*). Contrary to the trends observed for EPO30% and 50% QHD melts extrudates, the release from EPO70%QHD is detectable on the electronic tongue.

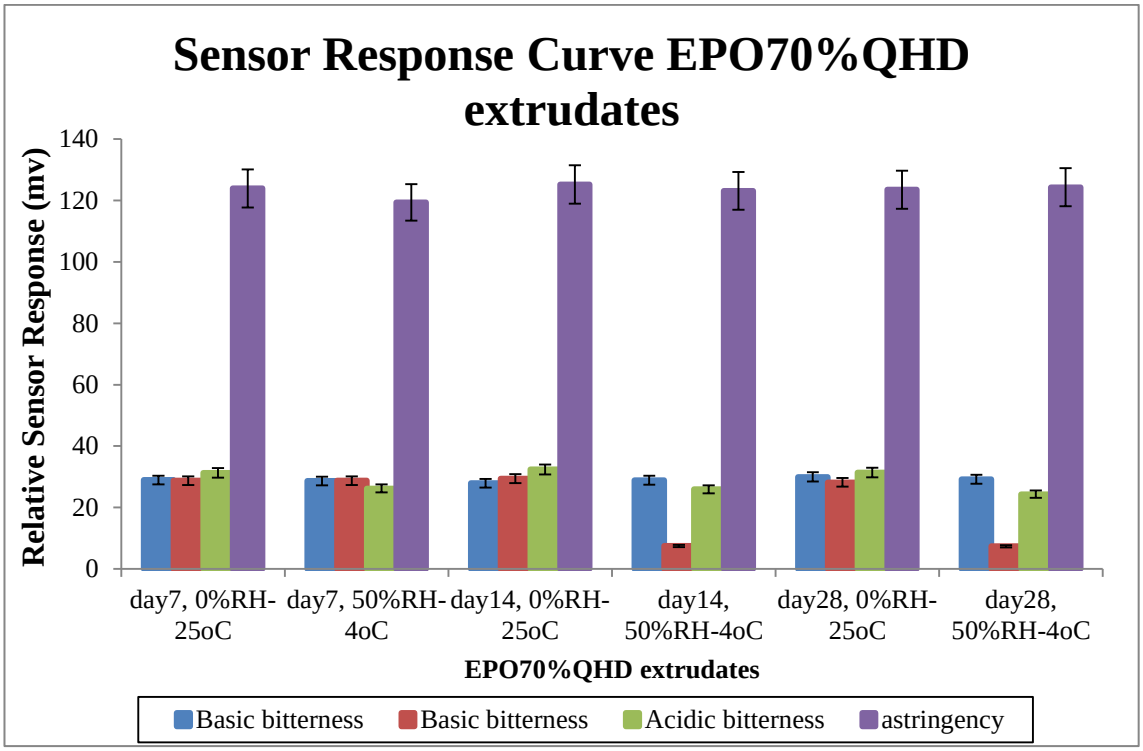


FIGURE 5. 49 RELATIVE SENSOR RESPONSE CURVE OF EPO70%QHD EXTRUDATES DISSOLVED IN DE-IONISED WATER, SHOWING SENSOR RESPONSES AS A FUNCTION OF CONCENTRATION (N=3, $\bar{x}$±SD).

## SUMMARY OF RESULTS

This section sought to describe the taste masking efficacy of the Eudragit®EPO melt extrudates using a modified dissolution apparatus in conjunction with spectrophotochemical analysis. The Insent® electronic tongue was also used as basis of comparison. The first major observation was that less than 10% of QHD was released from EPO30%QHD, EPO50%QHD and EPO70%QHD after three minutes. In comparison, the corresponding physical mixtures all released 10 -20% in the first three minutes of sampling. The EPOQHD melt extrudates had more than50% reduction on the release of QHD in comparison to the physical mixtures. 90% of QHD (in the

absence of polymer) was released within the first three minutes of sampling. What is also clear is that after two hours in the dissolution medium, up to 60% of QHD is released from the melt extrudates while 100% is released from the physical mixtures. Further analysis of the melt extrudates on the electronic tongue showed that there was no significant difference with increasing time. This suggests that even though QHD could be detected spectrophotochemically the amounts released were below the detection of the electronic tongue. This observation applied to EPO30%, 50% and 70% QHD.

Analysis of the release profiles of QHD from the melt extrudate after stress condition of temperature and humidity was also examined. The release profiles of QHD from EPO30%QHD and EPO50%QHD melt extrudates did not change with increasing time despite exposure to both 0% relative humidity, 25$^{o}$C and 50% relative, 4$^{o}$C. However, EPO70%QHD showed interesting behaviour. In the first instance, EPO70%QHD stored at 0% relative humidity and 25$^{o}$C showed a statistically significant release compared to fresh samples after seven days. This release was the same right through to twenty eight days. In contrast, EPO70%QHD stored at 50% relative humidity and 4$^{o}$C, showed similar release rates between the fresh samples and those analysed after seven days. The picture after fourteen days was statistically different as the melt extrudates' release rate mirrored that of the physical mixtures. In both cases, 100% of QHD was released at day twenty eight.

## 5.4 DISCUSSION

### 5.4.1 CHARACTERISATION OF QUININE HYDROCHLORIDE DIHYDRATE

The initial objective of the work described in this chapter was to characterise quinine (Qn), quinine hydrochloride dihydrate (QHD) and quinine hemisulphate dihydrate (QhS) with a view to describe the similarities and / or differences between the salts. The initial characterisation focussed on the crystallinity of the quinine and its salts. The PRXD diffractograms of quinine, quinine hydrochloride dihydrate and quinine

hemisulphate are given in Figures 5.1, 5.2 and 5.3 respectively. The first observation to report is that all quinine molecules show distinct peaks which therefore can be interpreted as being crystalline. The most prominent peak positions observed are $8^o$ for QHD and $18^o$ for Qn and QhSD. Quinine hydrochloride dihydrate has four other peaks at $12^o$, $18^o$, $22^o$ and $28^o$. Quinine also has four other peaks at $6^o$, $8^o$, $12^o$ and $20^o$. Quinine hemisulphate dihydrate has three other peaks at $8^o$, 22 and $26^o$. Based on these observations it can be concluded that all three quinine molecules are crystalline in nature.

Very little was found in the literature pertaining to the thermal characteristics of the quinine molecules. Hence in keeping with the objective to characterise quinine, quinine hydrochloride dihydrate and quinine hemisulphate dihydrate, their comparative DSC thermographs are shown in Figure 5.12. What is clear from this figure is that quinine only has one transition i.e. a melt with onset at $177^oC$. Quinine hydrochloride dihydrate and quinine hemisulphate dihydrate both exhibit a similar broad endotherm with onset at $45^oC$. The corresponding TGA analysis suggests that this endotherm corresponds to water loss. Quinine hemisulphate then shows one further transition corresponding to a melt with onset at $228^oC$. Quinine hydrochloride dihydrate show interesting thermal behaviour in that following on from the broad endotherm ascribed to water loss, it undergoes a melt (onset at $135^oC$), recrystallisation (onset at $171^oC$),melt (onset at $221^oC$). These transitions are observed on the DSC traces as well at the hot stage images shown in Figure 5.14. This was an unanticipated finding. Reports in the literature have stated that the melting point of quinine hydrochloride dihydrate was 115-$116^oC$. It is possible that the melting point reported in the literature refers the loss of water which has been illustrated by DSC, TGA and HSM. What is clear, especially via HSM is formation of a different crystal after the loss of water. In addition, it is also clear that the second crystal melts at temperature over $200^oC$. The most important finding in this analysis aided to selection of quinine hydrochloride dihydrate as model drug for

formulation of Eudragit® QHD extrudates. Quinine and quinine hemisulphate dihydrate were not suitable for this formulation because their melt onset were at 177$^{o}$C and 221$^{o}$C respectively, which would mean that processing temperatures would need to be excessively high i.e. approximately 190$^{o}$C and 230$^{o}$C. It is worth mentioning that at 180$^{o}$C Eudragit® EPO begins to burn, this is say it undergoes substantial discoloration. The TGA trace of Eudragit® EPO (Figure 5.31) shows a weight loss with onset approximately 178$^{o}$C, which could be ascribed to degradation. This observation has not been previously reported in the literature. Conversely, quinine hydrochloride dihydrate (QHD) had a melt with onset 135$^{o}$C therefore this provided the lowest possible processing temperature hence QHD was selected as model drug for extrusions. It also noteworthy to remind the reader that all three drug were detectable on the Insent® TS5000Z electronic tongue hence they were selected in the first instance.

As already alluded to, anhydrous quinine hydrochloride dehydrate melts and then recrystallizes. With this in mind the processing temperature for the hot melt extrusion was set at 140$^{o}$C. This was because at this temperature the anhydrous form of quinine hydrochloride is molten and this temperature is prior to the recrystallisation which has onset temperature at 171$^{o}$C. For Eudragit® EPO 70%QHD a processing temperature of 160$^{o}$C, this was because processing at 140$^{o}$C resulted in high torque values therefore temperature was increased negated this issue and additionally this temperature was below the onset of the recrystallisation.

With regards to the crystallinity of Qn, QhS and QHD, it is clear from the both the PXRD and SEM images that all the molecules are crystalline in nature. Interestingly, the positioning of the peaks on the PXRD diffractograms was similar across the three molecules, however the intensity differed. This significance of this is not apparent at this stage and is outside the scope of this study; however an investigation using crystallography techniques would offer substantial information particularly when comparing the native crystal with that formed following dehydration in the case of

quinine hydrochloride. Even more interesting would be to understand the crystal behaviour of the anhydrous form and how this influences its thermal properties particularly how easily it reverts back to the hydrated form.

### 5.4.2 CHARACTERISATION OF EUDRAGIT®EPO – QHD

The second objective of the work detailed in this chapter sought to characterise the form of quinine hydrochloride dihydrate present in the EPO-QHD melt extrudates. In addition to this an analysis of the miscibility between API and polymer is also described. An investigation into the thermal stability of this form was investigated. This was done by exposing each extrudate concentration to 0% relative humidity, 25$^{o}$C, 50% relative humidity, 4$^{o}$C and 75% relative humidity, 40$^{o}$C.

What is abundantly clear from the thermal analysis is that the low drug loading concentration i.e. EPO10%QHD is not affected by these stress conditions. On the other end of the spectrum, the EPO 70%QHD is vastly affected by the stress conditions, hence reverting back to hydrated form of quinine hydrochloride when tested after seven days. In addition, these powders congealed into a compact mass to the point where any downward investigations where not possible without further processing of the sample i.e. further grinding. In this study, this was not attempted because as highlighted in **chapter 2, section 2.4.3**, milling generates heat therefore this heat could alter the thermal character of the stored sample and as such give significantly different results. This limitation was more apparent for PXRD, were the holding pans for the Rigaku miniflex 600 required at least 1g of sample for processing. Therefore, future considerations could side step this limitation by casting in situ. This is to say, the samples for Eudragit® EPO70%QHD can be stored in the sample holders while under the stress conditions. Of course, caution needs to be taken to ensure that the sample holders (which are usually made from aluminium) do not degrade and interact with the samples to be investigated. An attempt was made to mount the congealed mass onto

the PXRD sample holder; however the resulting diffractogram showed that this ordering of the molecules was not detectable.

Another interesting observation is that fresh samples of EPO30%QHD, EPO50%QHD and EPO70%QHD have PXRD diffractograms that clearly show crystallinity. This observation has not been reported in the literature. In addition, exposure to stress conditions does not result in alteration in the crystallinity of all three EPO-QHD extrudates. DSC traces of these extrudates also confirm crystallinity. This is also supported by HSM. This result is encouraging in that it shows that at these concentrations the EPOQHD extrudates are stable for up to twenty eight days.

*ESTIMATION OF DRUG POLYMER MISCIBILITY*

The issue of thermodynamic miscibility between quinine hydrochloride dihydrate and Eudrgit® EPO can be predicted using the Hansen solubility parameters (δ) of drugs and polymer. This is calculated from their respective chemical structures using the van Krevelen and Hoftyzer methods described in Equations 5.1 and 5.2. The total solubility parameter ($\delta_t$) is determined from the interactions between dispersive forces ($\delta_d$), polar interaction ($\delta_p$) and hydrogen bonding ($\delta_h$) of the functional groups in the parent molecule divided by the molar volume (V). The units of solubility parameters are $MPa^{1/2}$.

$$\delta^2 = \delta_d^2 + \delta_p^2 + \delta_h^2$$

EQUATION 5.15

$$\delta = \sqrt{\left(\frac{\sum F_{di}}{V}\right)^2 \left(\frac{\sqrt{\sum F_{pi}^2}}{V}\right)^2 + \left(\sqrt{\frac{\sum E_{hi}}{V}}\right)^2}$$

EQUATION 5.16

where $F_{di}$, $F_{pi}$, and $E_{hi}$ are the group contribution of different components i.e. dispersive forces, polar interactions and hydrogen bonding respectively of the structural groups

reported in the literature. The Hansen solubility parameter (δ) for each component as reported in the literature is given in Table 5.10

TABLE 5 10 GROUP CONTRIBUTIONS TO HASSEN SOLUBILITY PARAMETERS FOR QUININE HYDROCHLORIDE DIHYDRATE AND EUDRAGIT®EPO(VAN KREVELEN *ET AL.* 2009A)

| **Molecule** | **Molecule component** | **Molar Volume($cm^3$/mol)** | **Hansen Solubility parameter δ (cal/mol)** |
|---|---|---|---|
| **Quinine hydrochloride dihydrate** | $CH_3$- | 33.5 | 1.125 |
| | -$CH_2$< | 16.1 | 1.18 |
| | -CH- | -1.0 | 820 |
| | >C< | -19.2 | 350 |
| | -OH | 10.0 | 7120 |
| | -O- | 3.8 | 800 |
| | N= | 4.5 | 2000 |
| | Cl- | 24.0 | 2760 |
| **Eudragit® EPO** | $CH_3$- | 33.5 | 1.125 |
| | -$CH_2$< | 16.1 | 1.180 |
| | N- | 6.7 | 5850 |
| | COO-ester | 18.0 | 4300 |

The drug-polymer parameter, χ, using the solubility parameters difference between the drug and the polymer, can be estimated as follows,

$$\chi = \frac{V_o}{RT}\left(\delta_{drug} - \delta_{polymer}\right)^2$$

EQUATION 5.17

where $V_o$ is the volume of the lattice site, R is the gas constant and T is the absolute temperature ($^oK$). The Hansen solubility parameter (δ) for each component, the difference between drug and polymer (Δδ) and the interaction parameter are given in Table 5.10. If drug and polymer have similar values of solubility parameter, i.e. Δδ < 7.0 $MPa^{1/2}$ they are more likely to be miscible. However, if Δδ > 10.0 $MPa^{1/2}$ this suggests that the compounds are more likely to be immiscible (Greenhalgh *et al.* 1999). Δδ = 3.7 therefore this implies that quinine hydrochloride dihydrate and Eudragit® EPO are miscible. If the drug-polymer parameter is closer to zero then this suggests greater interaction between drug and polymer (Van Krevelen *et al.* 2009b). In this case χ = 0.396 which is closer to zero therefore suggesting that there is interaction between drug and polymer. Results of these calculations are shown in Table 5.11.

TABLE 5 11 CALCULATED SOLUBILITY PARAMETERS AND INTERACTION PARAMETERS USING THE HANSEN GROUP CONTRIBUTION THEORY FOR QUININE HYDROCHLORIDE DIHYDRATE AND EUDRAGIT®EPO

| Compound | δ ($MPa^{1/2}$) | Δδ ($MPa^{1/2}$) | χ |
|---|---|---|---|
| **Quinine hydrochloride dihydrate** | 13.85 | 3.7 | 0.396 |
| **Eudragit®EPO** | 10.15 | | |

### 5.4.3 TASTE ASSESSMENT OF EUDRAGIT®EPO – QHD

The final objective of the work detailed in this chapter was to assess the taste masking effect of the EPO-QHD melt extrudates. A modified dissolution apparatus was used, the first modification was to reduce the volume of the dissolution medium. As previously illustrated the conventional 900ml volume is inappropriate for taste assessment as this volume mimics stomach contents rather that salivary volume in the oral cavity. 90ml was used in this study which was the minimum volume to allow for downward testing on both the electronic tongue and the UV spectrometer. Of course,

this volume is still not a true representative of volume present in the oral cavity, but is a step in the right direction towards making the volume used appropriate. De-ionised water was used as a solvent. Although, it could be argued that in order to mimic the oral cavity, then the solvent used should also mimic saliva. However, in **chapter 1**, it is highlighted that saliva is composite mixture of 99% water, salivary enzymes and buffering salts, which thus far has been difficult to formulate. In this study the use of de-ionised water is justified by the fact that a) water is the major constituent of saliva and b) use of buffering salts would affect the detection capability of the electronic tongue.

In this study in order to assess the taste masking efficiency of EPOQHD melt extrudates the concentration of drug release was measured initially at three minutes. This sampling time was chosen for practical operational reasons. Lee at al (2012) used a sampling time of two minutes while the FIP/AAPS guideline recommended five minutes. Since a single operator was operating the Incu® shaker, UV spectrophotometer and the Insent® electronic tongue, the sampling time was selected to allow a single operator to manage all three pieces of equipment simultaneously. According to FIP/AAPS taste masking guideline, a drug release of ≤ 10% within the first five minutes of dissolution indicates successful taste masking (Siewert *et al.* 2003a). The most clinically relevant finding from this study showed that the melt extrudates produced with drug loadings 30%, 50% and 70% all released 5.6%, 5.7% and 5.4% quinine hydrochloride respectively within the first three minutes. It is worth pointing out that although this guideline primarily addresses orodispersible preparations, it is the only guideline currently available in the literature relating to taste masking assessment. Therefore, the melt extrudates have demonstrated successful taste masking. This is further supported using the electronic tongue where the sensor responses are no statistically different to water when samples are tested after three minutes.

Another finding from the taste assessment showed that the EPO-30%QHD and EPO-50%QHD release profiles did not change with time, humidity or temperature. This observation mirrored the results also shown via PXRD diffractograms and DSC thermographs. EPO-70%QHD however had two different release profiles depending on the storage conditions. In the first instance when these melt extrudate were stored at 0% relative humidity and 25$^{o}$C, the release rate matched that of the physical mixtures after seven days thus releasing 18% QHD after three minutes. In contrast the EPO-70% QHD melt extrudate powders which were stored at 50% relative humidity and 4$^{o}$C released 5.6% after seven days, a percentage that similar to the fresh samples. However, after fourteen days, the amount of quinine hydrochloride released at the three minutes sampling time was similar to the physical mixture therefore releasing 41.4% quinine hydrochloride. It appears that when stored to 50% relative humidity and 4$^{o}$C, the EPO70%QHD is stable for up to seven days. At this stage it is unclear as to when the form of quinine hydrochloride reverts back to resemble its untreated counterpart because analysis was only done to day seven and day fourteen. Therefore, further investigation is required between those days to establish this.

A question that still remains to be discussed pertains to the relation between the crystalline nature of an API in a formulation and how that translates to taste masking ability of the same. The perception of the taste is dependent on the dissolution of the drug from the formulation. A literature review has looked at the issue of dissolution rate (Craig 2002). Essentially two mechanisms are identified. Carrier controlled and drug controlled systems. In the former, the dissolution rate of the drug is controlled by dissolution rate of the inert carrier which therefore implies the physical properties of the drug have no influence in the process. The other mechanism, drug –controlled dissolution so called because the dissolution rate is defined by the characteristics of the drug i.e size and physical form among others. In this study, the polymeric carrier used i.e. Eudragit®EPO is insoluble in water therefore it is highly unlikely that the

carrier controlled system is in play. Therefore, by default the dissolution mechanism is drug controlled. However, regardless of the dissolution mechanism, two factors are clearly important when discussing taste masking i.e. the proportion of API that is released within the residence time of the formulation within the oral cavity and the intrinsic taste of the API in question. At present, there is no consensus in the literature regarding both issues. A logical approach would suggest that the proportion of API released should vary in accordance with API. This is because each API has a difference detection threshold in humans. For example, human detection thresholds of quinine hydrochloride and caffeine are 0.0083±0.001mM and 1.2±0.12mM respectively (Keast *et al.* 2007). Therefore, the proportion of drug released should mirror the detection profile of the API. Using the example of the quinine and caffeine, quinine is one thousand time more detectable than caffeine which therefore 10% of quinine released should not be equated to 10% caffeine. This may not always be possible because unlike the APIs used in this study, in most cases the detection threshold of the drug under investigation is unknown. Therefore, it is reasonable to use 10% when considering in-vitro methods of taste assessment; however formulators should be prepared to adjust taste masking strategies when translating to human taste panel.

## 5.5 CONCLUSION

The thermal characterisation of quinine, quinine hydrochloride dihydrate and quinine hemisulphate dihydrate has shown that all three molecules are crystalline in nature. The first major finding from this analysis has shown that quinine hydrochloride dihydrate undergoes dehydration (range 48 – 102$^{o}$C). This is followed by melting of the anhydrous form which has onset at 135$^{o}$C. Recrystallisation occurs at onset temperature 168$^{o}$C, while the final melt has onset 232$^{o}$C. The dehydration, melt, recrystallisation and melt of quinine hydrochloride have not been reported in the literature. In addition, this finding contradicts previous reports in the literature which suggested that the melting point of quinine hydrochloride dihydrate was 115-116$^{o}$C.

The thermal behaviour of quinine and quinine hemisulphate dihydrate were both consistent with reports in the literature, although literature does not highlight the dehydration of quinine hemisulphate dihydrate. The implications of this finding indicate that were quinine hydrochloride dihydrate is being heat treated in order to form a solid dispersion, researchers need to be mindful of the resultant form of the quinine hydrochloride present in the solid dispersion as this study suggests that there are three different forms. A number of caveats are apparent from this study. The first one involves the issue examining the effect of different heating on formation of the anhydrous and subsequent forms of quinine hydrochloride. The other involves the characterisation of each of these forms using crystallography techniques with the aim of establishing the crystal habit similarities and differences if any between the forms of quinine hydrochloride dihydrate.

In addition to the characterisation of quinine and its salts, this study also characterised melt extrudates of Eudragit® EPO and quinine hydrochloride dihydrate. The most obvious finding to emerge from this study was that melt extrudate were successfully produced for 10, 30, 50 and 70% drug loadings. The freshly prepared 30% and 50% EPOQHD melt extrudate were shown to be crystalline and that the extrudate quinine hydrochloride existed in the dehydrated form. EPO70%QHD however reverted back to the hydrate after seven days of storage while the EPO30% and 50% remained dehydrated for up to twenty eight days. The PXRD diffractogram of EPO70%QHD did not match that of unprocessed QHD. This suggests that at the processing parameters used in this study EPO70%QHD may have a form that is different from that of pure quinine hydrochloride dihydrate. It is also clear that melt extrudates have different thermal behaviour in comparison to their physical mixture counterparts.

Another major objective of the work presented in this study was to analyse the taste masking efficacy of Eudragit®EPO quinine hydrochloride dihydrate extrudates in comparison to the same physical mixtures. The melt extrudates produced in this study all released ≤10% of quinine hydrochloride in the first three minutes of sampling. In addition the EPO-30% and 50% QHD melt extrudates continued to release less than 10% for up to and including twenty eight days. The EPO-70%QHD was only stable for fourteen days before the release profile began to match that of the physical mixtures. When analysing the fresh melt extrudates on the electronic tongue, there was no difference to the responses of water, therefore suggesting that the quinine hydrochloride was not detectable at these concentrations, therefore also suggesting successful taste masking.

# CHAPTER SIX
# CONCLUSIONS AND FUTURE WORK

# CHAPTER 6 – CONCLUSION AND FUTURE WORK

The publication of the European Paediatric Regulation (EC No. 1901/2006) that came into effect in January 2007 brought the taste and taste assessment to the forefront once again. This regulation requires the early submission of a pharmaceutical development plan for medicines: a paediatric investigation plan (PIP). The applicant is required to provide an overview of planned measures / performed studies of which taste masking and assessment are of particular relevance. Therefore, there has been an increased interest in the development of objective taste assessment methods. An overview of these taste assessment methods has been described in **chapter 1**. The main research objective presented here was to further the understanding of the mechanism of detection of the Insent electronic tongue TS 5000Z (a commercially available electronic tongue manufactured by Insent Japan). In addition, this research also set out to understand the utility of this electronic tongue in formulation development. Finally the taste masking efficacy of hot melt extrudates was assessed using the electronic tongue as well as UV spectrophotochemical techniques both of which are described in **chapter 2**.

Although the utility of electronic tongues in validating taste masking strategies is widely reported in the literature, very little is published concerning the mechanism of detection. The aim of the preliminary work detailed in **chapter 3** was to investigate the detection capability of the electronic tongue. The chapter detailed the investigation of the molecules with similar structures and demonstrated that caffeine, theobromine and theophylline were not detectable on this electronic tongue a finding which remains unpublished. In addition, the investigation of quinine, quinine hydrochloride dihydrate and quinine sulphate

revealed differences in sensor response for each molecule although they all possessed the same parent (quinine) molecule, another finding that is yet to be published. A comparison of the responses of quinine hydrochloride dihydrate and quinine sulphate to those of hydrochloric and sulphuric acid respectively, showed a similar pattern of response with a difference in magnitude. It was suggested that the difference observed can be attributed to the ionisation / dissociation profile of the API. Essentially, strong acids exhibit complete dissociation in solution therefore show a greater response on the electronic tongue and vice versa is true. The investigation of paracetamol and ibuprofen showed that these two APIs were not detected. In contrast, ibuprofen sodium and metformin hydrochloride were both detectable further supporting the ionisation/ dissociation profile theory. These findings have not been reported in the literature and furthermore, they contradict the adsorption theory suggested by Kobayashi et al 2010. However, they support the electro-chemical theory suggested by Woertz et al 2010 but further elucidates the understanding of the mechanism by also taking into consideration not only the molecule to be detected but also the solvent in which it is present.

A key concern that emerged during the course of the work detailed in **chapter 3** was the issue that the sensors registered a response for placebo including de-ionised water. The results from the work in **chapter 3** suggest that it is necessary to conduct sensor response studies using increasing concentrations of API under investigation. This is because the sensors are calibrated to record 0mV using a reference solution composed of 0.03mM tartaric acid and 3.0mM KCl (as per manufacturer's recommendation and design), therefore any other solution / solvent used would register a reading (mV) that would deviate from

this reference. That being the case, it is therefore important that sensor response curves be constructed initially in order to establish the true sensor response of the solution under investigation. Furthermore, during analysis the sensor response for the placebo should be accounted for. In **chapter 4** of this thesis, the placebo response has been subtracted from the overall response recorded therefore the responses reported only relate to API and excipients (if any).

The generalizability of these results is subject to certain limitations. For instance, although the study has successfully demonstrated that the detection mechanism is reliant on the ionisation / dissociation of the API and the solvent in which the API is dissolved, the issue of pH has not been fully explored. The pH of the resultant solutions was measured in order to allow for the use of the Henderson-Hasselbalch equation in order to understand the proportion of API that is ionised to that is unionised. Further research needs to examine more closely the impact of detection capability when the pH of the solution is varied because varying the pH of the solution will obviously affect the proportion of API that is ionised and that which is unionised. It goes without saying that this further experimentation needs to take into account that the use of any buffering solution to maintain pH may not only affect the API under investigation but the salts used to make buffer (which are generally ionic) will also be detectable. In addition to use of strong acids or strong alkali to obtain extremes of pH will not only affect sensor detection but may more than likely also affect sensor integrity since these are lipid based sensors. Therefore, care will need to be taken during the analysis to ensure that the sensor response under investigation only represents the tastant molecule rather than the buffering solution used as a

solvent. Caution will also need to be taken in order to maximise sensor integrity and this will not only affect detection capability but will also result increased consumable overheads.

In **chapter 4,** a “real life” application of the electronic tongue is presented in the form of an investigation of taste assessment of amlodipine (base), amlodipine besilate, maleate and mesilate using the electronic tongue. One of the more significant findings to emerge from this study is that the electronic tongue predominantly and consistently identifies astringency as the major descriptor of all the amlodipine salts. It would appear that amlodipine free base can be described in terms of basic and acidic bitterness while its salts are all described in terms of astringency. These findings are unique for several reasons. Firstly, this study has shown a difference in response patterns between amlodipine free base and its salts. It is clear the presence of cationic amlodipine and anionic besilate and maleate ions affects the detection profile, which further cements mechanism described in **chapter 3**. Secondly, the work reported in **chapter 4** has also shown that in addition to considering the dissociation profile of the salt forms, it is also important to consider the size of the resulting moieties. In the case where the cation is considerably larger than the corresponding anion, then more anions interact with the sensors therefore showing large response. Of course, this observation should be treated with caution because the interaction between the positively charged sensor and anions is an unusual occurrence in nature. This is to say that in nature most biological membranes are negatively charged therefore naturally expectation for positively charged ions would interact with them.

The third major observation from chapter 4 showed a difference in response patterns between the two negatively charged sensors, particularly when considering amlodipine free base. A clear reason could not be identified for this phenomenon which has not been reported this far. However, it is possible that the possibly different orientation of the lipids on the two sensors could be attributed to the difference in sensor response. With respect to the electronic tongue, the amlodipine besilate salt was identified as having the least palatability in comparison to the other amlodipine salts. Results from the electronic tongue showed that F1 formulations were the least palatable formulations, however, it was not possible to statistically distinguish between F2 and F3 formulations.

The final and most significant result reported in **chapter 4** is that a strong positive correlation was observed between the electronic tongue scores and those from the human taste panel when considering F1, F2 and F3 formulations of amlodipine besilate and mesilate. This finding adds to the limited body of evidence showing correlation between human taste and electronic tongue. Although this is a significant finding, these results need to be treated with caution as only amlodipine besilate and mesilate were investigated and furthermore a small sample size (n= 24) was used. Therefore, further research is required on different APIs and larger sample sizes in the human panels before suggestions that electronic tongue can replace human taste panels can be scientifically proven.

In **chapter 5**, the first objective was to characterise quinine, quinine hemisulphate dihydrate and quinine hydrochloride dihydrate using thermal

characterisation techniques with view of using this analysis to guide the selection of which quinine salt to use in the hot melt extrusion. The first major finding from this work showed that the quinine hydrochloride dihydrate had a number of transitions i.e. broad endotherm (onset 45$^{o}$C, ascribed to water loss), melt exotherm (onset 135$^{o}$C), recrystallisation exotherm (onset - 168$^{o}$C) and melt exotherm (onset 232$^{o}$C). This finding contradicts previous reports in the literature which suggested that the melting point of quinine hydrochloride dihydrate was 115-6$^{o}$C. This study adds to our knowledge on the dehydration of quinine hydrochloride dihydrate which is crucial particularly from a stability point of view. In addition the existence of a dehydrate form and subsequent melt and recrystallisation play a vital role in decision making with regards to temperature selection for the hot melt extrusion process. Other findings confirmed the melting points of quinine and quinine hemisulphate dihydrate to mirror those reported in the literature. It is important to note that quinine hemisulphate dihydrate also undergoes dehydration. Further work needs to be conducted on two fronts. The first one would focus on looking at the stability of dehydrate forms of quinine hemisulphate and quinine hydrochloride using crystallography techniques with a view of adding to our understanding of behaviour of hydrates and their dehydrate forms. Included in this could be explanations focussing the binding of water i.e. free water or otherwise. The second would zone in on the secondary form of quinine hydrochloride which is formed post melt and recrystallisation. Again, crystallography techniques could shed light on the identity of this crystal, which could potentially lead to identification of a novel crystal form of quinine hydrochloride.

Having decided to use quinine hydrochloride dihydrate as the API for producing melt extrudates using Eudragit®EPO, this study can report that it was possible to produce melt extrudates with drug loadings of 10%, 30%, 50% and 70% w/w. The next objective then set out to characterise these melt extrudates with a view of describing the form of quinine hydrochloride present in these extrudates. In addition, characterisation was conducted on melt extrudate powders after exposing them the stress of temperature, humidity and time. The work presented in **chapter 5, section 5.3.4.1 and 2** showed that it was possible to produce extrudate of Eudragit®EPO and quinine hydrochloride with drug loading at 10, 30, 50 and 70%. In addition, EPO10%, 30% and 50% QHD all demonstrated amorphous nature when analysed using PXRD. EPO70%QHD however showed crystallinity even when fresh. Interestingly, the PXRD diffractogram for EPO70%QHD did not match that of unprocessed hence suggesting the presence of the different crystal. This was mirrored by the DSC thermograph which showed a broad exotherm (onset 205$^{o}$C) ascribed to recrystallisation. This is a significant observation which remains to be published. Although, the identification of this crystal was not in the scope of this thesis, it would be interesting to do so and lead to reporting of a novel crystalline form of quinine hydrochloride. It is also worth noting that even though the generalised amorphous halo shown for 30 and 50% drug loading represents the amorphous nature of the polymer, however the drug remains crystalline as shown by the DSC thermographs and HSM images.

The final objective of **chapter 5** presented in **section 5**.was to assess the taste masking efficacy of the melt extrudates using a dissolution method designed to mimic the oral mucosa. The most clinically relevant finding from this study

showed that the melt extrudates produced with drug loadings 30%, 50% and 70% all released 5.6%, 5.7% and 5.4% quinine hydrochloride respectively within the first three minutes. The amount of drug released is less than 10% which is used as a benchmark in the AAPS/FIP taste masking guideline. It is worth pointing out that although this guideline primarily addresses orodispersible preparations, it is the only guideline currently available in the literature relating to taste masking assessment. Therefore, the melt extrudates have demonstrated successful taste masking. This is further supported using the electronic tongue where the sensor responses are not statistically different to water when samples are tested after three minutes.

Another finding from the taste assessment showed that the EPO30%QHD and EPO50%QHD release profiles did not change with time, humidity or temperature. This observation mirrored the results also shown via PXRD diffractograms and DSC thermographs. EPO70%QHD however had two different release profiles depending on the storage conditions. In the first instance when these melt extrudate were stored at 0% relative humidity and 25$^{o}$C, the release rate matched that of the physical mixtures after seven days thus releasing 18% QHD after three minutes. In contrast the EPO70% QHD melt extrudate powders which were stored at 50% relative humidity and 4$^{o}$C released 5.6% after seven days, a percentage that similar to the fresh samples. However, after fourteen days, the amount of quinine hydrochloride released at the three minutes sampling time was similar to the physical mixture therefore releasing 41.4% quinine hydrochloride. It appears that when stored to 50% relative humidity and 4$^{o}$C, the EPO70%QHD is stable for up to seven days. At this stage it is unclear as to when the form of quinine hydrochloride reverts back

to resemble its untreated counterpart because analysis was only done to day seven and day fourteen. Therefore, further investigation is required between those days to establish this

The work detailed in **chapter 5**, has highlighted that two factors are important when discussing taste assessment. These are **1)** the proportion of API that is released within the residence time of the formulation within the oral cavity and **2)** the intrinsic taste of the API in question. At present, there is no consensus in the literature regarding both issues. A logical approach would suggest that the proportion of API released should vary in accordance with API. This is because each API has a difference detection threshold in humans. For example, human detection thresholds of quinine hydrochloride and caffeine are 0.0083±0.001mM and 1.2±0.12mM respectively. Therefore, the proportion of drug released should mirror the detection profile of the API. Using the example of the quinine and caffeine, quinine is one thousand time more detectable than caffeine which therefore 10% of quinine released should not be equated to 10% caffeine. This may not always be possible because unlike the APIs used in this study, in most cases the detection threshold of the drug under investigation is unknown. Therefore, it is reasonable to use 10% when considering in-vitro methods of taste assessment; however formulators should be prepared to adjust taste masking strategies when translating to human taste panel.

# REFERENCES

Aframian D. J., Davidowitz T. and Benoliel R. (2006). "The distribution of oral mucosal ph values in healthy saliva secretors." Oral Diseases **12**(4): 420-423.

Aharoni S. M. (1998). "Increased glass transition temperature in motionally constrained semicrystalline polymers." Polymers for Advanced Technologies **9**(3): 169-201.

Ahmad M. N., Ismail Z., Chew O. S., Shafiqul Islam A. K. M. and Md Shakaff A. Y. (2006). "Development of multichannel artificial lipid-polymer membrane sensor for phytomedicine application." Sensors (Basel) **6**(10): 1333-1344.

Anand V., Kataria M., Kukkar V., Saharan V. and Choudhury P. K. (2007). "The latest trends in the taste assessment of pharmaceuticals." Drug Discov Today **12**(5–6): 257-265.

Aoki P. H. B., Caetano W., Volpati D., Riul Jr A. and Constantino C. J. L. (2008). "Sensor array made with nanostructured films to detect a phenothiazine compound." Journal of Nanoscience and Nanotechnology **8**(9): 4341-4348.

Aulton M. (2007). Aulton's pharmaceutics: The deisgn and manufacture of medicines, Churchill Livingstone Elsevier.

Baeuerle H. D. and Seelig J. (1991). "Interaction of charged and uncharged calcium channel antagonists with phospholipid membranes. Binding equilibrium, binding enthalpy, and membrane location." Biochemistry **30**(29): 7203-7211.

Behrens M., Brockhoff A., Kuhn C., Bufe B., Winnig M. and Meyerhof W. (2004). "The human taste receptor htas(2)r(14) responds to a variety of different bitter compounds." Biochemical and Biophysical Research Communications **319**(2): 479-485.

Beidler L. M. and Smallman R. L. (1965). "Renewal of cells within taste buds." The Journal of Cell Biology **27**(2): 263-272.

Bertolini A., Ferrari A., Ottani A., Guerzoni S., Tacchi R. and Leone S. (2006). "Paracetamol: New vistas of an old drug." CNS Drug Reviews **12**(3-4): 250-275.

Birch L. L. (1999). "Development of food preferences." Annual Review of Nutrition **19**: 41-62.

Bispo M. S., Veloso M. C. C., Pinheiro H. L. C., De Oliveira R. F. S., Reis J. O. N. and De Andrade J. B. (2002). "Simultaneous determination of caffeine, theobromine, and theophylline by high-performance liquid chromatography." Journal of Chromatographic Science **40**(1): 45-48.

## REFERENCES


Boltong A. and Campbell K. (2013). "'Taste' changes: A problem for patients and their dietitians." Nutrition & Dietetics **70**(4): 262-269.

Bose S. and Bogner R. H. (2007). "Solventless pharmaceutical coating processes: A review." Pharmaceutical Development and Technology **12**(2): 115-131.

Boughter J. D., St John S. J., Noel D. T., Ndubuizu O. and Smith D. V. (2002). "A brief-access test for bitter taste in mice." Chemical Senses **27**(2): 133-142.

Breitenbach J. (2002). "Melt extrusion: From process to drug delivery technology." European Journal of Pharmaceutics and Biopharmaceutics **54**(2): 107-117.

Breslin P. a. S. and Huang L. (2006). "Human taste: Peripheral anatomy, taste transduction, and coding." Taste and Smell: An Update **63**: 152-190.

Breslin P. a. S. and Spector A. C. (2008). "Mammalian taste perception." Current Biology **18**(4): R148-R155.

Bueno L. P. T. R. L. C. (2012). "A single platinum microelectrode for identifying soft drink samples." International Journal of Electrochemistry **2012**.

Bufe B., Breslin P. a. S., Kuhn C., Reed D. R., Tharp C. D., Slack J. P., Kim U. K., Drayna D. and Meyerhof W. (2005). "The molecular basis of individual differences in phenylthiocarbamide and propylthiouracil bitterness perception." Current Biology **15**(4): 322-327.

Bufe B., Hofmann T., Krautwurst D., Raguse J. D. and Meyerhof W. (2002). "The human tas2r16 receptor mediates bitter taste in response to beta-glucopyranosides." Nature Genetics **32**(3): 397-401.

Burleson W. R., Mantlo L. J., Self T. H. and Ryan M. R. (1978). "Taste preference test for oral liquid theophylline preparations." American Journal of Hospital Pharmacy **35**(5): 584-586.

Campbell K., Qi S., Craig D. Q. M. and Mcnally T. (2009). "Paracetamol-loaded poly(epsilon-caprolactone) layered silicate nanocomposites prepared using hot-melt extrusion." Journal of Pharmaceutical Sciences **98**(12): 4831-4843.

Cerea M., Zema L., Palugan L. and Gazzaniga A. (2008). "Recent developments in dry coating." Pharmaceutical Technology Europe **20**(2): 40-44.

Chandrashekar J., Hoon M. A., Ryba N. J. P. and Zuker C. S. (2006). "The receptors and cells for mammalian taste." Nature **444**(7117): 288-294.

## REFERENCES


Chandrashekar J., Mueller K. L., Hoon M. A., Adler E., Feng L., Guo W., Zuker C. S. and Ryba N. J. P. (2000). "T2rs function as bitter taste receptors." Cell **100**(6): 703-711.

Chaudhari N. and Roper S. D. (2010). "The cell biology of taste." The Journal of Cell Biology **190**(3): 285-296.

Ciosek P. and Wróblewski W. (2007). "Sensor arrays for liquid sensing - electronic tongue systems." Analyst **132**(10): 963-978.

Cowart B. J. (1981). "Development of taste perception in humans: Sensitivity and preference throughout the life span." Psychological Bulletin **90**(1): 43-73.

Craig D. Q. M. (2002). "The mechanisms of drug release from solid dispersions in water-soluble polymers." International Journal of Pharmaceutics **231**(2): 131-144.

Crowley M. M., Zhang F., Repka M. A., Thumma S., Upadhye S. B., Battu S. K., Mcginity J. W. and Martin C. (2007). "Pharmaceutical applications of hot-melt extrusion: Part i." Drug Development and Industrial Pharmacy **33**(9): 909-926.

Danilova V., Damak S., Margolskee R. F. and Hellekant G. (2006). "Taste responses to sweet stimuli in alpha-gustducin knockout and wild-type mice." Chemical Senses **31**(6): 573-580.

Devantier H. R., Long D. J., Brennan F. X., Carlucci S. A., Hendrix C., Bryant R. W., Salemme F. R. and Palmer R. K. (2008). "Quantitative assessment of trpm5-dependent oral aversiveness of pharmaceuticals using a mouse brief-access taste aversion assay." Behavioural Pharmacology **19**(7): 673-682.

Douroumis D. (2007). "Practical approaches of taste masking technologies in oral solid forms." Expert Opinion on Drug Delivery **4**(4): 417-426.

Eckert C., Pein M., Reimann J. and Breitkreutz J. (2013). "Taste evaluation of multicomponent mixtures using a human taste panel, electronic taste sensing systems and hplc." Sensors and Actuators B: Chemical **182**(0): 294-299.

El-Tawil S., Al Musa T., Valli H., Lunn M. P., El-Tawil T. and Weber M. (2010). "Quinine for muscle cramps." Cochrane Database Systematic Review(12): CD005044.

Evans J. S. O. and Radosavljevic Evans I. (2004). "Beyond classical applications of powder diffraction." Chemical Society Reviews **33**(8): 539-547.

Faulkner J. K., Mcgibney D., Chasseaud L. F., Perry J. L. and Taylor I. W. (1986). "The pharmacokinetics of amlodipine in healthy volunteers after single intravenous and oral doses and after 14 repeated oral doses given once daily." British Journal of Clinical Pharmacology **22**(1): 21-25.

## REFERENCES


Feng J., Xu L., Gao R., Luo Y. and Tang X. (2012). "Evaluation of polymer carriers with regard to the bioavailability enhancement of bifendate solid dispersions prepared by hot-melt extrusion." Drug Development & Industrial Pharmacy **38**(6): 735-743.

Finger T. E. (2005). "Cell types and lineages in taste buds." Chemical Senses **30**(suppl 1): i54-i55.

Fukunaga A., Uematsu H. and Sugimoto K. (2005). "Influences of aging on taste perception and oral somatic sensation." The Journals of Gerontology Series A: Biological Sciences and Medical Sciences **60**(1): 109-113.

Funasaki N., Uratsuji I., Okuno T., Hirota S. and Neya S. (2006). "Masking mechanisms of bitter taste of drugs studied with ion selective electrodes." Chemical and Pharmaceutical Bulletin **54**(8): 1155-1161.

Gao Y., Cui F.-D., Guan Y., Yang L., Wang Y.-S. and Zhang L.-N. (2006). "Preparation of roxithromycin-polymeric microspheres by the emulsion solvent diffusion method for taste masking." International Journal of Pharmaceutics **318**(1-2): 62-69.

Gibson J. and Beeley J. A. (1994). "Natural and synthetic saliva: A stimulating subject." Biotechnology and Genetic Engineering Reviews **12**: 39-61.

Gilbertson T. A. (1998). "Gustatory mechanisms for the detection of fat." Current,Opinion,in,Neurobiology **8**(4): 447-452.

Gittings S., Turnbull N., Roberts C. J. and Gershkovich P. (2014). "Dissolution methodology for taste masked oral dosage forms." Journal of Controlled Release **173**(0): 32-42.

Glendinning J. I., Gresack J. and Spector A. C. (2002). "A high-throughput screening procedure for identifying mice with aberrant taste and oromotor function." Chemical Senses **27**(5): 461-474.

Golenser J., Waknine J. H., Krugliak M., Hunt N. H. and Grau G. E. (2006). "Current perspectives on the mechanism of action of artemisinins." International Journal for Parasitology **36**(14): 1427-1441.

Golzi R., Boltri L. and Stollberg C. (2004). Microcapsules by coacervation containing a pharmaceutical incorporated in the coating polymer, Google Patents.

Greenhalgh D. J., Williams A. C., Timmins P. and York P. (1999). "Solubility parameters as predictors of miscibility in solid dispersions." Journal of Pharmaceutical Sciences **88**(11): 1182-1190.

Grisedale L. C., Jamieson M. J., Belton P. S., Barker S. A. and M. Craig D. Q. (2011). "Characterization and quantification of amorphous material in milled and spray-dried

salbutamol sulfate: A comparison of thermal, spectroscopic, and water vapor sorption approaches." Journal of Pharmaceutical Sciences **100**(8): 3114-3129.

Guhmann M., Preis M., Gerber F., Poellinger N., Breitkreutz J. and Weitschies W. (2012). "Development of oral taste masked diclofenac formulations using a taste sensing system." International Journal of Pharmaceutics **438**(1-2): 81-90.

Hayashi K., Yamanaka M., Toko K. and Yamafuji K. (1990). "Multichannel taste sensor using lipid-membranes." Sensors and Actuators B-Chemical **2**(3): 205-213.

Henrist D. and Remon J. P. (1999). "Influence of the process parameters on the characteristics of starch based hot stage extrudates." International Journal of Pharmaceutics **189**(1): 7-17.

Hetal P. (2014). Metformin tablets flim coating - sanofi aventis.

Hughes J. M., Li L., Chinn S. and Rona R. J. (1997). "Trends in growth in england and scotland, 1972 to 1994." Archives of Disease in Childhood **76**(3): 182-189.

Hui G. H., Mi S. S. and Deng S. P. (2012). "Sweet and bitter tastants specific detection by the taste cell-based sensor." Biosensors and Bioelectrics **35**(1): 429-438.

Hyde R. J. and Feller R. P. (1981). "Age and sex effects on taste of sucrose, nacl, citric acid and caffeine." Neurobiology of Aging **2**(4): 315-318.

Ito M., Ikehama K., Yoshida K., Haraguchi T., Yoshida M., Wada K. and Uchida T. (2013). "Bitterness prediction of h-1-antihistamines and prediction of masking effects of artificial sweeteners using an electronic tongue." International Journal of Pharmaceutics **441**(1-2): 121-127.

Jijun F., Lishuang X., Xiaoli W., Shu Z., Xiaoguang T., Xingna Z., Haibing H. and Xing T. (2011). "Nimodipine (nm) tablets with high dissolution containing nm solid dispersions prepared by hot-melt extrusion." Drug Development and Industrial Pharmacy **37**(8): 934-944.

Jones D. S. and Andrews G. P. (2010). "Cheminform abstract: Formulation and characterisation of hot melt extruded dosage forms: Challenges and opportunities." Chemical Informatics **41**(43): no-no.

Jones D. S., Margetson D. N., Mcallister M. S., Yu T., Shu L., Mccoy C. P. and Andrews G. P. (2014). "Thermodynamically stable amorphous drug dispersions in amorphous hydrophilic polymers engineered by hot melt extrusion." Chemical Engineering Research and Design **92**(12): 2046-2054.

Kalantzi L., Goumas K., Kalioras V., Abrahamsson B., Dressman J. B. and Reppas C. (2006). "Characterization of the human upper gastrointestinal contents under

conditions simulating bioavailability/bioequivalence studies." Pharmaceutical Research **23**(1): 165-176.

Kanny G., Hatahet R., Moneret-Vautrin D. A., Kohler C. and Bellut A. (1994). "Allergy and intolerance to flavouring agents in atopic dermatitis in young children." Allergie et Immunologie (Paris) **26**(6): 204-206, 209-210.

Karan M., Chadha R., Chadha K. and Arora P. (2012). "Identification, characterization and evaluation of crystal forms of quinine sulphate." Pharmacology & Pharmacy **3**: 129.

Kaufman L. and Rousseeuw P. J. (2009). Finding groups in data: An introduction to cluster analysis, John Wiley & Sons.

Kayitare E., Vervaet C., Mehuys E., Kayumba P. C., Ntawukulilyayo J. D., Karema C., Bortel V. and Remon J. P. (2010). "Taste-masked quinine pamoate tablets for treatment of children with uncomplicated plasmodium falciparum malaria." International Journal of Pharmaceutics **392**(1–2): 29-34.

Kayumba P. C., Huyghebaert N., Cordella C., Ntawukuliryayo J. D., Vervaet C. and Remon J. P. (2007). "Quinine sulphate pellets for flexible pediatric drug dosing: Formulation development and evaluation of taste-masking efficiency using the electronic tongue." European Journal of Pharmaceutics and Biopharmaceutics **66**(3): 460-465.

Kayumba P. C., Twagirumukiza M., Huyghebaert N., Ntawukuliryayo J. D., Van Bortel L., Vervaet C. and Remon J. P. (2008). "Taste-masked quinine sulphate pellets: Bio-availability in adults and steady-state plasma concentrations in children with uncomplicated plasmodium falciparum malaria." Annals of Tropical Paediatrics **28**(2): 103-109.

Keast R. S. J. and Roper J. (2007). "A complex relationship among chemical concentration, detection threshold, and suprathreshold intensity of bitter compounds." Chemical Senses **32**(3): 245-253.

Khan S., Kataria P., Nakhat P. and Yeole P. (2007). "Taste masking of ondansetron hydrochloride by polymer carrier system and formulation of rapid-disintegrating tablets." AAPS PharmSciTech **8**(2).

Knox C., Law V., Jewison T., Liu P., Ly S., Frolkis A., Pon A., Banco K., Mak C., Neveu V., Djoumbou Y., Eisner R., Guo A. C. and Wishart D. S. (2011). "Drugbank 3.0: A comprehensive resource for 'omics' research on drugs." Nucleic Acids Research **39**(suppl 1): D1035-D1041.

Kobayashi Y., Habara M., Ikezazki H., Chen R., Naito Y. and Toko K. (2010). "Advanced taste sensors based on artificial lipids with global selectivity to basic taste qualities and high correlation to sensory scores." Sensors (Basel) **10**(4): 3411-3443.

## REFERENCES


Kobayashi Y., Hamada H., Yamaguchi Y., Ikezaki H. and Toko K. (2009). "Development of an artificial lipid-based membrane sensor with high selectivity and sensitivity to the bitterness of drugs and with high correlation with sensory score." IEEJ Transactions on Electrical and Electronic Engineering **4**(6): 710-719.

Kojima T., Higashi K., Suzuki T., Tomono K., Moribe K. and Yamamoto K. (2012). "Stabilization of a supersaturated solution of mefenamic acid from a solid dispersion with eudragit® epo." Pharmaceutical Research **29**(10): 2777-2791.

Koyama N. and Kurihara K. (1972a). "Mechanism of bitter taste reception - interaction of bitter compounds with monolayers of lipids from bovine circumvallate papillae." Biochimica Et Biophysica Acta **288**(1): 22-&.

Koyama N. and Kurihara K. (1972b). "Mechanism of bitter taste reception: Interaction of bitter compounds with monolayers of lipids from bovine circumvallate papillae." Biochimica et Biophysica Acta (BBA) - Biomembranes **288**(1): 22-26.

Kuhn C., Bufe B., Winnig M., Hofmann T., Frank O., Behrens M., Lewtschenko T., Slack J. P., Ward C. D. and Meyerhof W. (2004). "Bitter taste receptors for saccharin and acesulfame k." Journal of Neuroscience **24**(45): 10260-10265.

Kurihara K. (1972). "Inhibition of cyclic 3′ , 5′ -nucleotide phosphodiesterase in bovine taste papillae by bitter taste stimuli." FEBS Letters **27**(2): 279-281.

Lagerlöf F. and Dawes C. (1984). "The volume of saliva in the mouth before and after swallowing." Journal of Dental Research **63**(5): 618-621.

Lawless H. T., Schlake S., Smythe J., Lim J., Yang H., Chapman K. and Bolton B. (2004). "Metallic taste and retronasal smell." Chemical Senses **29**(1): 25-33.

Lee J. H., Choi G., Oh Y. J., Park J. W., Choy Y. B., Park M. C., Yoon Y. J., Lee H. J., Chang H. C. and Choy J. H. (2012). "A nanohybrid system for taste masking of sildenafil." International Journal of Nanomedicine **7**: 1635-1649.

Legin A., Rudnitskaya A., Clapham D., Seleznev B., Lord K. and Vlasov Y. (2004). "Electronic tongue for pharmaceutical analytics: Quantification of tastes and masking effects." Analytical,and, Bioanalytical,Chemistry **380**(1): 36-45.

Li S., Jones D. S. and Andrews G. P. (2013). Hot melt extrusion: A process overview and use in manufacturing solid dispersions of poorly water-soluble drugs**:** 325-358.

Lurbe E., Cifkova R., Cruickshank J. K., Dillon M. J., Ferreira I., Invitti C., Kuznetsovah T., Laurent S., Mancia G., Morales-Olivas F., Rascher W., Redon J., Schaefer F., Seeman T., Stergiou G., Wuehl E. and Zanchetti A. (2009). "Management of high blood pressure in children and adolescents: Recommendations of the european society of hypertension." Journal,of,Hypertension **27**(9): 1719-1742.

## REFERENCES


Maniruzzaman M., Boateng J. S., Bonnefille M., Aranyos A., Mitchell J. C. and Douroumis D. (2012). "Taste masking of paracetamol by hot-melt extrusion: An in vitro and in vivo evaluation." European Journal of Pharmaceutics and Biopharmaceutics **80**(2): 433-442.

Maniruzzaman M., Bonnefille M., Aranyos A., Snowden M. J. and Douroumis D. (2014). "An in-vivo and in-vitro taste masking evaluation of bitter melt-extruded drugs." Journal of Pharmacy and Pharmacology **66**(2): 323-337.

Margetson D. N., Andrews G. P., Jones D. S. and Mcallister S. M. (2008). "Physico-chemical, rheological and drug-release characteristics of quinine and eudragit e100 prepared by hot-melt extrusion." Journal of Pharmacy and Pharmacology **60**: A47-A47.

Martin Alfred, Swarbrick James and Cammarata Arthur (1973). Physical pharmacy, Lea & Febiger.

Mattes R. D. (2011). "Accumulating evidence supports a taste component for free fatty acids in humans." Physiology & Behavior **104**(4): 624-631.

Mcburney D. H. and Gent J. F. (1979). "Nature of taste qualities." Psychological Bulletin **86**(1): 151-167.

Mennella J. A., Pepino M. Y. and Beauchamp G. K. (2003). "Modification of bitter taste in children." Developmental Psychobiology **43**(2): 120-127.

Milani G., Ragazzi M., Simonetti G. D., Ramelli G. P., Rizzi M., Bianchetti M. G. and Fossali E. F. (2010). "Superior palatability of crushed lercanidipine compared with amlodipine among children." British Journal of Clinical Pharmacology **69**(2): 204-206.

Miyazaki S., Kubo W., Itoh K., Konno Y., Fujiwara M., Dairaku M., Togashi M., Mikami R. and Attwood D. (2005). "The effect of taste masking agents on in situ gelling pectin formulations for oral sustained delivery of paracetamol and ambroxol." International Journal of Pharmaceutics **297**(1-2): 38-49.

Moffat J. G., Qi S. and Craig D. Q. M. (2014). "Spatial characterization of hot melt extruded dispersion systems using thermal atomic force microscopy methods: The effects of processing parameters on phase separation." Pharmaceutical Research **31**(7): 1744-1752.

Moribe K., Tozuka Y. and Yamamoto K. (2008). "Supercritical carbon dioxide processing of active pharmaceutical ingredients for polymorphic control and for complex formation." Advanced Drug Delivery Reviews **60**(3): 328-338.

Müller K., Figueroa C., Martínez C., Medel M., Obreque E., Peña-Neira A., Morales-Bozo I., Toledo H. and López-Solis R. O. (2010). "Measurement of saliva volume in the mouth of members of a trained sensory panel using a beetroot (beta vulgaris) extract." Food Quality and Preference **21**(5): 569-574.

## REFERENCES


Nahata M. C., Morosco R. S. and Hipple T. F. (1999). "Stability of amlodipine besylate in two liquid dosage forms." Journal of the American Pharmaceutical Association (Washington) **39**(3): 375-377.

Nakamura T., Tanigake A., Miyanaga Y., Ogawa T., Akiyoshi T., Matsuyama K. and Uchida T. (2002). "The effect of various substances on the suppression of the bitterness of quinine-human gustatory sensation, binding, and taste sensor studies." Chemical & Pharmaceutical Bulletin **50**(12): 1589-1593.

Ng K., Woo J., Kwan M., Sea M., Wang A., Lo R., Chan A. and Henry C. J. (2004). "Effect of age and disease on taste perception." J Pain Symptom Manage **28**(1): 28-34.

Nice. (2009). "The management of type 2 diabetes - cg87." Retrieved 31.04., 2014, from http://www.nice.org.uk/nicemedia/live/12165/44320/44320.pdf.

O'loughlin G. and Shanley C. (1998). "Swallowing problems in the nursing home: A novel training response." Dysphagia **13**(3): 172-183.

Oakley B. (1985). "Taste responses of human chorda tympani nerve." Chemical Senses **10**(4): 469-481.

Pearnchob N., Siepmann J. and Bodmeier R. (2003). "Pharmaceutical applications of shellac: Moisture-protective and taste-masking coatings and extended-release matrix tablets." Drug Development and Industrial Pharmacy **29**(8): 925-938.

Pickenhagen W., Dietrich P., Keil B., Polonsky J., Nouaille F. and Lederer E. (1975). "Identification of the bitter principle of cocoa." Helvetica Chimica Acta **58**(4): 1078-1086.

Pioggia G., Di Francesco F., Marchetti A., Ferro M. and Ahluwalia A. (2007a). "A composite sensor array impedentiometric electronic tongue part i. Characterization." Biosens Bioelectron **22**(11): 2618-2623.

Pioggia G., Di Francesco F., Marchetti A., Ferro M., Leardi R. and Ahluwalia A. (2007b). "A composite sensor array impedentiometric electronic tongue part ii. Discrimination of basic tastes." Biosensors and Bioelectronics **22**(11): 2624-2628.

Plomin R. and Mcclearn G. (1993). Nature, nurture and psychology. Nature and nurture: Perspective and prospective. R. Plomin and G. McClearn. Washington DC, Americal Psychological Association**:** 459-485.

Preis M., Pein M. and Breitkreutz J. (2012). "Development of a taste-masked orodispersible film containing dimenhydrinate." Pharmaceutics **4**(4): 551-562.

Preis M., Woertz C., Kleinebudde P. and Breitkreutz J. (2013). "Oromucosal film preparations: Classification and characterization methods." Expert Opinion on Drug Delivery **10**(9): 1303-1317.

## REFERENCES


Price S. (1973). "Phosphodiesterase in tongue epithelium - activation by bitter taste stimuli." Nature **241**(5384): 54-55.

Qi S., Belton P., Nollenberger K., Clayden N., Reading M. and Craig D. Q. M. (2010a). "Characterisation and prediction of phase separation in hot-melt extruded solid dispersions: A thermal, microscopic and nmr relaxometry study." Pharmaceutical Research **27**(9): 1869-1883.

Qi S., Deutsch D. and Craig D. Q. M. (2008a). "An investigation into the mechanisms of drug release from taste-masking fatty acid microspheres." Journal of Pharmaceutical Sciences **97**(9): 3842-3854.

Qi S., Gryczke A., Belton P. and Craig D. Q. M. (2008b). "Characterisation of solid dispersions of paracetamol and eudragit (r) e prepared by hot-melt extrusion using thermal, microthermal and spectroscopic analysis." International Journal of Pharmaceutics **354**(1-2): 158-167.

Qi S., Gryczke A., Belton P. and Craig D. Q. M. (2008c). "Characterisation of solid dispersions of paracetamol and eudragit® e prepared by hot-melt extrusion using thermal, microthermal and spectroscopic analysis." International Journal of Pharmaceutics **354**(1-2): 158-167.

Qi S., Marchaud D. and Craig D. Q. M. (2010b). "An investigation into the mechanism of dissolution rate enhancement of poorly water-soluble drugs from spray chilled gelucire 50/13 microspheres." Journal of Pharmaceutical Sciences **99**(1): 262-274.

Reed D. R., Tanaka T. and Mcdaniel A. H. (2006). "Diverse tastes: Genetics of sweet and bitter perception." Physiology & Behavior **88**(3): 215-226.

Reid A. W. and Becker C. H. (1956). "The use of cocoa syrups for masking the taste of quinine hydrochloride." Journal of the American Pharmaceutical Association **45**(3): 151-152.

Repka M. A., Battu S. K., Upadhye S. B., Thumma S., Crowley M. M., Zhang F., Martin C. and Mcginity J. W. (2007). "Pharmaceutical applications of hot-melt extrusion: Part ii." Drug Development and Industrial Pharmacy **33**(10): 1043-1057.

Repka M. A., Majumdar S., Kumar Battu S., Srirangam R. and Upadhye S. B. (2008). "Applications of hot-melt extrusion for drug delivery." Expert Opinion on Drug Delivery **5**(12): 1357-1376.

Riseman J. E. F. and Linenthal H. (1941). "The prolonged use of enteric-coated tablets of theobromine sodium acetate in the treatment of edema and angina pectoris." New England Journal of Medicine **224**(22): 933-936.

Roberts I. F. and Roberts G. J. (1979). "Relation between medicines sweetened with sucrose and dental disease." British Medical Journal **2**(6181): 14-16.

## REFERENCES


Rogers T. L. and Wallick D. (2011a). "Reviewing the use of ethylcellulose, methylcellulose and hypromellose in microencapsulation. Part 1: Materials used to formulate microcapsules." Drug Development and Industrial Pharmacy **38**(2): 129-157.

Rogers T. L. and Wallick D. (2011b). "Reviewing the use of ethylcellulose, methylcellulose and hypromellose in microencapsulation. Part 2: Techniques used to make microcapsules." Drug Development and Industrial Pharmacy **37**(11): 1259-1271.

Rogers T. L. and Wallick D. (2011c). "Reviewing the use of ethylcellulose, methylcellulose and hypromellose in microencapsulation. Part 3: Applications for microcapsules." Drug Development and Industrial Pharmacy **38**(5): 521-539.

Roper S. D. (1992). "The microphysiology of peripheral taste organs." Journal of Neuroscience **12**(4): 1127-1134.

Royal, Of C. and Physians (2012). National clinical guidlines for stroke cg68. R. C. o. Physicians.

Rudney J. D., Ji Z. and Larson C. J. (1995). "The prediction of saliva swallowing frequency in humans from estimates of salivary flow rate and the volume of saliva swallowed." Archives of Oral Biology **40**(6): 507-512.

Rudnitskaya A., Kirsanov D., Blinova Y., Legin E., Seleznev B., Clapham D., Ives R. S., Saunders K. A. and Legin A. (2013). "Assessment of bitter taste of pharmaceuticals with multisensor system employing 3 way pls regression." Analytica Chimi Acta **770**(0): 45-52.

Ruiz-Avila L., Ming D. and Margolskee R. F. (2000). "An in vitro assay useful to determine the potency of several bitter compounds." Chemical Senses **25**(4): 361-368.

Sakurai T., Misaka T., Ishiguro M., Masuda K., Sugawara T., Ito K., Kobayashi T., Matsuo S., Ishimaru Y., Asakura T. and Abe K. (2010). "Characterization of the beta-d-glucopyranoside binding site of the human bitter taste receptor htas2r16." Journal of biological chemistry **285**(36): 28373-28378.

Sathigari S. K., Radhakrishnan V. K., Davis V. A., Parsons D. L. and Babu R. J. (2012). "Amorphous-state characterization of efavirenz-polymer hot-melt extrusion systems for dissolution enhancement." Journal of Pharmaceutical Sciences **101**(9): 3456-3464.

Savage N. (2012). "Technology the taste of things to come." Nature **486**(7403): S18-S19.

Schiffman S. S. (1997). "Taste and smell losses in normal aging and disease." Journal of the American Medical Association **278**(16): 1357-1362.

## REFERENCES


Schiffman S. S. (2007). "Critical illness and changes in sensory perception." Proceedings of the Nutrition Society **66**(03): 331-345.

Schiffman S. S. (2009). "Effects of aging on the human taste system." Annals of the New York Academy of Sciences **1170**(1): 725-729.

Schiffman S. S., Gatlin L. A., Sattely-Miller E. A., Graham B. G., Heiman S. A., Stagner W. C. and Erickson R. P. (1994). "The effect of sweeteners on bitter taste in young and elderly subjects." Brain Research Bulletin **35**(3): 189-204.

Schiffman S. S., Suggs M. S., Graham B. G., Sattelymiller E. A. and Gatlin L. A. (1995). "The effect of bitter inhibitors on taste perception of urea, quinine hcl, magnesium chloride and caffeine." Chemical Senses **20**(6): 263-263.

Schiffman S. S., Suggs M. S. and Simon S. A. (1992). "Astringent compunds suppress taste responses in gerbil." Brain Research **595**(1): 1-11.

Schmidt A. C. and Schwarz I. (2005). "Solid state characterization of hydroxyprocaine hydrochloride. Crystal polymorphism of local anaesthetic drugs, part viii." Journal of Molecular Structure **748**(1–3): 153-160.

Schmidt R. and Fanchamps A. (1974). "Effect of caffeine on intestinal absorption of ergotamine in man." European Journal of Clinical Pharmacology **7**(3): 213-216.

Shpitzer T., Bahar G., Feinmesser R. and Nagler R. M. (2007). "A comprehensive salivary analysis for oral cancer diagnosis." Journal of Cancer Research and Clinical Oncology **133**(9): 613-617.

Siewert M., Dressman J., Brown C., Shah V., Aiache J.-M., Aoyagi N., Bashaw D., Brown C., Brown W., Burgess D., Crison J., Deluca P., Djerki R., Dressman J., Foster T., Gjellan K., Gray V., Hussain A., Ingallinera T., Klancke J., Kraemer J., Kristensen H., Kumi K., Leuner C., Limberg J., Loos P., Margulis L., Marroum P., Moeller H., Mueller B., Mueller-Zsigmondy M., Okafo N., Ouderkirk L., Parsi S., Qureshi S., Robinson J., Shah V., Siewert M., Uppoor R. and Williams R. (2003a). "Fip/aaps guidelines to dissolution/in vitro release testing of novel/special dosage forms." AAPS PharmSciTech **4**(1): 43-52.

Siewert M., Dressman J., Brown C. K., Shah V. P., Fip and Aaps (2003b). "Fip/aaps guidelines to dissolution/in vitro release testing of novel/special dosage forms." AAPS PharmSciTech **4**(1): E7-E7.

Silva O. S., Souza C. R. F., Oliveira W. P. and Rocha S. C. S. (2006). "In vitro dissolution studies of sodium diclofenac granules coated with eudragit l-30d-55® by fluidized-bed system." Drug Development & Industrial Pharmacy **32**(6): 661-667.

## REFERENCES


Sohi H., Sultana Y. and Khar R. K. (2004). "Taste masking technologies in oral pharmaceuticals: Recent developments and approaches." Drug Development and Industrial Pharmacy **30**(5): 429-448.

Stamatakis E., Primatesta P., Chinn S., Rona R. and Falascheti E. (2005). "Overweight and obesity trends from 1974 to 2003 in english children: What is the role of socioeconomic factors?" Archives of Disease in Childhood **90**(10): 999-1004.

Stark T., Bareuther S. and Hofmann T. (2005). "Sensory-guided decomposition of roasted cocoa nibs (theobroma cacao) and structure determination of taste-active polyphenols." Journal of Agricultural and Food Chemistry **53**(13): 5407-5418.

Stevens J. C. and Cain W. S. (1993). "Changes in taste and flavor in aging." Critical reviews in food science and nutrition **33**(1): 27-37.

Subramaniam B., Rajewski R. A. and Snavely K. (1997). "Pharmaceutical processing with supercritical carbon dioxide." Journal of Pharmaceutical Sciences **86**(8): 885-890.

Tahara Y. and Toko K. (2013). "Electronic tongues-a review." Ieee Sensors Journal **13**(8): 3001-3011.

Tepper B. J. and Nurse R. J. (1997). "Fat perception is related to prop taster status." Physiology & Behavior **61**(6): 949-954.

Thia T. H. H., Morel S., Ayouni F. and Flament M.-P. (2012). "Development and evaluation of taste-masked drug for paediatric medicines - application to acetaminophen." International Journal of Pharmaceutics **434**(1-2): 235-242.

Thies C., Dos Santos I. R., Richard J., Vandevelde V., Rolland H. and Benoit J. P. (2003). "A supercritical fluid-based coating technology 1: Process considerations." Journal of Microencapsulation **20**(1): 87-96.

Toko K. (1996). "Taste sensor with global selectivity." Materials Science & Engineering C-Biomimetic Materials Sensors and Systems **4**(2): 69-82.

Toko K., Matsuno T., Yamafuji K., Hayashi K., Ikezaki H., Sato K., Toukubo R. and Kawarai S. (1994). "Multichannel taste sensor using electric-potentials changes in lipid-membranes." Biosensors and Bioelectronics **9**(4-5): 359-364.

Uchida T., Tanigake A., Miyanaga Y., Matsuyama K., Kunitomo M., Kobayashi Y., Ikezaki H. and Taniguchi A. (2003). "Evaluation of the bitterness of antibiotics using a taste sensor." Journal of Pharmacy and Pharmacology **55**(11): 1479-1485.

Uchida T., Yoshida M., Hazekawa M., Haraguchi T., Furuno H., Teraoka M. and Ikezaki H. (2013). "Evaluation of palatability of 10 commercial amlodipine orally disintegrating tablets by gustatory sensation testing, od-mate as a new disintegration

apparatus and the artificial taste sensor." Journal of Pharmacy and Pharmacology **65**(9): 1312-1320.

Van Krevelen D. W. and Te Nijenhuis K. (2009a). Chapter 1 - polymer properties. Properties of polymers (fourth edition). D. W. V. K. by and K. T. Nijenhuis. Amsterdam, Elsevier**:** 3-5.

Van Krevelen D. W. and Te Nijenhuis K. (2009b). Chapter 7 - cohesive properties and solubility. Properties of polymers (fourth edition). D. W. V. K. by and K. T. Nijenhuis. Amsterdam, Elsevier**:** 189-227.

Warmke R. and Belitz H. D. (1993). "Influence of glutamic-acid on the bitter taste of various compounds." Zeitschrift Fur Lebensmittel-Untersuchung Und-Forschung **197**(2): 132-133.

Weinberger M. and Hendeles L. (1996). "Theophylline in asthma." New England Journal of Medicine **334**(21): 1380-1388.

Wilson M., Williams M. A., Jones D. S. and Andrews G. P. (2012). "Hot-melt extrusion technology and pharmaceutical application." Ther Deliv **3**(6): 787-797.

Winquist F. (2008). "Voltammetric electronic tongues – basic principles and applications." Microchimica Acta **163**(1-2): 3-10.

Wishart D. S., Knox C., Guo A. C., Cheng D., Shrivastava S., Tzur D., Gautam B. and Hassanali M. (2008). "Drugbank: A knowledgebase for drugs, drug actions and drug targets." Nucleic Acids Research **36**(suppl 1): D901-D906.

Woertz K., Tissen C., Kleinebudde P. and Breitkreutz J. (2010a). "Performance qualification of an electronic tongue based on ich guideline q2." Journal of Pharmeutical and Biomedical Analysis **51**(3): 497-506.

Woertz K., Tissen C., Kleinebudde P. and Breitkreutz J. (2010b). "Rational development of taste masked oral liquids guided by an electronic tongue." International Journal of Pharmaceutics **400**(1-2): 114-123.

Woertz K., Tissen C., Kleinebudde P. and Breitkreutz J. (2011a). "A comparative study on two electronic tongues for pharmaceutical formulation development." J Pharm Biomed Anal **55**(2): 272-281.

Woertz K., Tissen C., Kleinebudde P. and Breitkreutz J. (2011b). "Development of a taste-masked generic ibuprofen suspension: Top-down approach guided by electronic tongue measurements." Journal of Pharmaceutical Sciences **100**(10): 4460-4470.

## REFERENCES


Woertz K., Tissen C., Kleinebudde P. and Breitkreutz J. (2011c). "Taste sensing systems (electronic tongues) for pharmaceutical applications." International Journal of Pharmaceutics **417**(1–2): 256-271.

Woertz K., Tissen C., Kleinebudde P. and Breitkreutz J. (2011d). "Taste sensing systems (electronic tongues) for pharmaceutical applications." Int J Pharm **417**(1-2): 256-271.

Wu C. and Mcginity J. W. (1999). "Non-traditional plasticization of polymeric films." International Journal of Pharmaceutics **177**(1): 15-27.

Wulff M., Aldén M. and Craig D. Q. M. (1996). "An investigation into the critical surfactant concentration for solid solubility of hydrophobic drug in different polyethylene glycols." International Journal of Pharmaceutics **142**(2): 189-198.

Xin Z., Rui Y., Yu Z., Zhijun W., Xing T. and Liangyuan Z. (2007). "Part ii: Bioavailability in beagle dogs of nimodipine solid dispersions prepared by hot-melt extrusion." Drug Development & Industrial Pharmacy **33**(7): 783-789.

Yajima T., Itai S., Takeuchi H. and Kawashima Y. (2003). "Optimum heat treatment conditions for masking the bitterness of the clarithromycin wax matrix." Chemical and Pharmaceutical Bulletin **51**(11): 1223-1226.

Yan Y.-D., Woo J. S., Kang J. H., Yong C. S. and Choi H.-G. (2010). "Preparation and evaluation of taste-masked donepezil hydrochloride orally disintegrating tablets." Biological and Pharmaceutical Bulletin **33**(8): 1364-1370.

Yang Z., Nollenberger K., Albers J., Craig D. and Qi S. (2013). "Microstructure of an immiscible polymer blend and its stabilization effect on amorphous solid dispersions." Molecular Pharmaceutics **10**(7): 2767-2780.

Zheng J. Y. and Keeney M. P. (2006). "Taste masking analysis in pharmaceutical formulation development using an electronic tongue." International Journal of Pharmaceutics **310**(1–2): 118-124.

# APPENDICES

## A1 PREPARATION OF STANDARD SOLUTIONS

All reference solutions were adapted from Insent TS5000Z (2008) manual.

### A1.1 STANDARD REFERENCE SOLUTION

0.0455g of tartaric acid was dissolved in about 900ml of deionised water. 2.2452g of KCl was added to the tartaric acid solution and stirred until fully dissolved. The solution was transferred to a 1L volumetric flask and made up to the 1L mark using deionised water.

### A1.2 NEGATIVELY CHARGED MEMBRANE WASHING SOLUTION

150ml of ethanol was added to 250ml of deionised water and stirred thoroughly. 50ml of 1M hydrochloric acid solution was added to the ethanol and deionised water solution. Following thorough stirring the solution was transferred to a 500ml volumetric flask and made to volume using deionised water.

### A1.3 POSITIVELY CHARGED MEMBRANE WASHING SOLUTION

3.73g KCl was added to 250ml deionised water and stirred thoroughly. 150ml ethanol (99%) was added to the KCl solution and stirred thoroughly. 5ml of 1M KOH was added and again stirred thoroughly. The resulting solution was transferred to a 500ml volumetric flask and made to volume using deionised water.

### A1.4 SALTY REFERENCE SOLUTION

0.00453g of tartaric acid was dissolved in about 900ml deionised water. 22.368g of KCl was added to the tartaric acid solution and dissolved thoroughly. The solution was transferred to a 1L volumetric flask and made to volume using deionised water.

### A1.5 UMAMI REFERENCE SOLUTION

0.0458g of tartaric acid was added to about 900ml of deionised water and stirred thoroughly. 2.2525g of KCl was added to the tartaric acid solution. Following thorough stirring and full dissolution of KCl, 1.8694g of MSG was added to the KCl and tartaric acid solution and dissolved. The resultant solution was transferred to a 1L volumetric flask and made to mark using deionised water.

### A1.6 ASTRINGENT REFERENCE SOLUTION

0.04427g of tartaric acid was dissolved in about 900ml of deionised water. 2.4240g of KCl was added to the tartaric acid solution and stirred thoroughly. Finally, 0.4945g of tannic acid was added to tartaric acid – KCl solution. The resultant solution was transferred to a 1L volumetric flask and made to volume using deionised water.

### A1.7 BITTER (-) REFERENCE SOLUTION

0.045g of tartaric acid was dissolved in about 900ml of deionised water. 2.24g of KCl was added to the tartaric acid solution and stirred thoroughly. Finally, 100µl iso-α-acid was added and again stirred thoroughly. The resultant solution was transferred into a 1L volumetric flask and made to volume using deionised water.

### A1.8 BITTER (+) REFERENCE SOLUTION

0.045g of tartaric acid was dissolved in about 900ml of deionised water. 2.24g of KCl was added to the tartaric acid solution and stirred thoroughly. Finally, 0.04g quinine hydrochloride was added and again stirred thoroughly. The resultant solution was transferred into a 1L volumetric flask and made to volume using deionised water.

## A2 SCHEMATIC FOR PREPARATION OF F1 AND F2 FORMULATIONS

### A2.1 SCHEMATIC FOR PREPARATION FOR F1 FORMULATIONS

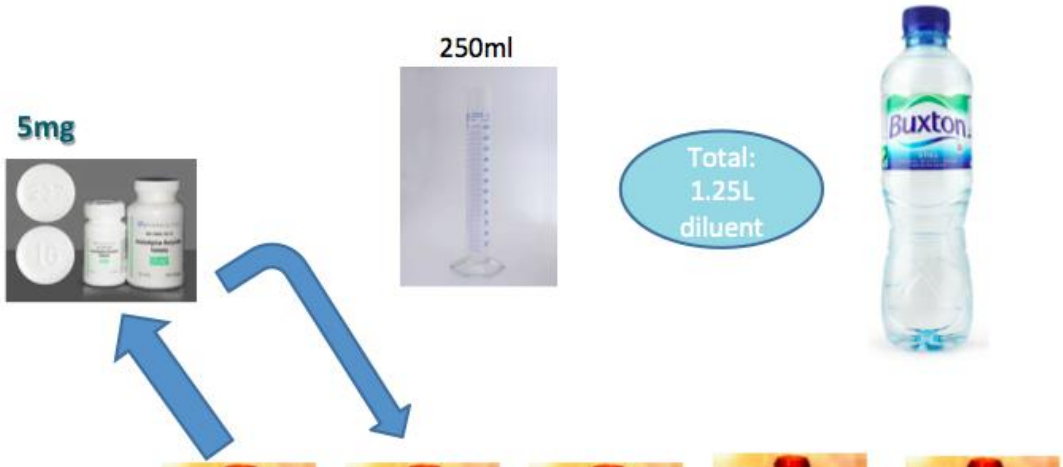


| | C0 | C1 | C2 | C3 | C4 |
|---|---|---|---|---|---|
| **Be / Ma** | 0 tabs<br>250ml | 12 ½ tabs<br>250ml | 25 tabs<br>250ml | 37 ½ tabs<br>250ml | 50 tabs<br>250ml |
| **Me (per 2h session)** | 0 tabs<br>100ml | 5 tabs<br>100ml | 10 tabs<br>100ml | 15 tabs<br>100ml | 20 tabs<br>100ml |

## A2.2 SCHEMATIC FOR PREPARATION OF F2 SUSPENSION

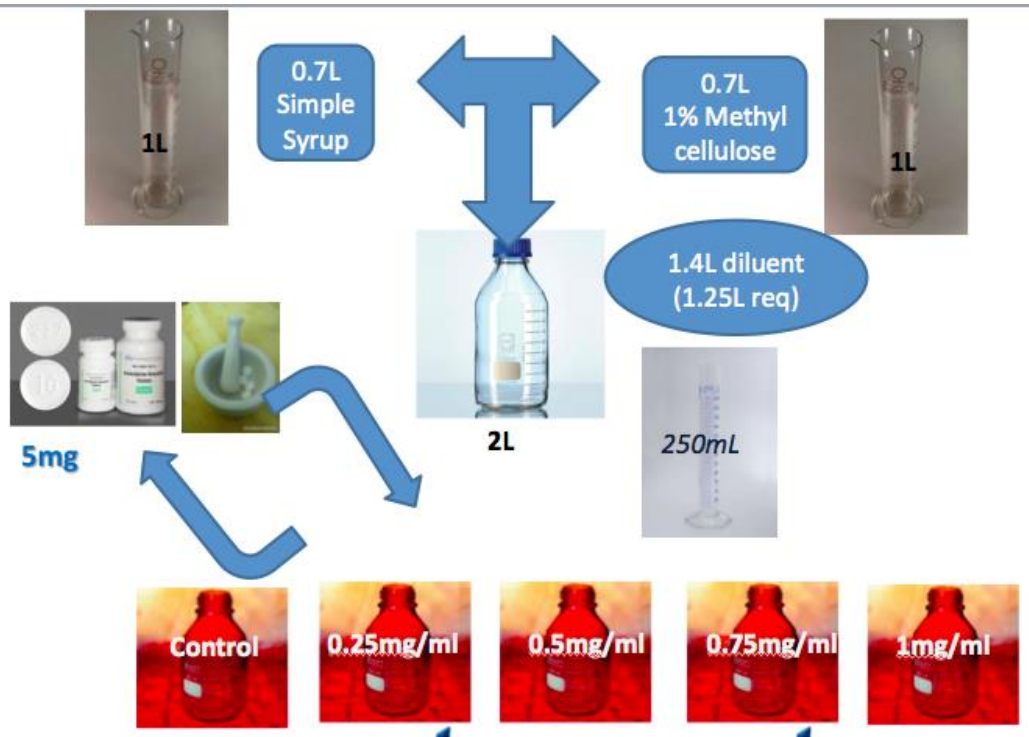


| | C0 | C1 | C2 | C3 | C4 |
|---|---|---|---|---|---|
| **Be / Ma** | 0 tabs | 12 ½ tabs | 25 tabs | 37 ½ tabs | 50 tabs |
| **Diluent** | 250ml | 250ml | 250ml | 250ml | 250ml |

## A3.2 POSTER FOR PARTICIPANT RECRUITMENT

*This study has been approved by the UCL Research Ethics Committee (Project ID Number): 4612/001*

# Volunteers Needed


We are carrying out a study to look at the taste of different **amlodipine** liquid formulations (a cardiovascular medicine) and are looking for some volunteers to help.

If you are healthy and over 18– open wide and take part in our study!

You will be asked to taste different samples for 5-20 seconds by 2 methods and rate them on a scale.

**You will not be asked to swallow the liquid.**

Finding out which one tastes better could help children and older adults who need to take this medicine, but can't swallow the tablets.

If you would like to participate, or find out more about this study, please contact us:ucnvxdg@live.ucl.ac.uk or ucnvjk1@live.ucl.ac.uk and we will send you an information sheet. As a small thank you for your time and commitment, you will be entered into a draw to win a £10 gift voucher

*All data will be collected and stored in accordance with the Data Protection Act 1998.*

*Principal Investigator: Dr Catherine Tuleu*

***UCL School of Pharmacy***

*29/39 Brunswick Square, London, WC1N 1AX*

*Tel: 020 7753 5857, Email: c.tuleu@ucl.ac.uk*

## A3.3 PARTICIPANT CONSENT FORM

Please complete this form after you have read the Information Sheet and/or listened to an explanation about the research.

Title of Project: **Amlodipine Palatability Assessment Study**

This study has been approved by the UCL Research Ethics Committee (Project ID Number): **4612/001**

Thank you for your interest in taking part in this research. Before you agree to take part, the person organising the research must explain the project to you.

If you have any questions arising from the Information Sheet or explanation already given to you, please ask the researcher before you to decide whether to join in. You will be given a copy of this Consent Form to keep and refer to at any time.

**Participant's Statement**

I

- have read the notes written above and the Information Sheet, and understand what the study involves.
- understand that I should not take part if I have had any dental care or medicinal treatment (except contraceptives) during the 15 days before the tests.
- understand that if I decide at any time that I no longer wish to take part in this project, I can notify the researchers involved and withdraw immediately without penalty.
- consent to the processing of my personal information for the purposes of this research study.
- understand that the information I have submitted will be published as a report and I can request a copy by contacting the researchers. Confidentiality and anonymity will be maintained and it will not be possible to identify me from any publications.
- understand that such information will be treated as strictly confidential and handled in accordance with the provisions of the Data Protection Act 1998.
- agree that the research project named above has been explained to me to my satisfaction and I agree to take part in this study.

Signed: Date:

## A4 PUBLICATION

# Inter-laboratory testing of Insent e-tongues

**Miriam Pein*[1], Xolani Dereck Gondongwe[2], Masaaki Habara[3] and Gesine Winzenburg[4]**

1) Institute of Pharmaceutics and Biopharmaceutics, Heinrich-Heine University Duesseldorf,
Universitaetsstr. 1, 40225 Duesseldorf, Germany
2) University College London, School of Pharmacy, 29-39 Brunswick Square, London, UK
3) Insent (Intelligent Sensor Technology), Inc., Atsugi, Kanagawa, Japan
4) Novartis Pharma AG, Basel, Switzerland

*Corresponding author. phone: +49 211 8114225; fax: +49 211 8114251

email addresses: miriam.pein@hhu.de, x.gondongwe@ucl.ac.uk,

habara.masaaki@insent.co.jp, gesine.winzenburg@novartis.com

**Abstract**

The first inter-laboratory testing of electronic taste sensing systems was performed within five participating centers, each working with the Insent (Insent Inc., Atsugi-Shi, Japan) e-tongue. Preparation of the samples for the comprised four experiments, shipping of the samples and evaluation of the results was performed at the University of Duesseldorf. The sensitivity (in this case the difference between lowest and highest sensor response) and slope of the regression line values, obtained within Experiment 1 and 2, have been found to serve as applicable evaluation criterions for inter-laboratory comparability. Modified sensor responses could be attributed to aged sensors, but did not influence the results of either Experiment 3, dealing with the evaluation of film formulations, or Experiment 4, dealing with the evaluation of minitablet formulations, in a great amount. Presented PCA Score and Loading Scatter Plots as well as Euclidean distance patterns based on the raw sensor responses confirmed the comparable performance of Insent e-tongues of the participating centers.

**1. Introduction**

With regard to a better understanding of electronic taste sensing systems (e-tongue), the "e-tongue usergroup" was set up in 2012 on behalf of the European Paediatric Formulation Initiative (EuPFi). Besides theoretical knowledge, data experimentally obtained within this group should be discussed. First studies have now been set up to evaluate inter-laboratory comparability of Insent e-tongue results. The inter-laboratory testing was based on four different experiments, comprising the evaluation of concentration series as well as drug containing film and minitablet formulations. To ensure comparability, production of the samples and data evaluation was done in one center (University of Duesseldorf).

## 2. Participants

The Institute of Pharmaceutics and Biopharmaceutics at the University of Duesseldorf, (HHUD, Duesseldorf, Germany) guided the inter-laboratory experiment and was responsible for the sample preparation and the data evaluation. All investigated samples were shipped to the participating centers Novartis (Basel, Switzerland), the School of Pharmacy at the University College of London (London, England) and the company Insent Inc. (Intelligent Sensor Technology, Inc. Atsugi-Shi, Japan). Every center worked with the Insent taste sensing system (Atsugi-Shi, Japan). Novartis, the University College London and the company Insent used the system TS5000Z, while the University of Duesseldorf (HHUD) used the TS5000Z and the SA402B, both with different sensor sets. In total, the results of 5 participating centers were the basis of this study.

Independent of the participating center, experiments with the TS5000Z were performed at ambient temperature. The samples measured with the SA402B at the HHUD were kept at 20 °C by water cooling.

## 3. Materials and methods

### 3.1 Chemicals

Quinine hydrochloride was purchased by Caesar & Loretz (Hilden, Germany) and potassium chloride by Gruessing (Filsum, Germany). Each film formulation contained 15 % (w/w) of the film forming agent hydroxypropyl methylcellulose (Pharmacoat® 606, Harke Group, Mühlheim a. d. R., Germany), 10 % (w/w) ethanol (96 %, VWR international, Darmstadt, Germany), 7 % (w/w) of anhydrous glycerol and the coloring agent E 124 (both excipients purchased by Caesar & Loretz, Hilden, Germany). Film

formulations A1 and B1 contained 3 % (w/w) of dimenhydrinate, and film formulations B1 and D1 were sweetened with 0.5 % of a 1:10 mixture of saccharin sodium:sodium cyclamate (both sweeteners purchased by Caesar & Loretz, Hilden, Germany). The minitablet formulations were prepared according to Stoltenberg based on the ready-to-use tableting excipient Pearlitol® flash (provided by Roquette, Lestrem, France) (Stoltenberg, 2012). Minitablets A2, B2 and D2 contained 0.16 % (w/w) of zinc sulphate (Riedel-de Haen, Sigma-Aldrich, Seelze, Germany), minitablets A2, C2 and D2 contained 9.8 % of sodium chloride (analytical grade, VWR international, Darmstadt, Germany) and minitablets B2, C2 and D2 contained 18.5 % of a 1:10 mixture of saccharin sodium:sodium cyclamate.

The sample compositions reduced to the API and the taste-masking excipient(s) are summarized in Table 1.

**Table 1: Sample composition, reduced to the API and the taste-masking agents**

| **sample** | **A1** | **B1** | **C1** | **D1** | **E1** | **F1** | **G1** |
|---|---|---|---|---|---|---|---|
| dimenhydrinate | 100 mg | 100 mg | - | - | 100 mg | 100 mg | - |
| saccharin sodium : sodium cyclamate | - | 17 mg | - | 17 mg | - | 17 mg | 17 mg |
| **sample** | **A2** | **B2** | **C2** | **D2** | **E2** | **F2** | **G2** |
| zinc sulphate | 20 mg | 20 mg | 20 mg | - | 20 mg | 20 mg | - |
| saccharin sodium : sodium cyclamate | | 23.1 mg | 23.1 mg | 23.1 mg | - | 23.1 mg | 23.1 mg |
| sodium chloride | 12.25 mg | - | 12.25 mg | 12.25 mg | - | 12.25 mg | 12.25 mg |

## 3.2 Preparation of the film and tablet formulations

To prepare the drug containing film formulations (film A1 and B1), dimenhydrinate (DMH) was dissolved in ethanol and added to a stirred water-glycerol mixture. To prepare film B1, the sweetener mixture was additionally added, while it was solely added to prepare film C1. To each of the solutions, the film forming agent was added stepwise. After 24 hours of continuous stirring, the viscous solutions were poured onto a release liner (Erichsen film applicator, Erichsen, Hemer, Germany) and casted directly afterwards at a speed of 6 mm/s.

The minitablets were compressed on a rotary die press (Pressima MX-Eu-B/D, IMA Kilian, Cologne, Germany) with 2 mm bi-concave punches. Prepared minitablets weighed 6.2 mg ± 0.26 mg.

### 3.3 Electronic tongue measurements

#### 3.3.1 Standard and washing solutions

Dependent on the incorporated artificial lipids, sensors should be dipped into either the (-)- or the (+)-washing solution. The (-)-washing solution was prepared by diluting 100 mM hydrochloric acid with ethanol (30 % (w/w)) and used for sensors with negatively charged lipids. The (+)-washing solution was used for sensors with positively charged lipids and prepared by dissolving 100 mM potassium chloride and 10 mM potassium hydroxide in ethanol (30 % (w/w)). The standard solution, which served as cleaning and reference solution, was prepared by dissolving 0.3 mM tartaric acid and 30 mM potassium chloride in distilled water.

#### 3.3.2 General procedure

Using the recommended measurement setup ABCABC (A, B, and C are representatives of sample beakers), the e-tongue measurement followed the standard procedure as described by (Woertz et al., 2010, 2011). The washing steps were conducted in the recommended (-)- or (+)-washing solution (see also section 3.3.3) as well as in the standard solution (preparation according to section 3.3.1). The whole measurement procedure was carried out 4 times in a row. Both, sensor responses and CPA (change of membrane potential due to adsorption) values were recorded.

#### 3.3.3 Specific procedure

To measure the samples with all 7 sensors, two measurement cycles have to be performed. For the first measurement cycle, the outer sensor head was equipped with sensor SB2AC0 at position 1 and SB2AN0 at position 2. During the washing procedure these sensors dipped into the (-)-washing solution.

After the first measurement cycle, the reference solution in the washing beakers was exchanged. For the second measurement cycle, the outer sensor head was then equipped with the sensors SB2AAE (position 1), SB2CT0 (position 2) and SB2CA0 (position 3), and the inner sensor head with sensors SB2C00 (position 5) and SB2AE1 (position 6).

The sensors at the outer sensor head dipped into the (-)-washing solution, whereas the sensors at the inner sensor head dipped into the (+)-washing solution.

### 3.4 Experiments 1 to 4 and sample preparation

A solution of quinine hydrochloride (0.5 mM, 0.1985 g/l) served as external standard, which was placed in the first sample beaker position (position sample A) for every experiment. A serial dilution series of quinine hydrochloride was prepared in water (Experiment 1) and in an aqueous 10 mM KCl-solution (Experiment 2). For Experiment 3, 20 films of each provided sample (A1-D1) and the according physical mixtures (E1-G1) were dissolved in 100.0 ml of purified water at 37 °C in an ultrasonic bath. For Experiment 4, 20 minitablets of each provided sample (A2-D2) were stirred for 3 min in 100.0 ml of purified water at 37 °C. To enable comparable filtration processes within the centers, the samples were immediately filtered through a paper filter, which was provided by the HHUD. The physical mixtures (E2-G2) were dissolved in 100.0 ml of purified water.

### 3.5 Data evaluation

The data was analyzed at the HHUD. For univariate evaluation and calculation of Euclidean Distances (Equation 1) based on the sensor signals, Excel 2010 (Microsoft, Redmond, US) was used.

Equation 1: $d\ (\mathrm{p}, \mathrm{q}) = \sqrt{\sum_{i=1}^{n}(p_i - q_i)^2}$

The single sensor responses of the external standard solution were subtracted from the sensor responses of the different experiment samples. Multivariate statistics were performed with SIMCA-P 12.01 (Umetrics AB, Umea, Sweden).

## 4. Results and Discussion

### 4.1 Evaluation Experiment 1 and 2 (dilution series)

A dilution series of quinine hydrochloride in water was analyzed to assess the performance of the Insent sensors, as it has already been shown by Woertz et al. that each sensor is sensitive towards changing quinine concentrations (Woertz et al., 2010). The model drug was moreover dissolved in aqueous KCl (10 mM), to judge about the specificity of the sensors within the different laboratories. Resulting sensor responses

were compared with regard to sensitivity (in this case the difference between the highest and the lowest sensor response), onset, log-linear range, slope and the corresponding coefficient of determination ($R^2$) (Figure 1).

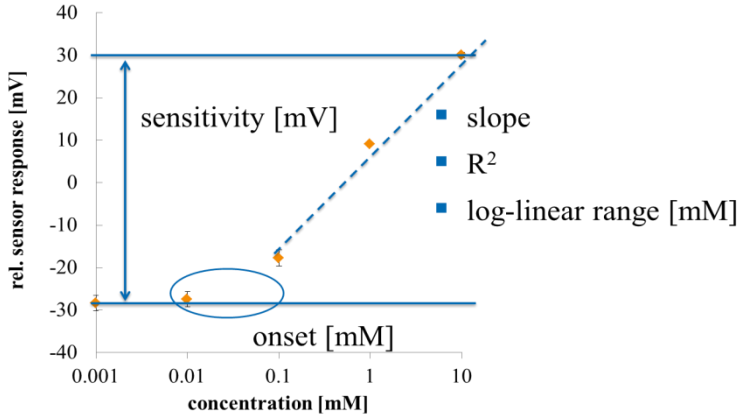


**Figure 1: Sensitivity, onset, log-linear range, slope and the corresponding coefficient of determination ($R^2$) as indicators for sensor performance comparability.**

The results of the concentration series in water are summarized in Table 2 and highlighted in the figures therein. As expected, and independent of the evaluating center, the bitter sensors SB2AC0 and SB2AN0 show the highest sensitivity towards changing quinine concentrations. Considering the slope as further parameter to describe the sensitivity, sensor SB2AN0 can be defined as more sensitive towards changing quinine concentrations between 0.1 and 10 mM (Table 2, slope (mean ± s) = 42.3 ± 1.3). Although sensor SB2AC0 provides a slighter slope compared to sensor SB2AN0, it shows the larger log-linear range (0.001-10 mM, Table 2). Both findings are in good agreement to (Woertz et al., 2010). The other five sensors are comparably sensitive towards changing quinine concentrations, represented in similar sensitivity values as well as similar absolute slopes. Noteworthy in this context are the comparable responses of sensor SB2AE1, indicating a robust performance of this sensor type. Sensors SB2C00 of center 4 and 5 are marked with a * in Table 1, because the according sensor responses do not only increase with increasing concentrations like those of 1 to 3, but decrease again after reaching a concentration of 0.1 (center 4) or 1 mM (center 5). Contrary to the other sensor types, SB2C00 sensors also show differing log-linear ranges within the centers.

Defining applicable evaluation criterions to judge about the inter-laboratory comparability of e-tongue results is one aim of this study, and sensitivity and slope

values have been selected for further investigation. Significance of different sensor behavior between the centers is proven based on the t-test for independent samples (α = 0.05). In this context, sensitivity and slope values of each sensor in each center are compared with the corresponding average values. For inhomogeneous variations a correction of the t-value according to Welch has been considered. Moreover, the corresponding confidence intervals (α = 0.05) are calculated based on the mean sensitivity and slope values.

**Table 2: Sensitivity, onset, log-linear range, slope and the coefficient of determination ($R^2$) as indicators for sensor performance; results are based on the concentration series in water; sensitivity and slope are highlighted in the figures on the right; the numbers in "sensor_center" represent the participant; the * indicates that according sensor responses do not only increase with increasing concentrations, but decrease again after reaching a concentration of 0.1 (SB2C00_4*) or 1 mM (SB2C00_5*); results were displayed with left up to right down scattered bares, if they were below mean ± CI (α = 0.05); results were displayed right up to left down scattered bars, if they were significantly different from the mean results within one sensor type according to the t-test for independent samples (α = 0.05); results were displayed with dotted bars, if they were below mean ± CI (α = 0.05) AND significantly different from the mean results within one sensor type according to the t-test for independent samples (α = 0.05).**

Both calculation methods recognized values tending towards and away from 0. As decreasing sensor performance is accompanied with values tending towards 0 (Pein et al., 2013), only those values have been highlighted in Table 2. Information, which can be obtained by the sensitivity values, confirms the assignment of the sensors. The slopes include however more specific information regarding sensor behavior (such as the orientation of the slope). SB2AAE and SB2CA0 of center 3, SB2C00 of center 4 and SB2C00 and SB2CT0 of center 5 behaved significant differently regarding both, sensitivity and slope values. While the reduced performance of the sensors of center 3 could be correlated with the high period of use (18 months), the reduced performance of the other sensors could not be explained.

The results of the concentration series aqueous KCl (10 mM) are summarized in table 3 and highlighted in the figures therein. Sensors SB2AC0, SB2AN0, SB2AAE and SB2CA0 show comparable sensitivity and slope patterns compared with those listed in Table 2. These results fit the assignment of the sensors: SB2AC0 and SB2AN0 are dedicated to cationic bitter substances, SB2AAE to umami tasting compounds and SB2CA0 to sour substances. Thus, they should not be influenced by either potassium cations or chloride anions. In contrast, the performance of the salty sensor (SB2CT0) is significantly decreased. This behavior is also displayed by the astringent sensor SB2AE1, which complies with the similar sensor membrane composition (Kobayashi et

al., 2010). Both sensors considerably lost their ability to differentiate between different concentrations of quinine hydrochloride. Their slopes decrease from -12.6 (±3.1) (SB2CT0) and -15.3 (±1.0) (SB2AE1) to -2.5 (±1.8) and -3.0 (±0.8) and their sensitivity values from 60.0 (±16.4) and 77.5 (±5.2) to 12.9 (±7.5) and 14.5 (±2.6). This behavior is additionally confirmed by the results of the linear regression. At least three concentrations have been used to calculate the coefficients of determination ($R^2$), even if the sensor responses neither significantly increase nor decrease until a concentration of 1 or 10 mM is reached (which is indicated by brackets around the corresponding log-linear ranges in Table 3). Especially for sensors SB2AE1 and SB2CT0, the resulting $R^2$ values are below 0.90. However, no explanation can be provided for the non-systemically changes of the responses of sensor SB2C00.

**Table 3: Sensitivity, onset, log-linear range, slope and the coefficient of determination ($R^2$) as indicators for sensor performance; results are based on the concentration series in 10 mM aqueous KCl; sensitivity and slope are highlighted in the figures on the right; the numbers in "sensor_center" represent the participant; the * indicates that according sensor responses do not only increase with increasing concentrations, but decrease again after reaching a concentration of 0.1 (SB2C00_4*); results were displayed with left up to right down scattered bares, if they were below mean ± CI (0.05); results were displayed with dotted bars, if they were below mean ± CI (0.05) AND significantly different from the mean results within one sensor type according to the t-test for independent samples (α = 0.05).**

The reduced performance of SB2AAE and SB2CA0 of center 3 and SB2CT0 of center 5 highlights the history of the sensors of center 3 as main influence.

## 3.2 Evaluation of the film formulations (Experiment 3)

Principle component analyses (PCA) were performed individually for each participating center, containing the information of all seven sensors. Moreover, a PCA was performed based on the merged information of all 5 centers, containing the information of 35 sensors. The corresponding PCA score and loading scatter plots are displayed in Figure 2.

**Figure 2: PCA maps of the results of Experiment 3, containing the information of 35 sensors (1) or 7 sensors (2-6). Each sample was measured in triplicate. Data was center scaled. A1 (black): films containing dimenhydrinate, B1 (red): films containing dimenhydrinate and sweetener, C1 (blue): placebo films, D1 (light green): films containing sweetener, E1 (yellow): dimenhydrinate, F1 (pink): dimenhydrinate and sweetener, G1 (dark green): sweetener**

The information of all dimenhydrinate containing samples is influenced by the responses of bitter sensors SB2AC0 and SB2AN0 (Figure 2.1: Loading Scatter Plot) and thus displayed on the right side of the PCA map 1. The information is mainly separated along principle component 1 (PC1:94.1 %), and only minor along PC2 (4.7 %). Regarding the distances between the data points, the dimenhydrinate containing formulations A1 and B1 and the corresponding physical mixtures E1 and F1 are detected comparably. While sweetener containing solutions (D1 and G1) are closer located, the placebo film sample (C1) is detected most differently compared to the dimenhydrinate containing samples. C1 is most distinctively recognized by sensors SB2AE1 and SB2CT0 (Figure 2.1: Loading Scatter Plot).

The PCA Score and Loading Scatter Plots of center 2, 4 and 5 are almost identical (Figure 2). The Score Scatter Plot of center 1 varies only little, representing sample C1 similar located as G1 regarding PC1. This might be due to the differing influences of sensors SB2C00 and SB2CA0 of center 1 (Figure 2.2: Loading Scatter Plot), if compared to those of center 2, 4 and 5. While the result of SB2CA0_1 complies with the reduced performance in Experiments 1 and 2, no such a correlation could be found for SB2C00_1. The PCA map of participant 3 is arranged mirror-inverted, although the results have been evaluated in the same manner as the results of the other centers. Moreover, scattered results for sample E1 are evident. These differing results could be due to the decreased sensor performance of sensor SB2AAE_3, SB2CT0_3 and SB2AC0_3, which have been proven as evident in Experiment 1 (Table 2) and Experiment 2 (Table 3). Moreover, sensor SB2AC0_3 is located in the same quadrant as sensor SB2AAE_3 (Figure 2.4: Loading Scatter Plot), which is not the case within the results of the other center. Nonetheless, the main information is comparable to those of the other centers: the dimenhydrinate containing samples are located at one side of the PCA map, while order and distance of the sweet and placebo samples as well as the information given on the x- and y-axes are the same as for each other PCA map.

Similar findings are confirmed by calculating and evaluation of the Euclidean distances (according to Equation 1) based on the mean sensor values. The Euclidean distances are calculated originating from the placebo film formulation (C1) and show similar patterns for all participating centers (Figure 3).

**Figure 3: Euclidean distances, calculated based on the mean sensor values (left) and CPA values (right) according to Equation 1. The Euclidean distances were calculated originating from the placebo film (C1). A1:**

**films containing dimenhydrinate, B1: films containing dimenhydrinate and sweetener, D1: films containing sweetener, E1: dimenhydrinate, F1: dimenhydrinate and sweetener, G1: sweetener**

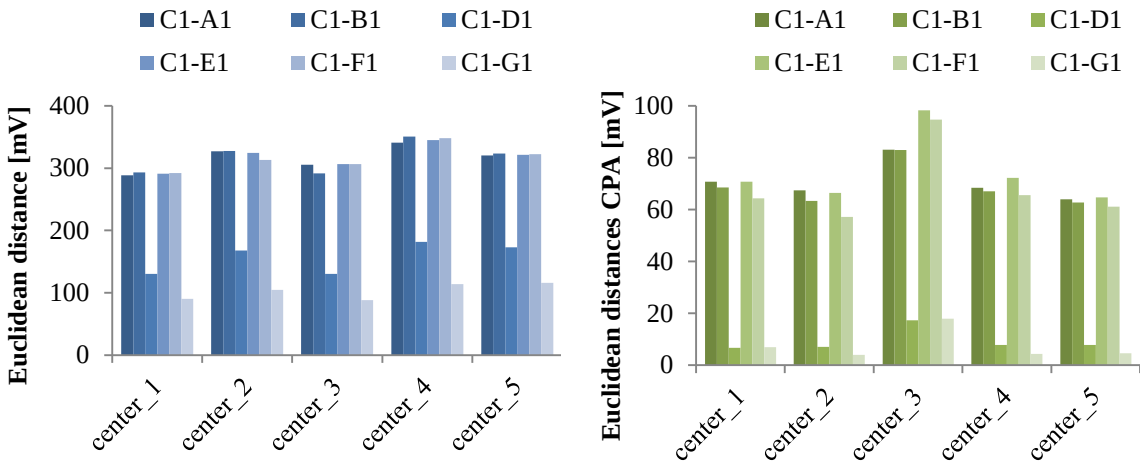


Interestingly, also the Euclidean distance patterns based on the mean CPA (change in membrane potential due to adsorption) values are comparable between the centers (Figure 3, right) but also to the patterns of the mean sensor values (Figure 3, left).

CPA values have already been correlated with gustatoric impressions by (Kobayashi et al., 2010) and are a measure for the lipophilic character of the analyzed substances. The obtained Euclidean distance patterns based on CPA values could therefore refer to adsorption of dimenhydrinate as the main contributor for the signal. This assumption is proven by evaluating the original CPA values (Figure 4). These values are by default measured in the standard solution after measuring a sample solution (followed by a subsequent slight washing). Distinctly recognized by the CPA values of the three bitter sensors (SB2C00, SB2AC0 and SB2AN0) are those samples that contain dimenhydrinate (Figure 4).

**Figure 4: Mean CPA values based on the CPA values of the different centers (mean ± s). A1 (black): films containing dimenhydrinate, B1 (red): films containing dimenhydrinate and sweetener, C1 (blue): placebo films, D1 (light green): films containing sweetener, E1 (yellow): dimenhydrinate, F1 (pink): dimenhydrinate and sweetener, G1 (dark green): sweetener**

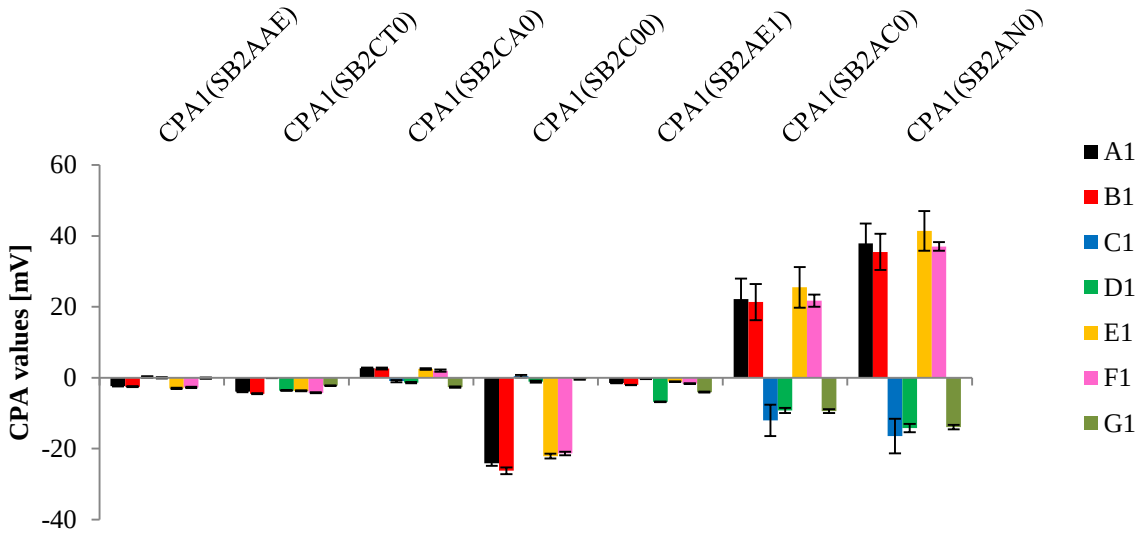


### 3.3 Evaluation of the minitablet formulations (Experiment 4)

For evaluating the minitablet formulations, PCAs were also performed individually for each participating center and based on the merged information of all 5 centers (Figure 5).

Contrary to the PCA maps of the film formulations, where around 95 % of the information is separated along the x-axes, PC1 of experiment 4 displays between 71-85.4 %. Thus, also the separation of the samples along PC2 (13.2-26.3 %) has to be regarded for the sample evaluation. PCA map 1 displays E2, containing only dissolved zinc sulphate, furthest to the right, mainly influenced by the response of astringent sensor SB2AE1 and to a lesser extent by SB2CT0 (Figure 5.1: Loading Scatter Plot). On the left side of the PCA map, the samples can be divided into two clusters: one representing the samples containing only NaCl and sweetener (C2 and G2) and one representing the samples, containing zinc sulphate in combination with NaCl and sweetener (D2 and F2). While the minitablet formulation containing zinc sulphate and only sweeteners (B2) is located in the second cluster, minitablets containing zinc sulphate and only NaCl (A2) can be found next to pure zinc sulphate (E2). This leads to the assumption that the included sweeteners direct to the left, while zinc sulphate directs to the right side of the PCA map. However, none of the applied sensors can unequivocally be dedicated to one or the other cluster (Figure 5.1: Loading Scatter Plot).

**Figure 5: PCA maps of the results of experiment 4, containing the information of 35 sensors (1) or 7 sensors (2-6). Data was center scaled. A2 (black): minitablets containing ZS and NaCl, B2 (red): minitablets containing ZS and sweetener, C2 (blue): minitablets containing NaCl and sweetener, D2 (light green): minitablets**

**containing ZS, NaCl and sweetener, E2 (yellow): ZS, F2 (pink): ZS, NaCl and sweetener, G2 (dark green): NaCl and sweetener**

While the PCA maps within Experiment 3 are very comparable (Figure 2), this is less the case for the PCA maps within Experiment 4 (Figure 5). Nonetheless, the cluster structure can be recognized independent of the center, and thus provide comparative results. No reason for the drifting results for each sample measured in center 4 could be found.

Calculating the Euclidean distances based on the mean sensor values lead to results summarized in Figure 6. In this case, the Euclidean distances are calculated originating from the zinc sulphate containing minitablet formulation (E2). The results support those of the PCA maps: Each center identified samples E2 and G2 on the one and B2, D2 and F2 on the other hand most likely to be similar. The decreased Euclidean distances of center 1 go along with the decreased scaling of the corresponding PCA map (Figure 5.2).

**Figure 6: Euclidean distances, calculated based on the mean sensor values (left) and CPA values (right) according to Equation 1. The Euclidean distances are calculated originating from pure ZS (E2). A2: minitablets containing ZS and NaCl, B2: minitablets containing ZS and sweetener, C2: minitablets containing NaCl and sweetener, D2: minitablets containing ZS, NaCl and sweetener, F2: ZS, NaCl and sweetener, G2: NaCl and sweetener**

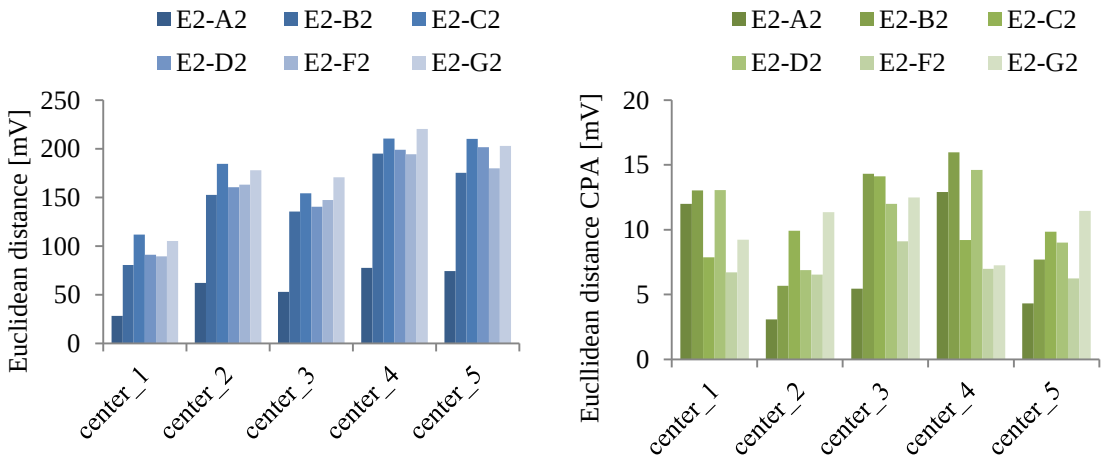


In contrast to the patterns obtained from Experiment 3 (Figure 3), the patterns based on the mean CPA values of Experiment 4 are not comparable to the Euclidean distance patterns of the sensor signals (Figure 6). Moreover, the highest Euclidean distances are decreased from approximately 70 mV (Figure 3, right) to 15 mV (Figure 6, right). The decreased values are additional proof for adsorption being the main signal creating process in Experiment 3, as zinc sulphate is not lipophilic and thus does not result in descriptive CPA values (Figure 7).

**Figure 7: Mean CPA values based on the CPA values of the different centers (mean ± s). A2 (black): minitablets containing ZS and NaCl, B2 (red): minitablets containing ZS and sweetener, C2 (blue): minitablets containing NaCl and sweetener, D2 (light green): minitablets containing ZS, NaCl and sweetener, E2 (yellow): ZS, F2 (pink): ZS, NaCl and sweetener, G2 (dark green): NaCl and sweetener**

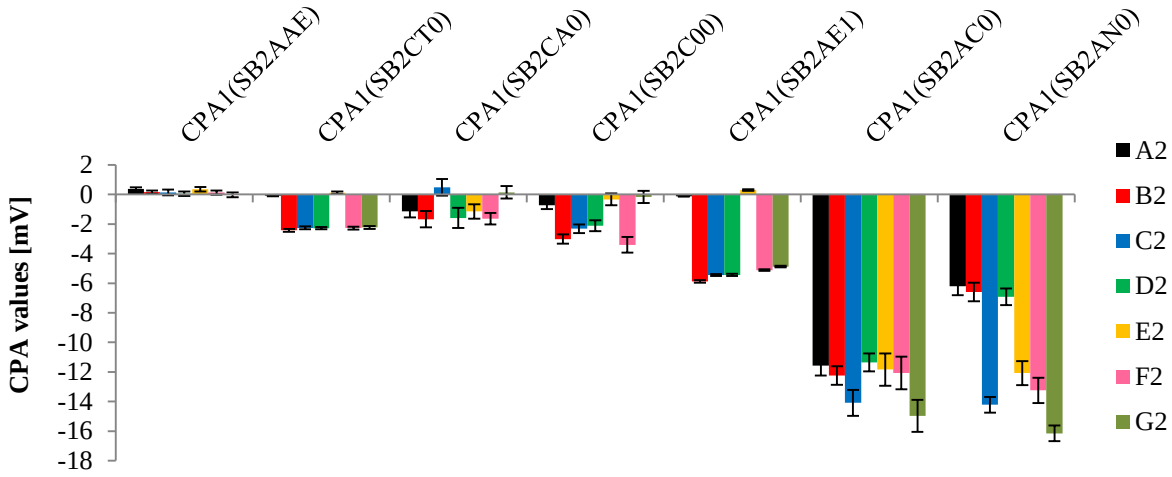


## 4. Conclusions

The first inter-laboratory testing of Insent e-tongues has successfully been performed based on four experiments, which were conducted by five different centers. Experiment 1 and 2, each based on a concentration series of quinine hydrochloride, served as some kind of additional sensor performance check. The resulting sensitivity (in this case the difference between lowest and highest sensor response) and slope of the regression line values have been found to serve as applicable evaluation criterions for inter-laboratory comparability. However, further investigations with other drugs than quinine hydrochloride are recommended for future studies to get more generalized information. . In Experiment 3 and 4, drug formulations were investigated and with regard to inter-laboratory comparability of the results different evaluation methods have been applied and discussed. PCA Score and Loading Scatter Plots and Euclidean distance patterns based on the raw sensor responses appeared as valuable evaluation tools for the inter-laboratory comparison. Varying PCA Score Scatter Plots between the centers were explained by the information of the Loading Scatter plots, which could be correlated with the results of Experiments 1 and 2. Information given by the CPA values enabled to dedicate adsorption of dimenhydrinate as main contributor for the results in Experiment 3. Although some (aged) sensors behaved differently in Experiment 1 and 2, the according sensors responses resulted in comparable PCA and Euclidean distances patterns in Experiment 3 and 4. In conclusion, participating e-tongues can be declared to perform comparably.

## 5. Future work

Modified sensor responses were found to be related to aged sensors. The supplier requires using only sensors that passed the routinely performed sensor check and the monthly required maintenance measurement. Both measures, considering defined substances in a defined concentration, fail, if the underlying information about the sensor response profiles differs from the measured one. These single point calibration procedures help to sort out weakly performing sensors. Thus, future work of the "e-tongue usergroup" intends to develop more sophisticated methods to judge about the sensor performance in connection with the sensor age or history, which will be beneficial for the users.

## 6. Acknowledgements

Our gratitude goes to Katharina Schneider and Daniel Sieber for their practical support and to Florian Kiene, Carolin Eckert and Maren Preis (University of Duesseldorf, Germany) for valuable scientific discussions.

## 7. Literature

Kobayashi, Y., Habara, M., Ikezazki, H., Chen, R., Naito, Y., Toko, K., 2010. Advanced taste sensors based on artificial lipids with global selectivity to basic taste qualities and high correlation to sensory scores. Sensors 10, 3411-3443.

Pein, M., Eckert, C., Preis, M., Breitkreutz, J., 2013. New protocol for αAstree electronic tongue enabling full performance qualification according to ICH Q2. J. Pharm. Biomed. Anal. 83, 157-163.

Stoltenberg, I., 2012. Orodispersible Minitabletten, Heinrich-Heine Universität, Düsseldorf.

Woertz, K., Tissen, C., Kleinebudde, P., Breitkreutz, J., 2010. Performance qualification of an electronic tongue based on ICH guideline Q2. J. Pharm. Biomed. Anal. 51, 497-506.

Woertz, K., Tissen, C., Kleinebudde, P., Breitkreutz, J., 2011. A comparative study on two electronic tongues for pharmaceutical formulation development. J. Pharm. Biomed. Anal. 55,